Modeling economic resilience

Célian Colon

NNT : 2016SACLX098

Thèse de doctorat de l'Université Paris-Saclay préparée à l'Ecole Polytechnique

Ecole doctorale n°129 — Sciences de l'Environnement d'Ile-de-France
Spécialité de doctorat : Mathématiques Appliquées

Par

M. Célian Colon

Modéliser la résilience économique

Thèse présentée et soutenue à l'Ecole Normale Supérieure, Paris, le 2 décembre 2016.
Composition du Jury :

M.	Jean-Philippe Bouchaud	Examinateur
M.	Fabio D'Andrea	Examinateur
M.	Michael Ghil	Directeur de thèse
M.	Antoine Mandel	Rapporteur
M.	Luciano Pietronero	Président du jury
M.	Gérard Weisbuch	Rapporteur

Ecole Polytechnique

Modeling Economic Resilience

PhD thesis

Célian Colon

supervised by

Michael Ghil

December 2016

Modeling Economic Resilience

Abstract: A wide range of climatic and ecological changes are unfolding around us. These changes notably manifest themselves through an increased environmental variability, such as shifts in the frequency, intensity, and spatial distribution of weather-related extreme events. If human societies cannot mitigate these transformations, to which conditions should they adapt? To many researchers and stakeholders, the answer is resilience. This concept seems to subsume a variety of solutions for dealing with a turbulent and uncertain world. Resilient systems bounce back after unexpected events, learn novel conditions and adapt to them. Theoretical models, however, to explore the links between socioeconomic mechanisms and resilience are still in their infancy. To advance such models, the present dissertation proposes a novel conceptual framework. This framework relies on an interdisciplinary and critical review of ecological and economic studies, and it is based on the theory of dynamical systems and on the paradigm of complex adaptive systems. We identify agent-based models as crucial for socioeconomic modeling. To assess their applicability to the study of resilience, we test at first whether such models can reproduce the bifurcation patterns of predator–prey interactions, which are a very important factor in both ecological and economic systems. The dissertation then tackles one of the main challenges for the design of resilient economic system: the large interconnectedness of production processes, whereby disruption may propagate and amplify. We next investigate the role of delays in production and supply on realistic economic networks, and show that the interplay between time delays and topology may greatly affect a network's resilience. Finally, we investigate a model that encompasses adaptive responses of agents to shocks, and describes how disruptions propagate even though all firms do their best to mitigate risks. In particular, systemic amplification gets more pronounced when supply chains are fragmented. These theoretical findings are fairly general in character and may thus help the design of novel empirical studies. Through the application of several recent ideas and methods, this dissertation advances knowledge on innovative mathematical objects, such as Boolean delay equations on complex networks and evolutionary dynamics on graphs. Finally, the conceptual models herein open wide perspectives for further theoretical research on economic resilience, especially the study of environmental feedbacks and their impacts on the structural evolution of production networks.

Remerciements

Ma première pensée va pour Denis-Didier Rousseau. Alors que je cherchais une équipe pour accueillir mon projet, il n'a pas hésité à m'ouvrir les portes du CERES. Conduire une recherche interdisciplinaire n'est pas chose aisée, et je dois beaucoup à l'ouverture d'esprit, la bienveillance et l'excellence des chercheurs de cette institution. Je remercie en particulier David Claessen, qui, tant sur le plan scientifique que pratique, m'a apporté un soutien précieux tout au long de ces trois années.

C'est avec un profond respet et une grande joie que je remercie Michael Ghil, mon directeur de thèse. Je lui suis extrêmement reconnaissant pour la confiance qu'il m'a accordée et pour son soutien sans faille dans toutes les phases de mon projet. Il m'a appris le métier de chercheur tout en laissant libre cours à ma curiosité, me permettant d'explorer des *terrae incognitae* de la connaissance.

Au cours de ces trois années, j'ai eu le plaisir de rencontrer et de collaborer avec des scientifiques remarquables : Fabio d'Andrea, Jean-Philippe Bouchaud, Åke Brännström, David Claessen, Ulf Dieckmann, Doyne Farmer, Stéphane Hallegatte, Antoine Mandel, Elena Rovenskaya, Gérard Weisbuch. Je les remercie pour les discussions stimulantes partagées et espère qu'elles se poursuivront. Je remercie également Luciano Pietronero pour m'avoir fait l'honneur de présider mon jury de soutenance.

Je suis, une nouvelle fois, redevable envers l'Ecole Polytechnique qui a financé mon travail via l'allocation doctorale Gaspard Monge. Je tiens à souligner le précieux concours de l'International Institute of Applied System Analysis de Laxenburg, ainsi que du Grantham Institute of Climate Change and the Environment de l'Imperial College de Londres.

J'ai travaillé dans d'excellentes conditions, et je dois beaucoup pour cela à Vincent Cassé, Guillaume Lapeyre et Bernard Legras. Je les remercie d'avoir toujours faciliter mon travail et mon intégration dans le LMD, laboratoire dans lequel j'ai fait de très belles rencontres.

J'exprime toute ma sympathie pour l'équipe de la graduate school de l'Ecole Polytechnique, qui ont avec constance allié gentillesse et efficacité : Fabrice Baronnet, Alexandra Belus, Emmanuel Fullenwarth et Audrey Lemaréchal. Ma gratitude va également à

Catherine Archat, Delphine Coudert, Nadine Razgallah, Micheline Rialet de l'ENS, Laurence Amsili de l'ED 129 ainsi qu'Aleksandra Cofala, Tanja Huber et Darina Zlatanova de l'IIASA pour leur précieux soutien administratif.

Le lancement de mon travail de thèse en octobre 2013 est le fruit d'une intense année d'échanges, au cours de laquelle j'ai construit et affiné mon projet. Je tiens à remercier, pour leurs conseils et encouragements, Denis Couvet, Guillaume Deffuant, Suren Erkman, Romain Ferrari, Cyrille Harpet, Jean-Louis Jourdan, John Mumford, Diogo Queiros-Conde, Muriel Tichit et Sebastien Treyer.

J'exprime enfin une pensée amicale à mes collègues et amis avec qui j'ai partagé de beaux moments de vie: les doctorants et post-docs du LMD, l'équipe CERES+EEM et les stagiaires qui y sont passés, les YSSPers 2015 et 2016, les participants la Moscow Summer Academy 2015, ceux de l'école d'été Modelling Environmental Resilience Paris 2016, et bien sûr toute la Lemon team. Je remercie enfin mes proches pour leur soutien sans faille, en particulier dans la dernière ligne droite.

Table of Contents

Introduction

We live in a time of fast-paced transformations. There are more humans on Earth than ever, and they are more educated, more interconnected, and consuming more resources than ever. Through soil degradation, contaminant dispersion and extensive illumination, the realm of the 'natural' is shrinking. Most living organisms have to adapt to an anthropogenized planet. Planetary processes are also becoming influenced by human societies, the most striking of these processes being the climate-related ones. Following Nobel Laureate Paul Crutzen, many scientists now propose to name our epoch the *Anthropocene*, the time of the humans.

These transformations have generated intense debates on how societies may, or should, adapt their *oiko-nomia*, the way they manage their home. In the 1960s, Kenneth Boulding was calling our planet 'Spaceship Earth', to stress its limits and the need to account for them in economic thinking. No decisions should be based on the view that the biosphere absorbs all pollutants and unlimitedly regenerates all basic resources.

The image of a spaceship also suggests a possibility for controlling the Earth's trajectory. If we gather around a negotiation table and act reasonably, we may put in place the adequate monitoring systems, use resources more efficiently, and thus maintain some indicators below certain targets, e.g., a 2°C increase in the planetary atmosphere's average surface temperature. Or, if we cannot reach these objectives in time, we may agree on measures to adapt our vessel: cool cities through green walls, protect coastal settlements with higher dams or displace some communities.

We are realizing, however, that environmental processes are not intrinsically 'balanced', and therefore such transformations may not be that smooth. Greenhouse gases change the mean temperature, but this in turn affects the frequency and intensity of extreme events, and, more generally, the climate's internal dynamics. The weather is likely to get more turbulent and warmer globally, and exact consequences on a local scale are still quite uncertain. In a more fluctuating environment, to what conditions should societies adapt?

To many, the answer is *resilience*. This intriguing concept seems to inspire solutions for adapting to a turbulent and uncertain future. Resilient societies may survive severe and unexpected events, bounce back after a shock, and reorganize their infrastructure, economies and policies to fit changing conditions. This flexible and dynamic notion is much harder to grasp than the eco-efficiency approach of the spaceship and its manageable indicators. Even so, this concept has recently become one of the key pillars of sustainability.

To become resilient, and to respond to the perturbed internal variability of the climate, societies need to change their own internal dynamics. In fact, socio-economic dynamics have also evolved rather rapidly over the past decades. Not only are there more people and organizations aboard the spaceship, but they interact much more intensely. Ideas, problems and solutions can spread like wildfire. Through heavier reliance on networked infrastructures, individuals and companies are less autonomous but they can also, paradoxically, engage more easily in decentralized activities.

As for economies in general, the production of goods and services is getting more global, and it involves therewith a multitude of specialized organizations connected through transnational and fragmented supply chains. As analyzed by Ingmar Granstedt already in the 1970s, these intricacies bind distant processes together. Such increased interconnectivity fosters the propagation of disruptions and may generate economic volatility. These economic phenomena may, in turn, be amplified by a potential increase in the amplitude, spatio-temporal extent and frequency of weather-and-climate–related extreme events. Systemic risk — whereby an unexpected event triggers a large domino effect — is a great concern, not only for people and businesses but also for insurers.

In this context, firms are themselves looking for resilient strategies. Through risk mitigation, increased agility, and permanent restructuring, they may better compete in a turbulent environment. Does such individual-firm behavior help the economy getting more resilient as a whole? How do individual risk reduction strategies interact with the complex structure of the economy? How can we even analyze the resilience in such interconnected systems?

The present dissertation aims to tackle these questions. We intend to advance the understanding of economic resilience, and focus on the supply side of economies, what we call "the production system." Our approach is based on the concepts and methods of dynamical and complex system analysis, through which we formulate and analyze mathematical models of the production system.

Given the relative novelty of the topic, our *first objective* is to carefully formulate the research approach, to define the key concepts, and to select the adequate tools. To that end, we embark in an interdisciplinary journey, carried out in three steps. We start in ecology, where resilience has first been mathematically introduced, go on with business management, economics, network and complex adaptive system theories, and end with the design of a conceptual framework for modeling economic resilience.

In Chapter 1, we present the sources and the originality of the concept of ecological resilience, and point to the avenue this structuring concept opens in the investigation of socioeconomic systems, along with its potential misuses. Chapter 2 then gives an account of the main economic trends affecting production systems and their vulnerability to shocks, in particular the complexification of supply chains and the emergence of systemic risks. We also analyze what resilience means for companies and their competitiveness. In Chapter 3, we review the tools available for studying the response of production systems to shocks. We then analyze how resilience has been framed in economics and discuss the theoretical challenges that remain for its modeling. From there, we design a novel conceptual framework for the study of economic resilience. This framework allows us to clearly define the concept, organize knowledge, generate hypotheses and formulate theoretical models.

Our *second objective* is to test and apply this conceptual framework. We tackle this goal in a series of three papers. The first one — reproduced as Chapter 4 in this dissertation — is of a rather methodological nature. It applies one of the modeling techniques that we identified in Chapter 3 to a predator–prey problem, and demonstrates its mathematical usefulness for the study of resilience.

We then build in the second and third paper two types of models representing productions systems, each of them focusing on different aspects of resilience that were highlighted by our conceptual framework. In the second paper Chapter 5, we study the interplay between the topological network structure, supply delays and their variability in affecting the networks' resilience. The third one (Chapter 6) investigates how the vertical fragmentation of supply chains may increase systemic risks and deteriorate resilience.

Based on the analysis of these two models, we are able to derive robust conclusions on the dynamics of production systems and on how decisions by economic agents may affect the resilience of networks they participate in. The understanding gained therewith can help generate hypotheses that are empirically testable. The novelty of these models and of the analysis methods applied to them herein also advances the broader mathematical knowledge on studying the resilience-related properties of complex dynamical systems. The research perspectives that this dissertation opens are discussed in Chapter 7.

Chapter 1

Persistence through resilience

Contents

Introduction

Resilience is about movement and dynamics. The word comes from the latin verb *resilire*, which means to rebound or leap back. Although "resilience" or "resiliency" is mentioned in some publications of the 19th century (Alexander, 2013), its development as an academic concept only started in the 1960s and 1970s. In the natural sciences, ecologist Holling introduced it in 1973 to interpret the persistence over time of highly fluctuating ecosystems. Through Kuhn's framework (1962), Holling's paper may be interpreted as an attempt to invalidate the equilibrium-based paradigm[1] that used to prevail in ecology. In parallel, the concept of resilience helped psychologists solve a gap between theory and observations on human development. Human development used to be understood as a linear process in which any adverse events would induce disorder (Werner, 1993). Several longitudinal studies however proved that some children had gone through positive development albeit adverse early exposure to stress, such as chronic poverty and family discord. Resilience opened a new scope for interpreting these observations: a person may be resilient, meaning able to recover from terrible life experiences.

In both fields, this concept was successful in opening new lines of interpretations. It allowed scientists to look at more complex and dynamic behavior. In Sec. 1.1, we present the key concepts of the resilience-based paradigm proposed by Holling. We particularly emphasize its original contribution, which contains the seeds of most of the further conceptual developments. In Sec. 1.2, we show how resilience evolved from a purely ecological concept to a truly interdisciplinary one. We also highlight the contribution of social scientists and the theory of complex adaptive systems in its conceptual refinement. Finally, Sec. 1.3 gives an account of how resilience diffused from ecology to many disciplines and from academics to policy-making realms, and uses as an example the field of disaster risk reduction. The diffusion of resilience has often been met with criticism, and has generated debates that we summarize in the last section.

The material comes from extensive review of literature in a variety of disciplines, including ecology, environmental sciences, economics, management sciences, along with grey literature from international institutions. It has been enriched from personal communications during seminars and conferences, including the Tenth Biennal Conference of the European Society for Ecological Economics, that was held in Lille in 2013, and the Third International Science and policy Conference on the Resilience of Social & Ecological Systems, that was held in Montpellier in 2014.

[1] Paradigm is used in the sense of Kuhn (1962): an "implicit body of intertwined theoretical and methodological belief that permits selection, evaluation, and criticism" (*Ibid.*, p. 16)

1.1 Resilience: reviving the dynamic nature of systems

Resilience casts a fresh light on the dynamic of systems. Framed in the theory of dynamical systems, it has enabled to move from an equilibrium-based view of ecosystems to an enriched theory that better embrace the complexity of living systems.

1.1.1 Resilience versus equilibrium in the study of ecosystems

Holling (1973) introduces **resilience** to challenge **stability**. Using both theoretical and empirical arguments, he disputes that the concept of stability limits our understanding of ecosystem dynamics. In his paper, the focus on stability implies postulating that ecosystems are fundamentally in equilibrium. This equilibrium hypothesis builds on a static view inspired from mechanical physics. Ecosystem analysis focuses on measuring abundance of species at an a postulated equilibrium point, and their dynamical behaviors around this point. This approach ignores the fact that ecosystems are fluctuating open systems that may undergo sudden changes.

Holling proposes instead to focus on the persistence of some qualitative properties, such as the coexistence of species. A resilient ecosystem is one in which species keep coexisting albeit large perturbations. Coexistence is compatible with fluctuations, and resilient systems may be unstable. He takes as example the periodic break out of spruce budworms. This pest regularly depletes spruce and balsam fir in Canadian forests, which leaves space for other tree species to develop. These large scale fluctuations help maintain the diversity of tree species, which would otherwise be reduced by competition.

Focusing on equilibrium and immediate stability tends to leave out of the scope some processes that are critical for the functioning of ecosystems. For instance, harvesting a seemingly stable fish population at the maximum sustained yield (MSY) may lead to its collapse[2]. Holling documents cases of fish populations that were harvested and suddenly collapsed, without any apparent perturbations. Such collapse happened to trouts in the American Great Lakes. Although fishing was not affecting their abundance, it had slowly made the population overall younger with smaller individuals. When a new species, sea lamprey, invaded the lake, the trout population collapsed. Fishing had made the population less resilient.

Sudden collapses of fisheries are still vivid issues. In the northwestern Atlantic, cod collapsed in the early 1990s due to overfishing[3]; see Fig. 1.1. Albeit a ban in 1992, the population has still not recovered, suggesting that fundamental processes have been lastingly

[2]The theory of MSY, nowadays called maximum sustainable yield, aims to determine the optimum extraction rate of a renewable resource; it is based on so-called surplus production models. One of the most popular ones for fisheries in Holling's time in environmental economics is the Schaefer model (Schaefer, 1954). Using the logistic growth model of Verhulst (1838), this model predicts that the best catch of a fish population occurs at its maximum growth rate.

[3]See Rose (2007) for a well-documented social and ecological account of the collapse of cod fisheries in this region.

disturbed. Focusing on MSY, which is based on the equilibrium paradigm, hides such processes. In a more recent paper, Holling further elaborates its critic of the dominant practices in resource management. He describes the side effects of command-and-control methods and efficiency-oriented approaches to ecosystems, which rely on simplistic understanding of ecological dynamics (Holling and Meffe, 1996).

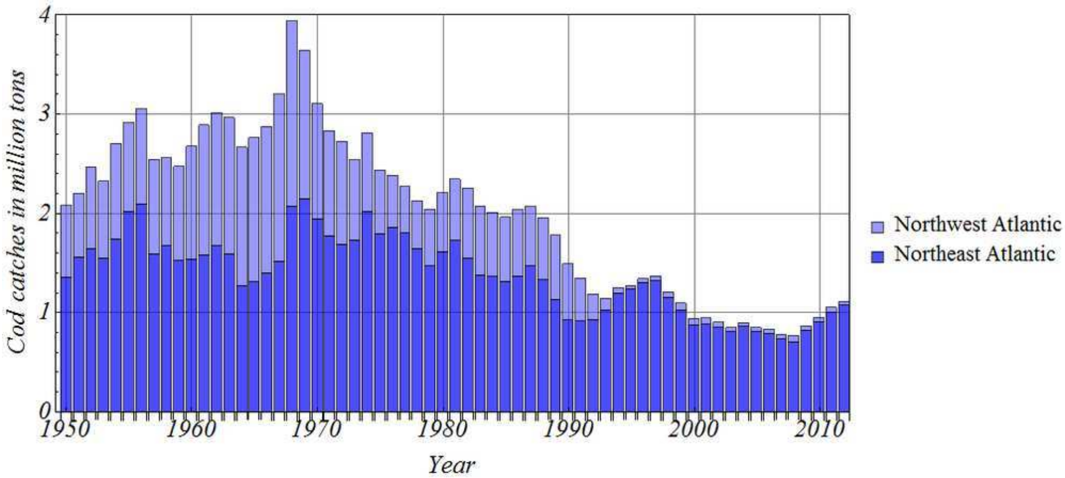

Figure 1.1: Cod catches in the Northeast and Northwest Atlantic Ocean in the period 1950-2012. Data provided by FAO. Source: Wikimedia Commons (2016).

By looking at how ecosystems persist through disturbances, Holling invites us to investigate the slowly changing processes that underpins their functioning, and how these processes interact with external factors at different scales in space and time. Studying resilience therefore provides a deeper understanding of the functioning of ecosystems. Table 1.1 summarizes the paradigmatic change proposed by Holling in terms of how ecosystems are viewed, and how they should be analyzed and managed.

He concluded by two hypotheses that are still under scrutiny nowadays. He argued that heterogeneous systems tend to be more resilient, because they offer wider set of options to react to unexpected events. This hypothesis has fed into the long-standing ecological debates on whether diversity increases stability. Next, he postulated that resilience results from evolutionary history. For instance, ecosystems that grow in self-contained environment, with steady climate conditions and few genetics exchanges with other ecosystems, have developed very context-specific structures. Although they seem stable, and are in fact very adapted to their biophysical constraints, they tend to be very sensitive a sudden change of these constraints. This tension between adaptation and adaptability will be central in further theoretical developments that are presented Sec. 1.2.2.

1.1.2 Alternative stable states, thresholds and tipping points

One of the central arguments for looking at resilience is the existence of **alternative stable states** (ASS) (Beisner et al., 2003). Ecosystems exhibit ASS when, under the

Table 1.1: Summary of the paradigmatic changes proposed by the resilience-based approach to system analysis, compared to the equilibrium-based approach.

Category	Equilibrium-based approach	Resilience-based approach
View	Unique equilibrium	Multiple state
	Short-term dynamical processes	Slow dynamical processes
	Fixed feedback structure	Changing feedback structure
Analysis	Quantitative	Qualitative
	Performance	Persistence
	Local dynamics	Global dynamics
Management	Plan according to predictions	Prepare for the unexpected
	Maximum sustainable yield	Adaptive management

exact same environmental conditions, they can be in several states that have important qualitative differences. One of the most documented examples is shallow lakes, which can be either in an oligotrophic, clear-water state or in a eutrophic, turbid one (Scheffer et al., 1997). Similarly, semi-arid savanna can have large areas of grass which enable grazing. Following extreme droughts, they can turn into a shrub-dominated landscape without grass (Walker et al., 1981) [4].

The detection of such behavior in simple theoretical models motivated Holling to work out the concept of resilience (Folke, 2006). They were systems of two coupled ordinary differential equations describing predator–prey interactions. In these models, ASSs emerge when the predation response is nonlinear and when one of the two populations suffers from the so-called Allee effect[5] — a setting that will be studied in our first paper (Chapter 4). In the 1960s and 1970s, the acknowledgement of the potential existence of alternate equilibra stimulated a significant number of theoretical works and empirical investigations (see the review by May, 1977).

Studying the dynamical behavior of systems with ASS requires not only to assess the local stability of each state, but also to identify how it can switch from one state to another. This switching behavior implies the existence of thresholds. Oligotrophic lakes can enter a phase of rapid eutrophication when nutrient inflows, from agricultural runoffs, cross certain rates. Drought-induced disappearance of grass in savanna rangeland is favored by large grazing intensities.

The possibility of discontinuous shifts in the qualitative state of a system has been known in the theory of dynamical systems since Poincaré (1885). He showed that a rotating fluid takes increasingly complex shapes as the angular speed increases, with discontinuous shift from one state to another, a prediction that was later confirmed experimentally (Hide, 1953). Poincaré coined the term bifurcation to describe this behavior, a first step towards what will become later the theory of bifurcations.

[4] Further examples of ASS, including those experimentally confirmed, can be found in the review by Schröder et al. (2005).

[5] The Allee effect describes the fact that the growth rate may particularly be low, even negative, for low population density. It is a nonlinear behavior often modeled by introducing a density threshold.

Empirical evidences that bifurcations take place in ecosystems have stimulated the search for '**tipping points**'[6] and other threatening 'catastrophic shifts' (Scheffer et al., 2001), drawing upon the theory of bifurcations. For instance, the dynamics of lake eutrophication was described as a saddle-node bifurcation, in which the unstable branch collides with a stable fixed point, giving rise to hysteresis (Scheffer, 2004).

For all compartments of the biosphere, there are attempts to find potential regime shifts at the global scale; see for instance (Lenton et al., 2008) for climate. In particular, Rockström et al. (2009) aims to define the thresholds delimiting the state of the world that enabled human development. A related stream of research aims to understand whether the advent of a tipping point can be anticipated by so-called early-warning signals (Scheffer et al., 2009). Although promising (Scheffer et al., 2012), the universality and actual performance of such signals have been criticized (Boettiger and Hastings, 2012). Our first paper (Chapter 4) touches upon this topic. It analyzes a class of bifurcation which differs from those studied in the literature on tipping points, which shows that more research is needed before being able to generalize the properties of early-warning signals.

1.1.3 Resilience in the theory of dynamical systems

As seen in the previous sections, resilience and the other concept it brings along are rooted in the theory of dynamical systems. For Holling (1973), the most important mathematical object to evaluate resilience is **the basin of attraction**. Holling, like many authors, defines resilience from the geometrical characteristics of this object. Let us consider the pitchfork bifurcation in its normal form:

$$\frac{\mathrm{d}x}{\mathrm{d}t} = x(\mu - x^2), \tag{1.1}$$

where μ is a real-value parameter. Fig. 1.2(a) presents the corresponding bifurcation diagram. For negative values of μ, there is only one fixed point. For positive values of μ, there are two of them: the system is called bistable. These features can be more intuitively represented with so-called stability landscapes. Such landscape can be rigorously defined for gradient systems by introducing pseudo-potentials. Fig. 1.2(b) presents this landscape for the pitchfork equation with $\mu = 1$. It derives from the following pseudo-potential V:

$$V(x) = -x^2(\mu - \frac{x^2}{4}). \tag{1.2}$$

For $\mu < 0$, the fixed point is globally stable. To understand the dynamics of this state, analyzing its local behavior would suffice. For $\mu > 0$, the resilience of each of the

[6]The term tipping was first used to describe neighborhood migrations in urban studies. Schelling (1978) popularized this term by showing that a few tipping can lead to sudden changes in migration flows, such as the emergence of community segregation. Since then, the concept of tipping point has been introduced in a variety of fields.

two fixed points is assessed by different geometric aspects of their respective basins of attraction: $[0, +\infty[$ and $]-\infty, 0]$.

The depth of each basin, called resistance by Walker et al. (2004), measures the strength of the attractor. Resistant system stays almost unchanged in the face of disturbance (Begon et al., 2006). The slopes of the basins determine the speed at which the perturbed system returns at equilibrium (Pimm, 1984; Peterson et al., 1998), or the management efforts it takes to move the system to another basin (Walker et al., 2004). In some fields, especially in engineering, these properties are called resilience. In material engineering, for instance, it describes how well elastic compounds autonomously recover from deformation.

Holling (1996) calls this view of resilience 'engineering resilience', in contrast to 'ecological resilience'. The latter focuses on the size of the attractor basins. The size is related to the amount of perturbation the system can sustain without switching to a new attractor. For the lower branch of Fig. 1.2(a), this amount is $\sqrt{\mu}$. Walker et al. (2004) adds another measure, called preciariousness, which is the proximity of the system to the boundary of the attractor basin.

By focusing on the boundaries of attractor basins, this approach de-emphasizes the nature of the attractor, whether fixed point, limit cycle, or more complex ones[7]. Although Holling draws a strong distinction between stability and resilience, assessing the geometry of attractor basins in mathematical models often starts with assessing the local stability of the attractors.

Even for non gradient systems, stability landscapes are often shown in the literature to convey these various measurements of resilience; see an example Fig. 1.3. However, such illustration suggests that landscapes are static. In fact, the resilience approach points to the possibility of changes in the landscapes. Through slow processes, existing basins may merge and new ones emerge. These reconfigurations can induce abrupt changes to the system within short time scale (Beisner et al., 2003). These processes are typically captured by the model parameters, the influence of which can be assessed by studying the bifurcation pattern. In the pitchfork example, the resilience of the upper branch $x = \sqrt{\mu}$ can be evaluated by the size of the parameter region in which this attractor exists, i.e. $\mu > 0$.

The viability theory of Aubin (2001) has been proposed to give a more precise mathematical definition of resilience (e.g., Deffuant and Gilbert, 2011). The aim of viability theory is to analyze whether a system, given constraints and external control processes, can stay within a specific region of the phase space. For a particular disturbance, Martin (2004) defines resilience as the inverse of the cost of driving the system back to a desired region. For an ensemble of disturbances, it is then possible to determine resilience at all

[7] Albeit Holling (1973) points out the generality of limit cycles, most resilience studies focus on fixed-point attractors.

points of the phase space (Deffuant and Gilbert, 2011). This framework has been applied to a variety of systems, and extended to stochastic dynamics (Rougé et al., 2013). These mathematical developments have however not diffused within resilience studies, which have now a more interdisciplinary and applied focus.

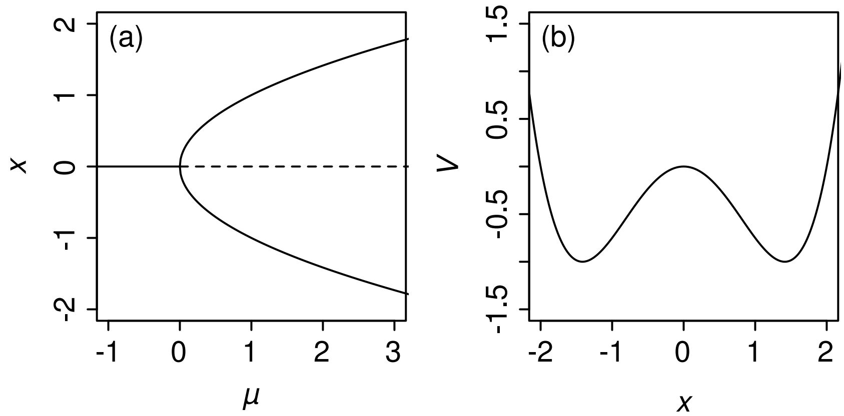

Figure 1.2: Geometric features of the pitchfork bifurcation $\frac{\mathrm{d}x}{\mathrm{d}t} = x(\mu - x^2)$. (a) Bifurcation diagram. Solid curves indicate stable fixed points, the dashed line indicates unstable ones. (b) Pseudo-potential for $\mu = 1$.

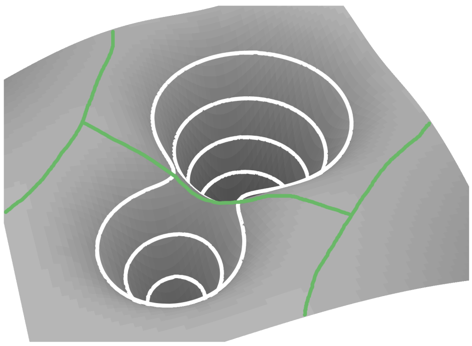

Figure 1.3: A fitness landscape. The green curves indicate the limit of the basins of attractions, while the white curves are level lines.

1.2 From ecology to interdisciplinary realms

From these ecological premises, the concept of resilience has been applied to a broader spectrum of systems. In particular, it was used to assess the management of natural resources, and was soon extended to socio-ecological systems (Sec. 1.2.1). This wider application has generated significant conceptual extensions, with contributions from social scientists and connections with the theory of complex adaptive systems (Sec. 1.2.2). These extensions have generated a wide range of resilience definitions, which we will summarize in three categories (Sec. 1.2.3).

1.2.1 From natural resources to socio-ecological systems

With the example of the collapse of fisheries, Holling (1973) pointed out the importance of identifying the processes underpinning the persistence of a resource, along with their interactions with larger systems. From this suggestion, some scholars proposed to study not only the dynamics of ecosystems but also the social dynamics that influence how resources are harvested. Social scientists studying the sustainable management of natural resources started cooperating with ecologists (Berkes and Folke, 2000; Adger, 2000; Folke, 2006). Berkes et al. (2003) proposed **socio-ecological systems** (SESs) as the adequate scope for studying the resilience of natural resources and local communities. This topic attracted considerable interests, and led to structuring of a new research community[8].

This stream of research highlights the constant interplay between social and ecological dynamics, which generates complex dynamical behaviors (Liu et al., 2007). A community adapts to the ecosystem it relies on, and thereby modifies some ecological processes. As with the example of fisheries, these modifications might lead to unexpected ecological responses, forcing the community to adapt to new conditions. The issue of finding new way of managing resources emerged. Novel management principles have been thus developed, such as community-based management (Berkes and Folke, 2000; Tompkins and Adger, 2004) or adaptive co-managment (Olsson et al., 2004). The contributions of social scientists are strongly connected to Ostrom's work on the governance of commons (Ostrom and Janssen, 2004). They revolve around learning, trust, local knowledge, self-organization and multilevel governance (Lebel et al., 2006). Examples of SESs studied through this lens are: forestry (Fischer et al., 2006), agroecosystems (Cabell and Oelofse, 2012) or coastal systems (Adger et al., 2005).

The study of SESs pointed to dynamical behaviors that were going beyond the concept of ecological resilience originally proposed. SESs proved to sometimes exhibit rapid structural changes, such as the introduction of technologies or new institutions. These

[8] Interdisciplinary research on resilience have long been undertaken at the Beijer Institute, Stockholm. Two research institutions have then been founded on the concept of SES: the Resilience Alliance, a network of scholars founded in 1999; the Stockholm Resilience Center, a research institute founded in 2007. Both institutions emphasize interdisciplinarity, a commitment to sustainability, and policy-oriented research.

results pointed out the limits of the metaphor of a slowly changing stability landscape. Such observations stimulated the development of an integrated theory on the transformation of SESs, called panarchy (Gunderson and Holling, 2002). The central element of this theory is the adaptive cycle; see Fig. 1.4. Originally developed to describe how productive ecosystems in temperate regions undergo changes, the adaptive cycle appeared to be a useful heuristic to qualitatively explore SES dynamics. The term 'panarchy' was used to stress that SES dynamics are not determined by a unidirectional, hierarchical causality. They are rather shaped by cross-scale interactions between multiple adaptive cycles: small-scale dynamics influence large-scale dynamics and vice-versa. Practical guidelines based on the panarchy theory have been published to facilitate the empirical assessment of SESs (Gunderson et al., 2010).

One of the successes of the panarchy theory is the description of several development traps that seem to arise in many types of systems, such as the poverty trap or the rigidity trap (Carpenter and Brock, 2008). According to this theory, poverty traps (Bowles et al., 2006), which have been particularly documented for poor rural communities (Dasgupta, 2003), occur when a system fails to activate the minimal level of resources to put in place the positive feedbacks that drive growth. On the other hand, the rigidity trap, or lock-in, occurs when a system has developed so complex structures and processes, than it has no room left for innovation, just for maintenance. They are strong but brittle, leading to strong collapse following an unexpected crisis. It has been for instance described for agricultural regions in West Australia (Allison and Hobbs, 2004). From a management perspective, Fath et al. (2015) argue that recognizing the different stages and preparing for them facilitate the successful 'navigation' through the adaptive cycle (Fath et al., 2015). They provide examples of applications of such adaptive management principles to business and public organizations.

1.2.2 Resilience and adaptive system theory

These latter conceptual developments have been strongly influenced by the paradigm of **complex adaptive systems** (CASs) (Holland, 1992; Gell-Mann, 1994). The idea of CAS has been shaped by a multidisciplinary corpus of theories from physics, genetics, evolutionary biology, computer sciences, mathematics and social sciences. We list here the most influencing theories: the theory of neural networks and cybernetics (McCulloch and Pitts, 1943), cellular automata and their self-reproductive behavior (von Neumann, 1966), general system theory (von Bertalanffy, 1969), thermodynamics of phase transition and dissipative structures (Nicolis and Prigogine, 1977), coevolution of self-organization at 'the edge of chaos' (Kauffman, 1993) and self-organized criticality (Bak and Chen, 1991). All these theories describe open, out-of-equilibrium systems through an holistic lens, such as living organisms, ecosystems, economies, brains and immune systems.

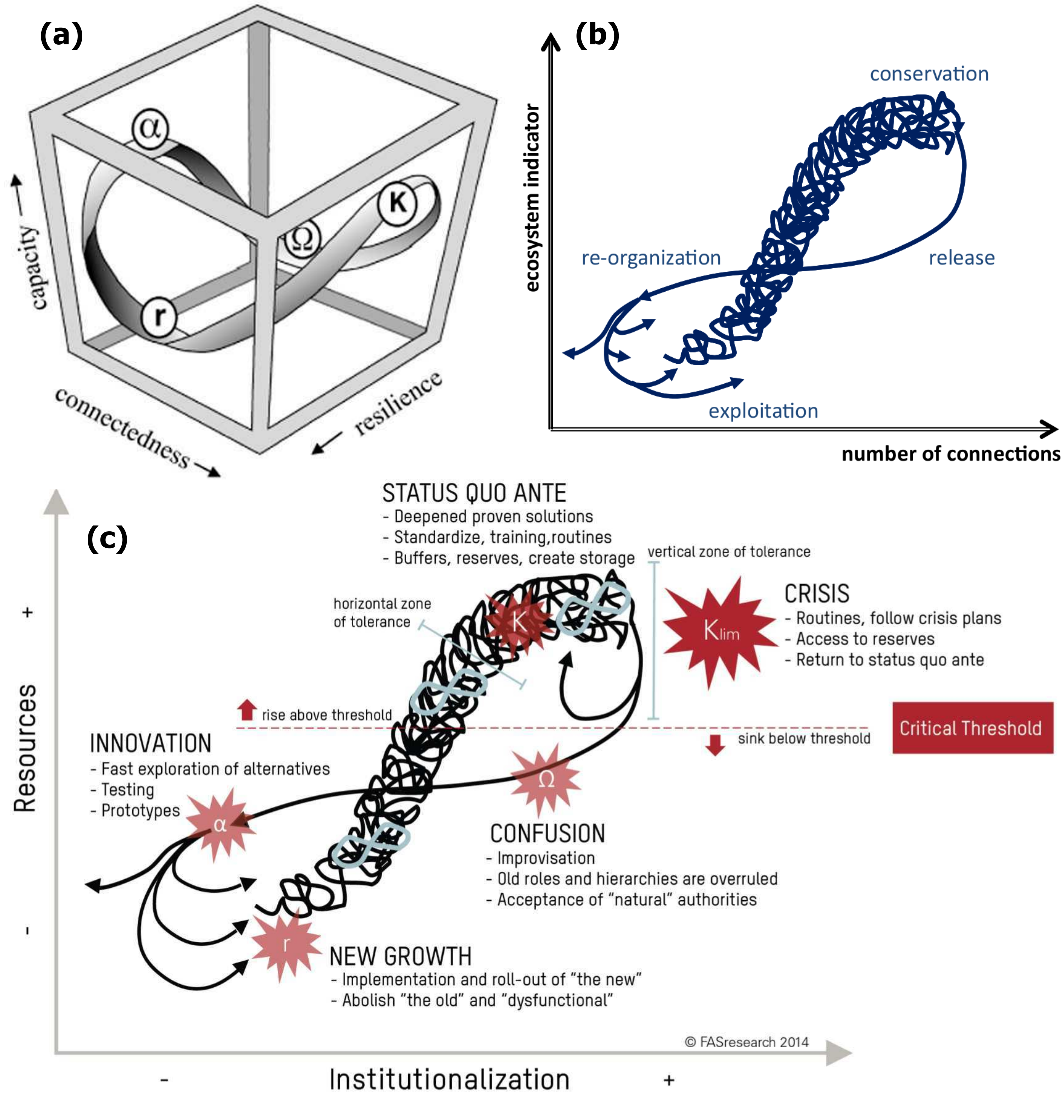

Figure 1.4: Three visual interpretations of the adaptive cycle. **(a)** A version proposed by Gunderson and Holling (2002, p.34) in three dimensions: capacity for change, connectedness and resilience. **(b)** The interpretation of Burkhard et al. (2011) emphasizes the erratic behavior of systems and the existence of smaller scale cycle in the growth phase. **(c)** The interpretation of Fath et al. (2015) adapted to the management of organizations.
(a–c) All adaptive cycles describe four stages, generally denoted by r, K, Ω and α. In the exploitation phase (r), the system is loosely structured, dominated by generalist agents that are robust to variability. They acquire resources and put in place positive feedback. Through self-organization, structures emerge and connectedness increases. When most resources have been exploited, the system enters the conservation phase (K). It is dominated by large and interconnected structures competing for scarce resources and resisting environmental variability. They however become rigid and their maintenance increasingly affects nearby systems. The system becomes less resilient. Eventually, one particular event triggers a crisis followed by a release phase (Ω), in which structures are dissolved and resources scattered. The system goes through a reorganization phase (α), where new linkages are tried, tested, until some become able to harness resources and grow, leading to a new exploitation phase.

CASs are composed of many interacting components which self-organize and create structures which in turn affect the behavior of the components, hence their complexity, the 'C' of CAS. Their second main feature is the 'A' of CAS, their ability to adapt to novel conditions through change of its internal structure. It implies self-regulating and learning processes, and the presence of enough diversity and degree of freedom to innovate, e.g. the genetic diversity of a population. This malleability is balanced by memory, by which successful structures persist through time and give to the system a persisting, yet evolving identity.

In this framework, resilience is then strongly connected to the adaptability of the system. It is its ability to self-organize and create new structures to maintain or reinvent its fundamental functions (Levin et al., 1998). This adaptability relies on a certain freedom to reorganize, which Ulanowicz interprets as a structural indeterminacy and tries to measure using information theory (Ulanowicz et al., 2009). He also calls this structural freedom the reserve capacity for adaptation. In the absence of perturbation, this capacity is harnessed by autocatalytic loops but tends to be restored through environmental variability (Ulanowicz, 1980). This theory is close to the hypothesis formulated by Holling (1973) on the influence of **evolutionary history** on resilience. Fittest systems are those maintaining a balance between adaptation and adaptability, between efficiency and resilience (Costanza and Mageau, 1999; Ulanowicz, 2002; Ulanowicz et al., 2009).

Thanks to the theory of CAS, strong analogies can be drawn between resilience and recent advances in system biology on robustness. Robustness generally describes models, engineered systems and decision-making processes, whose output barely changes when inputs widely vary. However, biology increasingly studies the robustness of organisms and biological processes, defined as their ability to "maintain [their] functions despite external and internal perturbations" (Kitano, 2004). In particular, such works focus on adaptive mechanisms, making robustness conceptually almost indistinguishable from resilience (Anderies et al., 2013). Although few connections have been made between these two corpuses, findings for biological systems, such as the intimate link between fragility and robustness described by Csete and Doyle (2002), may be profitably transferred to resilience studies.

1.2.3 The three dimensions of resilience

These conceptual expansions towards larger, more complex systems and more holistic theories may create perplexity and confusion (Brand and Jax, 2007)[9]. This confusion is reinforced by the diffusion of the term through a wide range of disciplines. In each of

[9]This confusion is however not specific to the concept of resilience. In ecology, for instance, it echoes discussions on the diversity of definitions of stability in the lasting diversity–stability debates, that authors regularly attempt to clarify (e.g., Harrison, 1979; Pimm, 1984; Grimm and Wissel, 1997; Ives and Carpenter, 2007). This confusion has not prevented this debate to yield very interesting insights, also from the perspective of resilience, on the response of ecosystems to global changes (see for instance McCann, 2000).

them, the definition of resilience has been adjusted with different wording and emphasis [10].

Albeit these diversity of interpretation and conceptual extensions, we have mapped these definitions along a complexity gradient. If the core idea of bouncing back after remains, this gradient reveals different views of what exactly bounces back and how. We distinguish three main levels on this gradient; see Tab. 1.2. This three-level distinction is now often made in the literature (e.g., Martin-Breen and Anderies, 2011).

First, '**engineering resilience**' characterizes a system that has good performance in enduring stress and in returning to a normal state once stress disappears. Systems have a single fixed point, and we analyze its local and global stability properties. For instance, this standpoint applies to the study of bridges and their resistance to wind or loads, or to the short-term effect of a drought on food prices.

Next, '**ecological resilience**' focuses on persistence of feedback structures and their functioning. Fluctuations do not matter, as long as the processes that sustain the most significant qualitative properties are maintained. The scope is enlarged to a greater complexity and includes the slow processes and interaction with connected systems. Systems can have multiple alternative attractors, possible complex ones. We analyze the basins of attractions, their size and how they might change through gradual parameter change. This approach is useful to examine how the overall functioning of an ecosystem or an economy can be lastingly affected by a change in environmental conditions.

Finally, '**adaptive resilience**' is also concerns with the persistence of functions, but acknowledges wide reorganizations, even changes of feedback structures and creations of new processes. From a system dynamics perspective, the basins of attractions are endogenously changing. Some parameters are no longer fixed but become adaptive traits influenced by internal variables and external stimuli. Using this standpoint, we can analyze how environmental perturbations — e.g., a hurricane — affect the internal structure of an ecosystem or an economy, which in turn may modify its ability to withstand new shocks.

This mapping is useful to identify the specific standpoint adopted by an author. Indeed, these three dimensions leads to different, yet complementary, inquiries on dynamical systems. As will be underlined in Sec. 3.3 of Chap. 3, the study of each of these dimensions requires the use of different modeling framework and of different methods. While we might have reached a limit in the refinement and extension of the concept of resilience, its diffusion to new fields is still ongoing.

[10] For instance, social scientists refer to institutions and organizations, while management scientists often focus on decision-makers. Brand and Jax (2007) and Bhamra et al. (2011) provide systematic reviews of resilience definitions.

Table 1.2: Three dimensions of resilience and their main characteristics

	What bounces back?	How?
Engineering	Quantitative property	Stability
System	Qualitative state	Persistence of process and feedback structure
Adaptive	Functions	Adaptability, reorganization, renewal

1.3 Spectacular diffusion and debated applications

The concept of resilience has spectacularly spread in a wide range of fields (Xu and Marinova, 2013). It has also crossed the boundary of academia[11] and reached a wider audience in both grassroots movements and global policy discussions. It is particularly pronounced for the topic of disaster risk reduction, which bridges science and policy. In contrast, the use of resilience in economics revolves around regional studies, and is absent from economic theory. In overall, the diffusion and application of the concept have sparked both scientific and political debates, which highlight important issues concerning its application.

1.3.1 Resilience of people, communities and cities to disaster

Given the failure to mitigate climate change and other large-scale perturbations such as the spectacular loss of biodiversity, human societies are likely to encounter novel environmental conditions. Since the IPCC third assessment report (2001), the agenda of climate change adaptation has been on the rise. However, given the levels of uncertainty and the difficulty to provide small-scale projections, it is hard to envision to what particular conditions societies will have to adapt. In this context, resilience appears to many as a potential solution, because it emphasizes preparedness and adaptability to unexpected changes (Comfort et al., 2010).

Resilience is now an essential part of the policy discussions on global sustainability (UNSG, 2012; FAO/OECD, 2012), and has become particularly prominent in the preexisting policy discussion on disaster risk reduction and international development. It has become a top priority of the United Nation International Strategy for Disaster Reduction (UNISDR, 2004), and enacted as the central objective of the 2005 Hyogo framework, brought forward in 2015 in the newly adopted Sendai framework (UNISDR, 2005, 2015).

The field of disaster risk reduction lies at the crossroad of policy, academia and practices. It is concerned with the vulnerability of communities to natural and man-made disasters. In this field, resilience can be build by providing risk-mitigating infrastructures and organizing responsive emergency services. Scholars also pointed out the central role played by social capital, and in particular by social bonds (Moser, 1998). This approach thus links ecological resilience with psychological resilience. The latter describes the context-specific coping strategies that enable people to positively respond to adverse conditions. In particular, Reich (2006) argues that public agencies dealing with natural disasters could foster resilience at the individual level. This should be done by giving people more control over their post-disaster recovery, by improving the diffusion of consis-

[11] Using bibliometric tools, Baggio et al. (2015) identified five main scientific fields that concentrate resilience studies: psychology, ecology, social sciences, engineering, and the hybrid field of socio-ecological systems (SES). Most fields tend to develop rather independently, especially in the sphere of engineering and business management. The notable exception is SES, which is by nature interdisciplinary.

tent information during a disaster, and by facilitating interpersonal communication and contacts.

The political success of the resilience concept, along with its wide range of implementation, is well illustrated by the recent adoption of the 2030 sustainable development goals (UN, 2015). Resilience appears in many goals, from poverty and food security to economic development, and is applied to communities, infrastructures, management practices and ecosystems. Resilience has become a central topic when discussing international development (Bahadur et al., 2013) and its funding (Muller, 2007), leading many NGOs to develop specific resilience-based programs.

Cities, which concentrate over half of the world's population, were identified as the adequate scale to develop context-specific resilience strategies against disasters (Ahern, 2011; Leichenko, 2011). In addition to climate events, urban resilience revolves around a wider spectrum of threat, from industrial accidents and terrorist attacks to geopolitical events (Godschalk, 2003). While urban resilience has first focused on urban planning and the design of robust infrastructures, the concept has been increasingly used to emphasize the role of adaptive mechanisms to deal with risks. It now largely extends to 'softer' considerations, such as institutions and local governance, social innovations (Ernstson et al., 2010) and decentralized organizations enabled by information technologies (Allenby and Fink, 2005).

1.3.2 Boundary object, buzzword or political agenda?

The spectacular diffusion of resilience, a 'viral spread' in Bristow's words (2010), may be attributed to the malleability, perceived accessibility and positive connotation of the concept. While the Cartesian idea of controlling nature[12] is fading, resilience seems to acknowledge the existence of surprise and uncertainty in a positive way (Davoudi, 2012). Moreover, with the perceived failure of getting anywhere closer to sustainability, resilience sketches out a way forward, stimulates novel solutions, and delivers a positive message. Resilience is now firmly established in "the so-called 'grey area' between academic, policy and practices discourses" (Bristow, 2010).

In each research community where it was introduced, debates have sparked between those arguing that resilience brings a fresh view on lasting issues and others who challenge its scientific value (Klein et al., 2003; Janssen et al., 2006; Brand and Jax, 2007; Hassink, 2010; Hudson, 2010) and highlight its potential political misuse (Pendall et al.,

[12] Opposing to a too speculative philosophy, Descartes considers that "it to be possible to arrive at knowledge highly useful in life; [...] to discover a practical, by means of which, knowing the force and action of fire, water, air, the stars, the heavens, and all the other bodies that surround us, as distinctly as we know the various crafts of our artisans, we might also apply them in the same way to all the uses to which they are adapted, and thus render ourselves like masters and possessors of nature. . And this is a result to be desired, not only in order to the invention of an infinity of arts, by which we might be enabled to enjoy without any trouble the fruits of the earth, and all its comforts, but also and especially for the preservation of health" (Descartes, 1637, sixth part).

2010; Reghezza-Zitt et al., 2012; Davoudi, 2012; Porter and Davoudi, 2012). Researchers introducing resilience in their research community seek to propose a novel approach, which usually rests on some of the central ideas presented in Sec. 1.1 the role of nonlinearities, the possibility of alternative equilibria, the need for an adaptive or evolutionary approach. By emphasizing local knowledge and the role of decentralized and grassroots institutions, the concept of resilience stimulated disruptive social innovations[13] (Shaw, 2012).

On the other hand, some scholars warn against the gradual dilution of the concept as it crosses disciplinary boundaries (Brand and Jax, 2007). They argue that resilience gets increasingly fuzzier because it is repeatedly stretched to describe more diverse systems. They note that resilience has now acquired both a descriptive and normative content, and warn that this confusion may hinder scientific progress. The interdisciplinary use of the word led some author to interpret it has a 'boundary object' (Star and Griesemer, 1989), i.e. a concept that enables people from different background to communicate, and that is plastic enough to satisfy different expectations. This malleability facilitates communication across disciplines, although each community may use it to legitimize their own research agenda.

In policy discourses, each party can stretch the concept to fit their own economical or political interests, which may lead to apparent, yet fragile consensus. Reghezza-Zitt et al. (2012) warn that operationalizing resilience may contain implicit political or ideological purposes. For instance, resilience, like sustainability, can be proposed as a one-size-fits-all solution to complex problems, and help disguise the lack of real strategy. Similarly, Porter and Davoudi (2012) argue that resilience can be used as a way to depoliticised topics. The Resilience Alliance states that it conducts research to foster sustainability, without a critical assessment of the use of sustainability in a social context (Reghezza-Zitt, 2013). For Porter and Davoudi (2012), the questions of agency, in the sociological sense, of fairness and justice need to be openly debated.

In international policies for disaster risk reduction, Reghezza-Zitt et al. (2012) noted that the introduction of resilience came with a change of attitude from international organizations such as the UN/ISDR towards vulnerable communities. These communities are not only victims, they are expected to take individual responsibility, to be proactive, and are otherwise stigmatized. By focusing on their adaptive capacity and self-reliance, Reghezza-Zitt et al. (2012) argue that these organizations tend to undermine the socioeconomical, political and historical contexts that underpin their vulnerability. Pushing it to the limit, being resilient could turn into a moral judgment, leading to a new sort of social Darwinism (Reghezza-Zitt et al., 2012; Porter and Davoudi, 2012).

Nevertheless, even critics acknowledge the main benefit of using resilience: building bridges between research communities and fostering interdisciplinary projects (Brand and

[13] Shaw (2012) mentions the case of the Transition Towns, a grassroots movement that aims to renew social, economic and environmental practices through local initiatives. The concept of resilience may have promoted the decentralized functioning of this movement and the idea of empowering local communities.

Jax, 2007). Debating resilience within communities are also opportunities to reassess assumptions and clarify research stances (Christopherson et al., 2010; Reghezza-Zitt, 2013). When it comes to its operationalization, the warnings formulated by social scientists should be integrated. They recall that, when aiming at implementations, we should not only analyze resilience of what to what (Carpenter et al., 2001), but also question for whom (Lebel et al., 2006) and finally understand who decides (Porter and Davoudi, 2012). This framework will prove useful to apprehend the discussion of business and resilience, respectively in Secs. 2.2 of Chapter 2 and 3.1.4 of Chapter 3.

Conclusion

Introduced in ecology in 1973, the concept of resilience was used by Holling to change the way ecosystems are seen and analyzed. Their dynamical nature reveals the need to adopt larger scopes and include more complexities. Instead of focusing on quantitative performance around postulated equilibria, Holling proposes to focus on the persistence of processes that sustain qualitative properties. This approach benefited from advances in the theory of nonlinear dynamical systems, which suggested the possibility of multiple stable states, threshold behaviors and tipping points. Such properties could be empirically observed in ecosystems.

Over the past two decades, the concept has been significantly extended, and has been applied to a wide spectrum of systems. With inputs from the theory of complex adaptive systems, resilience has become the building block of larger interdisciplinary frameworks. Resilient behaviors not only allow to remain within a fixed attractor basin but also enable the reorganization of structure and the creation of new processes in response to a shock. These more complex behaviors suggest potential trade-offs between adaptation and adaptability, between efficiency and resilience. These truly systemic questions connect many fields of research, from biology to engineering and economics.

For a complex system modeler, these interdisciplinary and conceptual extensions are real challenges. Even so, we could map resilience along a complexity gradient. This mapping provides guidance for modeling, by first focusing on simple behavior and then move to more complex ones. Starting from the local stability of attractors and their 'engineering' features, we can then study their attractor basins and identify bifurcations, and thus assess 'ecological resilience'. To dive into 'adaptive resilience', we can use tools from adaptive and evolutionary dynamics and analyze how emergent properties feedback to micro-components and how structural properties adapt to perturbations.

It is also important to acknowledge the strong diffusion of the concept in the policy arena, both in global discussions and practical implementations. To many, resilience sketches out potential solutions for our unsustainable era and inspires disruptive innovations. The operationalization of the concept can however favor some political or economical views, and some agents may use its relative fuzziness to impose their agenda. Such social dynamics are worth being known to scientists interested in applied works.

References

Adger, W. N., 2000. Social and ecological resilience: are they related? Progress in Human Geography 24 (3), 347–364.

Adger, W. N., Hughes, T. P., Folke, C., Carpenter, S. R., Rockström, J., 2005. Social-Ecological Resilience to Coastal Disasters. Science 309 (5737), 1036–1039.

Ahern, J., 2011. From fail-safe to safe-to-fail: Sustainability and resilience in the new urban world. Landscape and Urban Planning 100 (4), 341–343.

Alexander, D. E., 2013. Resilience and disaster risk reduction: an etymological journey. Natural Hazards and Earth System Science 13 (11), 2707–2716.

Allenby, B., Fink, J., 2005. Toward Inherently Secure and Resilient Societies. Science 309 (5737), 1034–1036.

Allison, H. E., Hobbs, R. J., 2004. Resilience, adaptive capacity, and the lock-in trap of the Western Australian agricultural region. Ecology and society 9 (1).

Anderies, J. M., Folke, C., Walker, B., Ostrom, E., 2013. Aligning Key Concepts for Global Change Policy: Robustness, Resilience, and Sustainability. Ecology & Society 18 (2).

Aubin, J. P., 2001. Viability Theory. Birkhauser, Basel.

Baggio, J. A., Brown, K., Hellebrandt, D., 2015. Boundary object or bridging concept? A citation network analysis of resilience. Ecology and Society 20 (2).

Bahadur, A. V., Ibrahim, M., Tanner, T., 2013. Characterising resilience: unpacking the concept for tackling climate change and development. Climate and Development 5 (1), 55–65.

Bak, P., Chen, K., 1991. Self-Organized Criticality. Scientific American 264 (1), 46–53.

Begon, M., Townsend, C. R., Harper, J. L., 2006. Ecology: From Individuals to Ecosystems. John Wiley & Sons.

Beisner, B., Haydon, D., Cuddington, K., 2003. Alternative stable states in ecology. Frontiers in Ecology and the Environment 1 (7), 376–382.

Berkes, F., Colding, J., Folke, C., 2003. Navigating Social-Ecological Systems: Building Resilience for Complexity and Change. Cambridge University Press.

Berkes, F., Folke, C., 2000. Linking social and ecological systems for resilience and sustainability. In: Berkes, F., Folke, C., Colding, J. (Eds.), Linking Social and Ecological Systems: Management Practices and Social Mechanisms for Building Resilience. Cambridge University Press, pp. 1–25.

Bhamra, R., Dani, S., Burnard, K., 2011. Resilience: the concept, a literature review and future directions. International Journal of Production Research 49 (18), 5375–5393.

Boettiger, C., Hastings, A., 2012. Quantifying limits to detection of early warning for critical transitions. Journal of the Royal Society Interface 9 (75), 2527–2539.

Bowles, S., Durlauf, S. N., Hoff, K., 2006. Poverty Traps. Princeton University Press, Princeton.

Brand, F. S., Jax, K., 2007. Focusing the meaning (s) of resilience: resilience as a descriptive concept and a boundary object. Ecology and Society 12 (1), 23.

Bristow, G., 2010. Resilient regions: re-'place'ing regional competitiveness. Cambridge Journal of Regions, Economy and Society 3 (1), 153–167.

Burkhard, B., Fath, B. D., Müller, F., 2011. Adapting the adaptive cycle: Hypotheses on the development of ecosystem properties and services. Ecological Modelling 222 (16), 2878–2890.

Cabell, J. F., Oelofse, M., 2012. An Indicator Framework for Assessing Agroecosystem Resilience. Ecology and Society 17 (1).

Carpenter, S., Walker, B., Anderies, J. M., Abel, N., 2001. From Metaphor to Measurement: Resilience of What to What? Ecosystems 4 (8), 765–781.

Carpenter, S. R., Brock, W. A., 2008. Adaptive capacity and traps. Ecology and society 13 (2), 40.

Christopherson, S., Michie, J., Tyler, P., 2010. Regional resilience: theoretical and empirical perspectives. Cambridge Journal of Regions, Economy and Society 3 (1), 3–10.

Comfort, L. K., Boin, A., Demchak, C. C., 2010. Designing resilience: preparing for extreme events. University of Pittsburgh Press, Pittsburgh, Pa.

Costanza, R., Mageau, M., 1999. What is a healthy ecosystem? Aquatic ecology 33 (1), 105–115.

Csete, M. E., Doyle, J. C., 2002. Reverse Engineering of Biological Complexity. Science 295 (5560), 1664–1669.

Dasgupta, P., 2003. Population, poverty, and the natural environment. In: Mäler, K., Vincent, J. (Eds.), Handbook of Environmental Economics. Elsevier, Amsterdam, pp. 191–247.

Davoudi, S., 2012. Resilience: A Bridging Concept or a Dead End? Planning Theory & Practice 13 (2), 299–307.

Deffuant, G., Gilbert, G. N., 2011. Viability and resilience of complex systems: concepts, methods and case studies from ecology and society. Springer Verlag, Berlin; New York.

Descartes, R., 1637. Discours de la méthode. Pour bien conduire sa raison, et chercher la vérité dans les sciences. Jean Maire, La Haye.

Ernstson, H., van der Leeuw, S. E., Redman, C. L., Meffert, D. J., Davis, G., Alfsen, C., Elmqvist, T., 2010. Urban transitions: on urban resilience and human-dominated ecosystems. AMBIO: a Journal of the Human Environment 39 (8), 531–545.

FAO/OECD, 2012. Building Resilience for Adaptation to Climate Change in the Agriculture Sector. Tech. rep., Organization for Economic Co-operation and Development & Foods and Agriculture Organization of the United Nations,, Rome.

Fath, B. D., Dean, C. A., Katzmair, H., 2015. Navigating the adaptive cycle: an approach to managing the resilience of social systems. Ecology and Society 20 (2).

Fischer, J., Lindenmayer, D. B., Manning, A. D., 2006. Biodiversity, ecosystem function, and resilience: ten guiding principles for commodity production landscapes. Frontiers in Ecology and the Environment 4 (2), 80–86.

Folke, C., 2006. Resilience: The emergence of a perspective for social–ecological systems analyses. Global environmental change 16 (3), 253–267.

Gell-Mann, M., 1994. Complex Adaptive Systems. In: Cowan, G., Pines, D., Meltzer, D. (Eds.), Complexity: Metaphors, Models, and Reality. Addison-Wesley, Reading, MA, pp. 17–45.

Godschalk, D., 2003. Urban Hazard Mitigation: Creating Resilient Cities. Natural Hazards Review 4 (3), 136–143.

Granstedt, I., 1980. L'impasse industrielle: un monde à réoutiller autrement en tous lieux. Seuil, Paris.

Grimm, V., Wissel, C., 1997. Babel, or the ecological stability discussions: an inventory and analysis of terminology and a guide for avoiding confusion. Oecologia 109 (3), 323–334.

Gunderson, L., Kinzig, A., Quinlan, A. E., Cundhill, G., Beier, C., Crona, B., Bodin, Ö., 2010. Assessing Resilience in Social-Ecological Systems: Workbook for Practitioners. Tech. rep., Resilience Alliance.

Gunderson, L. H., Holling, C., 2002. Panarchy: Understanding Transformations in Human and Natural Systems. Island Press.

Harrison, G. W., 1979. Stability under Environmental Stress: Resistance, Resilience, Persistence, and Variability. The American Naturalist 113 (5), 659–669.

Hassink, R., 2010. Regional resilience: a promising concept to explain differences in regional economic adaptability? Cambridge Journal of Regions, Economy and Society 3 (1), 45–58.

Hide, R., 1953. Some experiments on thermal convection in a rotating liquid. Quarterly Journal of the Royal Meteorological Society 79 (339).

Holland, J. H., 1992. Complex Adaptive Systems. Daedalus 121 (1), 17–30.

Holling, C., Meffe, G. K., 1996. Command and Control and the Pathology of Natural Resource Management. Conservation Biology 10 (2), 328–337.

Holling, C. S., 1973. Resilience and stability of ecological systems. Annual review of ecology and systematics 4, 1–23.

Holling, C. S., 1996. Engineering resilience versus ecological resilience. In: Schulze, P. (Ed.), Engineering Within Ecological Constraints. National Academies Press, pp. 31–44.

Hudson, R., 2010. Resilient regions in an uncertain world: wishful thinking or a practical reality? Cambridge Journal of Regions, Economy and Society 3 (1), 11–25.

IPCC, 2001. Climate Change 2001: Impacts, Adaptation, and Vulnerability. Tech. rep., Intergovernmental Panel on Climate Change, Cambridge, UK.

Ives, A. R., Carpenter, S. R., 2007. Stability and Diversity of Ecosystems. Science 317 (5834), 58–62.

Janssen, M. A., Schoon, M. L., Ke, W., Börner, K., 2006. Scholarly networks on resilience, vulnerability and adaptation within the human dimensions of global environmental change. Global Environmental Change 16 (3), 240–252.

Kauffman, S. A., 1993. The Origins of Order: Self-organization and Selection in Evolution. Oxford University Press.

Kitano, H., 2004. Biological robustness. Nature Reviews Genetics 5 (11), 826–837.

Klein, R. J. T., Nicholls, R. J., Thomalla, F., 2003. Resilience to natural hazards: How useful is this concept? Environmental Hazards 5 (1), 35–45.

Kuhn, T., 1962. The Structure of Scientific Revolutions. University of Chicago Press, Chicago.

Lebel, L., Anderies, J., Campbell, B., Folke, C., Hatfield-Dodds, S., Hughes, T., Wilson, J., 2006. Governance and the Capacity to Manage Resilience in Regional Social-Ecological Systems. Ecology and Society.

Leichenko, R., 2011. Climate change and urban resilience. Current Opinion in Environmental Sustainability 3 (3), 164–168.

Lenton, T. M., Held, H., Kriegler, E., Hall, J. W., Lucht, W., Rahmstorf, S., Schellnhuber, H. J., 2008. Tipping elements in the earth's climate system. Proceedings of the National Academy of Sciences 105 (6), 1786–1793.

Levin, S. A., Barrett, S., Aniyar, S., Baumol, W., Bliss, C., Bolin, B., Dasgupta, P., Ehrlich, P., Folke, C., Gren, I.-M., Holling, C., Jansson, A., Jansson, B.-O., Mäler, K.-G., Martin, D., Perrings, C., Sheshinski, E., 1998. Resilience in natural and socioeconomic systems. Environment and Development Economics 3 (02), 221–262.

Liu, J., Dietz, T., Carpenter, S. R., Alberti, M., Folke, C., Moran, E., Pell, A. N., Deadman, P., Kratz, T., Lubchenco, J., Ostrom, E., Ouyang, Z., Provencher, W., Redman, C. L., Schneider, S. H., Taylor, W. W., 2007. Complexity of Coupled Human and Natural Systems. Science 317 (5844), 1513–1516.

Martin, S., 2004. The Cost of Restoration as a Way of Defining Resilience: A Viability Approach Applied to a Model of Lake Eutrophication. Ecology and Society 9 (2).

Martin-Breen, P., Anderies, J. M., 2011. Resilience: A Literature Review. Tech. rep., The Rockefeller Foundation, New York, NY.

May, R. M., 1977. Thresholds and breakpoints in ecosystems with a multiplicity of stable states. Nature 269 (5628), 471–477.

McCann, K. S., 2000. The diversity–stability debate. Nature 405 (6783), 228–233.

McCulloch, W. S., Pitts, W., 1943. A logical calculus of the ideas immanent in nervous activity. Bulletin of Mathematical Biology 5 (1), 115–133.

Moser, C. O. N., 1998. The asset vulnerability framework: Reassessing urban poverty reduction strategies. World Development 26 (1), 1–19.

Muller, M., 2007. Adapting to climate change water management for urban resilience. Environment and Urbanization 19 (1), 99–113.

Nicolis, G., Prigogine, I., 1977. Self-Organization in Nonequilibrium Systems. Vol. 191977. Wiley, New York.

Olsson, P., Folke, C., Berkes, F., 2004. Adaptive Comanagement for Building Resilience in Social–Ecological Systems. Environmental Management 34 (1), 75–90.

Ostrom, E., Janssen, M. A., 2004. Multi-Level Governance and Resilience of Social-Ecological Systems. In: Spoor, M. (Ed.), Globalisation, Poverty and Conflict. Springer Netherlands, pp. 239–259.

Pendall, R., Foster, K. A., Cowell, M., 2010. Resilience and regions: building understanding of the metaphor. Cambridge Journal of Regions, Economy and Society 3 (1), 71–84.

Peterson, G., Allen, C. R., Holling, C. S., 1998. Ecological Resilience, Biodiversity, and Scale. Ecosystems 1 (1), 6–18.

Pimm, S. L., 1984. The complexity and stability of ecosystems. Nature 307 (5949), 321–326.

Poincaré, H., 1885. Sur l'équilibre d'une masse fluide animée d'un mouvement de rotation. Acta Mathematica 7, 259–380.

Porter, L., Davoudi, S., 2012. The Politics of Resilience for Planning: A Cautionary Note. Planning Theory & Practice 13 (2), 329–333.

Reghezza-Zitt, M., 2013. Utiliser la polysémie de la résilience pour comprendre les différentes approches du risque et leur possible articulation. EchoGéo 24 (1).

Reghezza-Zitt, M., Rufat, S., Djament-Tran, G., Blanc, A. L., Lhomme, S., 2012. What Resilience Is Not: Uses and Abuses. Cybergeo: European Journal of Geography.

Reich, J. W., 2006. Three psychological principles of resilience in natural disasters. Disaster Prevention and Management: An International Journal 15 (5), 793–798.

Rockström, J., Steffen, W., Noone, K., Persson, å., Chapin, F. S., Lambin, E. F., Lenton, T. M., Scheffer, M., Folke, C., Schellnhuber, H. J., Nykvist, B., de Wit, C. A., Hughes, T., van der Leeuw, S., Rodhe, H., Sörlin, S., Snyder, P. K., Costanza, R., Svedin, U., Falkenmark, M., Karlberg, L., Corell, R. W., Fabry, V. J., Hansen, J., Walker, B., Liverman, D., Richardson, K., Crutzen, P., Foley, J. A., 2009. A safe operating space for humanity. Nature 461 (7263), 472–475.

Rose, G., 2007. Cod: An Ecological History of the North American Fisheries. Breakwater Books, St. John's, Newfoundland.

Rougé, C., Mathias, J.-D., Deffuant, G., 2013. Extending the viability theory framework of resilience to uncertain dynamics, and application to lake eutrophication. Ecological Indicators 29, 420–433.

Schaefer, M. B., 1954. Some aspects of the dynamics of populations important to the management of commercial marine fisheries. Bulletin of the Inter-American Tropical Tuna Commission 1 (2), 27–56.

Scheffer, M., 2004. Ecology of Shallow Lakes. Springer Science & Business Media.

Scheffer, M., Bascompte, J., Brock, W. A., Brovkin, V., Carpenter, S. R., Dakos, V., Held, H., van Nes, E. H., Rietkerk, M., Sugihara, G., 2009. Early-warning signals for critical transitions. Nature 461 (7260), 53–59.

Scheffer, M., Carpenter, S., Foley, J. A., Folke, C., Walker, B., 2001. Catastrophic shifts in ecosystems. Nature 413 (6856), 591–596.

Scheffer, M., Carpenter, S. R., Lenton, T. M., Bascompte, J., Brock, W., Dakos, V., Koppel, J. v. d., Leemput, I. A. v. d., Levin, S. A., Nes, E. H. v., Pascual, M., Vandermeer, J., 2012. Anticipating critical transitions. Science 338 (6105), 344–348.

Scheffer, M., Rinaldi, S., Gragnani, A., Mur, L. R., van Nes, E. H., 1997. On the dominance of filamentous cyanobacteria in shallow, turbid lakes. Ecology 78 (1), 272–282.

Schelling, T. C., 1978. Micromotives and Macrobehavior. W. W. Norton & Company, New York.

Schröder, A., Persson, L., De Roos, A. M., 2005. Direct experimental evidence for alternative stable states: a review. Oikos 110 (1), 3–19.

Shaw, K., 2012. “Reframing” Resilience: Challenges for Planning Theory and Practice. Planning Theory & Practice 13 (2), 308–312.

Star, S. L., Griesemer, J. R., 1989. Institutional Ecology, ‘Translations’ and Boundary Objects: Amateurs and Professionals in Berkeley’s Museum of Vertebrate Zoology, 1907-39. Social Studies of Science 19 (3), 387–420.

Tompkins, E. L., Adger, W., 2004. Does adaptive management of natural resources enhance resilience to climate change? Ecology and society 9 (2), 10.

Ulanowicz, R. E., 1980. An hypothesis on the development of natural communities. Journal of Theoretical Biology 85 (2), 223–245.

Ulanowicz, R. E., 2002. The balance between adaptability and adaptation. BioSystems 64 (1), 13–22.

Ulanowicz, R. E., Goerner, S. J., Lietaer, B., Gomez, R., 2009. Quantifying sustainability: Resilience, efficiency and the return of information theory. ecological complexity 6 (1), 27–36.

UN, 2015. Transforming our World: The 2030 Agenda for Sustainable Development. Tech. Rep. A/RES/70/1, United Nations.

UNISDR, 2004. Living with risk: a global review of disaster reduction initiatives. Tech. rep., United Nations Office for Disaster Risk Reduction, New York and Geneva.

UNISDR, 2005. Hyogo Framework for Action 2005-2015: Building the resilience of nations and communities to disasters. Tech. rep., The United Nations Office for Disaster Risk Reduction, Geneva.

UNISDR, 2015. Sendai Framework for Disaster Risk Reduction 2015-2030. Tech. rep., The United Nations Office for Disaster Risk Reduction, Geneva.

UNSG, 2012. Resilient people, resilient planet: A future worth choosing. Tech. rep., United Nations Secretary-General's High-Level Panel on Global Sustainability, New York.

Verhulst, P. F., 1838. Notice sur la loi que la population suit dans son accroissement. Correspondance mathématique et physique 10 (4), 113–121.

von Bertalanffy, L., 1969. General System Theory: Foundations, Development, Applications, revised edition Edition. George Braziller Inc., New York.

von Neumann, J., 1966. Theory of Self-Reproducing Automata. University of Illinois Press, Champaign, IL, USA.

Walker, B., Holling, C. S., Carpenter, S. R., Kinzig, A., 2004. Resilience, Adaptability and Transformability in Social–ecological Systems. Ecology and society 9 (2), 5.

Walker, B. H., Ludwig, D., Holling, C. S., Peterman, R. M., 1981. Stability of semi-arid savanna grazing systems. Journal of Ecology 69 (2), 473–498.

Werner, E. E., 1993. Risk, resilience, and recovery: Perspectives from the Kauai Longitudinal Study. Development and Psychopathology 5 (4), 503–515.

Xu, L., Marinova, D., 2013. Resilience thinking: a bibliometric analysis of socio-ecological research. Scientometrics 96 (3), 911–927.

Chapter 2

Vulnerability and systemic risk of production systems

Contents

Introduction

All organizations involved in the production of a good or a service and its delivery to consumers form a **supply chain**. Typical supply chains include raw material providers, component producers, assemblers, wholesalers, retailers and transporters. It may sometimes be extended to financial intermediaries, marketing agencies, and other third party contractors (Mentzer et al., 2001). All together, supply chains constitute the **production system** of an economy. Some of them are highly critical — e.g., water, energy, communications — and support almost all other productive sectors. Many supply chains are intertwined, such as those of cars and electronic goods, of chemicals and food.

This chapter aims to analyze the vulnerability of the production systems by looking at its supply chains, which, over the past decades, have become increasingly global and fragmented. We describe these facts and the associated process of vertical specialization in Sec. 2.1, and analyze how they may have fostered the risk of disruptions and their propagation. If one member of the supply chain cannot timely deliver its production to the next one, delays and disruptions may occur and cascade down the chain. Recent natural disasters, such as the eruption of the Eyjafjallajökull volcano in Island in 2010 or the Tohoku earthquake and tsunami in Japan in 2011, have shown that, more than ever, localized events may have consequences in distant locations.

We present in Sec. 2.2 the main challenges that firms face trying to mitigate such domino effects. They are looking for novel solutions to design more resilient supply chains, which may be in tension with competitiveness objectives. For management specialists, resilience is also seen as a way to better compete in a turbulent business environment. In Sec. 2.3 highlights that some limits may exist in how much individual firms can mitigate these propagating disruptions. This share of unmanageable risk is often called **systemic**. Although there is not yet a clear definition of the concept, it is a shared concern in other types of highly interconnected systems, such as banking networks and power grids. In supply chains, insurers are increasingly asked to cover these risks.

The materials presented in this chapter come from a review of several fields, including trade economics, industrial organization, business management, and of documents published by consultancies and business organizations. This review is complemented by insights gained during five interviews[1] with several professionals, including supply chain managers, consultants and insurers.

[1] The purpose of these five interview was to provide insider insights on the topic. They were not meant to constitute a research material, and were not conducted using a particular scientific method. They however proved useful to deepen our understanding of the issue and to confront academic findings with practical experiences.

2.1 Interconnectedness and the propagation of disruptions

We present how production systems have become more globalized, specialized and fragmented (Sec. 2.1.1), and how these trends have generated new risks (Sec. 2.1.2).

2.1.1 More globalized production systems

Globalization has made economies more interconnected. International trade is reaching unprecedented levels, and represents now about 33% of the world GDP (UNCTAD, 2013; WTO, 2013, 2016). Trade is originally 'horizontal': goods and services are produced in one location then exported to another. Over the past decades, the growth of trade flows has been however increasingly driven by another type of trade, called vertical trade (Hummels et al., 1998, 2001). In such trade, goods and services are intermediaries: they are imported then used as inputs in production processes. It may occur within the same industry: a component is imported, processed, and then reexported (Grubel and Lloyd, 1975). Over the period 1990–2000, this vertical trade has grown globally at a yearly rate of 9.1%[2], while total trade was increasing by 6.5% per year (Jones et al., 2005).

These larger transnational flows of production inputs signal that supply chains are becoming more scattered geographically and fragmented functionally. This trend is called **vertical specialization**. It is particularly marked for the supply chains of technological products such as cars of electronic goods, which are made of an increasing number of component — modern cars are made of about 30,000 pieces. A mobile audio player may be designed in the USA but assembled in China, with components from South Korea, the USA, and Japan; those parts are themselves made of subcomponents from China, the Philippines, etc. (Timmer, 2010). According to Sheffi (2005), some electronic products travel half a dozen times the Pacific ocean before being sold.

This global fragmentation results from outsourcing and offshoring strategies. Some companies have opened subsidiaries in other countries to offshore, i.e. relocate, some of their activities. They generally seek to benefit from lighter production costs, in particular through lower wages. Other companies have chosen to only keep a small segment of their activities, the one where they are the most competitive and on which they will concentrate their R&D, marketing and logistic efforts. They outsource other segments to specialized suppliers and seek to benefit from their higher flexibility and reduced costs. Large manufacturing companies are thereby going through vertical dis-integration, and supply chains are getting **fragmented**.

[2]The exact figure depends on the precise definition given to vertical trade. In its broadest sense, even fully manufactured goods are intermediaries, because they still need to be marketed an distributed. Most trade — 76% — is then vertical (Baldwin and Lopez-Gonzalez, 2015). To isolate the exchange of goods at intermediate level of processing, other authors use more restricted definitions, and speak of trade in parts and components (Hummels et al., 2001; Jones et al., 2005).

These practices have been facilitated by the removal of tariffs[3] (Yi, 2003). Offshoring started in the 1960s with the development in Mexico of subsidiaries of U.S. companies, the so-called 'maquiladora' factories (Hummels et al., 2001). In Europe, Western European companies started to offshore activities in the Iberian Peninsula, and then largely in Central and Eastern Europe (Kaminski and Ng, 2005). But the largest boom of vertical specialization occurred in the 1980s with Japanese and US companies offshoring and outsourcing activities in South East Asia and China, respectively (Baldwin and Lopez-Gonzalez, 2015)[4].

Managing distant production units and suppliers has been enabled by the development, at affordable costs, of specific technologies and services, e.g., transportation and communication technologies, financial intermediation and insurance services (Jones et al., 2005). While the globalization of supply chains was initiated by multinational corporations (Helleiner, 1981), the lower cost and higher performance of these 'service links' gave small companies the capacity to engage in outsourcing[5].

In all sectors of the economy, supply chains are becoming longer and more specialized (Osadchiy et al., 2016). This trend has generated new types of risks.

2.1.2 Supply chain risks and shock propagation

In global and fragmented supply chains, distant processes are interdependent, and unexpected issues may quickly propagate. The 'Albuquerque accident' involving Swedish company Ericsson is prototypical (Norrman and Jansson, 2004; Sheffi, 2005). In 2000, a lightning bolt hits an electric line in Albuquerque, New Mexico's largest city, and induces a short power outage in a factory owned by the Dutch company Philipps. In the absence of alternative power generator, fire sparks; it is extinguished ten minutes later, but has affected some critical equipment. Two production lines are stopped for three weeks, and stay insufficiently productive for months. The disrupted process was very specific and Ericsson failed to promptly find an alternative supplier. In a booming market, the production of cellphone was disrupted. The losses incurred by Ericsson were about 50 times higher than the material damages[6].

Trigger events may be of different nature — e.g., a geopolitical crisis, a social movement, or, as in the 'Albuquerque' accident, a climate event — and they may disrupt

[3] The Auto Agreement reached in 1965 between the U.S.A. and Canada had for instance a well documented impact on the fragmentation of the North American car supply chains (Hummels et al., 2001).

[4] For an analysis of the global structure of vertical trades, see Baldwin and Lopez-Gonzalez (2015).

[5] As noted by Jones et al. (2005), financial firms in the City of London have been outsourcing computer maintenance to Asia already in the 1980s. Such practices has nowadays expanded to many organization, including in public ones.

[6] At the end of the year, the company announced a loss of US$2.3 billion for its mobile phone division, while the material damages for Philipps amounted to US$40 million (Sheffi, 2005). Following this accident, Ericsson sold its cellphone production activity to the joint venture Sony Ericsson, and profoundly renewed the management of supply chain risks (Norrman and Jansson, 2004).

production through a variety of mechanisms: damages on productive equipment, workforce or transporters unable to access the production site, disruptions of basic utilities such as gas, electricity, water, communication. After a natural disaster, many businesses may get disrupted, even though they were not directly affected, as shown by Tierney's study (1997) on the aftermath of the 1994 Northridge earthquake. Natural events need not be destructive to destabilize supply chains, as illustrated by the eruption of the Eyjafjallajökull volcano in 2010 and its impact on global businesses through the disruption of air transportation. Fujimoto (2011) documents similar chains of events that forced Toyota to close plants between 1979 and 2007. Many more case studies can be found in the literature (in particular in Sheffi, 2005).

Recent large natural disasters have cast the light on the role of supply chain in propagating risks. The 2011 Tohoku earthquake and the tsunami that followed generated the largest human and material damages in Japan since World War II. It also disrupted the production of many critical components, leading to significant production losses worldwide (World Economic Forum, 2012). In Japan only, Tokui (2012), cited by Todo et al. (2013), estimated that about 90% of the losses of economic output were due to supply chain disruptions. The same year, central Thailand was hit by floodings, the highest in 70 years, which heavily disrupted the global supply chains of cars and electronic components (Chongvilaivan, 2012).

Since they are longer and more global, supply chains are more exposed. Events that are rare for each firm become more likely when the whole chain is considered. But Barrot and Sauvagnat (2016) also showed that vertical specialization — the fact that inputs are more specific and sourced from distant suppliers — largely increases the propagation of risks. In particular, disruptions not only cascade from suppliers to customers, but may also affect supply chains horizontally: if a firm is affected by the disruption of one specialized supplier, its other suppliers tend to suffer from losses due to demand reduction.

These supply chain intricacies may be one of the drivers behind the rising economic impact of natural disasters (Stecke and Kumar, 2009; Swiss Re, 2014, 2016). In surveys by the Business Continuity Institute (BCI)[7], adverse weathers and climate extreme events almost always rank among the three main sources of supply disruption (BCI, 2014). These threats are not likely to fade out with climate change, which is likely to induce a shift in the frequency, intensity and spatial distribution of weather-related extreme events (Ghil et al., 2011).

[7]The Business Continuity Institute is a private consultancy specialized in supply chain disruptions. It runs yearly surveys on 500 to 550 companies from about 70 countries.

2.2 The quest for resilient supply chains

These phenomena are of high concern for businesses, insurers, and in general for organizations operating through such multi-tiered, complex web of intermediaries, such as humanitarian organizations. Managing supply chain risks faces specific challenges, some of which have been analyzed through the lens of resilience (Sec. 2.2.1). Although, competitiveness objectives may hamper the design of resilient supply chains, certain aspects of resilience, such as agility and permanent reorganization, are seen as being a way to better compete (Sec. 2.2.2).

2.2.1 The challenges of mitigating risks in complex supply chains

Supply chain disruptions are rather frequent — at least one per year for 80% of the respondents the BCI survey (2014). Their negative impact on the financial performance of companies has been empirically confirmed (Hendricks and Singhal, 2003, 2005). Mitigating the risk of supply chain disruptions widely differs from the management of other operational risks. Supply chains may indeed bring to your door the risks taken by another firm far away, both its operational risks — e.g., an accident on a production line — and its environmental risks — e.g., a climate or geopolitical event.

Managers therefore need to increase their monitoring capacity. However, they often lack visibility over their supply chain. While firms usually know their direct suppliers, they often struggle to keep track of their sub-suppliers, also called tier-2 suppliers, and of entities further away in the chain (BCI, 2014; Wang et al., 2015). Half of the disruptions seem however to originate from this deeper segment (BCI, 2014). In addition, supply chains are fluctuating systems — e.g., suppliers change their contractors, firms go bankrupt, others enter the market — and are therefore hard to map in real time.

Inherent difficulties of interorganizational communication may also accentuate the propagation of supply disruptions. Jüttner et al. (2003) identify such network-related risks: unclear responsibility, lack of responsiveness or overreaction, distorted information and mistrust. A small fluctuation in demand at one point of the chain may be magnified as orders cascade up the chain, leading to excess inventory, production down time, and transportation peaks. This phenomenon, known as the bullwhip effect (Lee et al., 1997), is well known by supply chain managers, empirical documented (e.g. Thun and Hoenig, 2011) and was has been experimentally tested for decades through the so-called beer game (Sterman, 1989).

Managing the risk of supply disruption has become a prominent topic of supply chain management (SCM)[8]. The main pillar of SCM is the coordination of processes across organizational boundaries, in which managers need to engage to avoid these issues.

[8]SCM is a management philosophy that views the supply chain as a whole. It is oriented towards cooperative efforts to coordinate operational and strategic capabilities within and across the boundary of firms in order to enhance the value created to the end customer (Mentzer et al., 2001). This field

Management scientists have published frameworks to identify supply chain risks and mitigation strategies, derived from interviews, focus groups and case studies — the 'Albuquerque accident' for instance (Chopra and Sodhi, 2004; Blackhurst et al., 2005; Manuj and Mentzer, 2008). Such frameworks permeate across the business field towards humanitarian aid (Wassenhove, 2005; Cozzolino, 2012). In some of them, resilience is set as the target for SCM, without explicitly referring to the ecological or psychological concept (Christopher and Peck, 2004; Blackhurst et al., 2005; Abe and Ye, 2013). Instead of defining resilience for the supply chain as a whole, they focus on the development of resilient strategies for individual firms, and emphasize the engineering standpoint described in Sec. 1.2.3: shortening the return to normal operation.

Two types of measures are typically put forward. A first set aims to increase the inbuilt robustness of the supply, e.g., hold safety stocks and multiple production facilities, enlarge the supplier base, standardize inputs. Another set aims to improve the organizational agility to handle unexpected disruptions, e.g., collaboratively develop rescue plans with suppliers, decentralize decision-making, increase communication between services. These latter measures often go with the development of a more responsive corporate culture (Sheffi, 2005).

Such measures can be well calibrated to deal with high-probability low-impact risks, using, for instance operation research models (for a recent review, see Snyder et al., 2016). However, preparing for rare events that may generate high damages is far more challenging (Norrman and Lindroth, 2004). In the absence of meaningful metrics to handle such uncertainties, managers may use stress tests, in the form of 'what if' scenarios, to identify bottlenecks and particularly vulnerable points (Chopra and Sodhi, 2004; Christopher and Peck, 2004).

Some measures aiming at designing a resilient supply chain, such as safety stocks and multiple sourcing, are costly, and the benefits they generate may be hard to evaluate. Therefore competitiveness often set the limit to how much resilient a supply chain can be.

2.2.2 Is resilience competitive?

Staying competitive is a matter of survival for firms, and balancing risks and return their very nature. Supply chain managers permanently deal with contradicting objectives (Cooper et al., 1997): reducing inventories while ensuring product availability, source standardized inputs for customized products, maintaining a diverse supplier base but reducing sourcing costs.

With heightened competitive pressure globally, companies have tended to streamline their supply chains to cut costs. The number of suppliers per firm has often decreased (Osadchiy et al., 2016). Some of the principles of the so-called Toyota model (Enkawa and

was originally concerned by inventory reduction and the involvement of suppliers to speed up product development (Cooper et al., 1997).

Schvaneveldt, 2001), such as just-in-time or lean management, have had a strong impact on supply chain practices. Following them, firms develop stronger relationships with fewer suppliers, which enable them to rely on fewer inventories and shorter time delivery. They can also better manage product quality and design more customized products, and thereby gain competitive advantages. These practices may even be implemented in conjunction with global outsourcing (Das and Handfield, 1997).

According to many, these optimization processes have made supply chain more sensitive to disruptions (Stecke and Kumar, 2009; World Economic Forum, 2012). For instance, Fujimoto (2011) underlines that the high rate of customer-specific or buyer-specific processes in Japanese industries has contributed to lengthen economic recovery after the 2011 Tohoku earthquake. Similarly, Todo et al. (2013) have established the positive effect on post-earthquake recovery of having geographically diverse suppliers and customers, but have stressed that this diversification strategy might erode competitiveness.

Fujimoto (2011) argue that some Japanese sectors are globally competitive specifically because of highly concentrated technology providers. He identified the 'diamond structure' of many Japanese supply chains of manufactured goods: few final producers, many tier-1 and tier-2 suppliers, and few tier-3 suppliers for basic components. This concentration at the base of the chain, driven by cost-effective technologies, came with large economies of scale that boosted the competitiveness of many sectors. At the same time, the chain has become less resilient, since a disruption affecting these few suppliers may generate very large consequences.

The structural aspects that foster supply chain resilience, i.e. their in-built robustness, seem too costly to allow firms to stay competitive. As shown in Sec. 2.1.1, outsourcing has been driven by competitive pressures, but has amplified supply chain risks. Some companies have however managed to compensate this loss of structural robustness by an enhanced agility. They have developed the internal organizational capability to proactively identify and manage unexpected events (Chopra and Sodhi, 2004). Incidentally, Toyota is one of the top performers in this regards; it has often managed to resume production much earlier than expected after disasters (Nishiguchi and Beaudet, 1998; Fujimoto, 2011).

Businesses may compete through resilience by developing such capabilities of adaptation and responsiveness (Sheffi, 2005). For Ponis and Koronis (2012), who reassess the ecological foundations of the concept, resilience is not only about restarting the production line, but how firms may learn from disruptions and reorganize. This view joins the broader business strategy literature, in which, as proposed by Hamel and Välikangas (2003), resilience is the capacity for continuous reconstruction in a fast changing environment. This view of resilience recognizes the possibility of sudden and abrupt changes, and that firms alone cannot fully control their supply chain. This 'limit of control' connects to the idea of a systemic risk.

2.3 Systemic risks and the limits of risk mitigation

For some supply chain managers, even with mitigating efforts, a low-probability hazard will inevitably occur, unexpectedly propagate and generate losses. This share of risks is often called 'systemic'. To many, **systemic risk** conveys the idea of a small event creating unexpectedly large consequences. It recalls the image that popularized the mathematical concept of chaos: a butterfly flapping its wings in one part of the world can create a hurricane in another. However, while chaos may emerge in very small systems, systemic risks arise precisely because systems are complex and highly connected (Helbing, 2009).

In the context of supply chains, the World Economic Forum (2012) defines a risk as systemic when it has the three following property: it is triggered by an unexpected event, it propagates and induces ripple effects, and it gets amplified because of the inability of the network structure to absorb it. This definition emphasizes the role of the network structures and implies that some structures are more prone to risk propagation than others. From an economic standpoint, Lorenz et al. (2009, p. 441) defines systemic risk "as an undesired externality arising from the strategic interaction of the agents". It is an externality, what individual firms cannot do about.

This perspective connects with two other networked systems where systemic risks are a prominent issue: power grids and financial systems. In these networks, systemic risks are also what the individual node — electricity consumers and power stations in the first case, banks and financial firms in the second — cannot manage alone. In power grids, a systemic risk is the potential occurrence of a sizeable and unexpected blackout resulting from a small perturbation or a minor reconfiguration of the grid. The concept of systemic risks is most used in finance, and is a central concern for central banks (National Research Council of the National Academies, 2007)[9]. As experienced in many financial crises, strong interlinkages between banks and other players make the system prone to domino effects and bankruptcy chains. Contagion risks are well illustrated by the 2007 subprime mortgage crisis, which paved the way to the largest financial crisis since the 1930s. Information of systemic risks in power grids, financial systems and supply chains are summarized in Tab. 2.1.

Table 2.1: Three domains concerned with systemic risks

Domain	Power grid	Financial system	Supply chains
Nodes of the network	Power plants, lines and substations	Banks, funds and firms	Non financial firms
Agent managing systemic risk	Transmission network operators	Central banks	Insurers?
Examples of trigger events	Disconnection of a line	Misevaluation of an asset	Accident in a facility
Propagation mechanisms	Load redistribution	Financial interdependence	Supply disruption
Amplification mechanisms	—	Herding behavior	Bullwhip effect
Consequences	Blackout	Bankruptcy chain	Economic output loss

[9]This report is based on the conference *New Directions for Understanding Systemic Risk* organized in 2006 by the US National Academy of Science and the Federal Reserve Bank of New York. It was published in 2007, a few months before the 2007–2009 financial crisis, and presciently starts with the following words: "guarding against systemic risk in the financial system is a key undertaking for central banks". Interestingly, ecologists and engineers were invited to this conference, in addition to economists, regulators and financial professionals, illustrating that an interdisciplinary stances may help understand the complex mechanisms that underpin systemic risks.

Supply chains differ in that no organization is supposed to tackle systemic risks. Central bankers play this role for the financial system, although they only manage parts of the global system. Power grids are managed by transmission system operators, which are either public or heavily regulated.

Increasingly, firms are asking insurers to cover the economic loss generated by supply chain disruptions (Allianz, 2012). Insurers, and especially reinsurers, might therefore be the organizations that will have to deal with system risks in the global production system. This transfer of risk is highly challenging to insurers, because of the difficulty to evaluate the contribution of a particular firm to supply chain risks (Munsch, 2013). With fragmentation and high connectivity of the production system, double counts and misevaluation of potential damages triggered by one event are likely.

Systemic risks are indeed tricky to manage. The frequency and magnitude of blackout have not decreased through time in the USA (Hines et al., 2008), neither have financial crises at the global level (Reinhart and Rogoff, 2008). In this context, the word resilience is often used as an antonym of systemic risks. Insurers, as central bankers and transmission operators, are in high demand to better understand the role of the network structure on systemic risks (Munsch, 2013). Newly developed tools to carry out such investigation will be presented in the next chapter.

Conclusion

Driven by competitive pressures, production systems are becoming more globalized, fragmented and vertically specialized. Consequently, localized disruptions may propagate through supply chains and create considerable economic losses. For firms, such risks are difficult to mitigate, because they often lack visibility over their supply chain, and coordinating with other firms can be particularly challenging.

In the business management literature, frameworks have been proposed to deal with supply chain risks, and many of them refer to engineering resilience as the goal: resume activity as quick as possible. However, competition has streamlined supply chains, especially through inventory reduction and more concentrated supply base. Another aspect of resilience, called agility, is then put forward. By being responsive, and by resuming operations quicker than a competitor, firms may also gain market shares.

This capability also connects with a wider understanding of resilience, which connects to the concept of adaptive resilience presented in Sec. 1.2.3: the ability to reorganize, change internal structure to adapt to novel conditions. This view acknowledges the turbulence of the business world, and turns it into an opportunity to compete. It also acknowledges that some risks cannot be avoided, especially systemic risks.

Systemic risks are common to many networked systems, and are not yet well defined in the context of supply chains and production systems. They seem to emerge from the network structure and manifest through disruption cascades. They are also externalities — what managers cannot do about. This peculiarity of systemic risks thus suggests that firm-level decisions are not enough to manage the resilience of the whole economy. Articulating the micro-level of firms with the macroeconomic will be the key to design a conceptual framework of economic resilience.

References

Abe, M., Ye, L., 2013. Building Resilient Supply Chains against Natural Disasters: The Cases of Japan and Thailand. Global Business Review 14 (4), 567–586.

Allianz, 2012. Managing disruptions: Supply chain risk: an insurer's perspective. Tech. rep., Allianz Global Corporate & Specialty, Munich.

Baldwin, R., Lopez-Gonzalez, J., 2015. Supply-chain Trade: A Portrait of Global Patterns and Several Testable Hypotheses. The World Economy 38 (11), 1682–1721.

Barrot, J.-N., Sauvagnat, J., 2016. Input Specificity and the Propagation of Idiosyncratic Shocks in Production Networks. The Quarterly Journal of Economics, qjw018.

BCI, 2014. Supply Chain Resilience 2014: An international survey to consider the origin, causes & consequences of supply chain disruption. Tech. rep., Business Continuity Institute, Caversham, UK.

Blackhurst, J., Craighead, C. W., Elkins, D., Handfield, R. B., 2005. An empirically derived agenda of critical research issues for managing supply-chain disruptions. International Journal of Production Research 43 (19), 4067–4081.

Chongvilaivan, A., 2012. Thailand's 2011 flooding: Its impact on direct exports and global supply chains. Tech. Rep. 113, ARTNeT Working Paper Series.

Chopra, S., Sodhi, M. S., 2004. Managing risk to avoid supply-chain breakdown. Mit Sloan Management Review 46 (1), 53–61.

Christopher, M., Peck, H., 2004. Building the Resilient Supply Chain. The International Journal of Logistics Management 15 (2), 1–14.

Cooper, M. C., Lambert, D. M., Pagh, J. D., 1997. Supply Chain Management: More Than a New Name for Logistics. The International Journal of Logistics Management 8 (1), 1–14.

Cozzolino, A., 2012. Humanitarian Logistics and Supply Chain Management. In: Humanitarian Logistics. Springer Berlin Heidelberg, Berlin, Heidelberg, pp. 5–16.

Das, A., Handfield, R. B., 1997. Just-in-time and logistics in global sourcing: an empirical study. International Journal of Physical Distribution & Logistics Management 27 (3/4), 244–259.

Enkawa, T., Schvaneveldt, S. J., 2001. Just-in-Time, Lean Production, and Complementary Paradigms. In: Salvendy, G. (Ed.), Handbook of Industrial Engineering. John Wiley & Sons, Inc., pp. 544–561.

Fujimoto, T., 2011. Supply chain competitiveness and robustness: a lesson from the 2011 Tohoku earthquake and supply chain "virtual dualization". Manufacturing Management Research Center (MMRC) Discussion paper Series (362).

Ghil, M., Yiou, P., Hallegatte, S., Malamud, B. D., Naveau, P., Soloviev, A., Friederichs, P., Keilis-Borok, V., Kondrashov, D., Kossobokov, V., Mestre, O., Nicolis, C., Rust, H. W., Shebalin, P., Vrac, M., Witt, A., Zaliapin, I., 2011. Extreme events: dynamics, statistics and prediction. Nonlinear Processes in Geophysics 18 (3), 295–350.

Grubel, H. G., Lloyd, P. J., 1975. Intra-industry trade: the theory and measurement of international trade in differentiated products. John Wiley & Sons, New York.

Hamel, G., Välikangas, L., 2003. The quest for resilience. Harvard Business Review 81 (9), 52–63, 131.

Helbing, D., 2009. Systemic risks in society and economics. Tech. Rep. 2009-12-044, Santa Fe Institute, Santa Fe, NM.

Helleiner, G. K., 1981. Intra-Firm Trade and the Developing Countries. Springer.

Hendricks, K. B., Singhal, V. R., 2003. The effect of supply chain glitches on shareholder wealth. Journal of Operations Management 21 (5), 501–522.

Hendricks, K. B., Singhal, V. R., 2005. An Empirical Analysis of the Effect of Supply Chain Disruptions on Long-Run Stock Price Performance and Equity Risk of the Firm. Production and Operations Management 14 (1), 35–52.

Hines, P., Apt, J., Talukdar, S., 2008. Trends in the history of large blackouts in the United States. In: 2008 IEEE Power and Energy Society General Meeting - Conversion and Delivery of Electrical Energy in the 21st Century. pp. 1–8.

Hummels, D., Ishii, J., Yi, K.-M., 2001. The nature and growth of vertical specialization in world trade. Journal of International Economics 54 (1), 75–96.

Hummels, D. L., Rapoport, D., Yi, K.-M., 1998. Vertical specialization and the changing nature of world trade. Economic Policy Review (Jun), 79–99.

Jones, R., Kierzkowski, H., Lurong, C., 2005. What does evidence tell us about fragmentation and outsourcing? International Review of Economics & Finance 14 (3), 305–316.

Jüttner, U., Peck, H., Christopher, M., 2003. Supply chain risk management: outlining an agenda for future research. International Journal of Logistics Research and Applications 6 (4), 197–210.

Kaminski, B., Ng, F., 2005. Production disintegration and integration of Central Europe into global markets. International Review of Economics & Finance 14 (3), 377–390.

Lee, H. L., Padmanabhan, V., Whang, S., 1997. The Bullwhip Effect in Supply Chains. Sloan Management Review 38 (3), 93–102.

Lorenz, J., Battiston, S., Schweitzer, F., 2009. Systemic risk in a unifying framework for cascading processes on networks. The European Physical Journal B 71 (4), 441–460.

Manuj, I., Mentzer, J. T., 2008. Global supply chain risk management strategies. International Journal of Physical Distribution & Logistics Management 38 (3), 192–223.

Mentzer, J. T., DeWitt, W., Keebler, J. S., Min, S., Nix, N. W., Smith, C. D., Zacharia, Z. G., 2001. Defining supply chain management. Journal of Business logistics 22 (2), 1–25.

Munsch, W., 2013. La supply chain est-elle encore assurable? Banque & Stratégie: cahier de prospective bancaire & financière 319 (ENASS paper 6), 16–19.

National Research Council of the National Academies, 2007. New directions for understanding systemic risk: a report on a Conference Cosponsored by the Federal Reserve Bank of New York and the National Academy of Sciences. Tech. rep., Federal Reserve Bank of New York, National Research Council, Washington, DC.

Nishiguchi, T., Beaudet, A., 1998. The Toyota Group and the Aisin Fire. Sloan Management Review 40 (1), 49–59.

Norrman, A., Jansson, U., 2004. Ericsson's proactive supply chain risk management approach after a serious sub-supplier accident. International Journal of Physical Distribution & Logistics Management 34 (5), 434–456.

Norrman, A., Lindroth, R., 2004. Categorization of supply chain risk and risk management. In: Brindley, C. (Ed.), Supply chain risk. Transport Systems and Logistics. Ashgate, Farnham, pp. 14–27.

Osadchiy, N., Gaur, V., Udenio, M., 2016. Evolution of Supply Networks.

Ponis, S. T., Koronis, E., 2012. Supply Chain Resilience: Definition Of Concept And Its Formative Elements. Journal of Applied Business Research 28 (5), 921–929.

Reinhart, C. M., Rogoff, K. S., 2008. This time is different: A panoramic view of eight centuries of financial crises. Tech. rep., National Bureau of Economic Research.

Sheffi, Y., 2005. The Resilient Enterprise: Overcoming Vulnerability for Competitive Advantage. MIT Press, Cambridge, MA.

Snyder, L. V., Atan, Z., Peng, P., Rong, Y., Schmitt, A. J., Sinsoysal, B., 2016. OR/MS models for supply chain disruptions: A review. IIE Transactions 48 (2), 89–109.

Stecke, K. E., Kumar, S., 2009. Sources of Supply Chain Disruptions, Factors That Breed Vulnerability, and Mitigating Strategies. Journal of Marketing Channels 16 (3), 193–226.

Sterman, J. D., 1989. Modeling Managerial Behavior: Misperceptions of Feedback in a Dynamic Decision Making Experiment. Management Science 35 (3), 321–339.

Swiss Re, 2014. Natural catastrophes and man-made disasters in 2013: large losses from floods and hail; Haiyan hits the Philippines. Tech. rep., Swiss Re, Zürich.

Swiss Re, 2016. Natural catastrophes and man-made disasters in 2015: Asia suffers substantial losses. Tech. rep., Swiss Re, Zürich.

Thun, J.-H., Hoenig, D., 2011. An empirical analysis of supply chain risk management in the German automotive industry. International Journal of Production Economics 131 (1), 242–249.

Tierney, K. J., 1997. Business Impacts of the Northridge Earthquake. Journal of Contingencies and Crisis Management 5 (2), 87–97.

Timmer, M., 2010. Measuring Global Value Chains with the WIOD (World Input-Output Database).

Todo, Y., Nakajima, K., Matous, P., 2013. How Do Supply Chain Networks Affect the Resilience of Firms to Natural Disasters? Evidence from the Great East Japan Earthquake. Tech. Rep. 13-E-028, Research Institute of Economy, Trade and Industry, Tokyo.

UNCTAD, 2013. Global value chains: investment and trade for development. Tech. rep., United Nations Conference on Trade and Development, New York.

Wang, Y. I., Li, J., Anupindi, R., 2015. Risky Suppliers or Risky Supply Chains? An Empirical Analysis of Sub-Tier Supply Network Structure on Firm Performance in the High-Tech Sector. Tech. Rep. No. 1297, University of Michigan, Ann Arbor, MI.

Wassenhove, L. N. V., 2005. Humanitarian aid logistics: supply chain management in high gear. Journal of the Operational Research Society 57 (5), 475–489.

World Economic Forum, 2012. New Models for Addressing Supply Chain and Transport Risk. Tech. rep., World Economic Forum.

WTO, 2013. World Trade Report 2013: Factors shaping the future of world trade. Tech. rep., World Trade Organization, Geneva.

WTO, 2016. World Trade Report 2016: Speeding up trade: benefits and challenges of implementing the wto trade facilitation agreement. Tech. rep., World Trade Organization, Geneva.

Yi, K.-M., 2003. Can Vertical Specialization Explain the Growth of World Trade? Journal of Political Economy 111 (1), 52–102.

Chapter 3

The modeling of production systems and their resilience

Contents

Introduction

Productions systems seem to internally amplify their vulnerability to external shocks. To make them more resilient, we should investigate such internal dynamics, and identify the critical processes that accentuate disruptions.

In this dissertation, we have chosen to tackle this challenge by means of theoretical models. To make a start, we need a modeling strategy. This chapter reviews a large set of tools and theories. We first discuss them in light of the empirical facts and the insider insights reported in Chapter 2. Next, we assess whether they can help us evaluate the three dimensions of resilience presented in Chapter 1 — engineering, ecological and adaptive resilience. The outcome of this analysis is the design of a conceptual framework that outlines our modeling strategy.

Specifically, Sec. 3.1 reviews the tools and data available for studying the ripple effects of natural disasters across firms and sectors. We also present insights from regional economists, who have discussed the use of resilience in economics. These considerations highlight the need to closely assess the kind of economic assumptions we aim to use in our models. To that end, we revisit in Sec. 3.2 different schools of thought and the perspectives they may or may not open on resilience. We try to identify the approach that can best articulate the role of firms, the propagation of disruptions, and resilience. We eventually present in Sec.3.3 the modeling framework.

The materials presented in the present chapter come from a review of the economic literature, in particular the theory of input–output, the general equilibrium theory, the economics of natural disasters, spatial economics, evolutionary economics, complexity economics and econophysics. We also benefited from discussions during workshops and seminars, in particular the Tenth Workshop on Economic Heterogeneous Interacting Agents (WEHIA) that was held in June 2015 in Sophia Antipolis, France.

3.1 Economic resilience and the challenge of interdependence

Mapping production interdependencies (Sec. 3.1.1) is the first necessary step towards the analysis of the ripple impacts of natural disasters (Sec. 3.1.2). We highlight that finer models are still lacking to capture the propagation of disruptions and systemic risks (Sec. 3.1.3). The differentiated responses of regions to disasters, but also to macroeconomic shocks, have motivated some economists to investigate economic resilience (Sec. 3.1.4).

3.1.1 Mapping the structure of production

As discussed in Chapter 2, what makes a production system particularly vulnerable to a localized disruption is that one produces what another needs. Mapping such interdependencies at the national scale was Leontief's key motivation when developing the theory of input–output tables (1936). Instead of describing the interactions between specific firms, this theory views the whole production system as a network of sectors[1]. Each sector is connected to others through financial flows, which correspond to exchanges of goods and services. Each flow is the output of one sector and the input of another. To balance the total amount of inputs consumed and of outputs produced, input–output tables also account for imports, exports, and household consumption.

Input–output tables meaningfully aggregate business census data collected by national administrations, and may help guide public policies. Leontief published the first tables of the U.S. economy for the year 1919 and 1929 with data from the U.S. National Bureau of Economic Research (Polenske, 2004)[2]. Since then, the methodology has been refined, standardized, and national statistics services of many countries now provide tables with 15 to 70 sectors[3].

Because of their high consistency, input–output tables are still nowadays the main empirical tool to assess how economies are structured. For instance, with a 426-sector table published by the U.S. Bureau of Economic Analysis for the year 2002, Xu et al. (2011) identified highly interconnected clusters of industries and pinpointed the sectors that play a pivotal role in bridging different part of the economy. International tables have been produced by interpolating national input–output data with trade records (Timmer et al., 2015); they have enabled Baldwin and Lopez-Gonzalez (2015) to follow over time the

[1]This view of the economy was inspired by *Les Tableaux Economiques* of Quesnay (1766), who analyzed in the 18th century the dependence of the French economy on agricultural production.

[2]An anecdote reported by Polenske (2004) highlights the incredible progress of computational power that were achieved over the past century. After using punchcards for the 1919 and 1929 tables, Leontief used a computer from Harvard labs, which was taking 56 hours to invert a 42-sector matrix. The same calculation takes today less than a millisecond

[3]In France, INSEE provides tables with 17 or 38 sectors. In the US, the Bureau of Economic Analysis provides tables with 15 or 71 sectors, and roughly every five years, 389 sectors.

unfolding of vertical specialization; see Sec. 2.1.1. The recent development of subnational tables opens novel perspectives for even finer analyses (Ploszaj et al., 2015).

3.1.2 Evaluating the economic impacts of a disaster

Natural disasters reveal the amplifying effect induce by such input–output interlinkages (Cochrane, 2004; Okuyama, 2007). Calibrated with regional tables, models have been developed to evaluate their costs.

The first approach uses a class of static models called computable general equilibrium (CGE). The pre-disaster economy is assumed to be at equilibrium: on all markets, supply equals demand. Because some facilities are hit by the disaster, some goods or services become undersupplied. In this post-disaster situation, CGEs compute the simultaneous adjustment of prices, purchase plans and production processes that lead the economy to a new equilibrium[4]. These models generally assume a certain degree of substitutability between production inputs, and are calibrated using input–output data. CGEs have been for instance used to anticipate the potential consequences of the disruption of a water utility in Portland (Rose and Liao, 2005) or the breakdown of the Los Angeles power grid (Rose et al., 2007).

From an economic standpoint, these models represent the best possible response of an economy: prices perfectly capture the availability of goods and services, firms and households make the most informed and rational decisions. These models do not describe the dynamic process whereby the economy moves from pre- to post-disaster equilibrium.

The empirical insights exposed in Chapter 2 suggest, however, that most disruptions occur precisely during this ‘out-of-equilibrium’ period: firms under or overreact, production facilities fall short of workers or of inputs, basic service providers cannot cope with the surge in demand, etc. These adjustments may be very quick, but other may be lasting. According to Hallegatte (2014a), after hurricane Katrina hit New Orleans in 2005, the lack of housing and of health care services hindered the return of workers, and thereby the restart of the economy.

For these reasons, CGEs underestimate actual costs (Rose and Liao, 2005). But they also show how an effective price mechanism may facilitate economic recovery. We may assume, in contrast, that no economic adjustment takes place at all. This approach could in turn overestimate the costs, but may well apply for short-term costs. Regional input–output tables can then be readily used to assess how the loss of production in one sector affects all others. No price changes and firms do not substitute any input[5].

[4]A representative household adjusts its consumption basket to maximize a utility function given budget constraints. Each sector is represented by a single firm that maximizes profit given budget and technological constraints. The technology is typically captured by ‘constant elasticity of substitution’ (CES) production functions, such as the Cobb-Douglas function. Impacts on import and export may also be modeled.

[5]As in CGEs, each sector is modeled by a single firm, but its production technology is represented by a Leontief production function.

Based on simple matrix calculation, this approach also benefits from the large availability of input–output data. It has been adapted into many modeling frameworks(e.g., Haimes and Jiang, 2001; Santos and Haimes, 2004; Steenge and Bockarjova, 2007). It was used for instance by Brookshire et al. (1997) to assess the potential cost of earthquake hitting the Boston metropolitan area. More realistic versions include inventories and further technical details on production processes, and model how these quantities change in time during and after the disaster (e.g., Okuyama, 2004; Santos, 2006)[6]. The adaptive regional input–output (ARIO) model of Hallegatte (2008, 2014c) captures both the rigidity of some processes with the adaptive response of others. ARIO has been applied to hurricane Katrina (Hallegatte, 2008), to the Wenchuan earthquake (Wu et al., 2011), and to assess the potential impacts of flooding in Copenhagen and Mumbai (Hallegatte et al., 2010; Ranger et al., 2011).

This modeling of disaster impacts has provided general insights on the propagation of risks through the production system. First, when interdependent activities are simultaneously disrupted, the losses are nonlinearly amplified. Consequently, when disasters get more intense, indirect costs tend to grow quicker than direct costs. These insights matches the anecdotal evidences on supply chain disruptions presented in Sec. 2.1.2.

Next, the level of aggregation used in these models does matter. When sectors are represented by multiple heterogeneous firms instead of a single agent, the models indicate higher impacts (Henriet et al., 2012; Hallegatte, 2014c). These observations suggest that an explicit representation of input–output interlinkages at the firm-level may be necessary to identify the vulnerable points in production systems, and thereby uncovering systemic risks.

3.1.3 Analyzing systemic risks through networks

The sectoral aggregation of input–output tables prevents us to capture the fine grained structure of production systems. This limitation has been recently overcome, and some researchers have managed to reconstruct, from different firm-level data sets, a significant part of the Japanese production network[7], and a small part of the U.S. one[8]. Although

[6] Many dynamic input–output models are based on the so-called sequential interindustry model (SIM) of Romanoff and Levine (1981, 1986). SIM's purpose is to bring an engineering vision to the input-output tables. It encompasses a wide class of models to represent production scheduling, inventories, production capacity, etc.

[7] Two private databases were investigated. Both are built and maintained by private companies, which were originally credit rating agencies: Tokyo Shoko Research and Teikoku Databank. Both databases list the suppliers and customers of about a million firms, and cover about half of the Japanese economy.

[8] In the U.S., public firms — that means publicly traded firm, the equivalent of the French 'societé anonyme' — have to disclose several information to the Securities and Exchange Commission (SEC). Under the rule No. 131 of the Statement of Financial Accounting Standards, they have to disclose the names of any customer representing more than 10% of the yearly sales. These data are publicly available directly from the SEC, or through various private databases: CompuStat, Mergent Horizon, Bloomberg. The latter enrich these public data with additional information on suppliers and customers. In 2015 there were about 3,700 public firms in the U.S.

these databases do not quantify the financial flows between firms, they have enabled a fine topological characterization of these networks (Saito et al., 2007; Ohnishi et al., 2009, 2010; Fujiwara and Aoyama, 2010; Atalay et al., 2011). In addition, it has been possible to link these structural features with the actual locations of firms (Bernard et al., 2014), and with their dynamics of growth and bankruptcies (Fujiwara and Aoyama, 2010; Mizuno et al., 2014).

These data sets open the opportunity to research statistical regularities in the structure of supply chains (Osadchiy et al., 2016) and the propagation of disruptions (Barrot and Sauvagnat, 2016)[9]. In particular, they provide an empirical basis to investigate systemic risks through network modeling.

To that end, we may tap into the toolbox of graph theory. For systemic risks, this theory primarily analyzes how generic classes of network break into pieces when some nodes or links are removed (Albert et al., 2000; Callaway et al., 2000; Cohen et al., 2000, 2001). In production system, however, systemic risks result from a dynamical process, whereby disruptions propagate from one firm to another. In its most simple form, it is a process of contagion (Watts, 2002; Dodds and Watts, 2004), which applies to cultural phenomenon, diseases and of computer viruses (May and Lloyd, 2001; Newman, 2002). Findings from these studies provide some insights for production systems, such as the amplifying role of hubs.

For production systems, most models have focused on simple network structure. Using a lattice and an explicit modeling of inventories, Bak et al. (1993) and Scheinkman and Woodford (1994) have shown that the occurrence of disruption cascades is a very generic phenomenon in production systems[10]. Similar models have investigated the emergence of the bullwhip effect (Helbing et al., 2004; Lee et al., 2004). In operation research, modeling frameworks for disruption propagation have been proposed (Wu et al., 2007). They focus on simple supply chains and aim at a detailed modeling of the production and management processes, building on the field the industrial dynamics (Forrester, 1961; Towill, 1996).

Cascading failure in power grids and financial systems is easier to study. When an electric substation breaks down, the electric load it was carrying is redistributed to other nodes; some of them may receive a load that is larger than what they can stand, thus triggering new failures (Crucitti et al., 2004; Zhao et al., 2004; Wang and Rong, 2011). If a bank defaults, its liabilities — which are the asset of other banks — are written off, which may precipitate new defaults (May and Arinaminpathy, 2010; Haldane and May, 2011; Battiston et al., 2012b,a). In both cases, this process involves a redistribution of burden[11].

[9] The results of these two studies have been presented in Secs. 2.1.1, 2.1.2 and 2.2.2.

[10] These researchers uncovered a few years before the mechanisms behind the avalanches of sand piles, called self-organized criticality (SOC) (Bak and Chen, 1991). With this economic model, they have demonstrated that, to a certain extent, disruption cascades may be interpreted the same way.

[11] Lorenz et al. (2009) has recently showed that a modeling framework can account for both contagion and load redistribution processes(see also Tessone et al., 2013).

This financial domino effect has been also studied for supply chains, since suppliers and customers are also financially interdependent[12], (Battiston et al., 2007; Delli Gatti et al., 2009b), and Fujiwara (2008); Fujiwara and Aoyama (2010) could track such chains of bankruptcy in the Japanese production system.

With the exception of Weisbuch and Battiston (2007), Coluzzi et al. (2011) and Henriet et al. (2012), no model has yet tackled the cascade of supply disruptions and their potential systemic impact. Building on Coluzzi et al. (2011), our second paper fills this gap, using the recent empirical results on real production networks.

Such models tend however to overemphasize the importance of the network structure. This structure is not that rigid, and whether a disruption propagates also depends on the capacity of firms to find new suppliers.

3.1.4 Economic resilience of regions

The propagation of disruptions plays a crucial role in increasing vulnerability, and amplifying shocks. But the resilience of an economy depends on many more factors than the production structure.

For Rose (2007), economic resilience may be observed both during a disaster — how functional does the economy remain — and after — how it bounces back. From an economic perspective, the first aspect is determined by the efficient allocation of available resources, the second by the reinvestment pattern for reconstruction and the restart of activities. As done in the field of disaster risk reduction, presented in Sec. 1.3.1, economists aims to identify pre-disaster conditions that foster these two aspects, such as the financial resources of households, the quality of the infrastructure, the access to wider markets, and firm-level features that are common with the management literature on supply chain risks presented in Sec. 2.2.1. Significant efforts have been dedicated to build resilience indexes from these factors, which proved to be very challenging (see reviews by Rose and Krausmann, 2013; Modica and Reggiani, 2015).

Many economists actually study resilience through a wider class of shocks, and aim, for instance, to understand the differentiated responses of regions to a macroeconomic shock, such as recession. For instance, Martin (2012) investigates why the Greater London area and the South West region of England were more affected by the early 1990s recession than northern regions, and why they recovered quicker afterwards. There, the question of resilience connects to preexisting inquiries on regional innovation systems or regional competitiveness, and focuses more largely on economic and institutional structures.

[12] A creditor-debtor relationship necessarily settles between a supplier and a customer. When the buyer pays after the delivery of its command, it means that the supplier had financed the production costs. In the time period between production and the payment, the supplier is a creditor and the customer a debtor. On the other hand, if the customer pays upfront, until he receives its command it is a creditor and the supplier a debtor.

Resilience also invites economists to investigate the longer-term response of economy to shocks, and how it may become more or less resilient over time. Actually, whether disasters can have a positive impact on long-term growth remains a debated issue (Jaramillo, 2009; Hallegatte, 2014b). For Christopherson et al. (2010), the way to approach these questions depends on the underlying assumption made on the economic equilibrium. First, we may assume, as in Fig. 3.1(a), that there is a unique growth trajectory to which the post-disaster region will eventually return, then 'engineering resilience' is the adequate standpoint. Shocks are only delaying growth and what matters is the speed and efficiency of the recovery. Alternatively, we may consider multiple dynamical attractors, in which case a shock could push a region into another growth pathway. This view directly connects to the ecological or adaptive resilience standpoint, cf. Figs. 3.1(b)–(c).

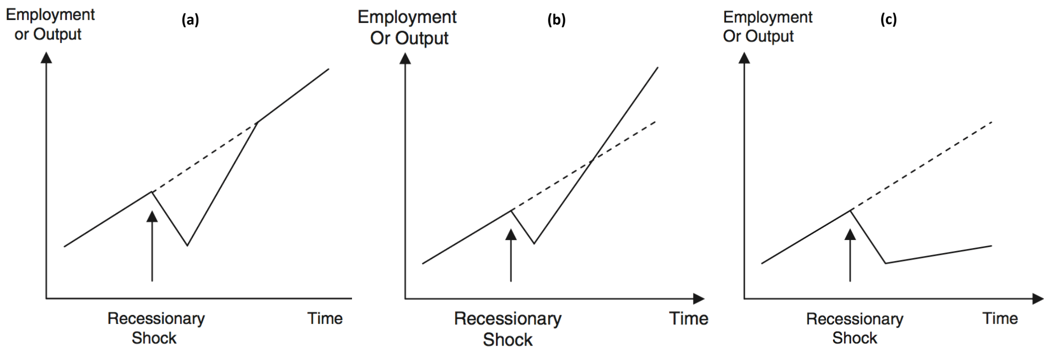

Figure 3.1: Hypothetical trajectories of economic output or employment in a region affected by a recessionary shock, published by Martin (2012). **(a)** Assuming the existence of a unique economic equilibrium, the region returns to the pre-shock growth trajectory. **(b)** and **(c)**: The shock leads to lasting negative or positive effects on the growth rate, suggesting that the economy has reorganized into a structurally different state.

Several authors from the fields of economic geography and spatial economics argue that economic resilience is conceptually richer in the second view (Christopherson et al., 2010; Simmie and Martin, 2010). This approach is also closer to the Holling's definition of resilience (1973). Shocks do not only deviate an economy from a fundamental trend, they may also spark profound changes and generate new development pathways. A prototypical example of such shock-induced redirection is that of Reunion and Mauritius islands in the early 19$^{\text{th}}$ century. Following a series of intense cyclones in 1806 and 1807, authorities decided to shift the entire agriculture from coffee to sugar cane, a radical change that may have had important impacts on the economic development of these islands (Garnier and Desarthe, 2013).

Tor these authors, reorientation and renewal are crucial to resilience. They are related to context-specific learning mechanisms, governance flexibility and civic capital (Pike et al., 2010; Wolfe, 2010; Martin, 2012). We note that these factors are close to those researched in the field of socio-ecological systems described in Sec. 1.2.1. To study the nonlinear trajectories of economies, these authors propose to adopt the framework of evolutionary economics (Dosi and Nelson, 1994). This branch of economics, which connects to the theory of complex adaptive systems described in Sec.1.2.2, acknowledges that path dependency, lock-in and hysteresis may occur. These theories will be useful to design our conceptual framework.

The conceptual richness of resilience, explored in Chapter 1, has been integrated in this branch of economics. The question of economic equilibrium seems particularly central to develop a conceptual framework on economic resilience. As for economic models, they tend to focus on the engineering aspects of resilience, and revolve around the following question: how quickly and how well does an economy recover from a shock. In fact, providing a robust answer to it is already very challenging. The usual approaches — whether CGEs or input–output models — rely on a level of aggregation in which disruptions are hard to track.

3.2 Where does resilience fit in economic models?

We aim to design models that capture the network structure of production systems, but that at the same time do not dwarf the role of firms. They should also allow us to investigate dynamical processes and bifurcations. We now need to identify the adequate economic assumptions.

The first question to be tackled is the status of equilibrium in economics. This notion is intrinsically linked with the assumptions made by the modelers on agent behavior. Different views may be taken, leading to important controversies between economic schools of thought (Sec. 3.2.1). Although many economic models are based on equilibrium conditions, there are many macroeconomic dynamic models in which resilience can be readily studied (Sec. 3.2.2). To capture the vulnerability of production systems, however, we need to fully account for the micro-level of firms and their interactions. We may study resilience from the 'bottom up' using agent-based modeling (Sec. 3.2.3). Since the network structure is so influential in driving resilience, we may use fairly simple, 'zero-intelligence', representation of firms, and gradually detail their behavior (Sec. 3.2.4).

3.2.1 Is resilience heterodox?

Resilience does not fit naturally within classical economic theory. As mentioned throughout Sec. 3.1, many models focus on equilibrium conditions. Bringing ecological resilience into economics could thus be seen as an attempt to provoke a paradigmatic change, as Holling (1973) did in ecology; see Sec. 1.1.1. In fact, such discussions have been ongoing for decades in economics, and the concept of equilibrium is one of the many debates in the antagonistic dispute between orthodox and heterodox economics. Without getting bogged down in these controversies[13], we will clarify the relationships between economic equilibrium and our proposal for a modeling of economic resilience.

The main obstacles that prevent us from applying the ecological approach of Chapter 1 are: (i) the forward-looking behavior of humans, and, connected to that, (ii) the normative implications of economic theories. While dynamic models in natural sciences can be expressed, for instance, as a dynamic map, where the future derives from the past (e.g., $x_{t+1} = f(x_t)$), most economic inquiries start the other way around, and investigate what could be the present decisions of agents given their expectations for the future (e.g., $x_t = f(x_{t+1})$). To reduce this almost infinite set of possible choices, economic theories generally focus on what agents 'should' do, given precise assumptions about their behavior and expectations. Classical economics focus on self-interested, fully rational and often omniscient individuals, while other fields investigating in human decisions may choose other assumptions.

[13]See Lavoie (2014, Chap. 1) for an overview of the different school of thoughts and of some aspect of the orthodox–heterodox dispute, from a Post-Keynesian, i.e. heterodox, perspective.

Economic equilibrium then describes the state of an economy when all agents do what they are supposed to do. The field of game theory has specialized in analyzing such equilibria. Because it focuses on the 'should do', such description has normative implications. In fact, economic theories sometimes generate interesting self-fulfilling phenomena. As pointed out by Farmer and Geanakoplos (2009), equilibrium-based models on the pricing of financial assets make accurate predictions once traders start to use them.

With these assumptions, the so-called general equilibrium theory aims to determine the set of prices that balance supply and demand for all markets of an economy composed of a multitude of agents. This theory has developed through the determination of the necessary conditions of existence, uniqueness, efficiency and finally stability of the equilibrium (Arrow and Debreu, 1954; Arrow, 1966).

However, the Sonnenschein–Mantel–Debreu theorem (e.g., Sonnenschein, 1973) demonstrates that, under general conditions, the economic equilibrium is neither unique nor stable. Albeit this result, which, to many, should have marked the end of equilibrium theories (e.g., Kirman, 1989; Ackerman, 2002), equilibrium-based models, such as CGEs, are still widely used. Instead of representing a multitude of agents, these models are based on the assumption of a 'representative agent' — one agent represents all households, one firm represents all firms in a sector, etc. — which enables the derivation of a single equilibrium. However, because of the absence of any out-of-equilibrium dynamics, these models miss processes that generate economic vulnerability, as discussed in Sec. 3.1.2.

The modeling of out-of-equilibrium behaviors has been an ongoing debate since the 19$^{\text{th}}$ century. It sparked a controversy between Walras, who produced the first complete version of the general equilibrium theory, and Edgeworth (Walker, 1987). For Walras, his theory had to explain how the equilibrium could be reached; to that end, he provided an out-of-equilibrium mechanism called tatonnement[14]. Edgeworth vividly rejected this. For him, only equilibrium can be known: the dynamics leading to it cannot be analyzed and is 'not part of the domain of the science' (Edgeworth, 1891, cited by Walker, 1987).

That economics should not deal with out-of-equilibrium processes is still a dominant view in orthodox economics. Even though the general equilibrium theory of Walras has set the bases of neoclassical economics, his view on dynamics has inspired a large body of works, especially in heterodox schools of thought, in which resilience seems to fit more naturally.

3.2.2 Economic dynamics

In fact, in parallel to equilibrium-based models, many economists have developed dynamic models in which bifurcations and basins of attraction may be analyzed. The tatonnement

[14]In the tatonnement process, the equilibrium is reached in a market through simultaneous auctions. Given an initial price, agents adjust their production and purchase plans, which are aggregated by an auctioneer and lead to a new price. This mechanism is iterated until the equilibrium prices are reached.

process has been studied using differential equations (Samuelson, 1941), as well as a large set of other out-of-equilibrium processes. These dynamical studies have shown that the equilibrium may be unstable and can lead to limit cycles (Negishi, 1962; Heal, 1986). Alternative theories have been elaborated to describe decisions made by agents when markets are unbalanced, called ‘arbitrage’, and to analyze ‘disequilbirium dynamics’ (Fisher, 1989; Barnett et al., 1996).

In fact, endogenous dynamics appear to be quite general as soon as the assumptions of omniscience and unlimited cognitive capability — the ‘god-like powers’ in the words of Farmer and Geanakoplos (2009) — are released. These undertakings are supported by psychological experiments that have demonstrated that human decisions are generally contextual, based on heuristics (Gigerenzer and Brighton, 2009), and framed by values and beliefs (Kahneman and Tversky, 1979, 2000). The fields of experimental and behavioral economics have developed novel theories based on these empirical assessments[15] (e.g., Camerer et al., 2011).

This equilibrium-versus-dynamics debate has important implications for the understanding of economic fluctuations. In particular, business cycles — these ample and somewhat periodic ups and down of economic aggregates (Groth et al., 2015; Sella et al., 2016) — are either interpreted as endogenous or as exogenous phenomena. In the equilibrium-based approach (e.g., Kydland and Prescott, 1982; Long and Plosser, 1983), business cycles are the consequences of the most rational decisions of agents[16] in response to exogenous shocks — e.g., new technologies, new policies, natural disasters. For others, business cycles result from endogenous instabilities. A very wide range of dynamical models have been proposed, in which limit cycles may emerge from Keynesian accelerators and multipliers (Kalecki, 1937; Harrod, 1939; Samuelson, 1939), from inertia and delays (e.g., Hallegatte et al., 2008), etc. Even with the assumptions of balanced markets and optimal forward-looking behavior, business cycles and chaotic trajectories may endogenously occur (e.g., Benhabib and Nishimura, 1979; Day, 1983; Baumol and Benhabib, 1989).

In macroeconomic dynamic models, which are now fairly developed (see for instance the textbook of Shone, 2002), we can use the theory of dynamical systems to study resilience. In particular, we note that the model proposed by Goodwin (1967), is made of a system of differential equations that is of the same class as the Lotka–Voltera predator–prey model used by Holling (1973). Investigating resilience in such models has not been undertaken yet, and we argue that tackling the following questions can lead to interesting studies: how external shocks may change the features of business cycles? Which macroeconomic processes may abruptly shift the dynamical regime?

[15] In particular, alternative models have been proposed to describe the forward-looking behavior of human beings. One of them is the heterogeneous expectation model (Brock and Hommes, 1997; Hommes, 2011), which, when implemented in economic models, leads to complex dynamical behavior. With this type of expectations, for instance, a higher use of *apriori* stabilizing financial instruments, such as hedging, can destabilize markets (Brock et al., 2009).

[16] These decisions concern how they plan to allocate money (the consumption–investment trade-off) and time (the labor–leisure trade-off) between the present and the end of their time horizon.

These models adopt, however, a macroeconomic standpoint, and encode dynamical relationships between economic aggregates, e.g., growth domestic product, investment, savings. Although analyzing resilience in these models may be of high interest, the degree of aggregation is not adapted to capture the vulnerability of production system described in Chapter 2. In particular, the propagation of disruptions and the indirect impacts of shock seem to be better captured by an explicit modeling of firms, as discussed in Sec. 3.1.

3.2.3 Resilience from the bottom up

Representing an aggregate property, such as resilience, from the modeling of economic agents connects to another fierce orthodox–heterodox debate on the 'microfoundation of macroeconomic behavior' (Kirman, 1992). As explained in Sec. 3.2.1, many equilibrium-based models represent a multitude of individuals or firms by a single agent who is also fully rational, omniscient etc. Many authors have been highlighted the weaknesses of this aggregation procedure, especially Kirman (1992). As soon as agents interact, a group does not behave like its average member, even when everyone is fully rational (Bouchaud, 2013). This absence of direct correspondence between the micro and the macro level is even more pronounced when the system is structured, as in production networks. In supply chains, tor instance, the bullwhip effect emerges spontaneously, even in small and linear structures and even if all firms act rationally (Lee et al., 2004).

In addition, the distributions of firms' size, income, number of suppliers and customers are highly unbalanced and exhibit fat tails (Axtell, 2001; Okuyama et al., 1999; Fujiwara and Aoyama, 2010). Averaging these characteristics to form a representative agent may thus be inappropriate. The importance of these heterogeneities in driving macroeconomic variables has been recently underlined even in equilibrium-based models (Gabaix, 2011; Acemoglu et al., 2012).

Providing an alternative to the representative agent is the key motivation behind **agent-based modeling** (ABM) (Gallegati and Kirman, 2012). ABMs are made of multiple autonomous agents, with internal and possibly heterogeneous rules on how they behave and interact with each others. Methods from statistical physics may be used to analytically aggregate this ensemble of behavior (Durlauf, 1997). The field of econophysics has specialized in applying such methods to economics, in particular to the study of financial time series. In addition, through the physical concept of phase transition, econophysicists have explored potential sudden changes of the qualitative structure of an economy (e.g., Bardoscia et al., 2015). We however note that, so far, detecting bifurcations in ABMs — a crucial step in the analysis of resilience — has hardly been tried, and remains to be tested. Our first paper tackles this gap (Chapter 4).

Through ABM, scientists may analyze the emergence of macro-level behavior and structures from the 'bottom up' (Simon, 1962; Schelling, 1978; Epstein and Axtell, 1996). They can then try to determine the kinds of agent-level behavior that lead to patterns observed in empirical data, often called 'stylized facts' (e.g., Delli Gatti et al., 2007). For instance, Mandel (2012) have designed an ABM to assess the emergence of multiple general equilibria, and to analyze whether the economy may shift from one equilibrium to another.

For production systems, the flexibility of ABMs may thus be harnessed to study how production networks emerge from the firm decisions. Game theory already provided results for the formation of innovation and social networks (Goyal, 2007), however the focus on fully rational and anticipating agents has somewhat limited its application to production systems. In the ABM of Gualdi and Mandel (2015), instead, a network emerges from the bottom up; it reproduces some features of real production systems, such as their scale-free topology. The longer-term evolution of a production system and their resilience may thus be modeled with this technique.

3.2.4 Rational versus 'zero intelligence' agents in structured systems

Which behavior should we then encode in our ABMs? The discussion on economic equilibrium in Sec. 3.2.1 highlights that the specificity of economic modeling — the rationality of agents and their expectation — needs a carefully assessment (Westley et al., 2002)[17]. Which alternative assumptions on rationality and expectation should we make for firms operating in interconnected production systems?

As seen in Chapter 2, production systems are highly structured. They are made of multiple specialized firms connected through long and intricate supply chains. As done in the various models presented in Sec. 3.1, production systems can be represented as a network. Although its topology is not fixed, it strongly constrains the actions undertaken by firms in the short term, especially in the event of a disruption. Small fluctuations may thus amplify as it ripples through the production network, as explained in Sec. 2.2.1. There are increasing empirical evidences that this amplification drives a sizeable portion of macroeconomic volatility (Foerster et al., 2011; Atalay, 2014; di Giovanni et al., 2014)[18].

To study how the network structure affects the aggregate dynamics, Farmer and Geanakoplos (2009) argue that the assumptions of perfectly rational and anticipating agents may be usefully released. They illustrate this approach with the examples of crowd dynamics and road traffic. Whatever the subtle assumptions we may think of for the

[17] In the context of SES modeling, Westley et al. (2002) warn that the absence of such considerations can negatively impact the interdisciplinary discussions on models made by natural scientists on socio-economic systems. They take as an example the report *Limits to Growth* by Meadows et al. (1972). It encountered fierce critics within the economic community, and still remains nowadays somewhat controversial, although the business-as-usual scenario of their model compares favorably with the data (Turner, 2008).

[18] Foerster et al. (2011) show that sectoral shocks are increasingly driving economy-wide fluctuations through shock propagation via input–output linkages between sectors. Atalay (2014) refines this analysis by showing that this effect is amplified when substitutability is low. di Giovanni et al. (2014) perform a similar analysis using more detailed data, and show that input–output relationships drive three times more macroeconomic fluctuations than firm-level shocks.

behavior and expectation of each driver, traffic is mostly determined by the road network[19]. Such systems may thus be effectively studied with simple behavioral assumptions.

This approach has been successfully applied to the study of financial markets. Financial time series exhibit some statistical regularities that indicate the presence of out-of-equilibrium dynamics, such as the power-law distributions of autocorrelation coefficients or transactions size (Lobato and Velasco, 2000; Bouchaud et al., 2006, 2009). ABMs with 'zero intelligence' traders have showed that many of these features were in fact related to the trading mechanisms, and not so much by the rationality of agents (Bouchaud et al., 2002; Farmer et al., 2005). The use of 'zero intelligence' firms might thus help us investigate the role of the network structure on resilience, at least over the time scale of disruption cascades.

We should not, however, dwarf the capacity of firms to react and manage disruptions, as well as their ability, in the longer run, to reorganize parts of their supply chain. Thanks to the flexibility of ABMs, we may thus gradually bring more rationality into the behavior of firms, and even allow them to act on the network structure.

[19]The dominance of the road structure over drivers' decisions is well illustrated by the so-called Braess's paradox (Braess, 1968): counterintuitively, the travel time of all road user may increase by the addition of new roads in the network, even assuming omniscience and full rationality.

3.3 Conclusion: A new conceptual framework for economic resilience

Economic resilience may be readily studied in a wide range of dynamic macroeconomic models. However, a large share of the vulnerability of production systems precisely comes from the micro-level. ABM represents a promising modeling paradigm to assess the link between agents' behavior and aggregate properties, such as resilience. We have identified that, because production systems are so structured, we may at first consider very simple behavioral rules for firms, and thereby isolate the effect of the network structure on resilience. More details may be added afterwards, using for instance the insights of operation research and business management, briefly exposed in Sec. 2.2 of Chapter 2. Finally, in the longer term, the production network is itself a result of the firm decisions.

In this section, we build a conceptual framework to articulate these feedback mechanisms across multiple scales. It will help us organize the pieces of knowledge reviewed in these three first chapters, and guide the formulation and interpretation of the models of our second and third papers (Chapters 5 and 6). The first paper (Chapter 4) will test the use ABM for resilience analysis.

We first explain how we intend to evaluate resilience in our models (Sec. 3.3.1). Next, we describe the conceptual framework (Sec. 3.3.2) and conclude by presenting our three papers (Sec. 3.3.3).

3.3.1 Evaluating resilience and systemic risks

We aim to design theoretical models for economic resilience. They will represent *in silico* artificial production systems made of interacting firms (Lane, 1993). We evaluate resilience by analyzing the responses of production systems to shocks, using a variety of analytical and statistical methods.

Table 3.1 summarizes the indicators[20] we intend to use and their associated mathematical objects. They correspond to the three main dimensions of resilience presented in Tab. 1.2 of Chapter 1. We have introduced a short and a long time scale. Adaptive resilience is evaluated by the long-term evolution of the short-term indicators. Through these metrics, we aim to analyze how some model ingredients affect resilience, e.g., how the probability of collapse varies with certain parameters.

From Tab. 1.2, we may now clarify the link between resilience and systemic risks. As discussed in Sec. 2.3, systemic risks are triggered by small events and have large consequences. They correspond to rather short time scale, i.e. to the first and second line of Tab. 1.2. From the engineering standpoint, systemic risk is the risk of disruption

[20]We emphasize that these indicators should not be equated to resilience, e.g., resilience is not the intensity of disruption cascades.

Table 3.1: Evaluating the three dimensions of resilience in theoretical models.

Dimension	Mathematical object	Indicators of resilience	Time scale
Engineering	Orbits	Intensity and duration of disruption cascades after shocks	Short
Ecological	Attractor basins and bifurcations	Shock intensity leading to a collapse, collapse probability given certain shocks, and how this change with parameters	Short
Adaptive	Evolutionary trajectories	Change over time of the measures of engineering and ecological resilience	Long

cascades, i.e. the expected loss due to disruption cascades. From the ecological standpoint, systemic risk is the risk of collapse, what Helbing and Balietti (2011) has called 'systemic shifts', e.g., for power grids, a large scale blackout. These two components of systemic risks will be investigated in our second paper.

Although this definition corresponds to most uses of the term, it seems to loosely encompass any network-related propagation of risks. In fact, as emphasized by Lorenz et al. (2009), and reported by managers, systemic risks are externalities: they are the shares of supply risks that firms cannot manage. We therefore define a risk as **purely systemic** if it occurs while all firms has mitigated their own supply risks. In other words, purely systemic risks are the risks of disruption cascades and of collapse that remain even though all firms have implemented their best possible 'resilient' strategy. As discussed in Sec. 2.2.2 of Chapter 2, many risk mitigation measures have to be balanced by competitive objectives. We hypothesize that stronger competitive pressures induce higher purely systemic risks. Our third paper will investigate this hypothesis. Because systemic risks are good indicators for short-term resilience, i.e. the first and second lines of Tab. 1.2, we may often refer to them in our papers.

3.3.2 Networks: a meso-level between agents and economic resilience

The conceptual framework, presented in Fig. 3.2, articulates three scales: firms at the micro-level, network of interaction at the meso-level, and the whole production system at the macro-level. Four links indicate interactions between these three scales.

That causality flows across scales is taken from the theory of complex adaptive systems (CASs) exposed in Sec. 1.2.2 of Chapter 1. It also connects with the panarchy theory presented in Sec. 1.2.1 of the same chapter. Studying the economy as a CAS as been suggested by many authors (Anderson et al., 1988; Arthur et al., 1997; Blume and Durlauf, 2005).

The originality of our conceptual framework is to introduce network a meso-scale between agents and the production system. This intermediary step facilitates our investigation.Arthur (2013) has suggested the use of meso-levels of aggregation. Related to our topic, Carvalho (2014) has also identified that input–output networks, detailed at the firm level, are powerful to study the link between micro and macroeconomics. Linking agents and economic macrostructure through networks has also been suggested by Schweitzer et al. (2009).

In addition, the production system is not *apriori* assumed to be at equilibrium. Instabilities may appear endogenously, as in Bonart et al. (2014). Such internal variability can be crucial for resilience (Hallegatte and Ghil, 2008)[21].

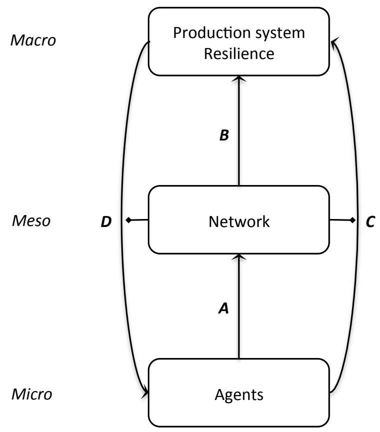

Figure 3.2: Conceptual framework for the modeling of economic resilience. The three upward-looking arrows A, B and C indicate emergence — from the bottom up — while the downward-looking arrow D represents the influence of the macro onto the micro. The two horizontal lines indicate that the network affects the two micro–macro relationships C and D.

We now detail the four different arrow of Fig. 3.2. The network emerges from the the decisions taken by the firms (A-arrow). ABMs are well suited to study this link (e.g., Gualdi and Mandel, 2015).

The various characteristic of the network — e.g., its topology, the nature of the links — strongly influence the short-term responses of the production system to shocks, and therefore its engineering and ecological resilience (B-arrow). We may study this link using ABM–network models, as in presented in Sec. 3.1.3, where the nodes are 'zero-intelligence' agents.

The internal agility and preparedness of firms also play a role in the disruption of cascades (C-arrow). We may use our ABM–network models and gradually add more agent-level details. These abilities, however, are constrained by the network structure (horizontal bar).

Macro-level resilience influence the exposure of agents to disruption cascades. Agents may react (D-arrow). This feedback enables adaptive resilience. For instance, considering their records of past disruptions, firms may change supplier (A-arrow).

[21]Hallegatte and Ghil (2008) have uncovered the 'vulnerability paradox': a natural disaster may have fewer impacts on an economy in recession than on the same one during a boom. During a recession, larger quantities of unused resources — inventories for instance — are available to cope with damages.

The network evolution becomes endogenous and depends on the agents' experience, as proposed by Kirman (1997). Firms may also update their emergency procedures (C-arrow). ABM–network models are flexible enough to model these feedback loops, and we may use the tools of evolutionary dynamics.

Over time, the D–A–B- and D–C-loops enable the production system to self-organize. Expressed in the wording used in Sec. 2.2.1, this process will change the 'in-built robustness' of the system (D–A–B-loop) and its agility (booth loops). Depending on the learning capacity of agents (D-arrow), the network structures and agent behavior that will evolve may depend on the pattern of exogenous shocks.

This conceptual framework offers many opportunities to generate research questions, build theoretical models, and integrate different tools and knowledge.

3.3.3 An introduction to the three papers

We now introduce the three papers (Chapters 4 to 6) that will be included thereafter. The main research perspectives they open are discussed in Chapter 7.

First paper (Chapter 4): *Bifurcation analysis of an agent-based model for predator–prey interactions.* Agent-based modeling seems adapted to study resilience as an emerging property of economic agents and their structure of interactions. We therefore aim to use ABMs to evaluate the dynamical trajectories of production systems, their attractor basins and possible bifurcations. However, analyzing ABMs is not yet backed, as for ordinary different equations (ODEs), by a large corpus of mathematical theories. In particular, while fairly standard theorems and numerical methods can be applied to ODEs for bifurcation analysis, no such well-established techniques exist for ABMs.

The first paper contributes to fill this gap. We study a Lotka–Voltera model for predator–prey interactions; one of the kinds that inspired Holling to conceptualize ecological resilience. We first perform the analysis of the model formulated as a system of ordinary differential equations (ODEs). Next, we design an ABM on a two-dimensional lattice that encodes, through the behavior of agents, the ingredients of the aggregate ODE model. In accordance to the ABM paradigm, these mechanisms are not built in at the aggregate level, and are entirely emerging from the bottom-up. We validate that, although the two modeling approaches — ODE and ABM — differ, both models exhibit similar bifurcation patterns.

Predator–prey interactions are not only at the origin of resilience thinking, they also correspond to a very generic behavior and may be found in many systems. The economic growth model of Goodwin (1967), mentioned in Sec. 3.2.2, exhibits for instance predator–prey dynamics leading to endogenous business cycles. Delli Gatti et al. (2009a) have found the same behavior from the study of industrial dynamics. In financial markets, Farmer (2002) uses all classes of Lotka–Voltera models, including competition, cooperation, and predator–prey interactions, to study investment strategies. These models may also describe economic interactions between social classes in more general socioeconomic models (Samuelson, 1971; Motesharrei et al., 2014).

This first paper also explains our approach to modeling, which is based on a hierarchy of models of different nature and level of complexity. By adding ingredients step by step, we are better able to keep track of their impact on the outcome. In addition, by employing a variety of modeling paradigms — e.g., ODEs, dynamical maps, ABMs — one can get a richer view on a phenomenon and draw more robust conclusions. As Levins (1966, 20) put it:

> "[I]f these models, despite their different assumptions, lead to similar results, we have what we can call a robust theorem that is relatively free of the details of the model. Hence, our truth is at the intersection of independent lies." (1966, 20)

Having multiple models is also helpful from a practical standpoint, since the results of one model may help formulate and analyze another.

Second paper (Chapter 5): ***Economic networks: Heterogeneity-induced vulnerability and loss of synchronization.*** This paper investigates resilience in production systems, both the engineering and ecological dimensions exposed in Tab. 3.1. It focuses on the B–arrow of the conceptual framework of Fig. 3.2. To that end, a network is populated with 'zero intelligence' agents with very simple behavior and no expectation. We analyze the interplay between topology, inventories and production delays, and how it affects the risk of disruption cascades and collapse.

This work builds on the literature presented in Sec. 3.1.3 on systemic risks and complex networks. The model is based on Coluzzi et al. (2011) and uses Boolean delays equations (BDEs). This framework allows us to focus on core nonlinear ingredients that influence the dynamics of propagation. The originality of the model is to study the dynamical interactions between heterogeneous inventories, heterogeneous delays, and complex topologies. We use a class of network calibrated with the empirical results of Fujiwara and Aoyama (2010), and a class of 'network of networks', which has recently be proposed to model interdependent supply chains and infrastructures (D'Agostino and Scala, 2013).

Third paper (Chapter 6): ***The fragmentation of production amplifies systemic risk in supply chains.*** This paper also investigates the dynamics of production networks subject to external perturbations, i.e. the B–arrow of Fig. 3.2. But, instead of studying complex topologies — we use rather small acyclic structures — we focus on the nature of supplier–customer interactions. Some agents may coordinate, others not. We compare ‘fully integrated’ structures, in which agents belong to the same firm and fully coordinate, with ‘fully fragmented’ ones, in which each agent is a single firm. Together with intermediate scenarios, they allow us to investigate how fragmentation may impact resilience.

In contrast with the BDE model, agents make decisions based on rules. By learning from past disruptions, they adjust inventory to increase profit. Their strategy depends on the pattern of disruption cascades, and thus on overall resilience (D–arrow). Resilience is in turn influenced by these firm-level decisions (C–arrow). Repeated over time, the C–D–loop forms an evolutionary process, which is determined by the network structure (horizontal line). Such application of evolutionary dynamics to production networks has not yet been explored (Lieberman et al., 2005). Eventually, by iterating this loop, each agent ends with the level of inventory that is the most adapted to the regime of perturbations. The risk of disruption cascades that remains is truly systemic.

References

Acemoglu, D., Carvalho, V. M., Ozdaglar, A., Tahbaz-Salehi, A., 2012. The Network Origins of Aggregate Fluctuations. Econometrica 80 (5), 1977–2016.

Ackerman, F., 2002. Still dead after all these years: interpreting the failure of general equilibrium theory. Journal of Economic Methodology 9 (2), 119–139.

Albert, R., Jeong, H., Barabási, A.-L., 2000. Error and attack tolerance of complex networks. Nature 406 (6794), 378–382.

Anderson, P., Arrow, K., Pines, D., 1988. The Economy as an Evolving Complex System. Addison-Wesley, Redwood City, CA.

Arrow, K. J., 1966. Economic Equilibrium. Tech. rep., Institute for Mathematical Studies in the Social Sciences, Stanford University.

Arrow, K. J., Debreu, G., 1954. Existence of an Equilibrium for a Competitive Economy. Econometrica 22 (3), 265–290.

Arthur, W. B., 2013. Complexity Economics: A Different Framework for Economic Thought. Tech. Rep. 2013-04-012, Santa Fe Institute, Santa Fe, NM.

Arthur, W. B., Durlauf, S. N., Lane, D. A., 1997. The Economy as an Evolving Complex System II. Proceedings Volume XXVII of the Santa Fe Institute Studies in the Science of Complexity. Addison-Wesley, Reading, MA.

Atalay, E., 2014. How Important are Sectoral Shocks? Tech. Rep. Paper No. CES-WP-14-31, US Census Bureau Center for Economic Studies, Washington, DC.

Atalay, E., Hortaçsu, A., Roberts, J., Syverson, C., 2011. Network structure of production. Proceedings of the National Academy of Sciences 108 (13), 5199–5202.

Axtell, R. L., 2001. Zipf Distribution of U.S. Firm Sizes. Science 293 (5536), 1818–1820.

Bak, P., Chen, K., 1991. Self-Organized Criticality. Scientific American 264 (1), 46–53.

Bak, P., Chen, K., Scheinkman, J., Woodford, M., 1993. Aggregate fluctuations from independent sectoral shocks: self-organized criticality in a model of production and inventory dynamics. Ricerche Economiche 47 (1), 3–30.

Baldwin, R., Lopez-Gonzalez, J., 2015. Supply-chain Trade: A Portrait of Global Patterns and Several Testable Hypotheses. The World Economy 38 (11), 1682–1721.

Bardoscia, M., Livan, G., Marsili, M., 2015. Complexity driven collapse of economic equilibria. arXiv preprint 1511.09203.

Barnett, W. A., Gandolfo, G., Hillinger, C., 1996. Dynamic Disequilibrium Modeling: Theory and Applications — Proceedings of the Ninth International Symposium in Economic Theory and Econometrics. Cambridge University Press.

Barrot, J.-N., Sauvagnat, J., 2016. Input Specificity and the Propagation of Idiosyncratic Shocks in Production Networks. The Quarterly Journal of Economics, qjw018.

Battiston, S., Delli Gatti, D., Gallegati, M., Greenwald, B., Stiglitz, J. E., 2007. Credit chains and bankruptcy propagation in production networks. Journal of Economic Dynamics and Control 31 (6), 2061–2084.

Battiston, S., Delli Gatti, D., Gallegati, M., Greenwald, B., Stiglitz, J. E., 2012a. Liaisons dangereuses: Increasing connectivity, risk sharing, and systemic risk. Journal of Economic Dynamics and Control 36 (8), 1121–1141.

Battiston, S., Puliga, M., Kaushik, R., Tasca, P., Caldarelli, G., 2012b. DebtRank: Too Central to Fail? Financial Networks, the FED and Systemic Risk. Scientific Reports 2.

Baumol, W. J., Benhabib, J., 1989. Chaos: Significance, Mechanism, and Economic Applications. The Journal of Economic Perspectives 3 (1), 77–105.

Benhabib, J., Nishimura, K., 1979. The hopf bifurcation and the existence and stability of closed orbits in multisector models of optimal economic growth. Journal of Economic Theory 21 (3), 421–444.

Bernard, A. B., Moxnes, A., Saito, Y. U., 2014. Geography and firm performance in the Japanese production network. Tech. Rep. 14-E-034, Research Institute of Economy, Trade and Industry, Tokyo.

Blume, L. E., Durlauf, S. N., 2005. The Economy As an Evolving Complex System, III: Current Perspectives and Future Directions. Oxford University Press.

Bonart, J., Bouchaud, J.-P., Landier, A., Thesmar, D., 2014. Instabilities in large economies: aggregate volatility without idiosyncratic shocks. Journal of Statistical Mechanics: Theory and Experiment 2014 (10), P10040.

Bouchaud, J.-P., 2013. Crises and Collective Socio-Economic Phenomena: Simple Models and Challenges. Journal of Statistical Physics 151 (3-4), 567–606.

Bouchaud, J.-P., Farmer, J. D., Lillo, F., 2009. How markets slowly digest changes in supply and demand. In: Hens, T., Reiner Schenk-Hoppé, K. (Eds.), Handbook of financial markets: dynamics and evolution. Handbooks in Finance. North-Holland, Elsevier, Amsterdam, pp. 57–160.

Bouchaud, J.-P., Kockelkoren, J., Potters, M., 2006. Random walks, liquidity molasses and critical response in financial markets. Quantitative Finance 6 (2), 115–123.

Bouchaud, J.-P., Mézard, M., Potters, M., 2002. Statistical properties of stock order books: empirical results and models. Quantitative Finance 2 (4), 251–256.

Braess, D., 1968. Über ein Paradoxon aus der Verkehrsplanung. Unternehmensforschung 12 (1), 258–268.

Brock, W. A., Hommes, C. H., 1997. A Rational Route to Randomness. Econometrica 65 (5), 1059.

Brock, W. A., Hommes, C. H., Wagener, F. O. O., 2009. More hedging instruments may destabilize markets. Journal of Economic Dynamics and Control 33 (11), 1912–1928.

Brookshire, D. S., Chang, S. E., Cochrane, H., Olson, R. A., Rose, A., Steenson, J., 1997. Direct and indirect economic losses from earthquake damage. Earthquake Spectra 13 (4), 683–701.

Callaway, D. S., Newman, M. E. J., Strogatz, S. H., Watts, D. J., 2000. Network Robustness and Fragility: Percolation on Random Graphs. Physical Review Letters 85 (25), 5468–5471.

Camerer, C. F., Loewenstein, G., Rabin, M., 2011. Advances in Behavioral Economics. Princeton University Press.

Carvalho, V. M., 2014. From Micro to Macro via Production Networks. The Journal of Economic Perspectives 28 (4), 23–47.

Christopherson, S., Michie, J., Tyler, P., 2010. Regional resilience: theoretical and empirical perspectives. Cambridge Journal of Regions, Economy and Society 3 (1), 3–10.

Cochrane, H., 2004. Economic loss: myth and measurement. Disaster Prevention and Management: An International Journal 13 (4), 290–296.

Cohen, R., Erez, K., ben Avraham, D., Havlin, S., 2000. Resilience of the Internet to Random Breakdowns. Physical Review Letters 85 (21), 4626–4628.

Cohen, R., Erez, K., ben Avraham, D., Havlin, S., 2001. Breakdown of the Internet under Intentional Attack. Physical Review Letters 86 (16), 3682–3685.

Coluzzi, B., Ghil, M., Hallegatte, S., Weisbuch, G., 2011. Boolean delay equations on networks in economics and the geosciences. International Journal of Bifurcation and Chaos 21 (12), 3511–3548.

Crucitti, P., Latora, V., Marchiori, M., 2004. Model for cascading failures in complex networks. Physical Review E 69 (4), 045104.

D'Agostino, G., Scala, A., 2013. Networks of networks: the last frontier of complexity. Understanding Complex System. Springer, New York.

Day, R. H., 1983. The Emergence of Chaos from Classical Economic Growth. The Quarterly Journal of Economics 98 (2), 201–213.

Delli Gatti, D., Gaffeo, E., Gallegati, M., 2009a. A look at the relationship between industrial dynamics and aggregate fluctuations. In: Faggini, M., Lux, T. (Eds.), Coping with the Complexity of Economics. New Economic Windows. Springer, pp. 33–49.

Delli Gatti, D., Gaffeo, E., Gallegati, M., Giulioni, G., Kirman, A., Palestrini, A., Russo, A., 2007. Complex dynamics and empirical evidence. Information Sciences 177 (5), 1204–1221.

Delli Gatti, D., Gallegati, M., Greenwald, B. C., Russo, A., Stiglitz, J. E., 2009b. Business fluctuations and bankruptcy avalanches in an evolving network economy. Journal of Economic Interaction and Coordination 4 (2), 195–212.

di Giovanni, J., Levchenko, A. A., Mejean, I., 2014. Firms, Destinations, and Aggregate Fluctuations. Econometrica 82 (4), 1303–1340.

Dodds, P. S., Watts, D. J., 2004. Universal Behavior in a Generalized Model of Contagion. Physical Review Letters 92 (21), 218701.

Dosi, G., Nelson, R. R., 1994. An introduction to evolutionary theories in economics. Journal of Evolutionary Economics 4 (3), 153–172.

Durlauf, S. N., 1997. Statistical Mechanics Approaches to Socioeconomic Behavior. In: Arthur, W. B., Durlauf, S. N., Lane, D. A. (Eds.), The Economy as an Evolving Complex System II. Addison-Wesley, Reading, MA.

Epstein, J. M., Axtell, R., 1996. Growing Artificial Societies: Social Science from the Bottom Up. Brookings Institution Press, Washington, DC.

Farmer, J. D., 2002. Market force, ecology and evolution. Industrial and Corporate Change 11 (5), 895–953.

Farmer, J. D., Geanakoplos, J., 2009. The virtues and vices of equilibrium and the future of financial economics. Complexity 14 (3), 11–38.

Farmer, J. D., Patelli, P., Zovko, I. I., 2005. The predictive power of zero intelligence in financial markets. Proceedings of the National Academy of Sciences of the United States of America 102 (6), 2254–2259.

Fisher, F. M., 1989. Disequilibrium Foundations of Equilibrium Economics. Cambridge University Press.

Foerster, A., Sarte, G., P.-D., Watson, M., 2011. Sectoral versus Aggregate Shocks: A Structural Factor Analysis of Industrial Production. Journal of Political Economy 119 (1), 1–38.

Forrester, J. W., 1961. Industrial Dynamics. MIT Press, Cambridge, MA.

Fujiwara, Y., 2008. Chain of firms' bankruptcy: a macroscopic study of link effect in a production network. Advances in Complex Systems 11 (05), 703–717.

Fujiwara, Y., Aoyama, H., 2010. Large-scale structure of a nation-wide production network. The European Physical Journal B 77 (4), 565–580.

Gabaix, X., 2011. The Granular Origins of Aggregate Fluctuations. Econometrica 79 (3), 733–772.

Gallegati, M., Kirman, A., 2012. Reconstructing economics: Agent based models and complexity. Complexity Economics 1 (1), 5–31.

Garnier, E., Desarthe, J., 2013. Cyclones and Societies in the Mascarene Islands 17th-20th Centuries. American Journal of Climate Change 02 (01), 1–13.

Gigerenzer, G., Brighton, H., 2009. Homo Heuristicus: Why Biased Minds Make Better Inferences. Topics in Cognitive Science 1 (1), 107–143.

Goodwin, R. M., 1967. A Growth Cycle. In: Feinstein, C. H. (Ed.), Socialism, Capitalism and Economic Growth. Palgrave Macmillan UK, pp. 54–58.

Goyal, S., 2007. Connections: An Introduction to the Economics of Networks. Princeton University Press, Princeton, NJ.

Groth, A., Ghil, M., Hallegatte, S., Dumas, P., 2015. The role of oscillatory modes in US business cycles. OECD Journal. Journal of Business Cycle Measurement and Analysis 2015 (1), 63–81.

Gualdi, S., Mandel, A., 2015. On the emergence of scale-free production networks. arXiv 1509 (01483).

Haimes, Y. Y., Jiang, P., 2001. Leontief-Based Model of Risk in Complex Interconnected Infrastructures. Journal of Infrastructure Systems 7 (1), 1–12.

Haldane, A. G., May, R. M., 2011. Systemic risk in banking ecosystems. Nature 469 (7330), 351–355.

Hallegatte, S., 2008. An Adaptive Regional Input-Output Model and its Application to the Assessment of the Economic Cost of Katrina. Risk Analysis 28 (3), 779–799.

Hallegatte, S., 2014a. Economic Resilience: Definition and Measurement. Tech. rep., The World Bank.

Hallegatte, S., 2014b. Economic Resilience: Definition and Measurement. Tech. rep., The World Bank.

Hallegatte, S., 2014c. Modeling the Role of Inventories and Heterogeneity in the Assessment of the Economic Costs of Natural Disasters. Risk Analysis 34 (1), 152–167.

Hallegatte, S., Ghil, M., 2008. Natural disasters impacting a macroeconomic model with endogenous dynamics. Ecological Economics 68 (1–2), 582–592.

Hallegatte, S., Ghil, M., Dumas, P., Hourcade, J.-C., 2008. Business cycles, bifurcations and chaos in a neo-classical model with investment dynamics. Journal of Economic Behavior & Organization 67 (1), 57–77.

Hallegatte, S., Ranger, N., Mestre, O., Dumas, P., Corfee-Morlot, J., Herweijer, C., Wood, R. M., 2010. Assessing climate change impacts, sea level rise and storm surge risk in port cities: a case study on Copenhagen. Climatic Change 104 (1), 113–137.

Harrod, R. F., 1939. An Essay in Dynamic Theory. The Economic Journal 49 (193), 14–33.

Heal, G., 1986. Macrodynamics and Returns to Scale. The Economic Journal 96 (381), 191–198.

Helbing, D., Balietti, S., 2011. How to Do Agent-Based Simulations in the Future: From Modeling Social Mechanisms to Emergent Phenomena and Interactive Systems Design. Tech. Rep. 2011-06-024, Santa-Fe Institute.

Helbing, D., Lämmer, S., Seidel, T., Seba, P., Platkowski, T., 2004. Physics, stability, and dynamics of supply networks. Physical Review E 70 (6), 066116.

Henriet, F., Hallegatte, S., Tabourier, L., 2012. Firm-network characteristics and economic robustness to natural disasters. Journal of Economic Dynamics and Control 36 (1), 150–167.

Hommes, C., 2011. The heterogeneous expectations hypothesis: Some evidence from the lab. Journal of Economic Dynamics and Control 35 (1), 1–24.

Jaramillo, C. R., 2009. Do Natural Disasters Have Long-Term Effects on Growth? SSRN Scholarly Paper ID 1543453, Social Science Research Network, Rochester, NY.

Kahneman, D., Tversky, A., 1979. Prospect theory: An analysis of decision under risk. Econometrica: Journal of the Econometric Society, 263–291.

Kahneman, D., Tversky, A., 2000. Choices, Values, and Frames. Cambridge University Press.

Kalecki, M., 1937. A Theory of the Business Cycle. The Review of Economic Studies 4 (2), 77–97.

Kirman, A., 1989. The Intrinsic Limits of Modern Economic Theory: The Emperor has No Clothes. The Economic Journal 99 (395), 126–139.

Kirman, A., 1992. Whom of what does the representative individual represent? Journal of Economic Perspectives 6 (2), 117–136.

Kirman, A., 1997. The economy as an evolving network. Journal of Evolutionary Economics 7 (4), 339–353.

Kydland, F. E., Prescott, E. C., 1982. Time to Build and Aggregate Fluctuations. Econometrica 50 (6), 1345–1370.

Lane, D. A., 1993. Artificial worlds and economics, part I. Journal of Evolutionary Economics 3 (2), 89–107.

Lavoie, M., 2014. Post-Keynesian economics: new foundations. Edward Elgar Publishing.

Lee, H. L., Padmanabhan, V., Whang, S., 2004. Information Distortion in a Supply Chain: The Bullwhip Effect. Management Science 50 (12), 1875–1886.

Leontief, W., 1936. Quantitative input and output relations in the economic systems of the United States. The Review of Economics and Statistics 18 (3), 105–125.

Levins, R., 1966. The strategy of model building in population biology. In: Sober, E. (Ed.), Conceptual issues in evolutionary biology. pp. 18–27.

Lieberman, E., Hauert, C., Nowak, M. A., 2005. Evolutionary dynamics on graphs. Nature 433 (7023), 312–316.

Lobato, I. N., Velasco, C., 2000. Long Memory in Stock-Market Trading Volume. Journal of Business & Economic Statistics 18 (4), 410–427.

Long, J. B., Plosser, C. I., 1983. Real business cycles. The Journal of Political Economy, 39–69.

Lorenz, J., Battiston, S., Schweitzer, F., 2009. Systemic risk in a unifying framework for cascading processes on networks. The European Physical Journal B 71 (4), 441–460.

Mandel, A., 2012. Agent-based dynamics in the general equilibrium model. Complexity Economics 1 (1), 105–121.

Martin, R., 2012. Regional economic resilience, hysteresis and recessionary shocks. Journal of Economic Geography 12 (1), 1–32.

May, R. M., Arinaminpathy, N., 2010. Systemic risk: the dynamics of model banking systems. Journal of The Royal Society Interface 7 (46), 823–838.

May, R. M., Lloyd, A. L., 2001. Infection dynamics on scale-free networks. Physical Review E 64 (6), 066112.

Meadows, D. H., Meadows, D. H., Randers, J., Behrens III, W. W., 1972. The Limits to Growth. Tech. rep., The Club of Rome, Rome.

Mizuno, T., Souma, W., Watanabe, T., 2014. The Structure and Evolution of Buyer-Supplier Networks. PLoS ONE 9 (7), e100712.

Modica, M., Reggiani, A., 2015. Spatial Economic Resilience: Overview and Perspectives. Networks and Spatial Economics 15 (2), 211–233.

Motesharrei, S., Rivas, J., Kalnay, E., 2014. Human and nature dynamics (HANDY): Modeling inequality and use of resources in the collapse or sustainability of societies. Ecological Economics 101, 90–102.

Negishi, T., 1962. The Stability of a Competitive Economy: A Survey Article. Econometrica 30 (4), 635–669.

Newman, M. E. J., 2002. Spread of epidemic disease on networks. Physical Review E 66 (1).

Ohnishi, T., Takayasu, H., Takayasu, M., 2009. Hubs and Authorities on Japanese Inter-Firm Network: Characterization of Nodes in Very Large Directed Networks. Progress of Theoretical Physics Supplement 179, 157–166.

Ohnishi, T., Takayasu, H., Takayasu, M., 2010. Network motifs in an inter-firm network. Journal of Economic Interaction and Coordination 5 (2), 171–180.

Okuyama, K., Takayasu, M., Takayasu, H., 1999. Zipf's law in income distribution of companies. Physica A: Statistical Mechanics and its Applications 269 (1), 125–131.

Okuyama, Y., 2004. Moldeling spatial economic impacts of an earthquake: input-output approaches. Disaster Prevention and Management: An International Journal 13 (4), 297–306.

Okuyama, Y., 2007. Economic Modeling for Disaster Impact Analysis: Past, Present, and Future. Economic Systems Research 19 (2), 115–124.

Osadchiy, N., Gaur, V., Udenio, M., 2016. Evolution of Supply Networks.

Pike, A., Dawley, S., Tomaney, J., 2010. Resilience, adaptation and adaptability. Cambridge Journal of Regions, Economy and Society, rsq001.

Ploszaj, A., Celinska-Janowicz, D., Rok, J., Zawalinska, K., 2015. Regional Input-Output Studies: A Systematic Literature Review. In: Proceedings of the 18th Annual Conference on Global Economic Analysis. Melbourne.

Polenske, K., 2004. Leontief's "magnificent machine" and other contributions to applied economics. In: Dietzenbacher, E., Lahr, M. L. (Eds.), Wassily Leontief and Input-Output Economics. Cambridge University Press, Cambridge, UK, pp. 30–46.

Quesnay, F., 1766. Analyse de la formule arithmétique du Tableau économique. Journal de l'agriculture, du commerce & des finances 2 (3), 11–41.

Ranger, N., Hallegatte, S., Bhattacharya, S., Bachu, M., Priya, S., Dhore, K., Rafique, F., Mathur, P., Naville, N., Henriet, F., Herweijer, C., Pohit, S., Corfee-Morlot, J., 2011. An assessment of the potential impact of climate change on flood risk in Mumbai. Climatic Change 104 (1), 139–167.

Romanoff, E., Levine, S. H., 1981. Anticipatory and Responsive Sequential Interindustry Models. IEEE Transactions on Systems, Man, and Cybernetics 11 (3), 181–186.

Romanoff, E., Levine, S. H., 1986. Capacity Limitations, Inventory, and Time-Phased Production in the Sequential Interindustry Model. Papers in Regional Science 59 (1), 73–91.

Rose, A., 2007. Economic resilience to natural and man-made disasters: Multidisciplinary origins and contextual dimensions. Environmental Hazards 7 (4), 383–398.

Rose, A., Krausmann, E., 2013. An economic framework for the development of a resilience index for business recovery. International Journal of Disaster Risk Reduction 5, 73–83.

Rose, A., Liao, S.-Y., 2005. Modeling Regional Economic Resilience to Disasters: A Computable General Equilibrium Analysis of Water Service Disruptions*. Journal of Regional Science 45 (1), 75–112.

Rose, A., Oladosu, G., Liao, S.-Y., 2007. Business Interruption Impacts of a Terrorist Attack on the Electric Power System of Los Angeles: Customer Resilience to a Total Blackout. Risk Analysis 27 (3), 513–531.

Saito, Y. U., Watanabe, T., Iwamura, M., 2007. Do larger firms have more interfirm relationships? Physica A: Statistical Mechanics and its Applications 383 (1), 158–163.

Samuelson, P. A., 1939. A Synthesis of the Principle of Acceleration and the Multiplier. Journal of Political Economy 47 (6), 786–797.

Samuelson, P. A., 1941. The Stability of Equilibrium: Comparative Statics and Dynamics. Econometrica 9 (2), 97–120.

Samuelson, P. A., 1971. Generalized Predator-Prey Oscillations in Ecological and Economic Equilibrium. Proceedings of the National Academy of Sciences of the United States of America 68 (5), 980–983.

Santos, J. R., 2006. Inoperability input-output modeling of disruptions to interdependent economic systems. Systems Engineering 9 (1), 20–34.

Santos, J. R., Haimes, Y. Y., 2004. Modeling the Demand Reduction Input-Output (I-O) Inoperability Due to Terrorism of Interconnected Infrastructures. Risk Analysis 24 (6), 1437–1451.

Scheinkman, J. A., Woodford, M., 1994. Self-Organized Criticality and Economic Fluctuations. The American Economic Review 84 (2), 417–421.

Schelling, T. C., 1978. Micromotives and Macrobehavior. W. W. Norton & Company, New York.

Schweitzer, F., Fagiolo, G., Sornette, D., Vega-Redondo, F., Vespignani, A., White, D. R., 2009. Economic Networks: The New Challenges. Science 325 (5939), 422–425.

Sella, L., Vivaldo, G., Groth, A., Ghil, M., 2016. Economic Cycles and Their Synchronization: A Comparison of Cyclic Modes in Three European Countries. Journal of Business Cycle Research 12 (1), 25–48.

Shone, R., 2002. Economic Dynamics: Phase Diagrams and Their Economic Application, second edition Edition. Cambridge University Press, Cambridge, UK.

Simmie, J., Martin, R., 2010. The economic resilience of regions: towards an evolutionary approach. Cambridge Journal of Regions, Economy and Society 3 (1), 27–43.

Simon, H. A., 1962. The Sciences of the Artificial. MIT Press, Cambridge.

Sonnenschein, H., 1973. Do Walras' identity and continuity characterize the class of community excess demand functions? Journal of Economic Theory 6 (4), 345–354.

Steenge, A. E., Bockarjova, M., 2007. Thinking about Imbalances in Post-catastrophe Economies: An Input–Output based Proposition. Economic Systems Research 19 (2), 205–223.

Tessone, C. J., Garas, A., Guerra, B., Schweitzer, F., 2013. How Big Is Too Big? Critical Shocks for Systemic Failure Cascades. Journal of statistical physics 151 (3-4), 765–783.

Timmer, M. P., Dietzenbacher, E., Los, B., Stehrer, R., de Vries, G. J., 2015. An Illustrated User Guide to the World Input–Output Database: the Case of Global Automotive Production. Review of International Economics 23 (3), 575–605.

Towill, D. R., 1996. Industrial dynamics modelling of supply chains. International Journal of Physical Distribution & Logistics Management 26 (2), 23–42.

Turner, G. M., 2008. A comparison of The Limits to Growth with 30 years of reality. Global Environmental Change 18 (3), 397–411.

Walker, D. A., 1987. Edgeworth versus Walras on the Theory of Tatonnement. Eastern Economic Journal 13 (2), 155–165.

Wang, J.-W., Rong, L.-L., 2011. Robustness of the western United States power grid under edge attack strategies due to cascading failures. Safety Science 49 (6), 807–812.

Watts, D. J., 2002. A simple model of global cascades on random networks. Proceedings of the National Academy of Sciences 99 (9), 5766–5771.

Weisbuch, G., Battiston, S., 2007. From production networks to geographical economics. Journal of Economic Behavior & Organization 64 (3–4), 448–469.

Westley, F., Carpenter, S. R., Brock, W. A., Holling, C. S., Gunderson, L. H., 2002. Systems of People and Nature. In: Gunderson, L. H., Holling, C. S. (Eds.), Panarchy: Understanding Transformations in Human and Natural Systems. Island Press, Washington, DC, pp. 103–119.

Wolfe, D. A., 2010. The strategic management of core cities: Path dependence and economic adjustment in resilient regions. Cambridge Journal of Regions, Economy and Society 3 (1), 139–152.

Wu, J., Li, N., Hallegatte, S., Shi, P., Hu, A., Liu, X., 2011. Regional indirect economic impact evaluation of the 2008 Wenchuan Earthquake. Environmental Earth Sciences 65 (1), 161–172.

Wu, T., Blackhurst, J., O'grady, P., 2007. Methodology for supply chain disruption analysis. International Journal of Production Research 45 (7), 1665–1682.

Xu, M., Allenby, B. R., Crittenden, J. C., 2011. Interconnectedness and Resilience of the U.S. Economy. Advances in Complex Systems 14 (05), 649–672.

Zhao, L., Park, K., Lai, Y.-C., 2004. Attack vulnerability of scale-free networks due to cascading breakdown. Physical Review E 70 (3), 035101.

Chapter 4

Bifurcation analysis of an agent-based model for predator–prey interactions

This paper has been published in 2015 in *Ecological Modelling*, under the following reference:
Colon C., Claessen D., Ghil M., 2015, Bifurcation analysis of an agent-based model for predator–prey interactions. Ecological Modelling, 317 (10): 93–106.

Authors: Célian Colon, David Claessen and Michael Ghil. DC is affiliated to the Ecole Normale Supérieure, Paris.

Abstract: The Rosenzweig–MacArthur model is a set of ordinary differential equations (ODEs) that provides an aggregate description of the dynamics of a predator–prey system. When including an Allee effect on the prey, this model exhibits bistability and contains a pitchfork bifurcation, a Hopf bifurcation and a heteroclinic bifurcation. We develop an agent-based model (ABM) on a two-dimensional, square lattice that encompasses the key assumptions of the aggregate model. Although the two modelling approaches – ODE and ABM – differ, both models exhibit similar bifurcation patterns. The ABM model's behaviour is richer and it is analysed using advanced statistical methods. In particular, singular spectrum analysis is used to robustly locate the transition between apparently random, small-amplitude fluctuations around a fixed point and stable, large-amplitude oscillations. Critical slowing down of model trajectories anticipates the heteroclinic bifurcation. Systematic comparison between the ABM and the ODE models' behaviour helps one understand the predator–prey system better; it provides guidance in model exploration and allows one to draw more robust conclusions on the nature of predator–prey interactions.

Ecological Modelling 317 (2015) 93–106

Contents lists available at ScienceDirect

Ecological Modelling

journal homepage: www.elsevier.com/locate/ecolmodel

Bifurcation analysis of an agent-based model for predator–prey interactions

C. Colon[a,b,d,*], D. Claessen[b,c], M. Ghil[a,b,e]

[a] Laboratoire de Meteorologie Dynamique, Ecole Normale Supérieure, F-75231 Paris Cedex 05, France
[b] Environmental Research and Teaching Institute, Ecole Normale Supérieure, F-75231 Paris Cedex 05, France
[c] Institut de Biologie de l'Ecole Normale Supérieure (CNRS UMR 8197, INSERM U1024), Ecole Normale Supérieure, 46 rue d'Ulm, 75005 Paris, France
[d] Applied Mathematics Department, Ecole Polytechnique, Route de Saclay, 91128 Palaiseau, France
[e] Department of Atmospheric and Oceanic Sciences, University of California at Los Angeles, Los Angeles, CA 90095-1565, USA

ARTICLE INFO

Article history:
Received 4 December 2014
Received in revised form 31 August 2015
Accepted 2 September 2015

Keywords:
ODE
Hopf bifurcation
Heteroclinic bifurcation
Time series analysis
Singular spectrum analysis
Critical transition
Early-warning signals

ABSTRACT

The Rosenzweig–MacArthur model is a set of ordinary differential equations (ODEs) that provides an aggregate description of the dynamics of a predator–prey system. When including an Allee effect on the prey, this model exhibits bistability and contains a pitchfork bifurcation, a Hopf bifurcation and a heteroclinic bifurcation. We develop an agent-based model (ABM) on a two-dimensional, square lattice that encompasses the key assumptions of the aggregate model. Although the two modelling approaches – ODE and ABM – differ, both models exhibit similar bifurcation patterns. The ABM model's behaviour is richer and it is analysed using advanced statistical methods. In particular, singular spectrum analysis is used to robustly locate the transition between apparently random, small-amplitude fluctuations around a fixed point and stable, large-amplitude oscillations. Critical slowing down of model trajectories anticipates the heteroclinic bifurcation. Systematic comparison between the ABM and the ODE models' behaviour helps one understand the predator–prey system better; it provides guidance in model exploration and allows one to draw more robust conclusions on the nature of predator–prey interactions.

1. Introduction and motivation

Ecologists are more and more frequently asked to make predictions about the potential effects of specific changes to an ecosystem or a community of species. This demand is particularly vivid in the context of climate change (Lavergne et al., 2010; Valladares et al., 2014) or resource management. It especially applies when anthropic harvesting is at play, as in fisheries (Lindegren et al., 2010), or when biological factors might disturb an established community of species, as in cases of non-endemic species invading an ecosystem (Crowl et al., 2008). Understanding these consequences is also relevant when the driver of changes is internal, in particular through evolutionary processes (Ferrière, 2009).

Whether the engine of change is external or internal, analysing the consequences requires a comprehensive understanding of the community dynamics. Achieving such an understanding has proven to be a challenging task. Observational and experimental data show that an ecological system composed of only two interacting species can exhibit non-trivial dynamics, such as bistability and oscillations (e.g., Fussmann et al., 2000). The importance of non-linear mechanisms in leading to such dynamics has motivated theoretical work on simple models to characterise the dynamical regimes, identify and circumscribe basins of attraction, and locate bifurcations or regime shifts. To do so, ecologists have borrowed mathematical concepts and tools from other disciplines and tried a variety of modelling techniques, especially using systems of ordinary differential equations (ODEs).

A recent innovation is the development of agent-based models (ABMs), also called individual-based models in the ecological literature. ABMs simulate systems described by the rules of interaction among autonomous individuals. According to DeAngelis and Mooij (2005), some scholars view ABMs as exploratory tools that extend classical aggregate models, whereas others suggest that ABMs provide a methodological basis on which to build a novel research paradigm (Grimm et al., 1999; Grimm and Railsback, 2005). In the field of population dynamics, ABMs have helped investigate the role of local interactions (Mccauley et al., 1993) and spatial dynamics (Dieckmann et al., 2000); they are also being increasingly employed to study evolutionary dynamics (Łomnicki, 1999; Gras et al., 2009).

* Corresponding author at: CERES, Ecole Normale Supérieure, F-75231 Paris Cedex 05, France. Tel.: +33 144323025
E-mail address: celian.colon@polytechnique.edu (C. Colon).

http://dx.doi.org/10.1016/j.ecolmodel.2015.09.004
0304-3800/

Can ABMs help the understanding of community dynamics? How can their use complement the classic ODE approach? In climate sciences, it has been proposed to advance knowledge by moving across a hierarchy of models of the same class of phenomena (Schneider and Dickinson, 1974; Ghil, 2001; Dijkstra and Ghil, 2005). This hierarchy ranges from low-resolution 'toy' models, which help understand the general behaviour of the system, all the way to very detailed 'realistic' models, which may be used for real-time forecasting of weather or climate. Moving up the hierarchy implies adding mechanisms and improving resolution, which often comes at the cost of losing analytical tractability and insight. Detailed models have to be integrated numerically, and analysing their outputs may require complex statistical manipulations. Going back and forth between different levels allows one to test the robustness of the conclusions and guide fruitful improvements of the models at each level of the hierarchy.

The hierarchical modelling approach could be insightfully applied to study the dynamics of communities and even ecosystems. It would thus appear that classical ODE systems, such as the Lotka–Voltera equations, are toy models – in the hierarchical modelling terminology (Ghil, 2001) – whereas the ABM framework is more appropriate for developing detailed models. ABMs can be seen as more realistic, since agents often correspond to observable organisms (Bonabeau, 2002). Contrasting the results of different models has already allowed ecologists to point out some mechanisms that a single-model approach may overlook, such as the influence of spatial distribution and localised interactions (Donalson and Nisbet, 1999; Durrett and Levin, 1994), of physiological structure (De Roos and Persson, 2005) and of heterogeneity (Hastings, 1990). In particular, Dieckmann et al. (2000) pointed out instances in which the dynamics of mean-field models differ from the ABMs they derive from, and proposed new mathematical methods to integrate the spatially distributed aspects of ABMs into ODEs, such as moment methods (Law and Dieckmann, 2000) or pair-wise approximations (van Baalen, 2000).

In this paper, we illustrate the hierarchical modelling approach by revisiting a classical predator–prey system and comparing the dynamical behaviour of an ABM with that of an ODE model. The guiding thread of this comparison is to determine whether the two models' bifurcation patterns – which summarise the key features of a system's dynamics – are qualitatively similar, even though each model is built upon distinct and complementary principles.

The key components of ODE models are the macro-level feedback mechanisms. Individuals, as distinct entities, do not play any role per se. The dynamics results from the relative abundance of each population, expressed through the principle of 'mass-action'. In ABMs, the system-level dynamics results from the micro-level actions of autonomous individuals. They follow rules, but their effective actions depend on local contingencies. In addition, agents may have only limited information on the system they are embedded in. Grimm and Railsback (2005) argue that reproducing results of a classical ODE model with ABMs often led to the design of models that are incomplete, not robust, and therefore lacking in interest.

In this paper, we do not aim to reproduce the outputs of an ODE model with an ABM, neither do we want to perform any quantitative comparison. Our objective is to establish whether the behaviour patterns of the two models are in qualitative agreement, i.e., whether the solution types – bistable, oscillatory and irregular – are in one-to-one correspondence, including the transitions between these regimes of behaviour, as long as the two models, while conceptually different, rely on the same key assumptions about the system under scrutiny. In addition, we are interested to find out – provided there is a good correspondence in regime types and bifurcations between the aggregate ODE model and the ABM – whether ideas on early warning that were developed for ODE models Scheffer et al. (2009) can help formulate such early warnings for ABMs.

The qualitative comparison between our ODE model and the ABM is carried out by computing the corresponding bifurcation diagrams of the two models. To do this, we need to locate the bifurcation points in our ABM. The identification of attractors has not been the main emphasis of ecological ABM studies, which tend to focus instead on the emergence of spatial patterns (Grimm and Railsback, 2005; Railsback and Grimm, 2011). Analysing attractor types and the transitions between them as significant model parameters change – i.e., studying the models' bifurcations – is quite helpful in understanding regime shifts. These shifts are crucial ecological phenomena and applying bifurcation-theoretical methods to ABM studies thus follows the call of Scholl (2001) to tighten connections between agent-based modelling and dynamical systems theory. In particular, we propose and apply a method to detect the transition between regular oscillations and irregular fluctuations around a steady state.

In Section 2.1, we present the behaviour of a classical ODE model of predator–prey systems: the Rosenzweig–McArthur model with strong Allee effect on the prey. In Section 2.2, we formulate an ABM in which the key mechanisms that enter the aggregate model emerge spontaneously; these mechanisms include the functional response and the Allee effect. We then define, in Section 2.4, the experimental protocol of the simulations and explain the methods we use to analyse the resulting ABM model.

In Section 3, we present the results and compare the bifurcation diagrams obtained for the two models, while focussing on the Hopf bifurcation in Section 3.2 and on the heteroclinic one in Section 3.3. In Section 4, we explore early-warning signals for the global transitions and test them when endogenous processes or exogenous forcing modify slowly the model parameters. Finally, we discuss the methodological implications of our work within ABM studies.

2. Models and methodology

2.1. The aggregate model and its behaviour

We study the Rosenzweig–McArthur model with strong Allee effect on the prey. Boukal et al. (2007) analysed how the 'route to collapse' featured in Rosenzweig–McArthur models is influenced by the addition of either a weak or a strong Allee effect, and by the sigmoidicity of the functional response. The system's collapse occurs through a global bifurcation, characterised by an heteroclinic orbit (van Voorn et al., 2007). Wang et al. (2011) performed a rigorous analysis of the model, and focussed on the existence and uniqueness of limit cycles after the Hopf bifurcation. González-Olivares et al. (2006) performed a similar analysis with an Holling type III functional response.

Let X denote the prey population and Y the predator population. The dynamics is governed by the following two coupled ODEs:

$$\frac{dX}{dt} = rX\left(1 - \frac{X}{K}\right)(X - A) - \alpha\frac{X}{X + S}Y, \tag{1a}$$

$$\frac{dY}{dt} = \rho\alpha\frac{X}{X + S}Y - dY. \tag{1b}$$

This model has seven parameters, whose definitions and values are listed in Table 1. We will also use $\mathbf{Z}(t) = (X(t), Y(t))$ to denote the state of our two-species ecosystem as a function of time t.

The model's dynamics can be summarised in a two-dimensional regime diagram usually plotted in the (d, A)-plane; see, for instance, González-Olivares et al. (2006), Boukal et al. (2007) and van Voorn et al. (2007). We choose ρ instead of d, which leads to a very similar diagram, plotted here as Fig. 1. The regime boundaries between regions (1) and (2) and between regions (2) and (3) were obtained

Table 1
Summary of the parameters used in the ODE model.

Parameter	Definition	Value
r	Prey's maximal growth rate	1
K	Prey's carrying capacity	1
A	Prey's Allee effect threshold	0.1
α	Predator's attack rate	1
S	Predator's half saturation constant	0.4
ρ	Predators' conversion rate	$0 \leq \rho \leq 1$
d	Predator's death rate	0.4

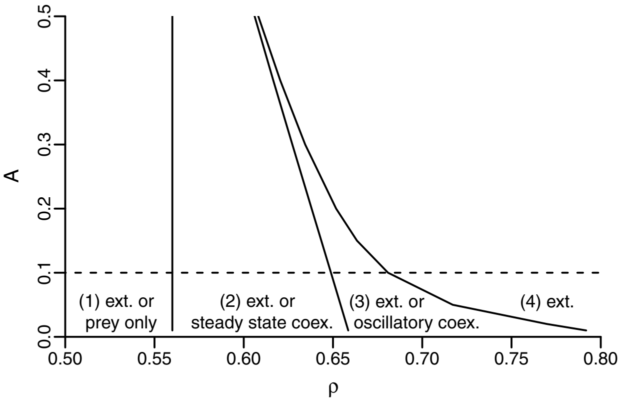

Fig. 1. Regime diagram of the aggregate model. The dashed line corresponds to the section along which the bifurcation diagram in Fig. 3 is calculated. 'Ext.' stands for extinction, 'coex.' for coexistence.

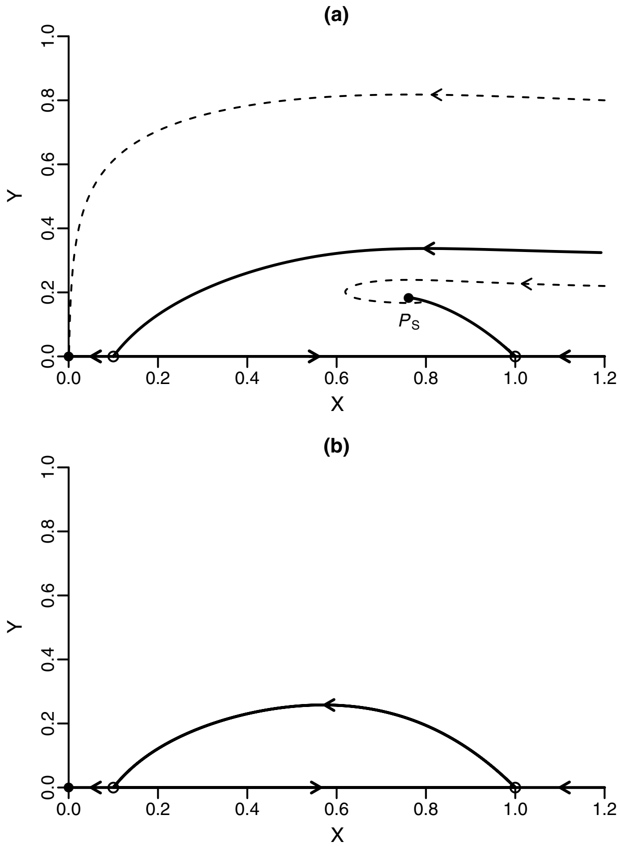

Fig. 2. Phase plane of the aggregate model with (a) $\rho = 0.61$ and (b) $\rho = 0.6808$. The solid curves correspond to the invariant manifolds of the saddle points (A, 0) and (K, 0), indicated by open circles. In panel (a), the stable manifold of (A, 0) is a separatrix that forms the mutual boundary of two regions. In either one of the two regions, all the trajectories – illustrated by one dashed curve in either region – converge to a fixed point, namely the origin and P_S, respectively; the latter two are indicated by a filled circle each. In panel (b), the unstable manifold of (K, 0) coincides with the stable manifold of (A, 0), thus forming a heteroclinic connection between the two saddles.

analytically. The location of the boundary between regions (3) and (4) was identified numerically, using continuation methods (Dhooge et al., 2003) to track the growth and collapse of the limit cycle.

In region (4) of the figure, there is only one attractor, which is a fixed point, and all orbits converge to the origin. Predators overexploit prey, whose density sinks below the Allee effect threshold. The prey go extinct, followed by the predators.

In the three other regions, the system is bistable: the state diagrams (not shown) exhibit two basins of attraction whose common boundary is a smooth separatrix, cf. Fig. 2a. In the portion of the phase plane located above the separatrix – i.e., at more abundant predator population – the system behaves as in region (4).

To understand better the dynamics below the separatrix in Fig. 2a, we calculated the bifurcation diagram shown in Fig. 3 with respect to the parameter ρ, at $A = 0.1$ (dashed line in Fig. 1).

Four types of behaviour are observed:

- *Prey-only*: for $\rho < 0.56$, ($X = K \neq 0$, $Y = 0$) is an attractor. The predators are not efficient enough and go extinct; the prey, freed from predation, fill the carrying capacity; see region (1) of Fig. 1.
- *Steady-state coexistence*: when ρ exceeds 0.56, the non-trivial steady state ($X = K$, $Y = 0$) changes from being a stable node, or sink, to being a saddle, and a new attracting fixed point P_S emerges: the two populations coexist at steady densities; see region (2) in the figure.
- *Oscillatory coexistence*: at $\rho = 0.65$, the new, stable fixed point undergoes a Hopf bifurcation and an attracting limit cycle emerges. The two populations coexist with periodic densities; see region (3).
- *Extinction*: as ρ increases further, the period and amplitude of the oscillations continue to increase until the limit cycle merges with the separatrix and becomes an heteroclinic orbit linking the two saddle points (K, 0) and (A, 0). This global bifurcation provokes the collapse of the bistability, and the system reaches region (4); see Fig. 2b.

To understand the nature of the bifurcation at $\rho = 0.56$, denoted by 'BP' in Fig. 3, requires a second look at the ODE system (2.1). In fact, the predator equation (1b) is invariant under a change of Y into $-Y$. While negative populations are not realistic, this mirror symmetry implies that BP is a pitchfork bifurcation, with transfer of stability from the prey-only fixed point (K, 0) to the new stable fixed point with non-zero predator population, $Y \neq 0$.

2.2. ABM model formulation

The model description follows the Overview, Design concepts, Details (ODD) protocol of Grimm et al. (2006, 2010).

2.2.1. Purpose

The purpose of the model is to understand how the dynamics of a simple predator–prey system varies according to the predator's mean conversion rate.

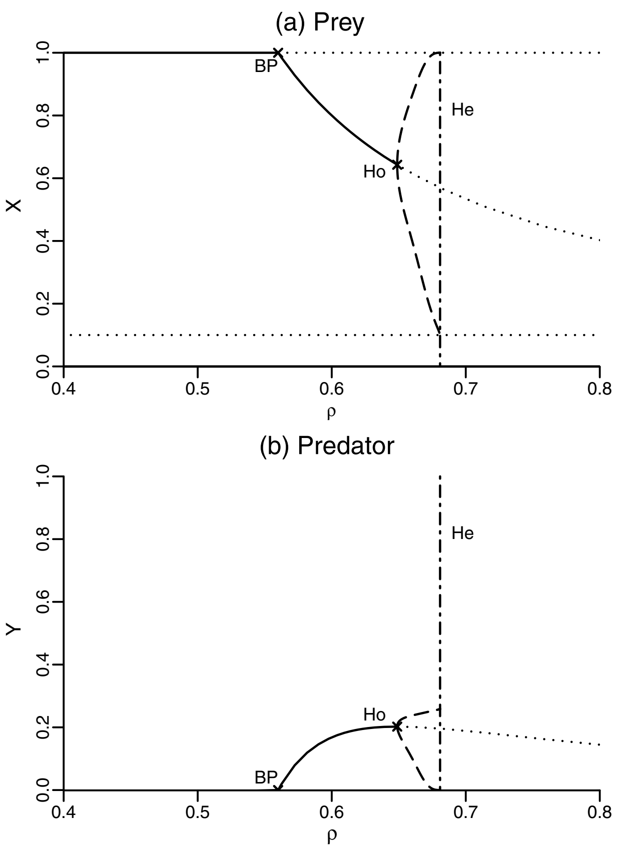

Fig. 3. Bifurcation diagram $\mathbf{Z}=\mathbf{Z}(\rho)$ of the ODE model with respect to the parameter ρ, for $A=0.1$; all the other parameters have the values in Table 1. (a) For the prey population $X=X(\rho)$; and (b) for the predator population $Y=Y(\rho)$. Solid lines represent stable equilibria, dotted lines unstable equilibria. The prey-only fixed point ($X=K$, $Y=0$) undergoes a one-sided pitchfork bifurcation, constrained by the positivity of Y, and is denoted in the figure by BP, for branching point; see text for details. This bifurcation from a single to two fixed points is followed by a Hopf bifurcation (Ho), with the dashed lines indicating the extrema of the limit cycles. The vertical dashed line represents the location of the next, global bifurcation, via the birth of a heteroclinic orbit (He); see Fig. 2(b).

2.2.2. Entities, state variables, and scales

Agents are of two types: predators and prey. Each agent is characterised by a specific identity number. The agent-level state variables are their two spatial coordinates.

Agents evolve on a two-dimensional, square lattice $\mathcal{L}^2$, whose boundary conditions are periodic, with no apriori limit on the number of agents that can be located in a cell; see Section 2.3 for the choice of the lattice parameter values. One time step represents one week and simulations were run for 1000 weeks, i.e., about 19 years.

2.2.3. Process overview and scheduling

At each time step, agents apply a set of rules, whose outcomes depend on random variables and on the local environments, defined as the cell where the agent stands and the eight surrounding cells. One time step corresponds to the implementation of eight modules. First, prey follow the sequence *move*, *reproduce* and *die*. Then predators act in the following order: *move*, *hunt*, *reproduce*, *die* and *migrate*. Within each module, the order between agents is random and updating is asynchronous.

2.2.4. Design concepts

Emergence. The model was formulated so that the emergent behaviour of both population matches the key assumptions of the Rosenzweig–MacArthur model with Allee effect on the prey, cf. Section 2.1; namely we expect the prey to exhibit logistic growth and a strong Allee effect, while the predator should collectively exhibit a Holling type II functional response.

Sensing. Each agent can sense the presence of other agents in their local environment.

Interactions. Three types of inter-agent interactions are explicitly modelled. First, prey interact directly through mating: two prey located in the same local environment can give birth to an offspring. Second, prey interact indirectly through density-dependence: mating cannot occur if the number of prey in the local environment exceeds a threshold. Third, predators and prey interact through hunting: predators can hunt the prey located in their local environment.

Stochasticity. Many processes involve stochasticity. First, there is spatial stochasticity: The movement of each agent is a two-dimensional random walk on $\mathcal{L}^2$. and each new offspring, prey and predator alike, is assigned to a random location. Next, behaviour is stochastic: Most actions, including breeding, dying, hunting, are probabilistic; specifically, they are realised if a random variable, generally drawn from a uniform distribution between 0 and 1, exceeds a threshold value.

Observation. The main data analysed are the prey and predator populations as a function of time, $X(t)$ and $Y(t)$, respectively.

2.2.5. Initialisation

The model is initialised by setting the initial prey and predator populations, $X(0)$ and $Y(0)$, and by assigning each agent a random location on the lattice $\mathcal{L}^2$. A wide range of initial populations $\mathbf{Z}(0)=(X(0), Y(0))$ was tested during preliminary model exploration. For the simulation experiments reported herein, we chose the initial population pair (4000, 500), which leads to the most interesting dynamics.

2.2.6. Input data

The model does not use input from external models or data files.

2.2.7. Submodels – prey modules

Move. Prey move to a randomly selected adjacent cell, whether occupied or not.

Reproduce. When a prey senses at least one other prey in its local environment, and if the local density of prey does not exceed a saturation density S, it has a certain probability b to give birth to another prey. This rule gives rise, at the population level, to two features of the aggregate model: (i) At high density, reproduction is limited by S, which leads to a density-dependent growth rate and (ii) below a certain density, low mating probabilities lead to extinction. The latter phenomenon corresponds to the Allee effect, cf. Fig. 15 in Appendix A. Offspring are assigned to a random cell; doing so avoids prey immediately mating with their offspring.

Die. Each prey dies with probability ν.

2.2.8. Submodels – predator modules

Move. Predators move to a randomly selected adjacent cell, whether occupied or not.

Hunt. When a predator senses prey in its local environment, it has a certain chance s to catch and kill them, but it cannot, in any event, kill more than N prey at a time. This limited handling capacity gives rise, at the population level, to a functional response of type II, cf. Fig. 17 in Appendix A.

Reproduce. After a successful hunt, a predator has a probability κ to breed a number of offspring equal to the number of prey it killed. Like the prey, offspring are randomly located on the lattice. Predators who did not catch any prey cannot breed.

Die. Each predator dies with probability w.

Table 2
Summary of the parameters used in the ABM model.

Parameter	Definition	Value
L	Number of cells along an edge of the square lattice	100
b	Prey's probability to breed when meeting another prey	1
S	Prey's local saturation density	5
ν	Prey's probability to die	0.05
s	Predator's probability to succeed in hunting	0.1
N	Predator's handling saturation	3
κ	Predator's mean conversion rate	$0.21 \leq \kappa \leq 0.7$
w	Predator's probability to die	0.1

Migrate. If all predators disappear but prey survive, a predator is added to the lattice; this model feature avoids premature disappearance of predators due to purely stochastic phenomena.

2.3. Choice of parameter values

The ABM has eight parameters, one more than the ODE model; these eight parameters are defined, and their values given, in Table 2. The objective choosing a set of parameters for the ABM is to approximate macro-level parameters of the aggregate model with corresponding ratios that emerge from the ABM simulations.

We first focus on the Allee effect. In the ODE model, it is characterised by its intensity, measured by the ratio $A/K = 0.1$. In the ABM, for $L = 100$, $b = 1$, $S = 5$, $\nu = 0.05$ and $\mathbf{Z}(0) = (4000, 500)$, the average prey population in the absence of predators is denoted by $\hat{K}$ and it equals 6080. This $\hat{K}$ is the emergent carrying capacity, which mirrors the explicitly-defined parameter K in the ODEs.

By carrying out a series of simulations, we also observe that, when the prey population sinks below 520, it is more likely to go extinct than to recover, cf. Fig. 15 in Appendix A. Additional experiments based on feedback control confirm that this value, denoted $\hat{A}$, is the emergent quantity that corresponds to the Allee effect threshold A; see Appendix A for details. We obtain therewith $\hat{A}/\hat{K} = 0.086$, which is close to $A/K = 0.1$ from Table 1.

The functional response, in turn, is characterised in the ODE model by a logistic curve with a half-saturation constant $S = 0.4$. In the ABM, for $s = 0.1$, $M = 3$ and $w = 0.1$, we observe that the average number of prey killed per predator plateaus at 0.3 when prey are abundant, i.e., $X \geq 9000$. When $X = 2750$, the average kill rate is $0.15 = 0.30/2$, which equals the emerging half-saturation constant $\hat{S}$, cf. Fig. 17 in Appendix A. We obtain $\hat{S}/\hat{K} = 0.45$, which is close to $S/K = 0.4$.

2.4. Numerical experiments and analysis methods

We choose the predator's mean conversion rate κ as the bifurcation parameter. For each value of κ between 0.21 and 0.70, in steps of 0.01, we run the model 100 times and monitor the prey population $X(t)$ and predator population $Y(t)$. Each run differs by the realisation of its random choices in agent actions and lasts for $T_f = 1000$ time steps, i.e., 1000 weeks $\simeq$19 years. We obtain a set of $50 \times 100 = 5000$ time series $X_i^{(\kappa)}(t)$ and $Y_i^{(\kappa)}(t)$, with $\kappa = 0.21, 0.22, \ldots, 0.70$; $i = 1, 2, \ldots, 100$; and $t = 1, 2, \ldots, 1000$. To characterise the dynamics and identify threshold values, we carried out a series of statistical analyses on this output. To deal only with statistically stationary data, we dropped the first 400 points of each time series, so our data set has $5000 \times 600 = 3\,000\,000$ points.

First, for each value of κ, we compute the probability distributions of the corresponding run $X^{(\kappa)}$ and $Y^{(\kappa)}$, and derive the proportion of runs in which prey go extinct (*extinction*), predators go extinct (*prey-only*), or both populations coexist (*coexistence*). Second, the time series in which the two species coexist were analysed using spectral methods. A few examples of such time series are displayed in Fig. 4.

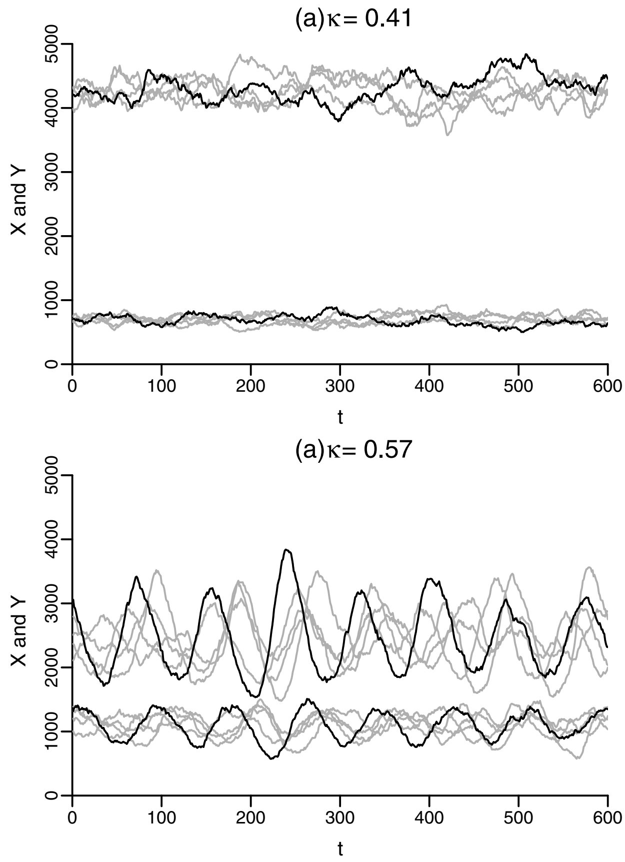

Fig. 4. Time series of the prey population $X^{(\kappa)}(t)$ and the predator population $Y^{(\kappa)}(t)$, shown as the upper and lower curves, respectively. Five simulations with $\kappa = 0.41$ and (b) five simulations with $\kappa = 0.57$. In each panel, one of the simulations is shown as the heavy solid curve, the other four as light solid. The fluctuations in panel (a) are more irregular and have smaller amplitudes than those in panel (b). The use of statistical and spectral methods helps locate the transition between these two regime types.

The ABM model was implemented using NetLogo (Wilenski, 1999). The statistical analyses were performed with the R package (R Core Team, 2012).

It is clear from this figure that the behaviour differs widely as a function of parameter value, with $\kappa = 0.41$ in panel (a) and $\kappa = 0.57$ in panel (b). But, because of the stochastic processes that enter agent behaviour, it is difficult to identify the structure of the underlying attractor: Are the irregular fluctuations of the simulated time series mere random noise around a fixed point, or do they exhibit oscillatory behaviour, which would point to a more complex attractor? How can we locate the transition between the two seemingly distinct regimes in Fig. 4a and b?

For each value of κ, we analyse the time series in which the two species coexist using singular spectrum analysis (SSA) (Vautard and Ghil, 1989; Vautard et al., 1992; Ghil et al., 2002) and Monte-Carlo SSA (MC-SSA) (Allen and Smith, 1989; Ghil et al., 2002). These methods have been widely used in climate dynamics and other areas, including population dynamics (Loeuille and Ghil, 1994). They are presented succintly here and more thoroughly in Appendix B.

SSA decomposes a time series into elementary components that can be classified into trends, oscillatory patterns and noise. Each component is associated with an eigenvector and an eigenvalue of the time series's lag-covariance matrix. An oscillation, whether harmonic or anharmonic, is captured by a pair of nearly equal eigenvalues, whose associated eigenvectors have the same dominant frequency and are in phase quadrature. Typically, oscillatory behaviour can be traced back to deterministic processes that contribute to generate the time series under study (Ghil et al., 2002).

MC-SSA tests the SSA results against a null hypothesis that is modelled by a simpler, purely stochastic process which could have generated it, typically white or red noise. Empirical analyses have shown that ecological time series, and in particular population time series, tend to have a 'red-shifted' spectrum (Pimm and Redfearn, 1988). Consequently, we have chosen to test the time series against the more stringent null hypothesis of red noise.

We are interested in detecting statistically significant oscillatory patterns and apply MC-SSA to identify pairs of eigenvalues at the 5% confidence level or better, as explained in Appendix B. Pairs that survive this test will be called significant pairs of eigenvalues (SPEs) and are indicative of oscillations produced by limit cycles, and not by purely stochastic effects.

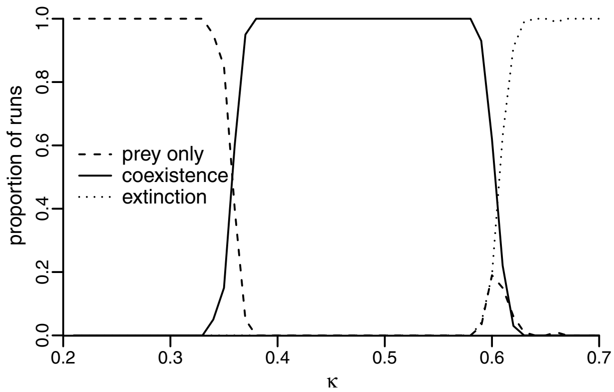

Fig. 5. Proportion of ABM runs reaching one of three possible regimes – prey-only (dashed line), coexistence (solid line) or extinction (dotted line) – as the parameter κ varies, $0.21 \leq \kappa \leq 0.70$.

2.5. Choice of time horizon

Our objective is to identify our predator–prey system's dynamical structure, namely the basins of attractions and bifurcation points. In this perspective, how satisfactory is our choice of $T_f = 1000$ weeks? To appraise the ecological significance of this time horizon, we evaluate the generation times of the two species, defined as the inverse of the respective death rate. We denote these quantities by T_C for the predator and by T_R for the prey. Since the predator death rate is $w = 0.1$ $T_C = 10$ weeks.

The death rate of the prey is the sum of the natural death rate $v = 0.05$ and a predation rate, while the latter is the product of the average number of prey killed per predator and of the predator abundance; this relationship is represented in Fig. 17 of Appendix A. Since the predator population typically ranges between 0 and 1500, as seen in Section 3 below, T_R varies between 8 and 20 weeks. The interval of 1000 weeks used in our study seems, therefore, long enough to capture ecologically significant dynamics, and it suffices in order to avoid the transients due to a choice of initial state alone.

Is this time horizon of 1000 weeks also sufficient in order to account for long-term behaviour? Due to the model's stochastic ingredients, and given long enough simulation intervals, it is quite possible that particular sequences of events that are a priori very unlikely will occur and lead trajectories to change basins of attraction. Since there is no external input of prey, extinction is the only absolutely inescapable regime, into which all trajectories will eventually fall. Focusing on genuinely asymptotic behaviour only would therefore prevent us from identifying the basins of attraction and bifurcation points that, according to the ODE model, do seem to play an important role. The ecologically significant dynamics might thus lie in what can be considered, from an asymptotic standpoint, as merely very long transients (Hastings, 2004). We carried out additional experiments with $T_f = 10\,000$ weeks $\approx$200 years and $T_f = 100\,000$ weeks $\approx$2000 years to assess the robust persistence of each attractor basin identified, along with evaluating associated probabilities.

3. ABM model results

3.1. Dominant regime and fixed points

As in the ODE model, if the initial predator population is large compared to the initial prey population, the prey will go extinct first, followed by the predators. For smaller initial predator populations, several regimes can occur: *extinction*, *prey-only* or *coexistence*, as shown in Fig. 5. As the parameter κ – which measures the reproduction efficiency of the predator – increases, two transitions are detected: the first one between 0.35 and 0.36, where the dominant regime switches from prey-only to coexistence, and the second one between 0.60 and 0.61, where it changes from coexistence to extinction.

During this second transition, we observe a small peak in the number of occurrences of the prey-only regime. In these simulations, the combination of stochastic events with moderate κ values leads to the following scenario: the predators deplete the prey population down to a level close to $\hat{A}$, which is insufficient for predator survival, while the prey population – being freed from predation and with the help of positive stochastic events – is able to persist. For higher κ values, predators deplete the prey population more rapidly, so that it falls well below $\hat{A}$ and thus induces extinction of both populations.

In Fig. 6 we plot, for each κ-value, the distribution of the populations $\{X_i^{(\kappa)}(t)\}$ and $\{Y_i^{(\kappa)}(t)\}$ over the realisations $i = 1, \ldots, 100$, and over the 600-week–long time interval $401 \leq t \leq 1000$. During the first transition, at $\kappa \simeq 0.36$, the average populations $\bar{\mathbf{Z}}^{(\kappa)} = (\bar{X}^{(\kappa)}, \bar{Y}^{(\kappa)})$ change rather smoothly, whereas the second transition, at $\kappa \simeq 0.61$, is marked by a sudden drop in both population averages. Before the collapse, the range of their values increases rather strikingly.

In the prey-only steady state, the prey population fluctuates around $\hat{K} = 6080$, i.e., around a value that is almost 12 times the Allee effect threshold. At this level, only a series of extremely high death rates – combined with very unlikely spatial distributions that severely limit reproduction – could lead the prey towards extinction. The probability of having more than 500 prey dying at once, i.e., still a fairly small number that only corresponds to one-eleventh of the road to extinction is less than 10^{-30}. This basin of attraction is so deep that, even on geological time scales, the prey-only regime can be considered as stable.

The coexistence regime requires a more thorough examination. The presence of predators creates new opportunities for adverse stochastic events; still, their probabilities remain extremely low for moderate κ-values. For $\kappa = 0.57$, additional, 2000-year-long simulations still show that less than 2% of the runs lead to extinction. As we approach the transition at $\kappa \simeq 0.61$, the depth of the basin of attraction decreases and coexistence is less and less likely to persist. Had we initially set the duration of the simulations to 2000 years, rather than 200 years, as in Fig. 6, the transition value of κ would be 0.59 instead of 0.61. This difference is still quite moderate with respect to the size of the basins of attraction, in terms of the parameter κ, as shown in Fig. 5. The robustness of our results upon

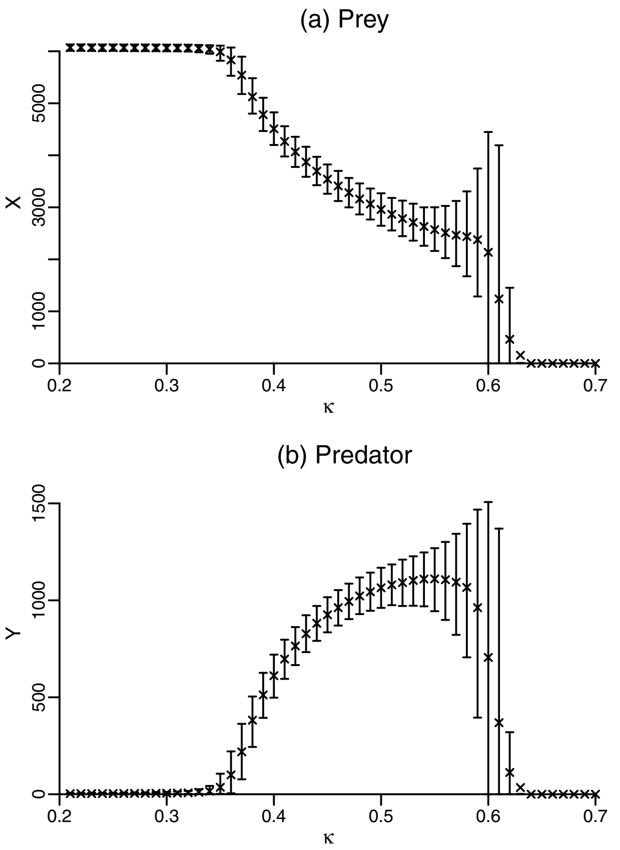

Fig. 6. Spread in the set of all population values for ABM model runs, for the realizations $i = 1, 2, \ldots, 100$ and the time interval $401 \le t \le 1000$, as a function of κ. (a) For the prey population $\{X_i^{(\kappa)}(t)\}$; and (b) for the predator population $\{Y_i^{(\kappa)}(t)\}$, at each κ-value. The $\times$ symbols indicate the average values $\bar{X}^{(\kappa)}$ and $\bar{Y}^{(\kappa)}$, respectively, of the distributions of $100 \times 600 = 60\,000$ points at each κ, while the bars indicate the interval between the 5th and 95th percentiles of this distribution.

using longer simulations thus validates our more computationally convenient time horizon of 1000 weeks $\simeq$200 years.

By examining, in the two panels of Fig. 7, the probability density function (PDF) of the 100 runs $\times$ 600 points in time of the

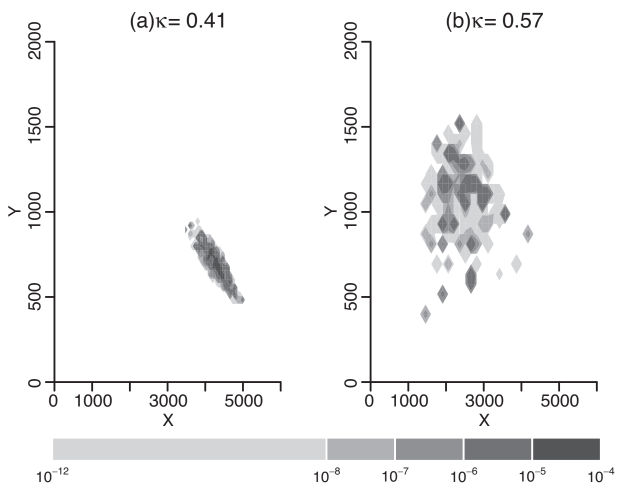

Fig. 7. Estimation of the two-dimensional probability density function (PDF), obtained from 100 runs with 600 points each. (a) $\kappa = 0.41$; and (b) $\kappa = 0.57$. The darker the area, the higher the density; see grey bar for shading values.

Table 3
Location of the Hopf bifurcation.

M	κ-Interval (MCSSA on prey)	κ-Interval (MCSSA on predator)
80	[0.49, 0.50]	[0.49, 0.50]
100	[0.49, 0.50]	[0.49, 0.50]
120	[0.48, 0.49]	[0.48, 0.49]
140	[0.47, 0.48]	[0.48, 0.49]
160	[0.46, 0.47]	[0.46, 0.47]
180	[0.46, 0.47]	[0.46, 0.47]
200	[0.46, 0.47]	[0.46, 0.47]

two simulations at $\kappa = 0.41$ vs. $\kappa = 0.57$, we can distinguish two distinct coexistence regimes. The first regime, in panel (a), is characterised by a well-defined density peak, with lower-density regions falling along a negatively slopped line in the (X, Y) phase plane. This regime corresponds to a fixed point, located at the peak of the PDF, and the negative correlation between prey and predator, away from the peak, reflects the predominance of a top-down regulation (McQueen et al., 1989; Pimm, 1991). The observed negative slope in Fig. 7a is also consistent with the ODE model: near the stable fixed point P_S associated with the coexistence regime, the flow into P_S is tangent to a unique characteristic direction, which has a negative slope; the direction is given by the tangent at P_S to the heteroclinic orbit form the saddle $(K, 0)$; see Fig. 2a.

The second regime, in Fig. 7b, displays no dominant peaks; here, the prey and predator populations are not distributed along a line, but fill a larger area. As we shall see in the next subsection, this regime corresponds to a stochastically perturbed limit cycle.

3.2. Hopf bifurcation and limit cycle

To locate the transition between the two coexistence regimes, we apply MC-SSA to the simulated time series with $0.35 \le \kappa \le 0.61$, using a set of lag-window lengths M between 80 and 200 weeks, in increments of 20; see Table 3. The transition occurs when MC-SSA identifies at least one SPE in more than 50% of the runs. For all values of M in the table, the numerical results locate the transition in the interval $0.46 \le \kappa \le 0.50$. MC-SSA analyses with $M \le 60$ weeks (not shown) rarely reject the null hypothesis of red noise, because the period of the actual oscillations is larger than M; see Table 4. The transition to a statistically significant SPE is illustrated in Fig. 8 by the statistics of the MC-SSA analyses applied to the predator time series with $M = 120$ weeks.

Results based on prey time series and on predator time series are consistent. In most simulations, only one SPE is detected. The application of MC-SSA thus identifies the emergence of a limit cycle for κ in the transition interval [0.46, 0.50]. This transition is equivalent to a Hopf bifurcation. The *oscillatory coexistence* regime lasts from $\kappa = 0.50$ until the transition to the extinction regime, which occurs at $\kappa \simeq 0.60$.

Throughout the oscillatory coexistence regime, the average frequency of the limit cycle is $f = 0.012$ cycle/week, i.e., a period

Table 4
Average periods P in weeks and frequencies $f = 1/P$ in cycles/week that are associated with the main SPEs detected via MC-SSA. The entries in the table are computed for κ-values at which SPEs are detected for more than 50% of the runs.

M	P [weeks] ($f = 1/P$) (SSA on prey)	P [weeks] ($f = 1/P$) (SSA on predator)
80	86.2 (0.0116)	80.6 (0.0124)
100	87.7 (0.0114)	84.7 (0.0118)
120	89.3 (0.0112)	80.6 (0.0124)
140	90.1 (0.0111)	76.9 (0.0130)
160	88.5 (0.0113)	80.0 (0.0125)
180	90.1 (0.0111)	78.1 (0.0128)
200	89.3 (0.0112)	78.7 (0.0127)

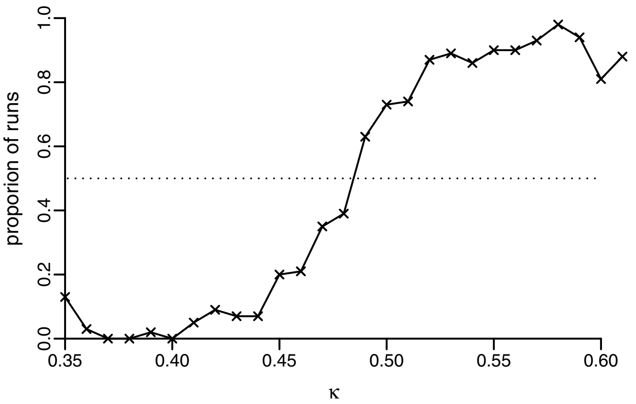

Fig. 8. Proportion of runs for which MC-SSA applied to the predator time series yields at least one SPE; $M = 120$ weeks. We locate the transition κ^* at the point at which the curve crosses the 50% threshold, represented as a dotted line; here $0.48 \leq \kappa^* \leq 0.49$.

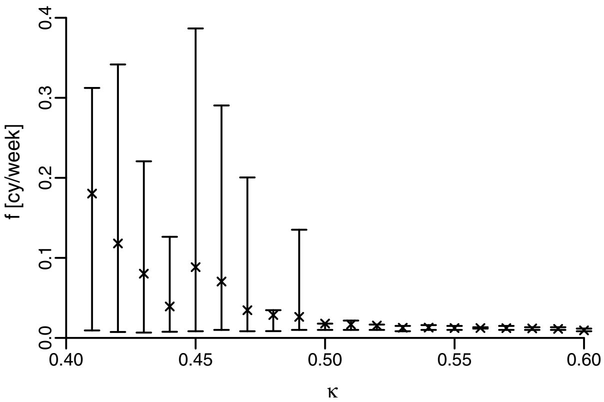

Fig. 9. Average frequencies, expressed in cycle per week, associated with the main SPEs detected by MC-SSA on the predator time series for the same $M = 120$ weeks as in Fig. 8. Same symbols for average and spread as in Fig. 6. The average frequencies before the transition, i.e., for $\kappa \simeq 0.48$, are on the average five times higher than those after the transition, $0.49 \leq \kappa$, namely 0.063 weeks^{-1} and 0.012 weeks^{-1}, respectively.

of about 83 weeks, cf. Table 4. The choice of M barely impacts the identification of the periods, and the results using prey and predator time series are in satisfactory agreement. We do observe a slight bias towards longer periods for the prey, though.

For instance, for $M = 120$ weeks, in 89% of the runs in which SPEs are detected in both time series, the period associated with the prey is identical to the one associated with the predator. But in 86% of the runs in which the periods are not equal – and especially when κ is close to the transition interval [0.46, 0.50], the prey time series displays a larger period. This difference disappears as κ increases, i.e., as the amplitude of the oscillations increases. While this phenomenon has not specifically been addressed here, a method to investigate it in further work is proposed in Section 4.1.

In the steady-state regime, the generation times of the predators and the prey, denoted by T_C and T_R, were 10 weeks and 8–20 weeks, respectively. In the oscillatory coexistence regime, the period of the oscillations varies between 70 and 94 weeks. This periodicity is consistent with the finding of Murdoch et al. (2002), who established that most consumer-resources cycles exceed $4T_C + 2T_R$.

The transition from steady-state to oscillatory coexistence also becomes apparent when looking at the frequencies of the SPEs. We notice in Fig. 9 that the average frequencies of the few SPEs detected before the transition are several times higher than the average frequencies of the SPEs detected after the transition. This transition

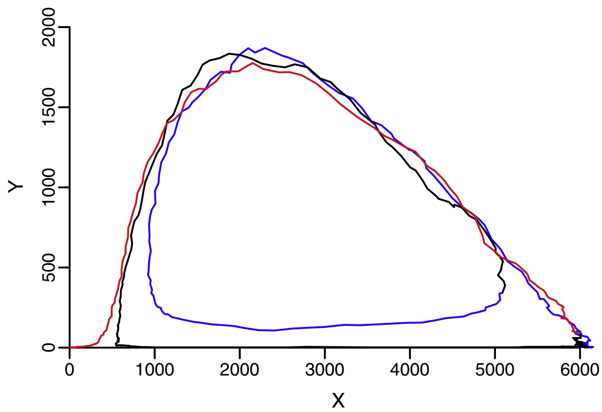

Fig. 10. An ABM simulation that illustrates the model's global bifurcation from a stable limit cycle to a single fixed point, via a heteroclinic orbit; in this particular simulation, $\kappa = 0.61$, $X(0) = 6080$ and $Y(0) = 0$. Along this single trajectory, the colour changes from blue to black to red, in order to highlight the two transient, nearly closed loops, blue and black, before the red segment that terminates in the origin. The larger, black loop is very similar to the heteroclinic curve of the ODE model in Fig. 2b.

from high to low frequencies is also associated with a marked drop in variance. The box-and-whisker diagram (not shown) of the frequencies plotted in Fig. 9 shows that the distributions are markedly asymmetric around the transition, for $0.45 \leq \kappa \leq 0.52$, with the mean lying outside the interquartile range.

The simultaneous jump in period and drop in spread reveals a regime shift between noisy fluctuations around a fixed point – in which rapid and irregular oscillations are detected in a minority of runs, with periodicities between 2 and 20 weeks – and a regular pattern of oscillations with longer periods and larger amplitudes that occur in most runs, with periodicities of 70–94 weeks.

3.3. *Heteroclinic bifurcation*

In the ABM, we observe a global bifurcation pattern that does resemble the one found in the aggregate model, cf. Section 2.1, and illustrated in particular in Figs. 2b and 3: as the limit cycles grow larger, prey have a higher chance to fall below the Allee effect threshold and go extinct, as shown here in Fig. 10. Additional experiments indicate that the actual transition takes place for $0.607 \leq \kappa \leq 0.608$; above this κ-value, extinction occurs in more than half of the runs.

This numerically inferred heteroclinic bifurcation shows two further features: a marked increase of the limit cycle's amplitude (Fig. 6), and period (Fig. 11). These features are present in the ODE model as well – as ρ is increased, the limit cycle that arises from the Hopf bifurcation expands in size and moves closer to the separatrix. The associated increase in amplitude is clearly apparent in Fig. 3 for both prey and predator, in panels (a) and (b), respectively.

Another consequence is that the trajectories get closer to the two saddle points, $(A, 0)$ and $(K, 0)$. They approach each one of them along its stable manifold, and move away along the corresponding unstable manifold. In the vicinity of these two saddles, the rate of change becomes exponentially small. Thus, as ρ tends towards the bifurcation point, the system increasingly slows down in the vicinity of the two saddles, and so the period tends towards infinity; see Fig. 12.

In the ABM, the average periodicity associated with the SPEs is nearly constant throughout most of the oscillatory coexistence domain. When κ exceeds 0.58 and approaches the transition point, the periods get longer and longer; see Fig. 11. After the transition,

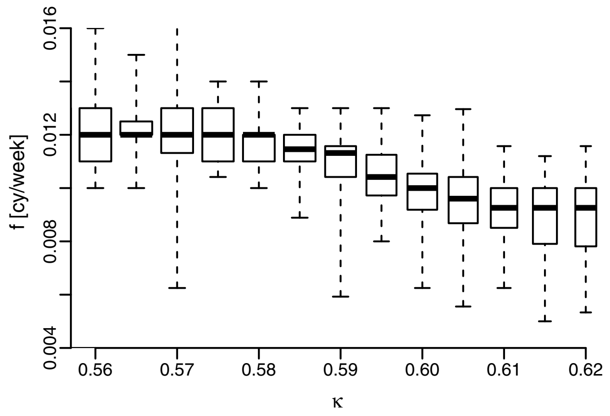

Fig. 11. Box-and-whisker diagram of the frequencies, expressed in cycles per week, associated with the main SPEs detected by MC-SSA on the predator time series for $M = 120$ weeks. The bottom and top of the boxes are the first and third quartiles, the heavy horizontal lines inside the boxes are the medians, and the ends of the whiskers are the extrema. The width of a box is proportional to the square root of the number of observations. There is a marked decrease in the frequencies of the SPEs for $\kappa \geq 0.58$. The results for the prey time series exhibit a similar pattern (not shown).

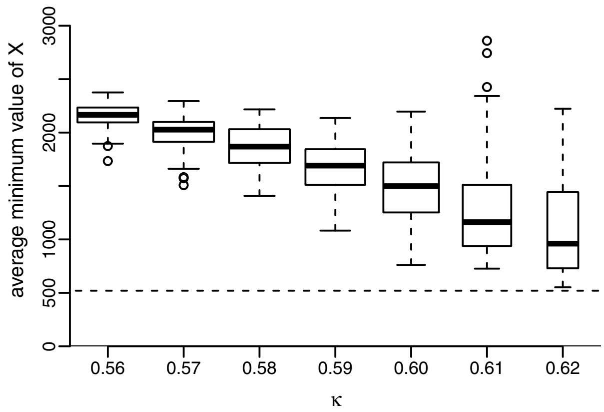

Fig. 13. Box-and-whisker diagram of the average minimum prey abundance during oscillations, as a function of κ. Same conventions as in Fig. 11. The horizontal dashed line shows the Allee effect threshold $\hat{A}$.

in the few runs where extinction does not occur, the periods keep on increasing, but at a slower pace.

The occurrence of a slowing down in the ABM is consistent with the ODE model. As predators become more efficient, they push the prey towards the Allee effect threshold; see Fig. 13. The fewer prey survive, the slower they find partners and repopulate the lattice. More acute depletions of prey lead to larger depletions of predators, whose recovery is delayed. This delay allows prey to get closer to the carrying capacity, before predators recover. This cycle repeats until prey fail to recover and go extinct.

The period in the ABM, though, increases less than that in the ODE model. Because of the discreteness of the state variables and the resulting demographic stochasticity, trajectories do not stay on the limit cycle along which the asymptotic slowing down occurs. They either move back into the hinterland of the coexistence region, where the dynamics is faster, or cross the boundary and fall into extinction. Hence, due to the noise in the ABM, the increase in periodicity remains moderate.

The implications of this slowing-down phenomenon for a potential early warning ahead of the heteroclinic bifurcation will be discussed in Section 4.2.

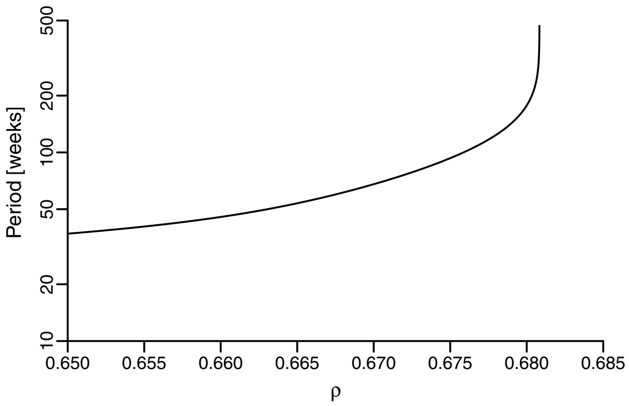

Fig. 12. Period of the limit cycle of the ODE model, in log scale, as a function of ρ.

4. Concluding remarks

4.1. Summary and discussion

Even simple ecological systems can exhibit complex dynamics. In this paper, we have shown that an approach based on a hierarchy of models can be highly effective in exploring such a complex system. At one end of the modelling spectrum, ABMs are arguably best adapted for 'realistic' modelling, inasmuch as many observed features of the individuals that are an ecosystem's building blocks can be plugged in directly. We argue that ABMs should, as much as possible, be developed in conjunction with simpler 'toy' models. Doing so facilitates the analysis, allows one to compare results, and finally to draw robust conclusions. This back-and-forth between different models is also well illustrated by Siekmann (2015) in the case of the dynamics of a two-strain infection process.

In this paper, we focused on a simple predator–prey system, using a deterministic ODE model and a stochastic ABM. Running ABM simulations and analysing their output were computationally intensive and time-consuming tasks. For instance, the application of MC-SSA required the generation and analysis of 200 surrogate data – 100 for the prey time series, and 100 for the predator time series – for each one of the 100 simulations run per ρ value. Given the 50 ρ values used, this yields $200 \times 100 \times 50 = 10^6$ runs.

Nevertheless, the analysis could be conducted efficiently because it was guided by the existence of a much simpler and, in part, analytically tractable ODE model. The process was quite straightforward in this case, since the ABM model was built a priori to share certain features of the aggregate model. Still, the striking success of the guidance provided by the simpler model suggests that this approach might be of great interest across a richer hierarchy of models.

An interesting addition would be a model of intermediate complexity based on stochastic differential equations (SDEs), which combine some of the stochastic features of ABMs with the simple deterministic ones of ODE models. Bifurcations of nonlinear SDEs have been studied by Kuehn (2011), and their usefulness in the climate modelling hierarchy has been demonstrated by Ghil et al. (2008) and Chekroun and Ghil (2011), among others. In particular, SDEs could be used to explore the possible stochastic origin of the bias towards larger periodicities of the prey time series observed in Tab. 4. An explanation might be that stochastic perturbations occasionally block the oscillations of the prey population, leading to larger average periods. To investigate this hypothesis, one could perturb the deterministic aggregate model by adding multiplicative noise – first to one ODE at a time, then to both.

The guidance provided by the ODE model helped us decide on which parameter to control and which bifurcations to expect. But to actually perform the analysis, we needed to carefully design simulation experiments and develop or adapt appropriate statistical methodology. Simple tests were used to detect transitions between the main regimes. For more challenging tasks, such as the detection of the Hopf bifurcation, we tapped into well-established methods of time series analysis. The advanced spectral methods of SSA and its derivatives were used to distinguish large-amplitude, regular and stable oscillations from small-amplitude, irregular fluctuations. A statistical test based on a Monte Carlo algorithm was used to identify oscillatory patterns that significantly differ, at the 5% level, from a red noise process.

Whether applied to the predator or to the prey time series, the analysis indicates a similar location of the Hopf bifurcation, which in addition was robust to changes of the window-width. The transition region from steady states to oscillatory behaviour was also marked by a sharp decrease in the mean and variance of the oscillations' frequencies; this decrease provides further evidence for a transition from a regime of small, rapid and erratic fluctuations to a regime of ample, regular and stable oscillations. MC-SSA thus appears to be well-suited for the detection and analysis of oscillatory dynamics in ABM-simulated time series.

Further methods of time series analysis could be integrated into the toolbox of ABM users. For instance, Kolmogorov entropy or Lyapunov exponents could provide further insights into whether a deterministically chaotic process has participated in generating a given time series (Kantz, 1994; Schouten et al., 1994). The application of such observables to experimental time series is often hampered by the limited length and accuracy of such series; this impediment does not exist for ABM-generated output.

Time series analysis alone does, however, not take advantage of the modeller's ability to freely design simulation experiments. The application of control-based methods – such as the one used to locate the Allee effect threshold, cf. Appendix A – seems to be a promising approach for the dynamical analysis of ABMs. Besides, Kevrekidis and colleagues have developed an 'equation-free' approach, in which macroscopic variables and their derivatives are obtained from microscopically defined models – such as ABMs – through the systematic implementation of a set of appropriately initialised simulations (Kevrekidis et al., 2004). This *coarse-graining* process enables one to use numerical bifurcation methods and it was applied to ABMs describing an epidemiological network (Reppas et al., 2010) and a financial market (Siettos et al., 2012).

Our approach to bifurcation in ABMs conceptually differs from the classic mathematical framework for bifurcation analysis in ODEs. In the latter, bifurcations are precisely defined using the same type of mathematical objects as those used to build the model. For instance, Hopf bifurcations can be precisely detected through the application of the Poincaré–Andronov–Hopf theorem. When needed, numerical methods are employed to compute the local structure of the Jacobian matrix and identify a bifurcation. Bifurcations are, in other words, endogenous to the model.

In this paper we used MC-SSA and defined the Hopf bifurcation as the point at which, in a majority of simulations, we observed the emergence of oscillations that are different from a red noise, at a preset significance level. In this approach, the analytical method used is as important as the ABM formulation for the analysis of the bifurcations.

4.2. Early warnings of a global bifurcation

Studying a hierarchy of models is also instructive in testing results on critical transitions and their ex-ante detection through 'early-warning signals'. The heteroclinic bifurcation present in both of our models belongs to the class of global bifurcations, which are structurally unstable and hence harder to detect numerically (Hale and Koçak, 1991). Moreover, Scheffer et al. (2009) and Boettiger et al. (2013) noted, in fact, that the early-warning signals of such bifurcations have been studied relatively little: most early-warning signals proposed in the literature – namely slowing down of trajectories, as well as increased variance, autocorrelation and skewness – derive from the properties of the saddle-node bifurcation, which belongs to the class of local bifurcations (Hale and Koçak, 1991).

In Section 3.3 we have seen that, in both models, some key features of the limit cycles change as the system approaches the heteroclinc bifurcation. The limit cycles get closer to the boundary of the basin of attraction, their amplitudes increase, and the oscillations slow down as a result of approaching the infinite period of the exact heteroclinic orbit.

This type of period increase differs from the phenomenon known as critical slowing down (CSR) (Wissel, 1984; Nes and Scheffer, 2007). The latter refers to the increase of return time after perturbations near a threshold, due to the real part of the dominant eigenvalue of a fixed point approaching zero. CSR has been theoretically demonstrated, and empirically tested, for a range of local bifurcations, especially for saddle-node bifurcations (Boettiger et al., 2013), and it is interpreted as a loss of resilience in the vicinity of a tipping point (Nes and Scheffer, 2007; Dai et al., 2012).

In the ODE model, after the Hopf bifurcation, the unstable fixed point of region (4) of Fig. 1 becomes more repellent as ρ increases, and the geometry of the flow near it changes. As a consequence, trajectories become gradually more affected by the specific dynamics that occurs in the vicinity of the two saddle points, $(A, 0)$ and $(K, 0)$. The slowing down does not originate from the real part of any eigenvalue vanishing; instead, it is due to a geometrical change of the basin of attraction. Another difference with respect to CSR is that this phenomenon is not observed through exogenous perturbations, but affects the endogenous dynamics of the system, i.e., the limit cycle. Even so, a broad-brush interpretation that is similar to CSR could be proposed, namely, as the parameter ρ – which is the conversion rate of the predator – increases, each population, which is periodically perturbed by the other one, recovers more and more slowly, i.e., it is less resilient.

The system as a whole is also less resilient, as it lies closer to the boundary of the basin of attraction, i.e., it is more 'precarious', in the sense of Walker et al. (2004). This aspect is more adequately captured by the amplitude of the limit cycles, to be compared with some known boundaries of the basin, such as the Allee effect threshold.

The slowing down near the two saddle points is also expected to induce an asymmetry in the distribution of the population abundance. This asymmetry can be captured by computing the skewness of the probability distribution in the time series. Guttal and Jayaprakash (2008) have proposed skewness γ as a potential early-warning signal for local bifurcation: γ is simply a distribution's third standardised moment, and it measures its degree of asymmetry. Given a random variable Z, with mean μ and standard deviation σ, skewness γ is defined as

$$\gamma = E\left[\left(\frac{Z-\mu}{\sigma}\right)\right]. \tag{2}$$

Results presented in Fig. 14 show that, in the ODE model, the asymmetry of both trajectories markedly increases as ρ approaches the bifurcation value 0.6801. The system slows down in regions with few predators, and accelerates when predators are abundant, so that the oscillations of the predator population are unbalanced towards low values. We can show analytically that, due to the strong Allee effect, prey recovery near $(A, 0)$ is much quicker than predator recovery near $(K, 0)$. As a consequence, the slowing down near $(K, 0)$ is more marked than the slowing down near $(A, 0)$, and

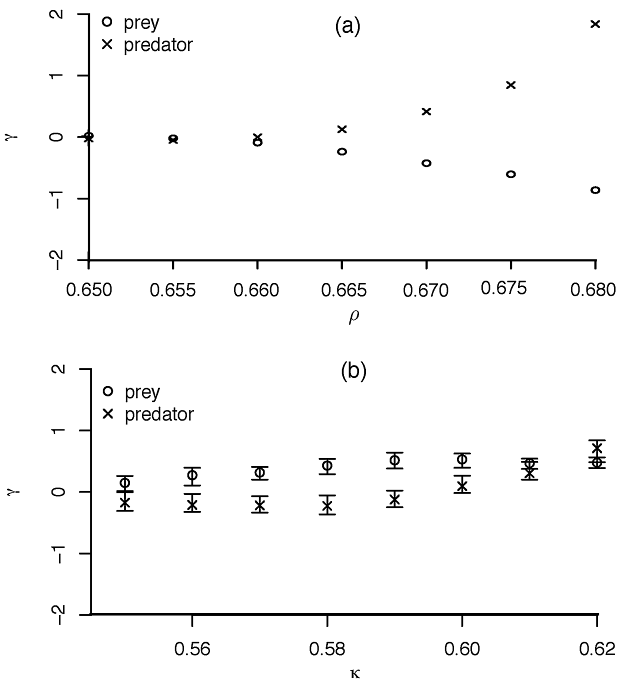

Fig. 14. Skewness γ of the predator and prey time series (a) in the ODE model as a function of ρ and (b) in the ABM model as a function of κ. In panel (b), the vertical bar represents the interquartile range.

the prey distribution tends to be unbalanced towards high values. While Guttal and Jayaprakash (2008) applied skewness to study perturbed trajectories around a fixed point in the vicinity of a local bifurcation, we see in Fig. 14a that this measure can also be used for oscillatory regimes approaching a global bifurcation, but for different dynamical reasons.

Skewness results for the ABM differ widely from the ODE ones; see Fig. 14b. Before the transition, which occurs for $\kappa \simeq 0.60$, the skewness of predator time series moderately increases in average, but we do not observe a decrease for the prey time series. Moreover, the signs of the skewness seem surprising with regards to the ODE results. This points out at one major difference between the two models. In the ABM, the mating requirements for prey, which is not modelled in the ODE, significantly slows down the systems in the $(\hat{A}, 0)$ region. In the ODE, the situation is opposite: because of the strong Allee effect, the growth rate of the prey in the $(A, 0)$ region is higher than in the other regions. The two models therefore exhibits opposite results.

The preceding discussion stresses an interesting slowing down phenomenon, which is different from CSR but, like it, also has considerable potential as an early warning signal. Skewness, however, seems to be more ambiguous as a signal, since its behaviour differs between the aggregate model and the ABM. This discrepancy allowed us to identify rather subtle differences in the formulation of the two models. By using a hierarchy of models, we are, therewith, able to precisely understand the role of each mechanism in the overall dynamics.

4.3. Exogenous and endogenous changes of parameter values

In the ABM, the analyses were carried out for fixed κ-values that are kept constant over the duration of a run. This type of analysis can remain valid for rates of change of κ that are slow compared to the characteristic times of the system's endogenous dynamics, i.e., in the 'adiabatic limit'. We sketch now two possible applications in which κ varies with time.

The simplest application is to add an exogenous rate of change $c = \text{const}.$ for $\kappa(t)$. This scenario could help one study the effect of external forcing that varies smoothly on an ecosystem or a community of species. Rising temperatures have a direct effect on the metabolism, physiology and phenology of organisms; see for instance Bale et al. (2002) for insect herbivores. Exogenously increasing κ can model, for instance, a situation in which rising temperatures tend to increase the predators' reproductive efficiency. We performed additional simulations with $\kappa(0) = 0.55$ and various c-values.

When $c \leq 10^{-5}\kappa$-unit/week, the results obtained in Sections 3 and 4.2 still apply. Both populations go extinct for $\kappa \simeq 0.60$, and this extinction is preceded by a marked increase in the amplitudes and periods of the oscillations. For higher rates of change, extinction occurs more rapidly and fewer oscillations are observed, but it tends to occur for a higher κ-value. For instance, with $10^{-5} < c \leq 10^{-4}\kappa$-unit/week, the prey population crosses the Allee effect threshold after 17 years, on average, and about 10 oscillations are observed. While this number of oscillations suffices in order to observe their increase in amplitude, the increase in period cannot be robustly established.

Another application is to introduce a process which internally modifies κ. We use an evolutionary framework, and set κ as the evolving trait. Instead of being exogenous and common to all predators, we turn this parameter into an endogenous agent-level variable, that predators hand down to their offspring. The transmission process occurs with an additive white noise, characterised by its standard deviation σ. The starting κ-value is set to 0.55 for all predators, and the initial prey and predator abundances are set to (2500, 1400), respectively, in the vicinity of the limit cycle.

In this formulation, the average κ-value of the predator population increases. Predators with higher reproduction efficiency always tend to invade, driving the system to extinction, a situation referred to as evolutionary suicide (Gyllenberg et al., 2002; Ferrière, 2009). With $\sigma = 10^{-3}$, and using 100 repetitions, extinction is reached on average after 85 years, and the final average κ-value is 0.61, as in Fig. 6. Here the average κ varies linearly in time, although some runs exhibit phases of acceleration and deceleration. The amplitude and period of the oscillations increase, as expected. Note that in some runs, prey succeed to survive and repopulate the lattice, which corresponds to the small peak identified in Fig. 5.

4.4. Conclusions

We have built an ABM that reproduces the key mechanisms of the Rosenzweig–McArthur model with strong Allee effect on the prey; the mechanisms of interest are the density-dependent growth rate of the prey and the Allee effect on it, as well as the Holling type II function response of the predator. The bifurcation analysis of the classic ODE model shows that the system can exhibit bistability between extinction and either a prey-alone or a coexistence regime. A Hopf bifurcation divides the coexistence regime into steady-state and oscillatory coexistence. Bistability collapses into a single fixed point through a global bifurcation: the limit cycle becomes a heteroclinic orbit and merges with the separatrix between the two attractors.

The ABM displays the same qualitative behaviour as the aggregate model. Early-warning signals of the critical transition associated with the heteroclinic orbit include the increase in the amplitude and periodicities of the oscillations of both populations.

The study of the ABM was guided by knowledge of the ODE model's behaviour. Going back and forth between the two models allowed us to identify and describe the role of each mechanism, as well as testing the robustness of assumptions about early-warning signals. The solid understanding of the system's dynamical

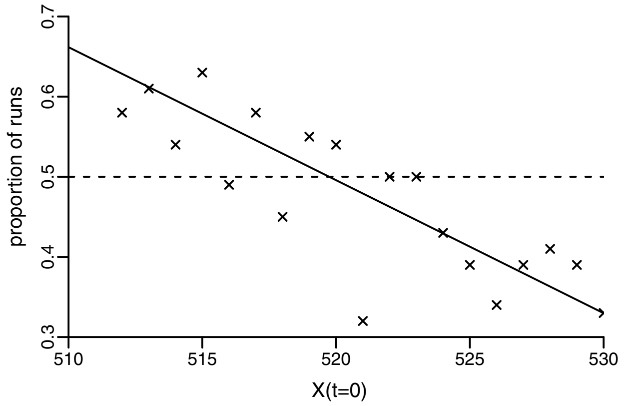

Fig. 15. Proportion of predator-free runs, $Y(0) = 0$, in which prey go extinct as a function of the initial number of prey $X(0) \neq 0$. The $\times$ symbols are the outcomes of numerical simulations, the dashed horizontal line indicates the 50% threshold, and the solid line is the result of linear regression. The two straight lines are used to determine the emerging Allee effect threshold $\hat{A}$.

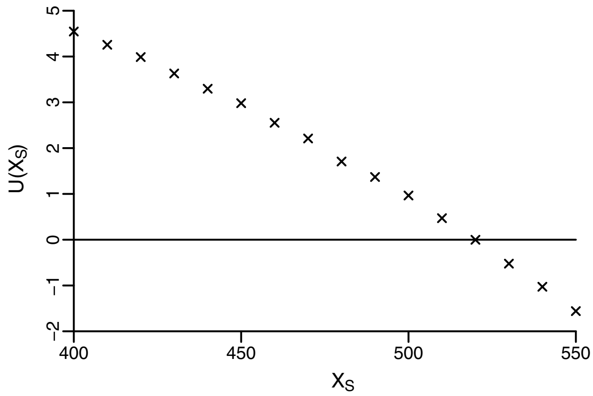

Fig. 16. Average feedback intensity that needs to be applied to the prey after each iteration to maintain the population at X_S. This quantity is the average value of $X(t) - X_S(t)$ for $10\,001 \leq t \leq 20\,000$. Each points correspond to the average value computed for 10 runs; see text for details.

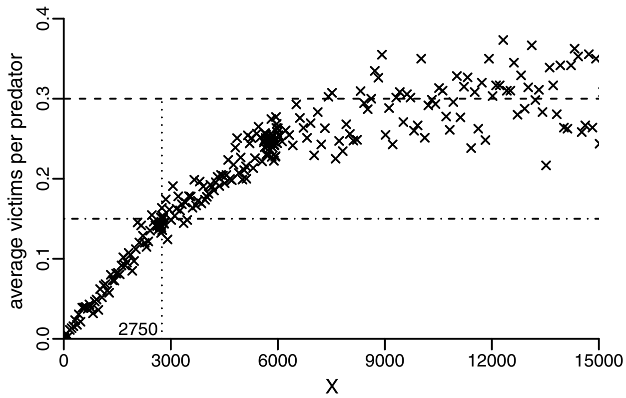

Fig. 17. Average number of prey killed per predator, as a function of prey population X. The horizontal dashed line shows the saturation value of 0.3 that is attained at roughly $X = 9000$, while the dash-dotted horizontal line corresponds to the half-saturation point at 0.15; the latter is attained at the value $X = 2750$, which is indicated by the dotted vertical line.

structure can then be used to evaluate the response of the system to parameter changes, whether these changes are exogenous or endogenous.

The ABM's bifurcations were detected through the use of singular spectrum analysis (SSA) and its derivatives. We argue that ABM practioners facing noisy and seemingly oscillatory responses may benefit from methods of time series analysis. We showed that MC-SSA can reliably detect the transition corresponding to Hopf bifurcation. Studying their Lyapunov exponents and the Kolmogorov entropy could also be of interest in assessing the chaotic behaviour of an ABM-generated process.

We further argue that jointly developing models of different level of complexity, from simple 'toy' models to detailed 'realistic' models, is an appropriate approach to study complex ecological systems. Such a hierarchical approach can effectively guide single-model exploration, help cross-check results, and derive more robust conclusions.

Acknowledgements

It is a pleasure to thank Régis Ferrière and the Ecologie-Evolution (EcoEvo) team from the Ecole Normale Supérieure for discussions and suggestions. Particular thanks are due to Andreas Groth and the Theoretical Climate Dynamics (TCD) group of the University of California at Los Angeles for their help on implementing and applying SSA. This work was supported by a Monge Fellowship of the Ecole Polytechnique (C.C.), by the Agence Nationale de la Recherche through grant PHYTBACK (ANR-10-BLAN-7109) (D.C.), and the European Union project ENSEMBLES, Grant no. 505539 (M.G.).

Appendix A. Choice of parameter values

In this appendix, we illustrate the connection between certain local rules used in our ABM modelling of Section 2.2 and the aggregate properties of our ODE model in Section 2.1. Thus Fig. 15 shows that, below a population of $X = 520$ the prey is more likely to become extinct than not. To confirm that this value is associated with the Allee effect threshold $\hat{A}$, we conducted an additional set of experiments based on feedback control, as suggested by an anonymous reviewer.

In the ODE model, $(X = A, Y = 0)$ is an unstable equilibrium that lies on the X–axis. To locate this point in the ABM, we run at each time step – after implementing all the other procedures in the ODD protocol described in Section 2.2 – a feedback procedure that artificially maintains the prey population at a given value, denoted by X_S. This procedure performs the following tasks: if $X > X_S$, $X - X_S$ prey are randomly removed; conversely, if $X < X_S$, $X - X_S$ prey are randomly added. The asymptotic mean value of $X - X_S$, denoted by $U(X_S)$, measures the sign and the intensity of the feedback that maintain the prey population at X_S. Fig. 16 shows that $U(X_S)$ equals zero when $X_S = 520$ and that it changes sign at this point: when $X_S < 520$, on average, individuals have to be added to maintain the population, while for $X_S < 520$, on average, individuals have to be removed. This result precisely locates the value of $\hat{A} = 520$, which leads in turn to the ABM's emergent $\hat{A}/\hat{K} = 0.086$ being a good approximation to the aggregate model's pre-defined $A/K = 0.1$; see Section 2.2 for details.

The effectiveness of this method at identifying the saddle-node suggests further explorations of the potential applications of control-based approaches for the study of ABMs and their dynamics. It could, in particular, be employed to perform numerical continuation of unstable equilibria or to track periodic solutions, as demonstrated by Barton and Sieber (2013) for physical experiments.

The intersection of the horizontal dash-dotted line in Fig. 17 with the dotted vertical line at $X = 2750$ gives the ABM's emerging half-saturation constant $\hat{S}$ and, therewith, an emerging $\hat{S}/\hat{K} = 0.45$, which is close to the aggregate model's $S/K = 0.4$; see Section 2.2 for details.

Appendix B. Singular spectrum analysis (SSA)

The SSA methodology involves three basic steps: (1) embedding a time series $\{X(t): t = 1, 2, \ldots, N\}$ of length N in a vector space of dimension M – for the choice of M, see Vautard et al. (1992) and Ghil et al. (2002); (2) computing the $M \times M$ lag-covariance matrix C_D of the data – see the two different approaches of Broomhead and King (1986) and Vautard and Ghil (1989); and (3) diagonalizing C_D:

$$\Lambda_D = E_D^T C_D E_D; \tag{B.1}$$

here $\Lambda_D = \mathrm{diag}(\lambda_1, \lambda_2, \ldots \lambda_M)$, with $\lambda_1, \lambda_2, \ldots \lambda_M > 0$ the real, positive eigenvalues of the symmetric matrix C_D, and E_D is the $M \times M$ matrix having the corresponding eigenvectors $\mathbf{E}_\kappa$, $\kappa = 1, \ldots M$, as its columns.

For each $\mathbf{E}_\kappa$ we construct the time series of length $N - M + 1$, called the κ-th principal component (PC); this PC represents the projection of the original time series on the eigenvector $\mathbf{E}_\kappa$, also called empirical orthogonal function (EOF). Each eigenvalue λ_κ gives the variance of the corresponding PC; its square root is called a singular value.

The Monte Carlo version of SSA (MC-SSA) is used to reliably identify oscillations in a time series (Allen and Smith, 1989; Ghil et al., 2002). In MC-SSA, one assumes a simple, random model for the analysed time series, referred to as the null hypothesis. We choose an autoregressive process $Z(t)$ of order one, also called a red noise, as the null hypothesis. The process $Z(t)$ solves

$$Z(t) = a_1[Z(t-1) - Z_0] + \sigma\xi(t) + Z_0, \tag{B.2}$$

where a_1, Z_0 and σ are parameters and ξ is a normally distributed white noise of mean 0 and variance 1. For each time series $X(t)$, the three parameters of the corresponding $Z(t; a_1, Z_0, \sigma)$ are computed by maximum-likehood fitting.

Next, a Monte Carlo ensemble of surrogate time series is generated from the null hypothesis and SSA is applied to the data and to the surrogates, to test whether it is possible to distinguish the original time series from the surrogates. Specifically, the $M \times M$ lag-covariance matrix of the Monte Carlo ensemble is projected onto the EOFs of the analysed time series, and one computes the statistics of the diagonal elements of the projected matrices. If the eigenvalue of a specific EOF of the analysed time series is larger than 95% of the corresponding diagonal elements computed from the surrogates, then the null hypothesis is rejected with a 95% confidence level.

Ghil et al. (2002) provide an overview and a comprehensive set of references; see also their free software at http://www.atmos.ucla.edu/tcd/ssa/.

References

Allen, M., Smith, L., 1989. Monte Carlo SSA: detecting irregular oscillations in the presence of coloured noise. J. Clim. 9, 3373–3404.

Bale, J.S., Masters, G.J., Hodkinson, I.D., Awmack, C., Bezemer, T.M., Brown, V.K., Butterfield, J., Buse, A., Coulson, J.C., Farrar, J., Good, J.E.G., Harrington, R., Hartley, S., Jones, T.H., Lindroth, R.L., Press, M.C., Symrnioudis, I., Watt, A.D., Whittaker, J.B., 2002. Herbivory in global climate change research: direct effects of rising temperature on insect herbivores. Glob. Change Biol. 8 (1), 1–16.

Barton, D.A.W., Sieber, J., 2013. Systematic experimental exploration of bifurcations with noninvasive control. Phys. Rev. E 87 (5), 052916.

Boettiger, C., Ross, N., Hastings, A., 2013. Early warning signals: the charted and uncharted territories. Theor. Ecol. 6 (3), 255–264.

Bonabeau, E., 2002. Agent-based modeling: methods and techniques for simulating human systems. Proc. Natl. Acad. Sci. U. S. A. 99, 7280–7287.

Boukal, D.S., Sabelis, M.W., Berec, L., 2007. How predator functional responses and Allee effects in prey affect the paradox of enrichment and population collapses. Theor. Popul. Biol. 72 (1), 136–147.

Broomhead, D., King, G., 1986. Extracting qualitative dynamics from experimental data. Physica D 20, 217–236.

Chekroun, M.D., Simonnet, E., Ghil, M., 2011. Stochastic climate dynamics: random attractors and time-dependent invariant measures. Physica D 240 (21), 1685–1700.

Crowl, T.A., Crist, T.O., Parmenter, R.R., Belovsky, G., Lugo, A.E., 2008. The spread of invasive species and infectious disease as drivers of ecosystem change. Front. Ecol. Environ. 6 (5), 238–246.

Dai, L., Vorselen, D., Korolev, K.S., Gore, J., 2012. Generic indicators for loss of resilience before a tipping point leading to population collapse. Science 336 (6085), 1175–1177.

De Roos, A.M., Persson, L., 2005. Unstructured population models: do general assumptions yield general theory? In: Cuddington, K., Beisner, B. (Eds.), Ecological Paradigms Lost: Routes of Theory Change. Theoretical Ecology Series. Elsevier Academic Press, Burlington, MA, USA, pp. 31–62.

DeAngelis, D.L., Mooij, W.M., 2005. Individual-based modeling of ecological and evolutionary processes. Annu. Rev. Ecol. Evol. Syst. 36 (1), 147–168.

Dhooge, A., Govaerts, W., Kuznetsov, Y.A., 2003. Matcont: a Matlab package for numerical bifurcation analysis of ODEs. ACM Trans. Math. Softw. 29, 141–164.

Dieckmann, U., Law, R., Metz, J.A.J., 2000. The Geometry of Ecological Interactions: Simplifying Spatial Complexity. Cambridge University Press.

Dijkstra, H.A., Ghil, M., 2005. Low-frequency variability of the large-scale ocean circulation: a dynamical systems approach. Rev. Geophys. 43, RG3002.

Donalson, D.D., Nisbet, R.M., 1999. Population dynamics and spatial scale: effects of system size on population persistence. Ecology 80 (8), 2492–2507.

Durrett, R., Levin, S., 1994. The importance of being discrete (and spatial). Theor. Popul. Biol. 46 (3), 363–394.

Ferrière, R., 2009. Evolutionary Conservation Biology, first ed. Cambridge University Press, Cambridge, UK.

Fussmann, G.F., Ellner, S.P., Shertzer, K.W., Hairston Jr., N.G., 2000. Crossing the Hopf bifurcation in a live predator–prey system. Science 290 (5495), 1358–1360.

Ghil, M., 2001. Hilbert problems for the geosciences in the 21st century. Nonlinear Process. Geophys. 8, 211–222.

Ghil, M., Allen, M.R., Dettinger, M.D., Ide, K., Kondrashov, D., Mann, M.E., Robertson, A.W., Saunders, A., Tian, Y., Varadi, F., Yiou, P., 2002. Advanced spectral methods for climatic time series. Rev. Geophys. 40 (1), 3-1–3-41.

Ghil, M., Chekroun, M.D., Simonnet, E., 2008. Climate dynamics and fluid mechanics: natural variability and related uncertainties. Physica D 237, 2111–2126.

González-Olivares, E., González-Yañez, B., Mena-Lorca, J., Ramos-Jiliberto, R., 2006. Modelling the Allee effect: are the different mathematical forms proposed equivalents? In: Mondaini, R. (Ed.), Proceedings of the 2006 International Symposium on Mathematical and Computational Biology BIOMAT 2006.

Gras, R., Devaurs, D., Wozniak, A., Aspinall, A., 2009. An individual-based evolving predator–prey ecosystem simulation using a fuzzy cognitive map as the behavior model. Artif. Life 15 (4), 423–463.

Grimm, V., Berger, U., Bastiansen, F., Eliassen, S., Ginot, V., Giske, J., Goss-Custard, J., Grand, T., Heinz, S.K., Huse, G., Huth, A., Jepsen, J.U., Jørgensen, C., Mooij, W.M., Müller, B., Pe'er, G., Piou, C., Railsback, S.F., Robbins, A.M., Robbins, M.M., Rossmanith, E., Rüger, N., Strand, E., Souissi, S., Stillman, R.A., Vabø, R., Visser, U., DeAngelis, D.L., 2006. A standard protocol for describing individual-based and agent-based models. Ecol. Model. 198 (1–2), 115–126.

Grimm, V., Berger, U., DeAngelis, D.L., Polhill, J.G., Giske, J., Railsback, S.F., 2010. The ODD protocol: a review and first update. Ecol. Model. 221 (23), 2760–2768.

Grimm, V., Railsback, S.F., 2005. Individual-Based Modeling and Ecology. Princeton University Press, Princeton.

Grimm, V., Wyszomirski, T., Aikman, D., Uchmanski, J., 1999. Individual-based modelling and ecological theory: synthesis of a workshop. Ecol. Model. 115 (2–3), 275–282.

Guttal, V., Jayaprakash, C., 2008. Changing skewness: an early warning signal of regime shifts in ecosystems. Ecol. Lett. 11 (5), 450–460.

Gyllenberg, M., Parvinen, K., Dieckmann, U., 2002. Evolutionary suicide and evolution of dispersal in structured metapopulations. J. Math. Biol. 45 (2), 79–105.

Hale, J.K., Koçak, H., 1991. Dynamics and Bifurcations. No. 3 in Texts in Applied Mathematics. Springer-Verlag, New York.

Hastings, A., 1990. Spatial heterogeneity and ecological models. Ecology 71 (2), 426–428.

Hastings, A., 2004. Transients: the key to long-term ecological understanding? Trends Ecol. Evol. 19 (1), 39–45.

Kantz, H., 1994. A robust method to estimate the maximal Lyapunov exponent of a time series. Phys. Lett. A 185 (1), 77–87.

Kevrekidis, I.G., Gear, C.W., Hummer, G., 2004. Equation-free: the computer-aided analysis of complex multiscale systems. AIChE J. 50 (7), 1346–1355.

Kuehn, C., 2011. A mathematical framework for critical transitions: bifurcations, fast-slow systems and stochastic dynamics. Physica D 240 (12), 1020–1035.

Lavergne, S., Mouquet, N., Thuiller, W., Ronce, O., 2010. Biodiversity and climate change: integrating evolutionary and ecological responses of species and communities. Annu. Rev. Ecol. Evol. Syst. 41 (1), 321–350.

Law, R., Dieckmann, U., 2000. Moment approximations of individual-based models. In: Dieckmann, U., Law, R., Metz, J.A. (Eds.), The Geometry of Ecological Interactions: Simplifying Spatial Complexity. Cambridge University Press, Cambridge, pp. 252–270.

Lindegren, M., Möllmann, C., Nielsen, A., Brander, K., MacKenzie, B.R., Stenseth, N.C., 2010. Ecological forecasting under climate change: the case of Baltic cod. Proc. R. Soc. Lond. B: Biol. 277 (1691), 2121–2130.

Loeuille, N., Ghil, M., 1994. Intrinsic and climatic factors in North-American animal population dynamics. BMC Ecol. 4 (6), 12.

Łomnicki, A., 1999. Individual-based models and the individual-based approach to population ecology. Ecol. Model. 115 (2–3), 191–198.

Mccauley, E., Wilson, W.G., De Roos, A.M., 1993. Dynamics of age-structured and spatially structured predator–prey interactions: individual-based models and population-level formulations. Am. Nat. 142 (3), 412–442.

McQueen, D.J., Johannes, M.R.S., Post, J.R., Stewart, D.J., Lean, D.R.S., 1989. Bottom-up and top-down impacts on freshwater pelagic community structure. Ecol. Monogr. 59 (3).

Murdoch, W.W., Kendall, B.E., Nisbet, R.M., Briggs, C.J., McCauley, E., Bolser, R., 2002. Single-species models for many-species food webs. Nature 417 (6888), 541–543.

Nes, E.H.V., Scheffer, M., 2007. Slow recovery from perturbations as a generic indicator of a nearby catastrophic shift. Am. Nat. 169 (6), 738–747.

Pimm, S.L., 1991. The Balance of Nature? University of Chicago Press, Chicago, IL, USA.

Pimm, S.L., Redfearn, A., 1988. The variability of population densities. Nature 334 (6183), 613–614.

R Core Team, 2012. R: A Language and Environment for Statistical Computing. R Foundation for Statistical Computing, Vienna, Austria http://www.R-project.org/, ISBN 3-900051-07-0.

Railsback, S.F., Grimm, V., 2011. Agent-Based and Individual-Based Modeling: A Practical Introduction. Princeton University Press, Princeton.

Reppas, A.I., Tsoumanis, A.C., Siettos, C.I., 2010. Coarse-grained bifurcation analysis and detection of criticalities of an individual-based epidemiological network model with infection control. Appl. Math. Model. 34 (3), 552–560.

Scheffer, M., Bascompte, J., Brock, W.A., Brovkin, V., Carpenter, S.R., Dakos, V., Held, H., van Nes, E.H., Rietkerk, M., Sugihara, G., 2009. Early-warning signals for critical transitions. Nature 461 (7260), 53–59.

Schneider, S.H., Dickinson, R.E., 1974. Climate modeling. Rev. Geophys. Space Phys. 12, 447–493.

Scholl, H.J., 2001. Agent-based and system dynamics modeling: a call for cross study and joint research. In: Proceedings of the 34th Annual Hawaii International Conference on System Sciences, Vol. 3, Manui, Hawaii.

Schouten, J.C., Takens, F., van den Bleek, C.M., 1994. Maximum-likelihood estimation of the entropy of an attractor. Phys. Rev. E 49 (1), 126–129.

Siekmann, I., 2015. Bifurcation analysis of individual-based models in population dynamics. Ecol. Complex., 21.

Siettos, C.I., Gear, C.W., Kevrekidis, I.G., 2012. An equation-free approach to agent-based computation: bifurcation analysis and control of stationary states. Europhys. Lett. 99 (4), 48007.

Valladares, F., Matesanz, S., Guilhaumon, F., Araújo, M.B., Balaguer, L., Benito-Garzón, M., Cornwell, W., Gianoli, E., van Kleunen, M., Naya, D.E., Nicotra, A.B., Poorter, H., Zavala, M.A., 2014. The effects of phenotypic plasticity and local adaptation on forecasts of species range shifts under climate change. Ecol. Lett. 17 (11), 1351–1364.

van Baalen, M., 2000. Pair approximations for different spatial geometries. In: Dieckmann, U., Law, R., Metz, J.A. (Eds.), The Geometry of Ecological Interactions: Simplifying Spatial Complexity. Cambridge University Press, Cambridge, pp. 359–387.

van Voorn, G.A.K., Hemerik, L., Boer, M.P., Kooi, B.W., 2007. Heteroclinic orbits indicate overexploitation in predator–prey systems with a strong Allee effect. Math. Biosci. 209 (2), 451–469.

Vautard, R., Ghil, M., 1989. Singular spectrum analysis in nonlinear dynamics, with applications to paleoclimatic time series. Physica D 35, 395–424.

Vautard, R., Yiou, P., Ghil, M., 1992. Singular spectrum analysis: a toolkit for short noisy chaotic signals. Physica D 58, 95–126.

Walker, B., Holling, C.S., Carpenter, S.R., Kinzig, A., 2004. Resilience, adaptability and transformability in social-ecological systems. Ecol. Soc. 9 (2), 5.

Wang, J., Shi, J., Wei, J., 2011. Predator–prey system with strong Allee effect in prey. J. Math. Biol. 62 (3), 291–331.

Wilenski, U., 1999. NetLogo. http://ccl.northwestern.edu/netlogo/.

Wissel, C., 1984. A universal law of the characteristic return time near thresholds. Oecologia 65 (1), 101–107.

Chapter 5

Economic networks: Heterogeneity-induced vulnerability and loss of synchronization

This paper has been submitted to the journal *Chaos*, for a focus issue entitled: *Synchronization in Large Networks and Continuous Media: Data, Models and Supermodels*.

Authors: Célian Colon and Michael Ghil

Abstract: Interconnected systems are prone to propagation of disturbances, which can under mine their resilience to external perturbations. Propagation dynamics can clearly be affected by potential time delays in the underlying processes. We investigate how such delays influence the resilience of production networks facing disruption of supply. We model interdependencies between economic agents via Boolean delay equations (BDEs), which allow one to introduce heterogeneity in production delays and in inventories. Complex network topologies are considered that reproduce realistic economic features, including a network of networks. Perturbations that would otherwise vanish can, because of delay heterogeneity, amplify and lead to permanent disruptions. This phenomenon is enabled by the interactions between short cyclic structures. Difference in delays between two interacting, and otherwise resilient, structures can in turn lead to loss of synchronization in damage propagation and thus prevent recovery. Finally, this study also shows that BDEs on complex networks can lead to metastable relaxation oscillations, which are damped out in one part of a network while moving to another part.

Economic networks:
Heterogeneity-induced vulnerability and loss of synchronization

Resilience is increasingly proposed as a highly desirable property of many socioeconomic systems, including populations that face natural disasters[1,2], communities living on natural resources[3], financial systems[4], or competitive companies[5]. Resilience building is seen as an adequate response to the perceived rising economic, geopolitical and environmental uncertainties, and to the threat of climate change and of the associated changes in the number and size of extreme events[6–8]. This trend is particularly marked for financial markets and supply chains, where globalization, decentralization and increased interconnectedness between economic agents are perceived as multiplying the sources of risks and their potential propagations[9,10]. We formulate a toy model for economic networks facing production disruptions, and identify mechanisms that foster or deteriorate resilience. Delays in production and inventories influence how localized disruptions ripple in the network and amplify. We found that heterogeneity in delays or inventories increases vulnerability to shocks, especially in strongly interdependent industries. The corresponding dynamics may be interpreted as a loss of synchronization between economic processes, that we uncover using Boolean delays equations (BDEs).

I. INTRODUCTION AND MOTIVATION

To frame our study, we use the well-established definitions of resilience proposed in ecology — where the concept originated[11] and adapted to the analysis of dynamical systems in general. Resilience can be evaluated using one or more of three metrics: the size of the basin of attraction of a specific dynamical regime[12,13]; the speed at which a system, after a given perturbation, bounces back to its attractor[14]; and the intensity of the perturbation that a system can sustain without switching to another, less desirable attractor[15]. The word 'metric' here is not used in its strict mathematical acceptance as a distance between two points in an arbitrary space but in the broader sense used in measuring performance[16].

We study these three metrics in a toy model for production networks. Dynamical models have been proposed to examine the propagation of supply disruptions in interfirm or intersector input–output networks. The emergence and the amplitude of cascading failures[17,18] and their potential consequences for production location[19] have been investigated. The relationship between network structure and vulnerability has recently been explored[20,21], as well as the role of adaptive agent behavior[22] and that of delays[23]. We note that the questions addressed by these models do have conceptual connections with epidemic modeling, which focuses on the spreading of human diseases or of computer viruses across a network of agents[24].

In this paper, we focus on the role of heterogeneities that are present at the network, node and link levels. First, production networks are reported to have high heterogeneity in connectivity, with few highly connected firms interacting with more peripheric ones. Fujiwara and Aoyama[25] have analyzed the power-law distributions of in- and out-degrees, which can influence how localized shocks aggregate Acemoglu *et al.*[26]. Vulnerability of various network structures has been studied in other types of models: in general network theory[27], in load network dynamics[28–31], in epidemic-spreading models[32,33] and, most recently, in networks of networks[34].

Furthermore, many node-level characteristics are heterogeneous in economic networks, such as their size[35]. Gabaix[36] found that a power-law distribution of firm size can affect the aggregate volatility of economies. Few models have incorporated firm-level heterogeneities in economic dynamics, with the exception of Hallegatte[37], who found that heterogeneity in capacity or in inventory can amplify supply-side shocks.

Finally, all links are not equivalent. In particular, they are associated with delays, which primarily originate from decision-making, production and transportation. They represent a key concern in operations research[38], since they can lead to mismanagement of inventories, synchronization issues and oscillations. A key example, which has been empirically and experimentally verified, is the bullwhip effect[39]. Still, with the exception of the stock market model developed by Miśkiewicz[40], no economic network model incorporates link delays. In epidemic models, delays have been shown to foster the outbreak of epidemics[41,42], but the effect of delay heterogeneity has not been tackled so far. Buzna, Peters, and Helbing[43] have developed a model of load dynamics on networks with uniformly distributed delays, but the role of inhomogeneity in the delays was not included.

Understanding the role of delay heterogeneity in networks is therefore of interest in a variety of fields. For economic networks Coluzzi *et al.*[23] took a first step in this direction, and their contribution is the basis of the present paper. We investigate here the influence of heterogeneity in connectivity, inventory and delays on the resilience of production networks. To do so, we formulate a model governed by a coupled system of Boolean delays equations (BDEs), whose Boolean variables evolve in continuous time[44,45].

The BDE framework is useful in building simple models of complex nonlinear systems. They allow one to simplify many components while fully retaining some core dynamical ingredients: threshold behavior, multiple feedbacks, and distinct time delays[46]. In fact, the behavior of Boolean networks with homogeneous delays that use exclusively the 'AND' operator is well documented[47]. More general BDEs — with arbitrary Boolean operators and with heterogeneous delays — have been successfully applied to the study of climate dynamics[48,49], earthquake physics[50,51] and genomics[52].

Our BDE model is based on Coluzzi *et al.*[23], extended to incorporate inventories. It encompasses four elements: (i) production based on complementary inputs; (ii) heterogeneous production and delivery delays; (iii) heterogeneous inventories; and (iv) supplier–buyer networks with heterogeneous connectivity. The addition of a simple economic process allows us to go one step beyond the static effect of network structures on resilience. Thanks to the BDE framework, we can focus on the key nonlinear components of this economic dynamics: production interdependencies, heterogeneous delays and inventories.

To analyze the effects of heterogeneous connectivity, we developed a class of scale-free networks that exhibits some empirical features of real economic networks. Specifically, Fujiwara and Aoyama[25] studied a large dataset of over 1 million Japanese firms and their supply relationships, provided by the company Tokyo Shoko Research Ltd. They found that the distributions of in- and out-degrees have a power-law distribution for degrees between 10 and 1000, followed by an exponential decay for higher degree, and an average connectivity of 4. The exponents of the cumulative distributions $P_>(k)$ of in- and out-degree are respectively 1.35 ± 0.02 and 1.26 ± 0.02, where the error corresponds to 1.96 times the estimated standard deviation. We generate a class of networks that reproduce these features, which we call SF–FA networks — SF for scale-free and FA for Fujiwara and Aoyama — and compare their behavior with that of Erdős–Rényi (ER) networks.

Finally, we also explore networks of networks, which can represent the interdependence between specific economic sectors, such as water, food and energy supply[34]. This setting allows us to study the effects of synchronization and the loss thereof on resilience.

We use our model to evaluate dynamical response to local perturbations. Initially, all agents fully produce except one who gets temporarily disrupted. This initial perturbation may spark a wave of disruptions, that may vanish or induce permanent disruptions. Through extensive simulations, we characterize the network behavior and evaluate the influence of heterogeneity in inventories and in delays. We use the three previously mentioned metrics to gauge resilience: size of the attractor basin of the full activity state, transient speed, and perturbation intensity. We then propose a resilience indicator and discuss its implications for resilience building. Our results also include intriguing synchronization behavior, such as metasable relaxation oscillations, recalling the importance of delays in network synchronization[53].

In Sec. II, we first formulate the BDE model and its delays. Next, the simulation routines and the algorithm generating the classes of networks investigated are specified. In Sec. III, we start our investigation by studying how a single perturbation propagates in fundamental network motifs. We build a probabilistic model to analyze the propagation in simple acyclic structures in Sec. III A, and in Secs. III B–III D, we identify the key mechanisms that can prevent network recovery.

Section IV provides results for large interfirm networks. Guided by the results of the previous sections, we study in Sec. IV A the global and local structures of SF–FA networks that influence resilience, and contrast this analysis with ER networks. Sec. IV B presents the effects of heterogeneity in inventories and in delays.

In Sec. V, we turn to systems of interdependent networks, and show how differences between the networks can affect vulnerability via loss of synchronization. We measure in Sec. VI the critical role played by individual agents and derive an aggregate resilience indicator. Finally, we discuss in Sec. VII potential implications for resilience building, suggest several extensions, and comment on the role of synchronization in network resilience.

II. METHOD

A. A dynamical model of supplier–buyer networks

The economy is modeled here as a network, in which each agent is represented as a node and produces using inputs from other agents. These dependence relationships are represented by directed links. The topology of the network is captured by an $n \times n$ connectivity matrix $M = (m_{ij})$, where n is the number of agents, and $m_{ij} = 1$ if agent i supplies agent j, and $m_{ij} = 0$ otherwise. No agent can supply itself, i.e. $m_{ii} = 0$. Some agents are primary producers, and produce without supplier.

Each of the n agents can only be in one state, modeled as a Boolean variable x_i with $i = 1, .., n$: either it is fully active, $x_i = 1$, or it is disrupted and $x_i = 0$. A fully active agent is able to deliver its outputs to its clients.

The Boolean variable x_i is continuously updated over time via delay equations. Each supplier–buyer relationship is characterized by a delay, denoted by τ_{ij}; this delay represents the time it takes agent j to produce and deliver inputs to agent i. With the exception of primary producers, all agents need inputs from each one of their suppliers, and they produce upon the simultaneous reception of all inputs.

In the absence of inventories, full activity of an agent i depends exclusively on the set $\mathcal{S}(i)$ of its suppliers, and the n variables are updated as follows:

$$x_i(t) = \begin{cases} 1, & \text{if } \mathcal{S}(i) = \emptyset, \\ \prod_{j \in \mathcal{S}(i)} x_j(t - \tau_{ji}), & \text{otherwise.} \end{cases} \tag{1}$$

Here the operator $\prod$ is the repeated Boolean product 'AND', and we use the usual notation AND $\equiv \wedge$ and OR $\equiv \vee$.

We assume that agents hold inventories that allow them to stay active when their supply is disrupted. A second Boolean variable, y_i, is attached to each agent: it represents the availability, $y_i(t) = 1$, or unavailability, $y_i(t) = 0$, of agent i's inventory at time t. Disruption, $x_i(t) = 0$, only occurs if agent i does not receive some supply while its inventory is depleted; see Eq. (2a) below.

Inventory is created through production: when agent i receives all its supply simultaneously, i.e. when $\prod_{j \in \mathcal{S}(i)} x_j(t - \tau_{ji}) = 1$, then i produces and it both delivers outputs to clients and replenishes its own inventory; the latter will be available after λ_i time units; see Eq. (2b) below. This real-valued quantity represents the size of the inventory: agents with large λ_i can stand longer external perturbations, because their production can be stored for a larger period of time.

For non-primary producers, the dynamical system for $x_i(t)$ and $y_i(t)$ is:

$$x_i(t) = y_i(t) \vee \prod_{j \in \mathcal{S}(i)} x_j(t - \tau_{ji}), \tag{2a}$$

$$y_i(t) = \prod_{j \in \mathcal{S}(i)} x_j(t - \tau_{ji} - \lambda_i). \tag{2b}$$

Equation (2b) can be substituted into (2a), yielding a single dynamical equation for activity:

$$x_i(t) = \prod_{j \in \mathcal{S}(i)} x_j(t - \tau_{ji} - \lambda_i) \vee \prod_{j \in \mathcal{S}(i)} x_j(t - \tau_{ji}). \tag{3}$$

Note that the system of BDEs in this equation is partially dissipative, in the precise sense defined by Ghil and Mullhaupt [45] and reviewed by Ghil, Zaliapin, and Coluzzi [46]. Therefore, we expect the solutions for all the network topologies and combinations of delays and inventories that will be considered herein to contain initial transients and lead to asymptotic behavior — whether stationary, periodic or aperiodic — in finite time. Some of the transients, however, may be very long, as found already by Coluzzi *et al.* [23].

B. Small perturbations and key observables

This dynamical system has a trivial fixed-point attractor: if all agents are active, i.e. if $x_i(t) = 1$ for $i = 1, \ldots, n$, the system remains stationary. We study the resilience of this attractor, called full activity, to small perturbations: How quickly and how far do external perturbations propagate? Does the network always get back to full activity, or can perturbations push the system into other alternative states? How does the network topology and the heterogeneity of delays and inventories influence such behavior?

An external perturbation is defined as the shutdown of a single agent's production over a certain time interval, denoted by δ_0. We primarily focus on the consequences of such perturbations that occur in isolation. For an initial perturbation δ_0 affecting agent r, the initial state is formulated as follows: for all $i = 1, \ldots, n$ and for $t \leq 0$, $x_i(t)$ equals one. From $t = 0$ onward, all the $x_i(t)$'s are updated according to Eq. (3), except $x_r(t)$, which is maintained at 0 for $0 \leq t < \delta_0$. Unless otherwise specified, we set $\delta_0 = 1$.

We will monitor how such initial perturbations propagate throughout the network. In particular, they may create propagating "waves" of disrupted agents that are either damped out or continue to propagate indefinitely. The key observable is the relative number of fully active agents over time, denoted by $\rho(t)$:

$$\rho(t) = \frac{\sum_{i=1}^{n} x_i(t)}{n}. \tag{4}$$

Alternative attractors are characterized by their dimension in the space $\mathbb{Z}_2^n$, where $\mathbb{Z}_2 = \{0, 1\}$, and by the average asymptotic value of fully active agents, denoted by ρ_∞. If the asymptotic regime is a fixed point, ρ_∞ is the value of $\rho(t)$ at this point. If it is periodic, ρ_∞ is the average value of $\rho(t)$ over one period. When ρ_∞ is below 0.5, most agents are not fully active anymore, and the network is said to have collapsed.

Transients are characterized by the speed and amplitude of the propagating wave. We observe the ensemble $\mathcal{A}$ of agents that get perturbed at least once following the initial perturbation. The cardinal of $\mathcal{A}$, denoted by α, measures the propagation amplitude. We also record the time at which each agent in $\mathcal{A}$ gets perturbed for the first time. The time of first perturbation, denoted by t_i, is such that $x_i(t) = 1$ for $t < t_i$ and $x_i(t_i) = 0$. The average time of first perturbation, denoted by θ, is a proxy for propagation speed: for comparable amplitudes α, wave with a small θ propagates faster than one with a high θ.

C. Numerical experiments and network topologies

We start in Sec. III by a detailed investigation on how perturbations propagate in fundamental network motifs, such as lines, trees, and loops. We particularly focus on interacting multiples loops. These studies allow us to identify the key propagation mechanisms that can lead, in more complex networks, to alternative attractors. For these simple structures, we build a probabilistic model to analyze how particular distributions of delays and inventories influence propagation. We use in particular lognormal, exponential and uniform probability distributions.

In Sec. IV, we analyze how the distributions of delays and inventories affect the resilience of SF–FA and ER networks. To generate SF–FA networks, we use the algorithm first proposed by Goh, Kahng, and Kim[54], in the form used by Chung and Lu[55]. The number of incoming and outgoing links attributed to each node is proportional to a weight, or load factor. For a network with n nodes, the factor of the i^{th} node is $(i+i_0-1)^{-1/(\gamma-1)}$, where γ is the targeted power-law exponent, and i_0 an integer used to introduce an exponential decay for high degrees. To match the results of Fujiwara and Aoyama[25] for their huge data set of Japanese firms, we use γ-values of 1.35 for in-degrees and of 1.26 for out-degrees, while i_0 is set to 12. The connectivity c is defined as the average number of in- and out-degrees per agent, and it is set to 4, i.e. there are 4 times more links than nodes.

Directed ER networks are generated through the so-called $\mathcal{G}(n, m)$ algorithms, where n denotes the number of nodes and m the number of links[56]. To compare with SF–FA networks, we choose $m = 4n$. Unless otherwise specified, all networks have $n = 10^3$ agents. This number is large enough to be in qualitative agreement with the behavior of larger networks, and low enough to be computationally feasible when exploring large regions of the parameter space.

We design a simulation routine to comprehensively assess the behavior of the network from all possible initial perturbations. For networks with n agents, this routine consists of n simulations. Each of these simulations corresponds to the initial perturbation of a different agent. For instance, in the k^{th} simulation, agent k is initially perturbed, and we measure the propagation amplitude $a^{(k)}$, the average time of first disruption $\theta^{(k)}$ and the asymptotic average density of fully active agents $\rho_\infty^{(k)}$. The statistics of the n-member ensembles $\{\alpha^{(k)}\}$, $\{\theta^{(k)}\}$ and $\{\rho_\infty^{(k)}\}$ captures the system's response to small perturbations. We denote the mean of these three ensembles by A, Θ and R_∞, respectively.

We first study the homogeneous case, where all delays and inventories are equal, i.e. $\tau_{ij} \equiv \tau$ and $\lambda_i \equiv \lambda$. We track how the three ensembles $\{\alpha^{(k)}\}$, $\{\theta^{(k)}\}$ and $\{\rho_\infty^{(k)}\}$ change in the two-dimensional (2-D) parameter space (τ, λ). Then, to assess the effect of heterogeneities in delays and inventories, we draw each delay τ_{ij} and each inventory λ_i from two lognormal distributions with means (μ_τ, μ_λ) and standard deviations $(\sigma_\tau, \sigma_\lambda)$, respectively. We then track how the dynamical response changes along an increase in σ_τ and σ_λ. We use as a baseline the homogeneous case where $\tau = 1$ and $\lambda = 0.2$.

In Sec. V, we study how heterogeneities in delays and inventories affect propagation in acyclic networks, where disruptions never persist indefinitely, i.e. where $R_\infty = 0$. Weisbuch and Battiston[19], for instance (see Fig. 1 there), used homogeneous delays and a regular lattice — which can be seen as a particularly simple case of acyclic topology — to model production networks.

In this paper, we generate random acyclic networks, abbreviated RAs, by building ER networks and removing the lower triangle of the connectivity matrix. In RAs, there is a

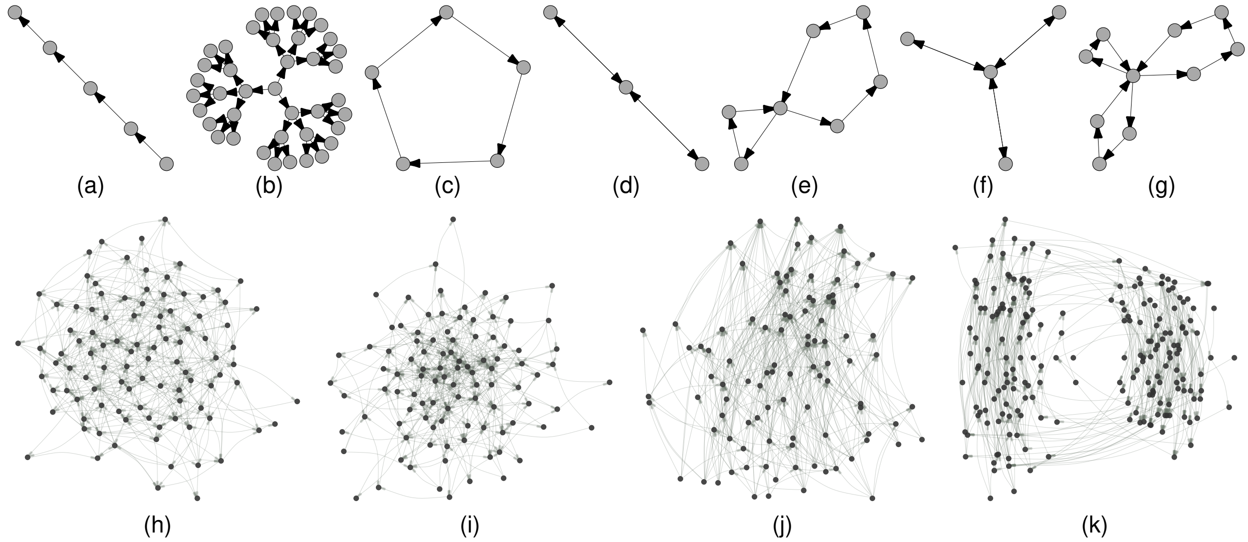

Figure 1. Schematic diagram of the classes of networks studied in this paper. The first row shows the simple network motifs analyzed in Sec. III: (a) linear networks; (b) trees; (c) isolated loops; (d) and (e) two interacting loops, connected through a pivotal node; (f) and (g) three interacting loops. The second row displays examples with $n = 100$ and connectivity $c = 4$ of the more complex classes of networks investigated in Secs. IV-to-VI: (h) directed Erdős–Rényi (ER) networks; (i) scale-free networks with specific SF–FA distributions of in- and out-degree; (j) random acyclic (RA) network in which production moves upward; and (k) a system of two interdependent RA networks — in the network placed on the left, production moves upward, while it moves downward in the one to the right.

natural direction of the production flow from primary producers, i.e. agents without a supplier, to final producers, i.e. agents without a customer. We characterize the sensibility of RAs to small perturbation by evaluating the extent to which final producers are impacted by initial perturbations of primary producers. We measure, for each primary producer, the average time final producers are disrupted. The average of this quantity, divided by the duration of the initial perturbation δ_0, defines the transfer coefficient, denoted by TC.

Finally, we examine the resilience of a network of interdependent RA networks. We focus on the case of two RA networks, where the primary producers of one network are supplied by the final producers of the other. To generate these interlocked networks, we produce two RA networks, and each primary producer of the first RA network randomly picks a supplier among the final producers of the second one; reciprocally, primary producers of the second

RA network pick suppliers among the final producers of the first one. Figure 1 illustrates all classes of networks studied in the paper. Table I summarizes the parameters, variables, Boolean operators and observables used in the model.

Table I. Summary of the variables, parameters, topologies, operators and observables used in the model.

Variable	Definition	Initial value
$x_i(t)$	Agent i is fully active, $x_i(t) = 1$, or disrupted, $x_i(t) = 0$	1
$y_i(t)$	Agent i has inventory, $y_i(t) = 1$, or not, $y_i(t) = 0$	1
Parameter	**Definition**	**Default**
n	Number of agents	10^3
c	Average number of suppliers per agent	4
τ_{ij}	Production and delivery delay from agent i to agent j	1
μ_τ	Mean of the lognormal distribution of delays	1
σ_τ	Standard deviation of the lognormal distribution of delays	0.2
λ_i	Duration of inventory hold by agent i	0.2
μ_λ	Mean of the lognormal distribution of inventories	0.2
σ_λ	Mean of the lognormal distribution of inventories	0.1
δ_0	Duration of the external perturbation	1
Topology	**Full name**	**Reference**
ER	Directed Erdős–Rényi network	[56]
SF–FA	Scale-free networks based on Fujiwara & Aoyama (2010)	[25]
RA	Random acyclic networks	[57]
Operator	**Definition**	
$\vee$	Boolean 'OR'	
$\wedge$	Boolean 'AND'	
$\prod$	Repeated Boolean product 'AND'	
Observable	**Definition**	
$\rho(t)$	Density of fully active agents, i.e. $\sum_i x_i(t)/n$	
$\rho_\infty^{(k)}$	Asymptotic density of fully active agents following the external perturbation of agent k	
R_∞	Mean of the ensemble $\{\rho_\infty^{(k)}\}$	
$\mathcal{A}^{(k)}$	Ensemble of agents that get disrupted following the external perturbation of agent k	
$\alpha^{(k)}$	Cardinal of $\mathcal{A}^{(k)}$	
A	Mean of the ensemble $\{\alpha^{(k)}\}$	
$t_i^{(k)}$	Time at which agent $i \in \mathcal{A}^{(k)}$ gets disrupted	
$\theta^{(k)}$	Mean of the ensemble $\{t_i^{(k)}\}$ over $i \in \mathcal{A}^{(k)}$	
Θ	Mean of the ensemble $\{\theta^{(k)}\}$	
TC	Transfer coefficient: average time a final producer spends in a disrupted state, following an external perturbation of a primary producer of unit duration.	
$\delta_c^{(i)}$	Critical perturbation: the duration of the external perturbation affecting agent i over which the OUT component collapses	
Δ_c	Mean of the ensemble $\{\delta_c^{(i)}\}$	

III. ROLE OF KEY NETWORK MOTIFS

A. Decaying waves in simple acyclic networks

Consider a linear network, illustrated in Fig. 1a, with $n \gg 1$ agents. Agent 0 is the primary producer, it supplies agent 1, which itself supplies agent 2, an so on up to agent $n-1$. With this structure, the dynamical system of Eq. (3) becomes, for $i > 0$:

$$x_i(t) = x_{i-1}(t - \tau_{i-1,i}) \vee x_{i-1}(t - \tau_{i-1,i} - \lambda_i). \tag{5}$$

If agent 0 is externally perturbed during δ_0 unit of time, we can demonstrate that agent 1 will be temporarily disrupted if the initial perturbation is longer than its inventory, i.e. if $\delta_0 > \lambda_1$. In that case, agent 1 will be perturbed at $t = \tau_{01} + \lambda_1$ for $\delta_0 - \lambda_1$ units of time. Recursively, we can demonstrate that agent i will be perturbed if the duration of the external perturbation exceeds the sum of the inventories of all agents between agent 1 and itself, i.e. if:

$$\delta_0 > \sum_{k=1}^{i} \lambda_k. \tag{6}$$

If inequality (6) is satisfied, then the duration of the perturbation affecting agent i is given by the difference between the duration of the initial perturbation and the sum of the inventories $\delta_0 - \sum_{k=1}^{i} \lambda_k$. Both the delays and the inventories determine the time of first perturbation:

$$t_i = \sum_{k=1}^{i} \tau_{k-1,k} + \lambda_k. \tag{7}$$

When all delays and inventories are homogeneous and equal to τ and to λ, respectively, the initial perturbation propagates up to agent $z \equiv \lfloor \delta_0/\lambda \rfloor$, where $\lfloor x \rfloor$ denotes the integer part of x. In linear networks, this ratio also corresponds to the number of disrupted agents. α, which is thus inversely proportional to the inventories λ, and is not affected by delays. The time t_i of first disruption of agents within the set $\mathcal{A}$ is $t_i = (\tau + \lambda)i$. The average time θ of first disruption is given by $\theta = (\tau + \lambda)(a + 1)/2$: it varies linearly with the sum of the delays and the inventories, $\tau + \lambda$. In such a linear network, there is no permanent disruption: perturbations eventually decay.

We can readily extend these results to trees which are illustrated in Fig. 1b. Layer 0 is occupied by one root agent, which supplies d agents in layer 1, d^2 in layer 2, and so on. Ternary trees, with $d = 3$, were used, for instance, by Zaliapin, Keilis-Borok, and Ghil[50,51].

In trees, the initial perturbation of the root agent can lead to significant propagating waves. The formula $z \equiv \lfloor \delta_0/\lambda \rfloor$, derived for linear networks, can be applied, where z now represents the level to which the perturbation propagates. Given that layer k is occupied by d^k agents, we have:

$$\alpha = \sum_{k=0}^{z} d^k, \qquad \theta = \sum_{k=0}^{z} \frac{k(\tau+\lambda)d^k}{\alpha}. \tag{8}$$

For the heterogenous case, we build a probabilistic model to assess the effect of a change in key features of the delay and inventory distribution on propagation. Letting each delay and inventory be an independent, identically distributed random variable, our probabilistic model is based on a recursive algorithm that yields the expected values of the amplitude and average time of first disruption, $\mathbb{E}(\alpha)$ and $\mathbb{E}(\theta)$. The algorithm is presented in Appendix A and its results are compared with those of numerical experiments. We find that, for both a uniform and a lognormal distribution, the more heterogeneous inventories are, the further the perturbation tends to propagate. In these simple network structures, in which pathways never interesect, delay heterogeneity does not affect the propagation amplitude.

B. Fast collapse in isolated loops

While propagating disturbances eventually vanish in acyclic networks, they can be sustained or even amplify in purely cyclic networks. Such isolated loops, in which agents belong to one and only one loop, are illustrated in Fig.1c; in them, the asymptotic behavior involves recovery, periodic disruptions or collapse.

In the absence of inventory, an initial perturbation propagates indefinitely around the loop: it periodically affects each agent, and the period is equal to the sum of the delays. If other agents depend directly or indirectly on this loop, they are also affected by the periodic wave of disruptions.

When some agents hold inventories, propagating waves are gradually damped and eventually die out; their behavior can be derived using the analytic approach taken for the linear network in Sec. III A. This damping can however be canceled by short time delays: if the initial perturbation propagates around the loop so rapidly that the first agent has not yet recovered from its initial perturbation, then all agents remain permanently disrupted. In an isolated loop with agents labeled $k = 0, 1, \ldots, n-1$, the condition for such fast collapse is:

$$\delta_0 \geq \sum_{k=0}^{n-1} \tau_{k,k+1} + \lambda_k. \tag{9}$$

C. Fine detuning in interacting loops

More complex types of behavior occur in networks in which multiple loops interact. In this case, a new type of phenomenon arises, which we call "fine detuning." Essentially, it involves a proximity of two or more periodicities associated with the distinct loops to their being commensurable i.e., to having an exact rational relationship. The precise definition is given in Eq. (10) below.

When two loops interact through one agent, as in Figs. 1d and e, any perturbation reaching this pivotal agent duplicates, inducing one propagating wave in each one of the two loops. In the absence of inventory, these two waves propagate freely, duplicate again at the pivotal agent, leading therewith to new propagating waves in each loop, and so on.

If the propagation times through either loop are equal, then the two waves return to the pivotal agent at the same time. This exact overlapping leads to a periodic regime, as it does in an isolated loop. More generally, if one propagation time is an integer multiple of the other then, in the absence of inventory, a periodic regime sets in. In the absence of such an integer-multiple relation between propagation times, any initial perturbation gradually amplifies through duplication and eventually leads to permanent disruption of all agents.

Contrary to isolated loops, explored in Sec. III B, inventories do not guarantee recovery in interacting loops, even for moderate initial perturbations. We refer to the case in which the sum of the delays in one loop and that in the other differ by a small amount as fine detuning. In this case, a single perturbation can permanently disrupt all agents through a process of successive duplication and recombination of propagating waves.

When the difference in delays between both loops — i.e., the detuning — is large and incommensurable, the wave that propagates in one loop behaves independently of the one in the other loop; both waves gradually decay due to inventories, as seen in isolated loops in the previous section. When both loops are tuned, i.e. when the sums of delays in each loop are equal, the waves are perfectly superimposed at the pivotal agent, and they synchronously decay. Only when the difference in delays is small, i.e. when detuning is fine, do the waves superimpose with a small shift and thus amplify.

Specifically, for an initial perturbation δ_0 affecting the pivotal agent, fine detuning occurs when the difference in total delays Δ_T between the two loops falls within the following range:

$$L_a < \Delta_\mathrm{T} < \delta_0 + \lambda_0 - L_b, \tag{10}$$

where L_a is the sum of inventories in the faster loop, labeled a, L_b the sum of inventories in the slower loop, and λ_0 the inventory of the pivotal agent. For this condition to hold, it is furthermore necessary that $\delta_0 > \max\{L_a, L_b\} - \lambda_0$, in other words that the inventories be low enough to allow the initial perturbation to propagate back to agent 0 in both branches. The derivation of these conditions is provided in Appendix B, along with relevant examples of time series.

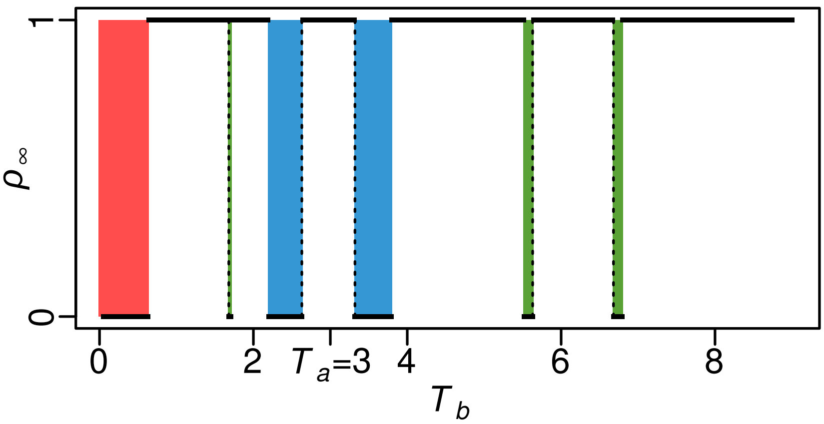

Figure 2. Asymptotic density ρ_∞ of fully active agents, as a function of the total delay T_b of loop b, for networks with two loops connected through a single pivotal agent, as in Figs. 1d and e. The total delay T_a in loop a equals 3. Initially, all agents are producing, except the pivotal agent, which is perturbed during a time interval $\delta_0 = 1$. The heavy horizontal solid line corresponds to ρ_∞. The colored areas indicate full collapse of the network, while the vertical dashed lines pinpoint the isolated occurrence of asymptotically periodic solutions. The red area corresponds to fast collapse, as described in Sec. III B, while the green and blue ones correspond to fine detuning; see main text for details. The total inventories in loops a and b are, respectively, $L_a = 0.35$ and $L_b = 0.4$; the inventory of the pivotal agent is $\lambda_0 = 0.15$. Note that the number of agents in each loop does not change the results.

For two loops as in Figs. 1d and e, Fig. 2 shows how the asymptotic density ρ_∞ of fully active agents varies with the total delay T_b of one of the two loops. The phenomenon of fine detuning occurs in the blue areas, on either side of T_a, i.e. for $T_b > T_a$, as in the inequalities (10), as well as for $T_b < T_a$, which also corresponds to these inequalities when the loops labeled a and b are interchanged.

We notice the appearance of periodic solutions on the less detuned side of a collapsed interval, i.e. closer to the "resonance" between the two "periods," T_a and T_b. On the farther side, there is an abrupt change from collapse to recovery, cf. Fig. 13 in Appendix B.

This detuning also occurs, to a lesser extent, when one of the total delays, T_a or T_b, is close to an integer multiple of the other, as shown by the narrower green areas of Fig. 2: when $(T_a = 3, T_b = 6)$ and when $(T_a = 3, T_b = 1.5)$. In the latter case, given the parameter set chosen, fine detuning only occurs for $T_b > T_a/2$. The red area of Fig. 2 corresponds to the phenomenon of rapid collapse described in the previous section: delays and inventories are so short that the propagating waves return to agent 0, while it has not yet recovered from the initial perturbation.

D. Synchronization in three interacting loops

When more than two loops interact, the process of wave duplication and recombination can lead to even more complex dynamical behavior. In particular, given three interacting loops, as illustrated in Figs. 1f and g, periodic regimes occur for continuous parameter intervals, while for two interacting loops such regimes only set in at isolated parameter values, as indicated by the vertical dotted lines in Fig. 2.

The dynamical response to initial perturbations of a specific network is shown in Fig. 3 for six sets of parameters. This network has $n = 4$ agents, structured into three loops connected through agent 0, as in Fig. 1f. As illustrated in panels (a) and (b), permuting delays within a loop modifies the finite-length transient but does not alter the asymptotic periodic solution. A minor change in one delay can lead to a discontinuous jump in period length: from 1 for $\tau_{02} = 2$ in panels (a,b) to 2 for $\tau_{02} = 1.9$ in panel (c). Such period doubling is well known in differentiable dynamical systems and has been discussed in the BDE context by Saunders and Ghil[49]. Changing inventories does not modify the period length but it does affect the actual periodic pattern; see panels (a), (d), (e) and (f).

In this network, additional numerical simulations (not shown) suggest that, in addition to full activity or collapse, periodic solutions occur in large regions of the 10-dimensional parameter space $(\tau_{01}, \tau_{10}, \tau_{02}, \tau_{20}, \tau_{03}, \tau_{30}, \lambda_0, \lambda_1, \lambda_2, \lambda_3)$. These regions have a finite volume in $\mathbb{R}^{10}$, in other words they are not points as in the case of two interacting loops, but are a union of several disconnected sets. Within such a set, the period length can remain stable or change discontinuously with a change in one delay. Additional results are shown in Appendix C and require further study.

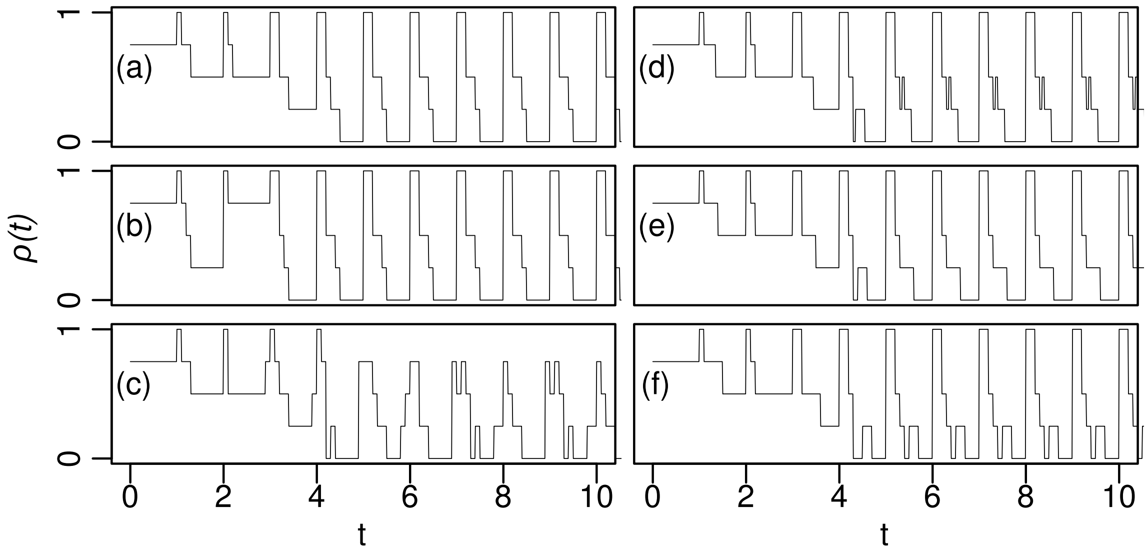

Figure 3. Time series of the density $\rho(t)$ of fully active agents in the 3-loop network of Fig. 1f. Agent 0 is the pivotal agent, which is initially perturbed for a time interval $\delta_0 = 1$. (a) Results for default values of delays and inventories — all delays are equal to 1 except $\tau_{02} = 2$, while the inventories are $\lambda_0 = 0$, $\lambda_1 = 0.1$, $\lambda_2 = 0.2$ and $\lambda_3 = 0.3$. (b,c) Results for changes in delays: (b) the values of τ_{02} and τ_{20} are interchanged; and (c) $\tau_{02} = 1.9$. (d)–(f) Changes in the inventory λ_3 of the third agent: (d) $\lambda_3 = 0.35$; (e) = 0.4; and (f) = 0.5.

IV. RESILIENCE OF COMPLEX NETWORKS

A. Influence of global and local structures

As shown in the previous sections, the presence of loops in a network, and in particular that of interacting loops, enable permanent disruption. In complex networks, loops are the constitutive motif of their so-called strongly connected component (SCC)[23,58]. An SCC is a maximal subset of agents within which each agent can reach and be reached by any other agent through directed links. SCCs are embedded in a weakly connected component (WCC), where the WCC is the maximal subset of agents within which each agent can reach and be reached be any other agent, disregarding the direction of the links.

If a permanent disruption reaches an SCC, all agents in the SCC itself, along with those that source their inputs in the SCC, get permanently disrupted. The whole disrupted region is called the out-component of the SCC, labeled OUT. Identifying all agents in OUT allows one to predict the potential extent of permanent disruptions. Conversely, an initial perturbation can only trigger permanent disruptions if it is located in the IN of an SCC, i.e. among the agents producing inputs used by any agents within the SCC. Investigating all IN agents allows one, therefore, to estimate the maximum probability that an initial perturbation triggers a permanent disruption. The major WCC, SCC, IN and OUT components of a network can be usefully mapped into a so-called bow-tie diagram; see Fig. 13 in Coluzzi *et al.*[23] and discussion therein.

In ER networks, a giant SCC arises when the average connectivity is larger than 1; see Fig. 4a. The expected sizes of the IN and OUT components of the giant SCC are equal, and reach half of the network for $c = 1.39$ when $n = 10^5$. At this specific connectivity, and in the absence of inventory, there is one chance in two that a random perturbation triggers a permanent disruption. Such a disruption would then affect half of the agents. In a scale-free network, the high concentration of links ensures that a giant SCC emerges for very low connectivities; this is the case also in our SF–FA networks, as seen in Fig. 4b. The asymmetry between in and out-degree distributions in SF–FA networks leads, moreover, to different sizes of the IN and OUT components.

According to the results of Sec. III, the asymptotic response is determined by the presence of interactions between multiple short loops. We investigate next the density of agents that are engaged in at least two loops of five agents or less, as a function of network structure; this quantity is denoted by D_{SIL}, where the subscript SIL stands for “short interacting loops.” Longer loops are expected to play only a minor role when the average inventory exceeds 0.2.

For both ER and SF–FA networks, D_{SIL} increases with the average connectivity (not shown), but tends to decreases with the network size, as shown in Fig. 4c. This decrease is, however, much sharper for ER networks; hence, for large n, almost no agent is engaged in

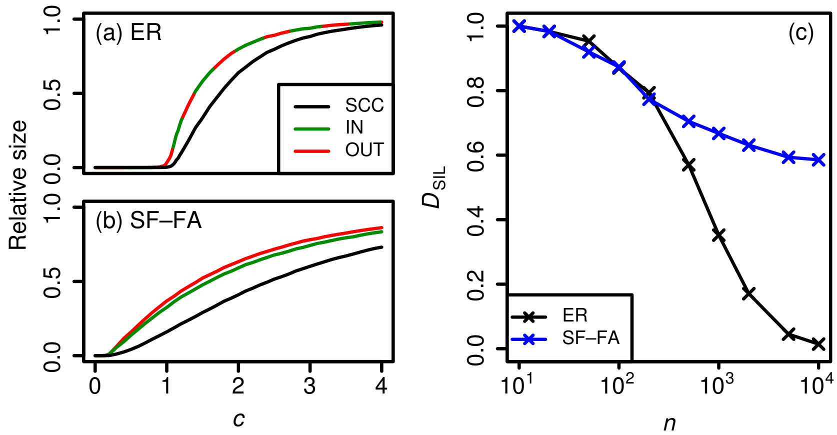

Figure 4. Properties of Erdős–Rényi (ER) networks vs. more realistic (SF–FA) supply networks. (a,b) Relative size of the giant strongly connected component (SCC; solid black line) and of the giant in and giant out components, IN (solid green) and OUT (solid red), as a function of the connectivity c: (a) numerical results for ER networks of size $n = 10^4$; and (b) analogous results for SF–FA networks of the same size. (c) Density D_{SIL} of agents engaged in at least two loops of less than five agents as a function of the network size n, for ER (black) and SF–FA (blue) networks of connectivity $c = 4$.

multiple short loops. This result is consistent with the findings of Bianconi, Gulbahce, and Motter [59], who showed that the number of short loops becomes negligible in ER networks in the limit of large n.

For SF–FA networks, though, the density of agents that are engaged in at least two short loops, D_{SIL}, stabilizes for large n and remains above 50%. Following Bianconi, Gulbahce, and Motter [59], this difference is likely to be related to the positive correlation in SF–FA networks between in-degree and out-degree [25].

The high occurrence of short interacting loops in SF–FA networks suggests that they are more prone to permanent disruptions than ER networks. Moreover, for connectivity below 1, SF–FA networks still exhibit SCCs, and can therefore permanently collapse, while ER networks cannot. For larger connectivities, SF-FA networks have a smaller giant OUT component than ER networks, suggesting that the extent of a possible collapse, in terms of the number of inactive nodes, is expected to be lower.

B. Heterogeneity in delays and inventories

In both ER and SF–FA networks, three asymptotic regimes are possible: full activity, periodic disruption or permanent disruption. In the homogeneous case with $\tau = 1$ and $\lambda = 0.2$, both ER and SF–FA networks fully recover from any initial perturbation. However, even a moderate level of heterogeneity in delays reduces resilience fairly abruptly; see Fig. 5a. This effect is due to the occurrence of fine detuning, cf. Sec. III C. Slight variability in the delays of multiple interacting loops can induce the collapse of these loops, which then extends to the whole giant SCC and OUT components.

For ER networks, the transition between full recovery and collapse occurs for a standard deviation of delays σ_τ between 0.06 and 0.12; see Fig. 5a. The rapid drop of R_∞ is due, in fact, to a change in the structure of the distribution of the individual values of $\{\rho_\infty^{(k)}\}$. Before the transition, the network always recovers and all $\rho_\infty^{(k)}$ equal 1. During the transition, a second mode — in the statistical sense of the term — appears in the distribution. It corresponds to the collapse of the giant OUT component, and it is equal to 1 minus the relative size of the giant OUT component; for ER networks with $n = 1000$ and $c = 4$, this mode equals $1 - (0.98 \pm 0.008)$. The weight of this mode in the statistical distribution of $\{\rho_\infty^{(k)}\}$ starts from 0% and reaches $82.5\% \pm 3.0\%$ after the transition.

In SF–FA networks, the transition is likewise shown in Fig. 5a and it occurs for even lower heterogeneity levels, because of the higher density of short interacting loops; see the values of D_{SIL} in Fig. 4c at $n = 10^3$. These networks have smaller giant OUT components than ER networks, namely 0.90 ± 0.02, but permanent disruption occurs more often, following $88.2\% \pm 0.9\%$ of the initial perturbations. Furthermore, the σ_τ-value at which transition occurs is more variable among different SF–FA than for ER networks; see the blue vs. the black interquartile ranges in Fig. 5a.

As σ_τ increases, no persistent periodic orbits arise, in either ER or SF–FA networks. Transients can, however, exhibit oscillations for moderate delay heterogeneity, $\sigma_\tau \lesssim 0.15$, as illustrated by the time series of Figs. 5b, c and d. The period of these small oscillations corresponds to the the mean delay μ_τ, and they quickly vanish for higher σ_τ-values. Delay heterogeneity tends to accelerate the disruption waves and shorten the transients. After the transition from full recovery to collapse, a further increase in σ_τ reduces the average time of first disruption Θ. In SF-FA networks, it is reduced by about 11% between $\sigma_\tau = 0.1$ and

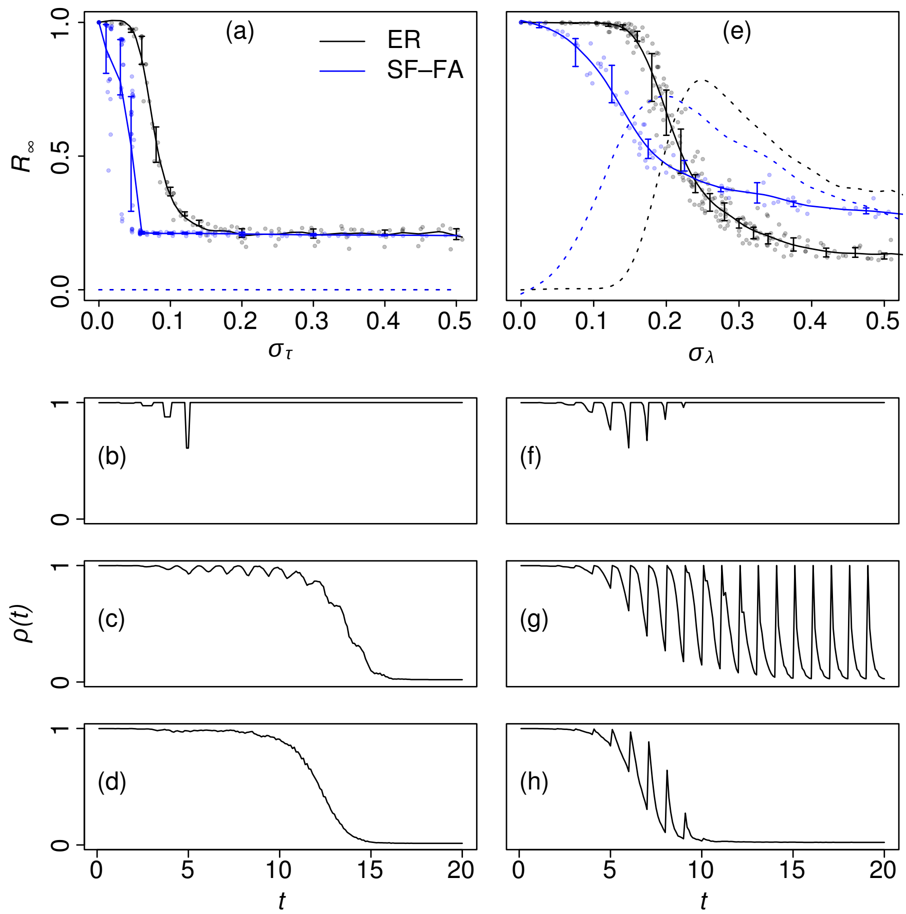

Figure 5. Effect of heterogeneity in delays and inventories on the asymptotic behavior of ER and SF–FA networks following small perturbations. (a,e) Average asymptotic number R_∞ of fully active agents as a function of (a) the standard deviation σ_τ of the lognormally distributed delays, when inventories are kept homogeneous; and (e) of the standard deviation σ_λ of inventories, when delays are kept homogeneous. In both panels, the data points are represented by semi-transparent dots (black for ER and blue for SF–FA networks), while the solid curves are trend lines based on locally weighted polynomial regressions, and the vertical bars represent interquartile ranges. In panel (e), the dashed curves represent the relative number of periodic attractors. Note that there are no periodic attractors in (a) because, when the delays are heterogenous, the transition from full activity to permanent disruption is too rapid. (b)–(d) Sample time series of $\rho(t)$ obtained in ER networks for $\sigma_\tau = 0$, 0.1 and 0.2; and (f)–(h) sample time series for $\sigma_\lambda = 0.1$, 0.2 and 0.5.

$\sigma_\tau = 0.5$, from 4.4 ± 0.09 to 3.9 ± 0.09.

Inventory heterogeneity also deteriorates the ability of the system to recover, i.e. its resilience. As seen in Fig. 5e, a similar transition occurs as σ_λ increases; this transition, however, occurs for much larger σ_λ-values. For instance, for ER networks, the decrease in R_∞ starts when the standard deviation of inventories σ_λ reaches 0.15, i.e. for a coefficient of variation of 75%, as opposed to a coefficient of variation of 6% for delay heterogeneity.

In this case, though, the transition between full recovery and collapse is accompanied by the emergence of asymptotically stable periodic orbits: these are represented by the dashed lines in Fig. 5e, and illustrated by the time series of Fig. 5g. In addition to full recovery and collapse of the giant OUT component, the distribution of $\rho_\infty^{(k)}$ has intermediate values, which correspond to the time average of $\rho(t)$ during one period of these oscillations. The presence of these periodic orbits tends to soften the transition from high to low $\langle\rho_\infty\rangle$-values, which is less abrupt than in Fig. 5a.

As for the delays, the transition in SF-FA networks occurs for lower σ_λ. The emergence of asymptotically periodic orbits is related to the interaction between multiple short loops, as illustrated in Sec. III D, and it is largely fostered by the homogeneity of the delays. As soon as delays become heterogeneous, fine detuning occurs and most oscillations become transient and lead to collapse. In this case, the counterpart (not shown) of the diagram in Fig. 5e does not exhibit periodic orbits.

C. Interplay between delays and inventories

The detrimental role of heterogeneity on resilience can be observed by comparing panels (a) and (c), in which delays and inventories are homogeneous, with panels (b) and (d) of Fig. 6, in which they are heterogeneous with a coefficient of variation of 50%. For both ER and SF–FA networks, the portion of the parameter plane (μ_τ, μ_λ) corresponding to full recovery (dark blue) is significantly reduced. As previously illustrated, this detrimental effect of heterogeneity on resilience mostly comes from the heterogeneity of delays. When delays are heterogeneous, the exact mean value of the distribution has almost no impact on resilience; see Figs. 6b and d. This result provides additional evidence for permanent disruption occurring through fine detuning, in which only the difference in delays matters and not their absolute value, in agreement with inequalities (10).

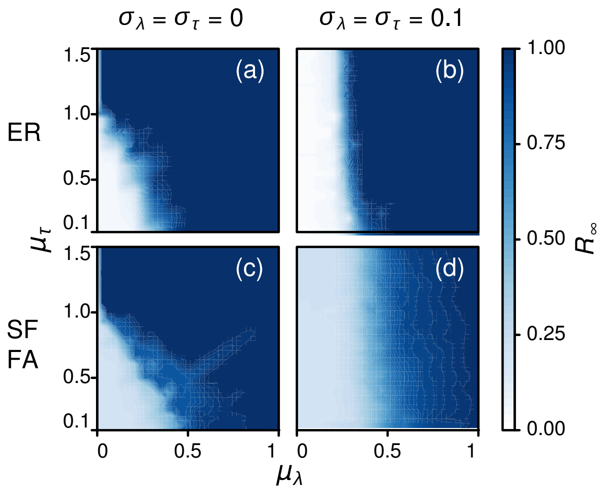

Figure 6. Average asymptotic density R_∞ of fully active agents, as a function of the mean inventory μ_λ and the mean delay μ_τ, for ER networks in panels (a) and (b) and SF–FA networks in panels (c) and (d). In the two panels on the left, (a) and (c), inventories and delays are homogeneous: they are all equal to μ_λ and μ_τ, respectively. In the two panels on the right, (b) and (d), they are heterogeneous. The inventories are lognormally distributed with standard deviation $\sigma_\lambda = 0.1$, and so are the delays, with standard deviation $\sigma_\tau = 0.1$. The four plots are based on interpolation of grid data, and represent average values of R_∞ for ten networks.

In the homogeneous case, collapse occurs for short delays only. Since all delays are equal, fine detuning can only occur between loops of distinct length, e.g. between a 2-loop and a 3-loop, or between a 2-loop and a 4-loop. The smallest difference in delays between such interacting loops — i.e., the quantity Δ_T in Eq. (10) — is therefore τ: that is why small τ-values are necessary for fine detuning. For instance, using Eq. (10), if the initial perturbation hit an agent connecting a 2-loop and a 3-loop, fine detuning occurs for $\lambda \leq \tau < 1 - \lambda$.

Small delays also enable fast collapse when the sum of delays and inventories in one loop falls below the initial perturbation, see Sec. III B. In loops of two agents, for instance, fast collapse occurs when $\tau < \delta_0/2 - \lambda$. Further mechanisms are also likely to induce collapse, such as those underlying the behavior of three interacting loops, as illustrated in Sec. III D.

Comparing Figs. 6b and 6d shows that SF–FA networks are less resilient than ER networks. The transition between full recovery — the dark region — and permanent disruption — the light region — occurs for larger inventory levels. According to the results of Sec. IV A, SF-FA networks have a larger number of short interacting loops, and thus a higher probability for fine detuning.

In the homogeneous case, Figs. 6a and 6c are very similar. However, because of the same topological feature, the parameter region of full activity is slightly reduced for SF–FA networks in the general area ($0 \leq \tau \leq 0.5, 0.25 \leq \lambda \leq 0.45$) of low delays and relatively high inventories. On the other hand, because SF–FA have smaller giant OUT component, the extent of collapse is lower than in ER networks. This can be seen in Figs. 6b and d, where the light region is slightly darker than in Figs. 6a and c, indicating larger R_∞-values.

V. NETWORK OF ACYCLIC NETWORKS

A. Propagation in acyclic networks

In an acyclic network, no permanent disruption occurs. Still, heterogeneities in delays and inventories do have an impact on certain features of the transient regime. A random acyclic (RA) network can be seen as a sequence of linear chains that intersect without forming a loop. Recalling the study of linear networks in Sec. III A, the amplitudes of the propagating waves induced by the perturbation of primary producers are likely to increase as inventory heterogeneity increases.

This prediction is confirmed in Fig. 7a, which shows that the transfer coefficent TC increases with σ_λ. This indicator measures the average disruption time of final producers following the external perturbation of a primary producer. In other words, a broader distribution of inventories makes an RA network more permeable, i.e. final producers are more likely to be disrupted due to the failure of primary producers. Since more agents get perturbed, full recovery takes longer.

Fig. 7b shows a positive, yet moderate, impact of delay heterogeneity on TC. This phenomenon is due to a process similar to fine detuning, which occurs between parallel pathways. The initial perturbation generates several propagating waves, some of which get recombined further down the network. This recombination can potentially amplify the disruption, as shown in Sec. III C for fine detuning between loops. This explanation is confirmed by the fact that TC increases only for small σ_τ-values; this amplifying effect then vanishes, as in the transition for cyclic networks illustrated in Fig. 5a, where fine detuning only requires a small degree of delay heterogeneity.

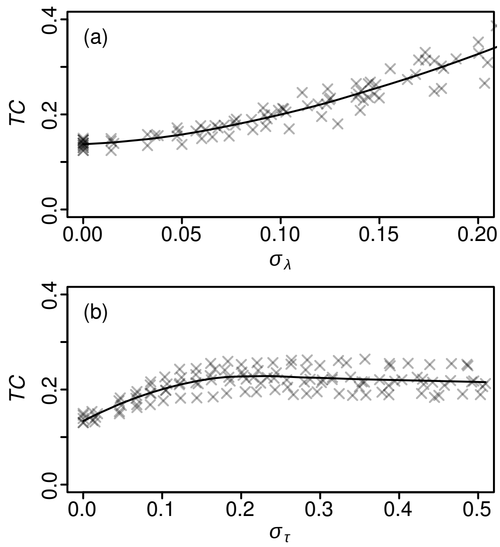

Figure 7. Transfer coefficient TC for random acyclic (RA) networks, as a function of (a) the standard deviation σ_λ of the inventories; and (b) the standard deviation σ_τ of the delays; see Tab. I for the definition of TC. Five networks were used for each plot. The $\times$ symbols indicate individual TC values obtained from simulations, and the solid curve indicates the local average.

B. Resilience of interdependent RA networks

In a system of two interdependent RA networks — where each primary producer of one network is supplied by one final producer of the other — delay heterogeneity significantly reduces resilience. When the delays in both networks are drawn from the same lognormal distribution, the behavior (not shown) is qualitatively similar to that of the ER and SF–FA networks in Fig. 5a, with a quick transition to collapse for moderate σ_τ.

Two time series are displayed in Fig. 8, where the red curves correspond to the network where the inital perturbation occurs. When delays are homogeneous or almost homogeneous, as in Fig. 8a, the propagating waves fade out, while in Fig. 8b they amplify through fine detuning due to delay heterogeneity. Inventory heterogeneity can also lead to collapse, but for even larger σ_λ-values than in ER and SF–FA networks, while periodic orbits arise to a smaller extent during the transition (not shown).

In all propagation phenomena in these paired networks, whether leading to recovery or to collapse, we observe a back-and-forth pendulum movement: disruptions are alternately stronger in one network, then in the other, an so on. In Figs. 8(a,b), the red curve starts

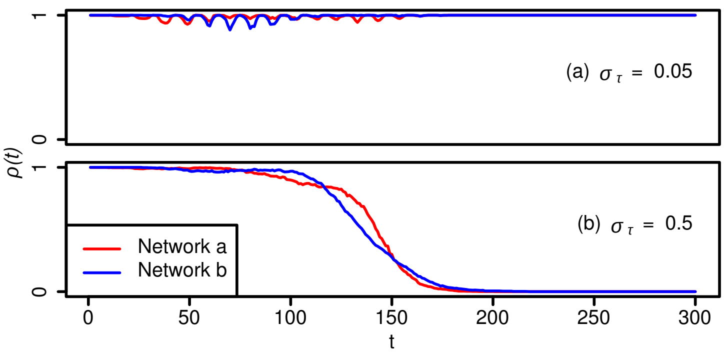

Figure 8. Time series of the density $\rho(t)$ of fully active agents in two systems of two interdependent RA networks, each with $n = 500$ agents and connectivity $c = 4$. The red curve indicates the time series corresponding to the network a where the initial perturbation occurs and the blue curve the second network, called network b. Both the delays and the inventories are lognormally distributed, with mean delay $\mu_\tau = 1$ in both panels, and inventories having mean $\mu_\lambda = 0.2$ and standard deviation $\sigma_\lambda = 1$. The two panels differ by a distinct value of the standard deviation σ_τ of the delay distribution that is common to both networks: (a) $\sigma_\tau = 0.05$; and (b) $\sigma_\tau = 0.5$.

below the blue curve, then crosses above it, and so on, until the asymptotically stationary regime is reached. Additional simulations show that the time between two crossings lasts between 3.5 and 5.5 time steps, which is slightly higher the total delays along an average pathway from primary to final producers. We also observe a slight acceleration of these crossing throughout the transients leading to collapse.

When the delay distributions are distinct from one network to the other, collapse can occur even for distributions that are both homogeneous. In the so-called dichotomous case, where all delays are equal to τ_a in network a and to τ_b in network b, a phenomenon of resonance occurs due to fine detuning, as shown in Fig. 9. When τ_a and τ_b are close to be multiple of one another, both networks recover; otherwise, they collapse. This process involves longer loops formed by the interconnection between the two networks, and thus occurs for lower inventories — $\lambda = 0.1$ in Fig. 9. Rebounds are observed for intermediate multiplicity, for $\tau_b \approx 1.5$ or 2.6. This observation suggests finer mechanisms of interactions between propagation waves, that could be examined in further work.

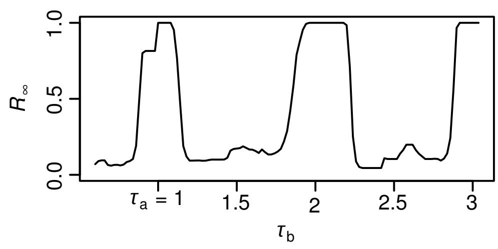

Figure 9. Average asymptotic density R_∞ of fully active agents in a system of two interdependent RA networks, a and b, connected as in Fig. 8; all inventories are homogeneous and equal to 0.1. In both networks, $n = 200$ and $c = 4$, while the delays are homogeneous and equal to 1 in network a. The figure shows how R_∞ varies with the delay τ_b.

VI. CRITICAL PERTURBATIONS

A. How critical are individual agents?

An important aspect of resilience is the maximum intensity of perturbations that the system can handle without leaving the attractor basin of full activity; this question connects to the original inquiry of Albert, Jeong, and Barabási [27] into the "tolerance" of complex network. In our Boolean setting, the intensity of an external perturbation is apprehended by its duration. For SF–FA and ER networks, we measure for each agent the critical duration of external perturbation beyond which the giant OUT component collapses. For all agents $i = 1, .., n$, we denote by $\delta_c^{(i)}$ this duration, also called the critical perturbation. We determine the values of $\delta_c^{(i)}$ through simulations. External perturbations lasting less than $\delta_c^{(i)}$ are called subcritical perturbations: they do not threaten the stability of the network.

Agents that are not in the giant IN component cannot induce permanent disruptions: they have no critical perturbation, i.e. $\delta_c^{(i)} = \infty$ for all agents $x_i \notin$ IN. All other agents in the giant IN component have a finite $\delta_c^{(i)}$-value, which depends on the topology, the delays and on the inventories of the other agents. The lower $\delta_c^{(i)}$, the more important agent i is for global resilience. Fig. 10a shows an example of how critical durations are spread over an SF–FA network with $n = 50$ agents. The spread of $\delta_c^{(i)}$-values is relatively limited.

This indicator is now compared with the canonical centrality measures developed in network theory[58]. We determine whether central nodes, according to closeness, betweenness and eigenvector centrality, have also low critical perturbations $\delta_c^{(i)}$. Additional simulations

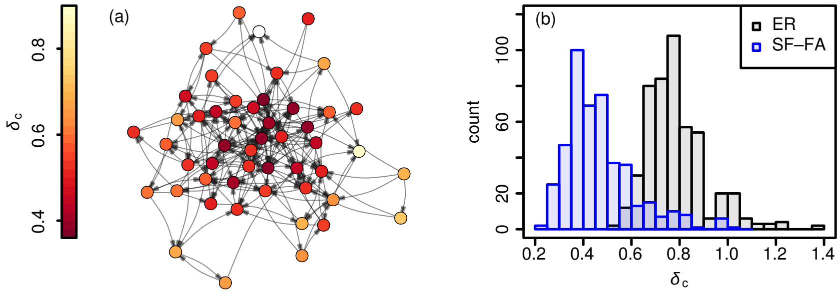

Figure 10. Distribution of critical perturbations δ_c over a network. (a) Distribution over an SF–FA network with $n = 50$ and $c = 4$. For each agent, $\delta_c^{(i)}$ is the maximal duration of perturbations that does not lead to collapse. Delays and inventories are lognormally distributed with parameters $(\mu_\tau = 1, \sigma_\tau = 0.5)$ and $(\mu_\lambda = 0.2, \sigma_\lambda = 0.1)$. Nodes are colored according to their $\delta_c^{(i)}$-value: dark red for highly critical agents, and light yellow for less critical one. The agent colored in white is not in the giant IN component and its $\delta_c^{(i)}$ is infinite. (b) Histogram of δ_c in an ER network (gray and black) and in an SF–FA network (light and dark blue). Both networks have the same characteristics as in (a), except for $n = 200$ in both. The sum of $\delta_c^{(i)}$ in the ER network is 389.4, while it is 216.2 in the SF–FA network.

are performed for five ER and five. SF–FA networks with lognormally distributed delays with parameters $(\mu_\tau = 1, \sigma_\tau = 0.5)$ and inventories with $(\mu_\lambda = 0.2, \sigma_\lambda = 0.1)$.

We observe that, on average, the ensemble $\{\delta_c^{(i)} : i \in \text{IN}\}$ is satisfactorily correlated with closeness centrality: -0.72 ± 0.066 for ER networks and -0.68 ± 0.031 for SF–FA networks. Closeness centrality is the inverse of the average geodesic distance linking one node to all other nodes, and therefore captures the potential damages that the failure of this node could cause. The correlation coefficient is not higher, in absolute terms, when the geodesic distance is replaced by the propagation time, i.e. by the sum of delays and inventories.

The remaining variability that is not captured by closeness centrality is due to the particular propagation phenomena studied in Sec. III, especially fine detuning. These mechanisms, enabled by the interaction between short loops, occur more often in SF–FA networks. This behavior is a plausible explanation for the correlation coefficient being lower for SF–FA networks than for ER ones.

Correlations are weaker for betweenness centrality: -0.36 ± 0.06 for ER networks and $-0.37 \pm 0.04\%$ for SF–FA networks; they are also weaker for eigenvector centrality: $-0.01\% \pm$

0.06% for ER networks and $-0.36\% \pm 0.04\%$ for SF–FA networks. Betweeness centrality, which measures how important a node is in connecting each pair of nodes, captures wider information on the structure of the incoming links, which are not relevant for propagation. Eigenvector centrality, based on in and out-degree concentration, has a particularly low correlation coefficient for ER networks, where degrees are more evenly spread.

B. Aggregate indicators of resilience

The ensemble $\{\delta_{\mathrm{c}}^{(i)}\}$ condenses information on one of the three aspects of resilience. We study how this ensemble varies with a change in the topology and the distribution of delays and inventories. In particular, the sum Δ_{c} of the $\delta_{\mathrm{c}}^{(i)}$'s over the complement of the IN set can be used as a scalar indicator for resilience: the higher this indicator, the larger perturbations a network can sustain without collapsing. The following results present quantities that are averaged over five repetitions of the same class of networks, and confirm the findings in Sec. IV concerning the attractor basins and propagation speed.

First, the Δ_{c}-values of SF–FA networks are lower by almost 50% than those of ER networks with similar delay and inventory distributions. In networks of 1000 agents with heterogeneous delay and inventory distribution, $\Delta_{\mathrm{c}} = 817 \pm 34$ in the ER networks and $\Delta_{\mathrm{c}} = 440 \pm 37$ in the SF–FA neworks.

To illustrate this result, two distributions of $\delta_{\mathrm{c}}^{(i)}$'s are shown in Fig. 10b, one for SF–FA networks, the other for ER networks. First, the shape of the two histograms is similar and their widths are approximately equal. Second, as expected from the results of Sec. IV, delay heterogeneity tends to reduce Δ_{c}. For ER networks with $\sigma_\tau = 0.05$ (not shown), i.e. before the sharp drop in R_∞ apparent in Fig. 5a, $\Delta_{\mathrm{c}} = 910 \pm 51$, while it drops to 817 ± 34 in Fig. 10b, where $\sigma_\tau = 0.5$.

C. Resilience to recurrent perturbations

The networks under consideration here recover from any initial subcritical perturbation. However, the critical perturbations $\delta_{\mathrm{c}}^{(i)}$ were determined for initial perturbations occurring one by one only. They apply to situations where, after each perturbation, the system has enough time to recover. What happens when additional subcritical perturbations occur during the recovery process?

Additional simulations where carried out, where, instead of imposing a unique perturbation at the beginning of the run, random perturbations occur. Specifically, agents have a certain probability to get perturbed per unit of time; this failure rate is denoted by f. The duration of theses subcritical perturbations is set to $0.8\delta_{\mathrm{c}}^{(i)}$ for agents that are in the giant IN component and to 1 for agents that are not in it. The following results are based on a limited set of numerical simulations, and should therefore be considered as merely indicative.

SF–FA networks with 1000 agents and lognormally distributed delays and inventories — where $(\mu_\tau = 1, \sigma_\tau = 0.5)$ and $(\mu_\lambda = 0.2, \sigma_\lambda = 0.1)$ — are robust when f is lower than 0.3%, i.e. when 3 subcritical perturbations occur on average per unit of time. For higher rates, collapse occurs within 500 units of time; this latency time interval decreases dramatically as f increases. For smaller networks, collapse occurs for even lower f-values. For instance, in SF–FA networks with 100 agents, collapse often occurs within 500 units of time for f as low as 0.03%. The two situations are illustrated in Figs. 11(a,b).

We observe that, at such low rates, collapse occurs following two perturbations that are very close to each other in time, within one or two units of time. It suggests that the combined perturbations, even subcritical, of interacting agents could lead to collapse. The different behavior observed in large and small networks could originate from the higher density of short interacting loops in smaller networks, as shown in Sec. IV A. The probability that two perturbations concomitantly affect the same loops or two loops in interaction is therefore higher.

These analyses show that large networks are robust to random subcritical perturbations occurring at a moderate rate — less than 3 per time steps for $n = 1000$. However, if perturbations are not random and exhibits some spatial correlations, even lower failure rates can induce collapse. Combination of localized perturbations occurring in specific regions of the network, whether ER or SF–FA, can have significant economy-wide impacts.

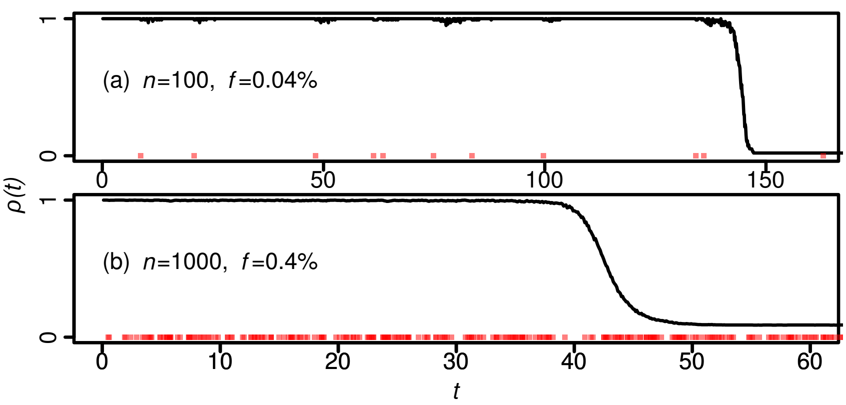

Figure 11. Time series of the density $\rho(t)$ of fully active agents, for two SF–FA networks, given recurrent subcritical perturbations; both networks have lognormally distributed delays and inventories, with parameters ($\mu_\mathcal{T} = 1, \sigma_\mathcal{T} = 0.5$) and ($\mu_\lambda = 0.2, \sigma_\lambda = 0.1$), respectively. (a) 100 agents, while $f = 0.04\%$; and (b) 1000 agents, while $f = 0.4\%$. Along the the x-axis, each red dot indicates the occurrence of a subcritical perturbation.

VII. CONCLUDING REMARKS

A. Summary and discussion

The point in time at which dynamical processes occur on networks does matter. In this paper, we have demonstrated that heterogeneity in delay values significantly influences how economic networks react to small, localized perturbations. Several aspects of a network's resilience are affected by the heterogeneity of its delays: the size of the economically desirable basin of attraction is reduced, the intensities of the perturbations from which the network can recover are smaller, and the speeds at which perturbations propagate are higher. We argue that the distribution of delays is crucial in influencing the dynamics of input–output networks, a factor well worth considering when building or analyzing such economic models.

In particular, the destabilizing effect of short delays in production and delivery is rather counterintuitive. Unlike feedback control systems, in which short delays prevent oscillations and instabilities, quick interactions between interdependent processes speed up the propagation of a disruption, resulting in a longer recovery or a collapse.

We found that inventory heterogeneity can also play a major role in acyclic supply chains, by increasing the permeability of the network, i.e. the probability that final producers get affected by the failures among primary producers. This finding confirms the conclusions of Hallegatte[37], who found an adverse effect of both capacity and inventory heterogeneity upon a network's recovery from natural disasters. Imbalances in inventories, though, have a weaker effect on a network's vulnerability than the one induced by delay heterogeneity.

We identified the key mechanisms underpinning these results. Of particular significance is the process of fine detuning, whereby a single perturbation induces multiple disturbance waves in a network with interacting loops; these waves subsequently recombine and form new, longer perturbations. The latter originate from interactions between loops with short and slightly distinct time delays. The aggregate behavior of large, complex networks was thus found to be related to their local topological features. This finding allowed us to explain why real production-and-supply networks, represented here as SF–FA networks, are consistently less resilient than comparable ER networks. The higher vulnerability of scale-free networks is consistent with conclusions drawn from epidemic-spreading models[32,33], a consistency that suggests conceptual linkages between contagion dynamics and disruption propagation. Our findings on SF–FA networks could be refined by incorporating other features of real economic networks identified by Fujiwara and Aoyama[25], in particular disassortativity, clustering, and community structures.

The process of fine detuning was also observed in networks of networks, and it is induced by heterogeneity in delays between networks. An acyclic network with homogeneous delays can safely interact with other acyclic structures, as long as their respective delays are integer multiples of each other. But the absence of integer multiplicity between delays leads to a loss of synchronization between the disruption waves, and may thus prevent the joint recovery of the networks Buldyrev *et al.*[60] have shown, in effect, that interacting networks can exhibit very different failure behavior than single networks, and our findings here contribute therewith to the study of networks of networks.

Finally, while aiming mainly at gaining insight into their resilience, we explored many aspects of a network's behavior, such as the size of its attractor basins, as well as the transient speed of damage propagation and the effects of the intensity of exogenous perturbations. Studying these various aspects separately, as well as in combination with each other, allowed us to increase the robustness of our conclusions.

We argue that, although sometimes it may be presented as ill-defined, the concept of resilience can usefully guide system analyses and stimulate original investigations.

B. The challenge of resilience indicators

In Sec. VI, we evaluated how critical individual agents are for overall resilience. We built an agent-level indicator $\delta_c^{(i)}$ based on the maximum perturbation intensity — measured here by its duration — that an agent i can handle without causing permanent disruptions to a large fraction of the network. The importance of individual agents can be partly predicted by closeness centrality, but not by two additional, commonly used centrality measures that we considered — betweenness and eigenvector centrality.

It appears, therewith, that no one-size-fits-all indicator can measure the importance of nodes, independently of context. Hence, vulnerability indicators need to be specifically tailored to capture the relevant dynamical processes at stake. In a real-world context, to evaluate how critical a specific firm is using the concept of a critical perturbation, one would need to quantify the levels of inventory of its direct partners, and the extent to which they depend on each other, as well as on the travel times of the damages.

How powerful can such vulnerability indicators be in mitigating risks? Section VI C shows that our indicator $\delta_c^{(i)}$ can be used to map the vulnerability of the production networks to localized perturbations. From this information, critical nodes could be targeted with measures that speed up their post-shock recovery. Such a strategy could help alleviate the system-wide consequences of events that are uncorrelated, both in time and in space.

Our study suggests, however, that vulnerability assessments based on single-failure scenarios do not capture the whole risk landscape: they have serious limitations, for instance, when it comes to large-scale events, such as natural disasters, or to coordinated attacks, which can lead to concomitant failures of specific combinations of agents. Comprehensively assessing the individual role of firms for such low-probability high-impact risks is particularly challenging.

We argue that progress can be made by identifying critical network structures, as done in Sec. III. We found that it is the interactions between basic structures, more than the structures themselves taken in isolation, that give rise to vulnerabilities. For large, complex networks, it is likely that no single indicator can cover all types of damage mechanisms. From a regulatory perspective, then, several vulnerability or resilience indicators should be combined in applications, without underestimating the remaining uncertainties.

C. Synchronization

Besides our results on network resilience, this work has revealed some intriguing aspects of Boolean processes with delays. Rosin *et al.*[61,62] observed somewhat similar characteristics of such processes in experimental realizations of BDEs using electronic logic circuits.

In large regions of parameter space, we found relaxation oscillations emerging in the density $\rho(t)$ of undamaged agents. This was the case, in particular, for networks consisting of three interacting loops, as apparent in the time series of Figs. 3 and 14, as well as for complex networks with homogeneous delays and heterogeneous inventories, cf. Figs. 5(f–h) and Fig. 15 in Appendix C below. These oscillations asymptote, after a transient, to a periodic limit cycle, over whose period the initial perturbation propagates and synchronously affects a large number of nodes.

Within a period, inventories first attenuate the beginning of the disruption, but are not large enough to stop it completely. Next they are gradually emptied out, thus leading to the reappearance of disruptions. Finally, inventories get replenished, the disruptions temporarily disappear again entirely, and the cycle can start all over.

Since delays are homogeneous, the replenishment of the inventories occurs simultaneously, so that all disruptions disappear more suddenly than they decrease, which leads to a very step upward slope of $\rho(t)$ within each period; see, for instance, Fig. 5g. The pattern of the relaxation dynamics, i.e. the downward slope of $\rho(t)$, is directly related to the fact that inventories become used gradually, one agent after the other.

We observe in Fig. 14 that modifying one inventory changes the relaxation pattern. The higher the average level of inventories, the longer the relaxation phase within each period.

Delays determine the return of the inventories, and therefore the timing of the steep upward peak in $\rho(t)$. They therefore determine the periodicity. As seen in Sec. III, these oscillations are due to interactions between multiple loops. A change of delay in one loop can desynchronise different loops, and lead to a different period. A small change in delay can have a strong discontinuous effect on the length of the period; see Figs. 14(a–c). However, delays that are too heterogeneous tend to desynchronize the loops, which can lead either to recovery or to complete collapse. These phenomena are further discussed in Appendix C.

The patterns seen in Fig. 15 below suggest that metastable oscillations can stabilize and persist indefinitely. The fact that, within a given network, the same propagation phenomena can lead at first to a relaxation pattern, that lasts for several periods, and then to a different pattern, with sometimes a distinct periodicity, suggests that relaxation oscillations may temporarily set in over different regions of the network. The transition from one oscillatory regime to another is marked by a temporary desynchronization, and can span multiple periods; see Figs. 15(b–f). This behavior gives rise to increasingly long transients. D'Huys *et al.*[63] found experimentally a different phenomenon that also generates very long transients in Boolean loops with 'NOT' operators.

The fact that oscillations can move throughout the network is of particular interest for networks with several centers, such as the system of interdependent networks studied in Sec. V. This movement is likely to be at the origin of the pendulum alternation between two acyclic networks observed in Fig. 8.

D. Conclusion

In this paper, we have formulated a simple model of an economic network, and analyzed how heterogeneity in delays, inventories and connectivity negatively affect resilience to small perturbations. We identified the key underpinning mechanisms leading to different dynamical responses, and established robust correspondences between the local structure of the networks and their aggregate behavior. We investigated resilience using three major network characteristics: size of attractor basins, duration of transients, and intensity of perturbations. These three characteristics allowed us to compare and combine our partial results throughout this paper and provide more robust final findings.

The use of BDEs allowed us to capture the highly nonlinear processes at work without modeling the exact production levels. Thanks to this key simplification, we were able to perform extensive numerical simulations on complex networks and study large portions of the models' parameter space. Even if the quantitative results herein cannot be tested directly on real data, the qualitative understanding gained allows us to identify new directions for empirical studies.

We argue that variability in production and delivery delays and inventory unbalances could amplify the economy-wide impacts of localized supply disruptions. This hypothesis is empirically verifiable using econometric methods. We also suggest that, beyond the simple message that interdependencies between key industries increase vulnerability, it is the time scale over which the connections actually happen that matters, as well as the existence and nature of a given connection. Case studies could reveal whether, indeed, short interactions between interdependent industries can lead to sizeable disruption risks.

Albeit restricted to Boolean variables, it was possible to satisfactorily model inventories. The BDE framework seems therefore flexible enough to integrate more detailed representations of economic processes. Our model could thus incorporate, for instance, a certain degree of substitutability between inputs, known to alleviate propagation phenomena. Such a modification could be achieved by replacing the operator AND by OR, or by introducing other Boolean operators. Agents could also be allowed, when disruptions become severe, to switch to alternative suppliers within the same network, or, as implemented by Coluzzi *et al.*[23], to receive external provisions of inputs.

ACKNOWLEDGMENTS

It is a pleasure to thank F. D'Andrea and G. Weisbuch for numerous suggestions; G. Weisbuch also read attentively and provided constructive comments on an earlier version of the paper. This work was supported by a Monge Fellowship of the Ecole Polytechnique (CC), and by grants N00014-12-1-0911 and N00014-16-1-2073 from the Multidisciplinary University Research Initiative (MURI) of the Office of Naval Research and by the US National Science Foundation grant OCE 1243175 (MG).

Appendix A: Damage propagation in simple heterogeneous networks

1. Algorithm

We consider a linear network of $n \gg 1$ agents, where inventories and delays are random variables, respectively denoted by $\Lambda_0, ..., \Lambda_{n-1}$ and $T_{01}, ..., T_{1-2n-1}$. Each of these variables are independent, and follows a certain probability distribution. The duration of the disruption affecting each agent is also random variables, denoted by $\Delta_0, ..., \Delta_{n-1}$. We further denote by f_X the probability distribution function of a random variable X, and by g_X its cumulative distribution function. The duration of the initial perturbation, Δ_0, is exogenous, and its probability distribution function is given, along with those of each inventory and delay. We denote by Ω_k with $1 \leq k < n$ the occurrence of a disruption at agent k, following the initial perturbation of agent 0. We add to this set the event Ω_0, which represent the occurrence of the exogenous perturbation on agent 0. The probability of this event, $\Pr(\Omega_0)$, is 1.

The probability that the perturbation affecting agent 0 propagates to agent 1 corresponds to the probability that the inventory of agent 1 is lower than the initial perturbation. This probability, denoted by $\Pr(\Omega_1|\Omega_0)$ and called the transmission probability, is obtained through the following formula:

$$\Pr(\Omega_1 \mid \Omega_0) = \Pr(\Lambda_1 < \Delta_0) \tag{A1}$$
$$= \int_0^\infty \Pr(\Lambda_1 < x) f_{\Delta_0}(x) \mathrm{d}x \tag{A2}$$
$$= \int_0^\infty g_{\Lambda_1}(x) f_{\Delta_0}(x) \mathrm{d}x. \tag{A3}$$

We assume that the perturbation reaches agent 1. To determine whether it propagates further and reaches agent 2, we need to gauge the relative value of Δ_1 and Λ_2. To that end, we need to determine the probability distribution of $\Delta_1 = \Delta_0 - \Lambda_1$ conditional to the occurrence of Ω_1. It is the probability distribution for Δ_1 for positive values of Δ_1. We can write:

$$\Pr(\Delta_1 = x \mid \Omega_1) = \frac{\Pr(\Delta_0 - \Lambda_1 = x \bigcap x > 0)}{\Pr(\Omega_1 \mid \Omega_0)}. \tag{A4}$$

We can then use the convolution product only to determine the probability distribution of $\Delta_1 \mid \Omega_1$:

$$f_{\Delta_1 \mid \Omega_1}(x) = \frac{1}{\Pr(\Omega_1 \mid \Omega_0)} \int_x^\infty f_{\Delta_0}(u) f_{\Lambda_1}(u-x) \mathrm{d}u. \tag{A5}$$

We can use those results to initiate an iterative algorithm to compute the duration of all perturbations Δ_k conditional to their occurrence Ω_k. The following set of equations allows one to compute the probability distribution of $(\Delta_k \mid \Omega_k)$ given the probability distribution of $(\Delta_{k-1} \mid \Omega_{k-1})$ and the apriori probability distribution chosen for inventories:

$$\Pr(\Omega_k \mid \Omega_{k-1}) = \int_0^\infty g_{\Lambda_k}(x) f_{\Delta_{k-1} \mid \Omega_{k-1}}(x) \mathrm{d}x, \tag{A6}$$
$$f_{\Delta_k \mid \Omega_k}(x) = \frac{1}{\Pr(\Omega_k \mid \Omega_{k-1})} \int_0^\infty f_{\Delta_{k-1} \mid \Omega_{k-1}}(u) f_{\Lambda_k}(u-x) \mathrm{d}u. \tag{A7}$$

This algorithm yields as a by-product all transmission probabilities $\Pr(\Omega_k \mid \Omega_{k-1})$ for $k > 0$.

We compound these probabilities to obtain the probability that the k^{th} agent get disrupted:

$$\Pr(\Omega_k) = \prod_{i=1}^{k} \Pr(\Omega_i \mid \Omega_{i-1})\Pr(\Omega_0). \tag{A8}$$

The expected amplitude of the propagation is simply the sum of all probabilities:

$$\mathbb{E}(A) = \sum_{k=0}^{n} \Pr(\Omega_k). \tag{A9}$$

The discrete probability distribution of A can also be obtained. The probability that A equals an integer a is the probability that the initial perturbation propagates up to agent a without propagating further:

$$\Pr(A = a) = \Pr(\Omega_a) - \Pr(\Omega_{a+1}). \tag{A10}$$

For trees, we make the simplifying assumption that each pathways connecting the root agent to the final agents are independent. In a tree composed of L layers, with each agent supplying to d agents, the expected amplitude is $\mathbb{E}(A) = \sum_{k=0}^{K} d^k \Pr(\Omega_k)$. Figs. 12 shows how the average amplitude changes with the mean and standard deviation of inventories for different probability distribution, using numerical simulations and the algorithm described in this Appendix.

2. Application with exponential distributions

Suppose that the duration of the initial perturbation is a random variable which follow an exponential distribution probability with rate parameter r, and that all inventories follows the same exponential distribution with rate parameter q. The probability distribution function and cumulative distribution function of inventories are:

$$f_\Lambda(x) = q\mathrm{e}^{-qx} \tag{A11}$$

$$g_\Lambda(x) = 1 - \mathrm{e}^{-qx} \tag{A12}$$

$$\tag{A13}$$

Using Eqs. (A6) and (A7), we have:

$$\Pr(\Omega_1 \mid \Omega_0) = \frac{q}{r+q}, \tag{A14}$$

$$f_{\Delta_1 \mid \Omega_1}(x) = r\mathrm{e}^{-rx}. \tag{A15}$$

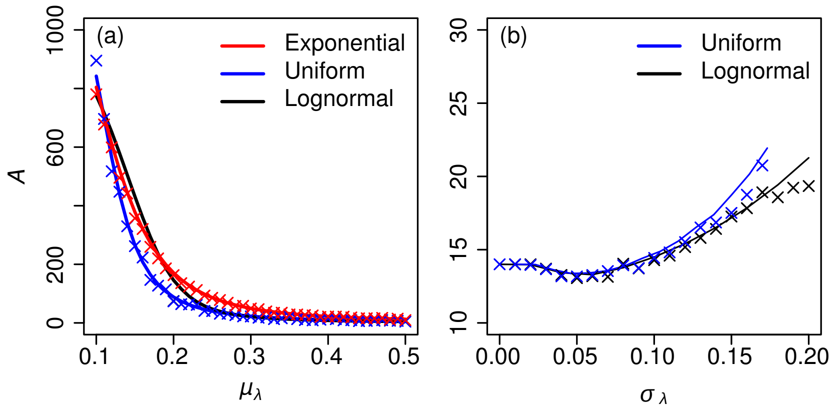

Figure 12. Propagation amplitude A in tree networks of 1023 agents, with one root agent and $d = 2$ descendants per agent, as a function of (a) the mean inventory μ_λ or (b) the standard deviation of inventories, and for different classes of probability distribution. In panel (a), the exponent of the exponential distribution, shown in red, is $1/\mu_\lambda$. In blue, the uniform distribution spans over the range $[0, \mu_\lambda]$, and in black the lognormal distribution has a standard deviation of 0.2. In panel (b), the lognormal distribution has mean $\mu_\lambda = 0.3$, and the uniform distribution is centered on the same value. The $\times$ symbol indicates the averages of numerical simulations, which are compared with the expected behavior predicted by the probabilistic model, indicated by the solid curves.

In other words, if agent 1 gets disrupted, the probability distribution of the duration of this disruption is the same as the probability distribution of the initial perturbation. This result applies to all agents. Consequently, for all $k = 1, .., n$, the transmission probability is constant and equal to $q/(r + q)$.

Appendix B: Analysis of fine detuning

Fine detuning can occur in a network composed of two interacting loops, whose topology is illustrated in Figs. 1d and 1e. Due to this phenomenon, an initial perturbation can amplify and lead to the full and permanent disruption of the network. In this appendix, we determine the conditions that lead to such small detuning. We denote by T_a and T_b the sum of the delays in each loop and assume, without loss of generality, that $T_a \geq T_b$. Similarly, we denote by L_a and L_b the sum of inventories in each loop, including the inventory of the pivotal agent, called agent 0, whose inventory equals λ_0. We assume that L_a and L_b are strictly positive.

When agent 0 gets perturbed at $t = 0$, two waves of disruption emerge, one in each loop. If we consider each loop as independent, then Eq. (6) states that agent 0 gets disrupted through loop a if the duration of the initial perturbation exceeds L_a. We call this event a direct disruption (a). Conversely, a direct disruption (b) occurs if the duration of the initial perturbation exceeds L_b. If either one of these two conditions is not met, then the study of the propagation in this system boils down to the one in isolated loops, where the propagating wave eventually vanishes.

If both propagating waves, though, reach agent 0 again, they can interact. We denote by a' the supplier of agent 0 belonging to loop a, and by b' its supplier from loop b. The dynamical equation governing the behavior $x_0(t)$ of agent 0 is:

$$x_0(t) = [x_a(t - \tau_{a'0}) \wedge x_{b'}(t - \tau_{b'0})] \vee [x_{a'}(t - \tau_{a'0} - \lambda_0) \wedge x_{b'}(t - \tau_{b'0} - \lambda_0)] \,, \tag{B1}$$

where $\tau_{a'0}$ and $\tau_{b'0}$ are the delays between agent a' and agent 0, and between agent b' and agent 0, respectively.

Direct disruption (a) corresponds to the case in which the inventory is emptied due the disruption of supplier a', and the production is stopped due to the same disruption, and likewise for direct disruption (b). But another disruption can also occur when the inventory of agent 0 is emptied by the disruption of one supplier, and the production is then stopped by the perturbation of another one. Specifically, agent 0 is disrupted at t if agent a' is disrupted at $t - \tau_{a'0} - \lambda_0$ and agent b at $t - \tau_{b'0}$. We call this phenomenon an (ab) cross-disruption. Conversely, a (ba) cross-disruption occurs when agent 0 is disrupted at t because agent b' is disrupted at $t - \tau_{b'0} - \lambda_0$ and agent a' at $t - \tau_{a'0}$.

To study these cross-disruptions, we need to know when the propagation waves hit suppliers a' and b'. From Eq. (7), supplier a' is perturbed at $(T_a - \tau_{a'0}) + (L_a - \lambda_0)$ until $(T_a - \tau_{a'0}) + \delta_0$, and supplier b at $(T_b - \tau_{b'0}) + (L_b - \lambda_0)$ until $(T_b - \tau_{b'0}) + \delta_0$. The conditions for an (ab) cross-disruption to occur are therefore:

$$(T_a - \tau_{a'0}) + (L_a - \lambda_0) \leq t - \tau_{a'0} - \lambda_0 \leq (T_a - \tau_{a'0}) + \delta_0, \tag{B2}$$

$$(T_b - \tau_{b'0}) + (L_b - \lambda_0) \leq t - \tau_{b'0} \leq (T_b - \tau_{b'0}) + \delta_0. \tag{B3}$$

They can be rewritten as:

$$T_a + L_a \leq t \leq T_a + \lambda_0 + \delta_0, \tag{B4}$$

$$T_b + L_b - \lambda_0 \leq t \leq T_b + \delta_0. \tag{B5}$$

Both conditions can be realized at the same time if:

$$T_a + L_a \leq T_b + \delta_0, \tag{B6}$$

$$T_b + L_b - \lambda_0 \leq T_a + \lambda_0 + \delta_0. \tag{B7}$$

Since $T_a < T_b$ and $L_a < \delta_0$, the first condition is always met. The second condition can be rewritten as: $\Delta_\mathrm{T} < \delta_0 - L_b + 2\lambda_0$.

The same analysis for a (ba) cross-disruption, yields that the first necessary condition for such a disruption to occur is $T_b + L_b \leq T_a + \delta_0$; under the present assumptions, the latter condition is not met. Hence, if $T_a < T_b$, only an (ab) cross-disruption is possible.

The starting and ending times of the cross-disruption (ab) are, respectively $\max\{T_a + L_a, T_b + L_b - \lambda_0\}$ and $\min\{T_a + \lambda_0 + \delta_0, T_b + \delta_0\}$. Since the direct disruption (a) occurs between $T_a + L_a$ and $T_a + \delta_0$, the cross-disruption (ab) always occurs after the direct disruption (a). Both disruptions overlap if disruption (ab) starts before the end of disruption (a), i.e. if $\Delta_\mathrm{T} < L_a - L_b + \lambda_0$ or if $\Delta_\mathrm{T} < \delta_0 - L_b + \lambda_0$. Since $\delta_0 > L_a$, the second condition $\Delta_\mathrm{T} < \delta_0 - L_b + \lambda_0$ is sufficient for overlapping to occur. Similarly, given that the direct disruption (b) occurs between $T_b + L_b$ and $T_b + \delta_0$, the cross-disruption (ab) always occurs before. Both disruptions overlap if disruption (ab) ends after the start of disruption (b), i.e. if $\Delta_\mathrm{T} < \lambda_0$ or if $\Delta_\mathrm{T} < \delta_0 - L_b + \lambda_0$. Since $\delta_0 > L_b$, the second condition $\Delta_\mathrm{T} < \delta_0 - L_b + \lambda_0$ is sufficient for overlapping to occur.

Thus, the cross-disruption (ba) never occurs, and the cross-disruption (ab) only occurs if $\Delta_\mathrm{T} < \delta_0 - L_b + 2\lambda_0$; if so, it overlaps with both direct disruptions (a) and (b) provided $\Delta_\mathrm{T} < \delta_0 - L_b + \lambda_0$. In such a case, the disruption of agent 0 spans the time interval from the beginning of disruption (a) up to the end of disruption (b), i.e. $T_a + L_a \leq t \leq T_b + \delta_0$. The duration of this disruption is therefore $\Delta_\mathrm{T} + \delta_0 - L_a$, which exceeds the initial perturbation if $\Delta_\mathrm{T} > L_a$. Conversely, if $T_b < T_a$, by exchanging a and b, we obtain that the cross-disruption (ba) occurs if $\Delta_\mathrm{T} < \delta_0 - L_a + 2\lambda_0$ and overlaps with both direct disruptions if $\Delta_\mathrm{T} < \delta_0 - L_a + \lambda_0$. Finally, the new disruption of agent 0 exceeds the initial perturbation if $\Delta_\mathrm{T} > L_b$.

To summarize, the phenomenon of fine detuning occurs when the difference Δ_T in delays between the two loops falls within the following range:

$$L_a < \Delta_\mathrm{T} < \delta_0 + \lambda_0 - L_b; \tag{B8}$$

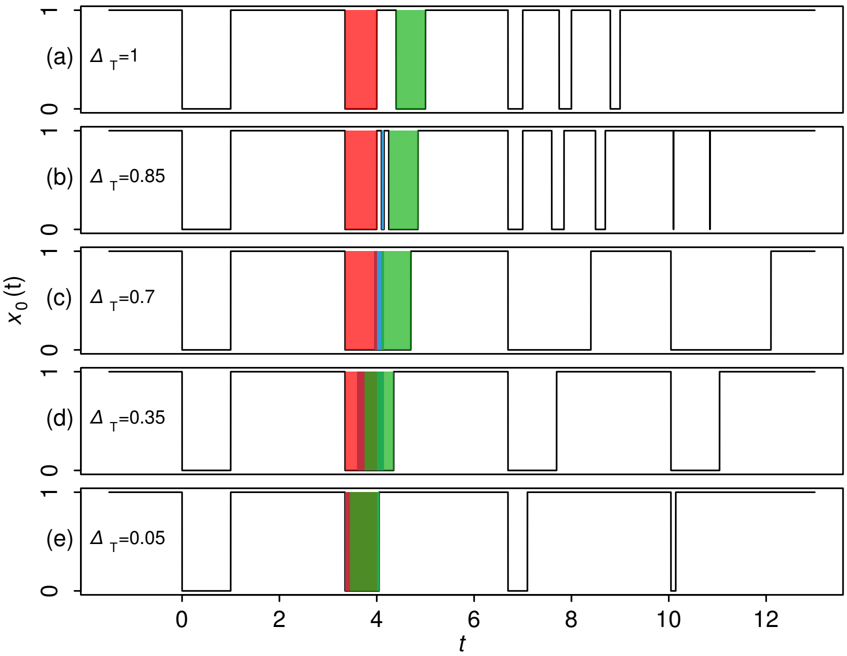

Figure 13. Time series of the production of the pivotal agent $x_0(t)$ connecting two loops, called loop a and loop b, as in Figs. 1d or 1e. The sum T_a of all delays in loop a is 3, and the sum of inventories, L_a is 0.35. The inventory λ_0 of agent 0 is 0.15. For loop b, $L_b = 0.4$ and $T_b = T_a + \Delta_\mathrm{T}$, where Δ_T is the fine detuning parameter, which decreases from panel (a) to panel (e) : (a) $\Delta_\mathrm{T} = 1$, (b) $\Delta_\mathrm{T} = 0.85$, (c) $\Delta_\mathrm{T} = 0.7$, (d) $\Delta_\mathrm{T} = 0.35$ and (e) $\Delta_\mathrm{T} = 0.05$. Colors are added to the second disruption wave, for $3.5 \leq t \leq 4.5$. The red color indicates a disruption coming from loop a, the green color indicates a disruption coming from loop b, and the blue color corresponds to so-called cross-perturbations originating from the interaction between the two loops; see text for details.

here L_a is the sum of inventories in the quick loop, L_b the sum of inventories in the slow loop and λ_0 the inventory of the pivotal agent. When $\Delta_\mathrm{T} < \delta_0 - L_b + 2\lambda_0$, as in Fig. 13a, no cross disruption (ab) is generated and the two direct disruptions do not overlap. Each propagation wave keeps propagating but the duration of each disruption keeps decreasing, until the propagation ends. If $\delta_0 - L_b + \lambda_0 < \Delta_\mathrm{T} < \delta_0 - L_b + 2\lambda_0$, as in Fig. 13b, a cross-disruption (ab) occurs but it fails to overlap with the direct disruptions.

When the inequalities (B8) is verified, then both overlapping and amplification occur,and thus the initial perturbation amplifies each times it returns to agent 0, until all agents are permanently perturbed; see Fig. 13c. In particular, when $L_a < \Delta_\mathrm{T} < \delta_0 - L_b$, both direct disruptions overlap, without being bridged by a cross-disruption. For $\Delta_\mathrm{T} = L_a$, the duration of the new disruption is exactly equal to the initial perturbation, such that a periodic regime sets in: the initial perturbation is identically regenerated at each period; see Fig. 13d. When Δ_T falls below L_a, overlapping is so strong that the new disruption is shorter than the initial perturbation, and the damage propagation eventually vanishes, cf. Fig. 13e.

Appendix C: Complex behavior for further investigation

Figure 14 presents additional results for the 3-loop network of Fig. 1f, which was studied in Sec. III D, with a second set of parameters, whose values are described in the caption of the figure. The periods of the oscillations seen in this figure are longer than for the first set of parameters studied in Fig. 3, for which the periods were of 1 or 2 units of time. The period of the reference case is 4 in panel (a), and it is modified by small changes in single delays to equal 2 in panel (b), 4.1 in panel (c).

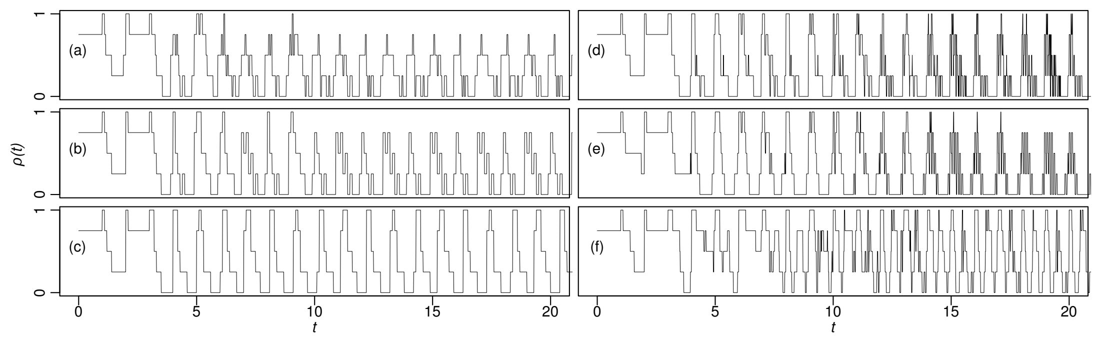

Figure 14. Time series of the density $\rho(t)$ of fully active agents in the 3-loop network shown in Fig. 1f. The three loops are only connected through a pivotal agent, called agent 0. The initial perturbation affects agent 0 during $\delta_0 = 1$ unit of time. (a) Results for the default delays — all delays are equal to 1 except $\tau_{20} = 2$ and $\tau_{30} = 3$ — and default inventories — $\lambda_0 = 0$, $\lambda_1 = 0.1$, $\lambda_2 = 0.2$ and $\lambda_3 = 0.4$. (b, c) Effects of changes in delays on $\rho(t)$: (b) $\tau_{20} = 1.9$; and (c) $\tau_{30} = 3.1$. (d)–(f) Effects of changes in the allocation of inventories on $\rho(t)$: (d) $\lambda_1 = 0.08$; (e) $\lambda_3 = 0.87$; and (f) $\lambda_2 = 0.57$.

The main difference with respect to Fig. 3 is a more heterogeneous distribution of the delays, with two delays different from 1: $\tau_{20} = 2$ and $\tau_{30} = 3$. The fact that each one of the three loops have distinct delays seems to give rise to longer transients — namely 3 to 4 times higher than in Fig. 3, to be exact. In panels (d), (e) and (f), specific inventories are changed which can widely modify the periodic pattern. Although these changes do not modify the period of the oscillation, they can induce disruption peaks in the middle of the period, as observed in panel (f).

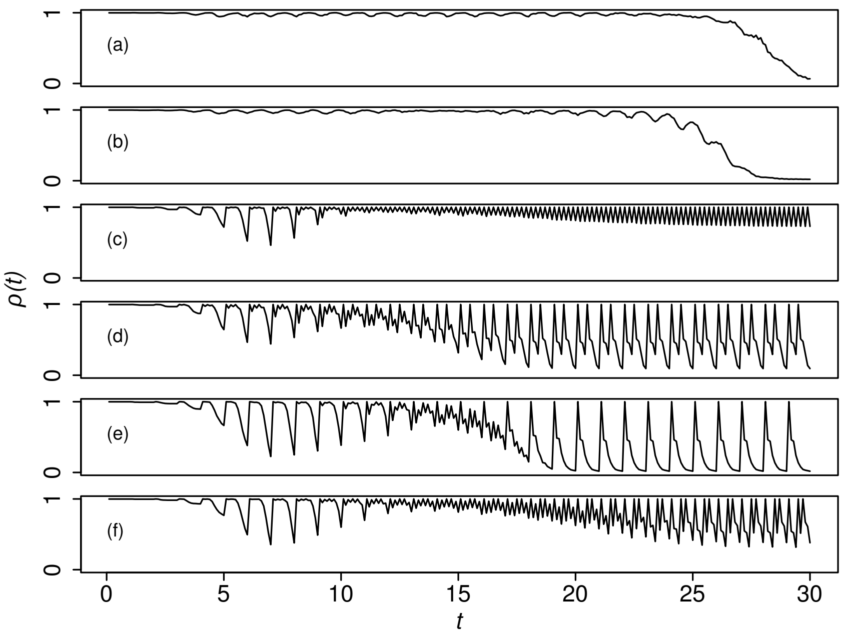

Figure 15. Examples of time series of the density $\rho(t)$ of fully active agents in ER networks. (a, b) Inventories are all equal to 0.2 and delays are lognormally distributed with $(\mu_\tau = 1, \sigma_\tau = 0.16)$. (c)–(f) Delays are homogeneous and equal to 1, while inventories are lognormally distributed with $\mu_\lambda = 0.2$ and (c, d) $\sigma_\lambda = 0.1$; (e) $\sigma_\lambda = 0.12$; and (f) $\sigma_\lambda = 0.13$.

Figure 15 displays additional results for large ER networks, with $n = 10^4$, that illustrate particularly interesting types of behavior. Panels (a) and (b) show long transients with a strong periodic component before collapse. Although delays are too heterogeneous for a limit cycle to occur, the transient lasts for about 20 oscillations. In panel (b), these oscillations even cease for a few periods before returning and eventually inducing collapse. This temporary damping of transient oscillations is also seen in panels (c) to (f), where delays are homogeneous. In these 4 panels, we observe at first an amplitude-modulated periodic pattern that sets in for 4–8 oscillations, and then evolves to another asymptotically stable one. This change of pattern suggests that the disruption waves move from one set of agents to another one. In panel (c), this movement even leads to a new periodicity, shifting from 1 to 0.2 time units.

REFERENCES

[1]United Nations Office for Disaster Risk Reduction, "Hyogo Framework for Action 2005-2015: Building the resilience of nations and communities to disasters," Tech. Rep. A/CONF.206/6 (The United Nations, Kobe, Hyogo, Japan, 2005).

[2]F. H. Norris, S. P. Stevens, B. Pfefferbaum, K. F. Wyche, and R. L. Pfefferbaum, "Community resilience as a metaphor, theory, set of capacities, and strategy for disaster readiness," American Journal of Community Psychology **41**, 127–150 (2008).

[3]E. L. Tompkins and W. Adger, "Does adaptive management of natural resources enhance resilience to climate change?" Ecology and Society **9**, 10 (2004).

[4]A. Narain, I. Ötker-Robe, and C. Pazarbasioglu, eds., *Building a More Resilient Financial Sector: Reforms in the Wake of the Global Crisis* (International Monetary Fund, Washington, DC, 2012).

[5]Y. Sheffi, *The Resilient Enterprise: Overcoming Vulnerability for Competitive Advantage* (MIT Press, Cambridge, MA, 2005).

[6]M. Ghil, P. Yiou, S. Hallegatte, B. D. Malamud, P. Naveau, A. Soloviev, P. Friederichs, V. Keilis-Borok, D. Kondrashov, V. Kossobokov, O. Mestre, C. Nicolis, H. W. Rust, P. Shebalin, M. Vrac, A. Witt, and I. Zaliapin, "Extreme events: dynamics, statistics and prediction," Nonlinear Processes in Geophysics **18**, 295–350 (2011).

[7]R. Gledhill, D. Hamza-Goodacre, and L. Ping Low, "Business-not-as-usual: Tackling the impact of climate change on supply chain risk," Tech. Rep. (PwC, 2013).

[8]S. Hallegatte, "Economic Resilience: Definition and Measurement," Tech. Rep. (The World Bank, 2014).

[9]I. Goldin, "Globalisation and risks for business: Implications of an increasingly interconnected world," Tech. Rep. (Lloyd's, 2010).

[10]WEF, "New Models for Addressing Supply Chain and Transport Risk," Tech. Rep. (World Economic Forum, 2012).

[11]C. S. Holling, "Resilience and stability of ecological systems," Annual Review of Ecology and Systematics **4**, 1–23 (1973).

[12]C. Holling, "The resilience of terrestrial ecosystems; local surprise and global change," in *Sustainable Development of the Biosphere*, edited by W. C. Clark and R. Munn (Cambridge University Press, Cambridge, UK, 1986).

[13]G. Peterson, C. R. Allen, and C. S. Holling, "Ecological resilience, biodiversity, and scale," Ecosystems **1**, 6–18 (1998).

[14]S. L. Pimm, "The complexity and stability of ecosystems," Nature **307**, 321–326 (1984).

[15]G. W. Harrison, "Stability under environmental stress: Resistance, resilience, persistence, and variability," The American Naturalist **113**, 659–669 (1979).

[16]E. Chavez, G. Conway, M. Ghil, and M. Sadler, "Ensuring food security by risk management in an uncertain climate," Nature Climate Change **5**, 997–1002 (2015).

[17]P. Bak, K. Chen, J. Scheinkman, and M. Woodford, "Aggregate fluctuations from independent sectoral shocks: self-organized criticality in a model of production and inventory dynamics," Ricerche Economiche **47**, 3–30 (1993).

[18]S. Battiston, D. Delli Gatti, M. Gallegati, B. Greenwald, and J. E. Stiglitz, "Credit chains and bankruptcy propagation in production networks," Journal of Economic Dynamics and Control **31**, 2061–2084 (2007).

[19]G. Weisbuch and S. Battiston, "From production networks to geographical economics," Journal of Economic Behavior & Organization **64**, 448–469 (2007).

[20]S. Battiston, D. Delli Gatti, M. Gallegati, B. Greenwald, and J. E. Stiglitz, "Liaisons dangereuses: Increasing connectivity, risk sharing, and systemic risk," Journal of Economic Dynamics and Control **36**, 1121–1141 (2012).

[21]F. Henriet, S. Hallegatte, and L. Tabourier, "Firm-network characteristics and economic robustness to natural disasters," Journal of Economic Dynamics and Control **36**, 150–167 (2012).

[22]S. Hallegatte, "An adaptive regional input-output model and its application to the assessment of the economic cost of Katrina," Risk Analysis **28**, 779–799 (2008).

[23]B. Coluzzi, M. Ghil, S. Hallegatte, and G. Weisbuch, "Boolean delay equations on networks in economics and the geosciences," International Journal of Bifurcation and Chaos **21**, 3511–3548 (2011).

[24]M. E. J. Newman, "Spread of epidemic disease on networks," Physical Review E **66** (2002), 10.1103/PhysRevE.66.016128.

[25]Y. Fujiwara and H. Aoyama, "Large-scale structure of a nation-wide production network," The European Physical Journal B **77**, 565–580 (2010).

[26]D. Acemoglu, V. M. Carvalho, A. Ozdaglar, and A. Tahbaz-Salehi, "The network origins of aggregate fluctuations," Econometrica **80**, 1977–2016 (2012).

[27]R. Albert, H. Jeong, and A.-L. Barabási, "Error and attack tolerance of complex networks," Nature **406**, 378–382 (2000).

[28]A. E. Motter and Y.-C. Lai, "Cascade-based attacks on complex networks," Physical Review E **66**, 065102 (2002).

[29]J. Lorenz, S. Battiston, and F. Schweitzer, "Systemic risk in a unifying framework for cascading processes on networks," The European Physical Journal B **71** (2009), 10.1140/epjb/e2009-00347-4.

[30]C. J. Tessone, A. Garas, B. Guerra, and F. Schweitzer, "How big is too big? Critical shocks for systemic failure cascades," arXiv:1209.0959 [cond-mat, physics:physics, q-fin] (2012).

[31]L. Zhao, K. Park, and Y.-C. Lai, "Attack vulnerability of scale-free networks due to cascading breakdown," Physical Review E **70**, 035101 (2004).

[32]R. Pastor-Satorras and A. Vespignani, "Epidemic dynamics and endemic states in complex networks," Physical Review E **63** (2001), 10.1103/PhysRevE.63.066117, arXiv: cond-mat/0102028.

[33]R. M. May and A. L. Lloyd, "Infection dynamics on scale-free networks," Physical Review E **64**, 066112 (2001).

[34]G. D'Agostino and A. Scala, *Networks of Networks: The Last Frontier of Complexity*, Understanding Complex System (Springer, New York, 2013).

[35]R. L. Axtell, "Zipf distribution of U.S. firm sizes," Science **293**, 1818–1820 (2001).

[36]X. Gabaix, "The granular origins of aggregate fluctuations," Econometrica **79**, 733–772 (2011).

[37]S. Hallegatte, "Modeling the role of inventories and heterogeneity in the assessment of the economic costs of natural disasters," Risk Analysis **34**, 152–167 (2013).

[38]J. Sterman, *Business Dynamics: Systems Thinking and Modeling for a Complex World* (Irwin/McGraw-Hill, Boston, 2000).

[39]C. E. Riddalls and S. Bennett, "The stability of supply chains," International Journal of Production Research **40**, 459–475 (2002).

[40]J. Miśkiewicz, "Economy with the time delay of information flow—The stock market case," Physica A: Statistical Mechanics and its Applications **391**, 1388–1394 (2012).

[41]X.-J. Xu, H.-O. Peng, X.-M. Wang, and Y.-H. Wang, "Epidemic spreading with time delay in complex networks," Physica A: Statistical Mechanics and its Applications **367**,

525–530 (2006).

[42]C. Xia, L. Wang, S. Sun, and J. Wang, "An SIR model with infection delay and propagation vector in complex networks," Nonlinear Dynamics **69**, 927–934 (2012).

[43]L. Buzna, K. Peters, and D. Helbing, "Modelling the dynamics of disaster spreading in networks," Physica A: Statistical Mechanics and its Applications **363**, 132–140 (2006).

[44]D. Dee and M. Ghil, "Boolean difference equations, I: Formulation and dynamic behavior," SIAM Journal on Applied Mathematics **44**, 111–126 (1984).

[45]M. Ghil and A. Mullhaupt, "Boolean delay equations, II. Periodic and aperiodic solutions," Journal of Statistical Physics **41**, 125–173 (1985).

[46]M. Ghil, I. Zaliapin, and B. Coluzzi, "Boolean delay equations: A simple way of looking at complex systems," Physica D: Nonlinear Phenomena **237**, 2967–2986 (2008).

[47]G. Weisbuch, *Complex Systems Dynamics: An Introduction to Automata Networks* (Addison-Wesley, Boston, 1991).

[48]M. Darby and L. Mysak, "A Boolean delay equation model of an interdecadal Arctic climate cycle," Climate Dynamics **8**, 241–246 (1993).

[49]A. Saunders and M. Ghil, "A Boolean delay equations model of ENSO variability," Physica D **2801**, 1–25 (2001).

[50]I. Zaliapin, V. Keilis-Borok, and M. Ghil, "A boolean delay equation model of colliding cascades. Part I: Multiple seismic regimes," Journal of Statistical Physics **111**, 815–837 (2003).

[51]I. Zaliapin, V. Keilis-Borok, and M. Ghil, "A boolean delay equation model of colliding cascades. Part II: Prediction of critical transitions," Journal of Statistical Physics **111**, 839–861 (2003).

[52]H. Öktem, R. Pearson, and K. Egiazarian, "An adjustable aperiodic model class of genomic interactions using continuous time Boolean networks (Boolean delay equations)," Chaos **13**, 1167–1174 (2003).

[53]C. Li and G. Chen, "Synchronization in general complex dynamical networks with coupling delays," Physica A: Statistical Mechanics and its Applications **343**, 263–278 (2004).

[54]K.-I. Goh, B. Kahng, and D. Kim, "Universal behavior of load distribution in scale-free networks," Physical Review Letters **87**, 278701 (2001).

[55]F. Chung and L. Lu, "Connected components in random graphs with given expected degree sequences," Annals of Combinatorics **6**, 125–145 (2002).

[56]P. Erdős and A. Rényi, "On random graphs. I," Publicationes Mathematicae Debrecen **6**, 290–297 (1959).

[57]B. Karrer and M. E. J. Newman, "Random acyclic networks," Physical Review Letters **102**, 128701 (2009).

[58]M. Newman, *Networks: An Introduction* (Oxford University Press, Oxford, U.K., 2010).

[59]G. Bianconi, N. Gulbahce, and A. E. Motter, "Local structure of directed networks," Phys. Rev. Lett. **100**, 118701 (2008).

[60]S. V. Buldyrev, R. Parshani, G. Paul, H. E. Stanley, and S. Havlin, "Catastrophic cascade of failures in interdependent networks," Nature **464**, 1025–1028 (2010).

[61]D. P. Rosin, D. Rontani, D. J. Gauthier, and E. Schöll, "Control of synchronization patterns in neural-like boolean networks," Physical Review Letters **110** (2013), 10.1103/PhysRevLett.110.104102.

[62]D. P. Rosin, D. Rontani, N. D. Haynes, E. Schöll, and D. J. Gauthier, "Transient scaling and resurgence of chimera states in networks of Boolean phase oscillators," Physical Review E **90** (2014), 10.1103/PhysRevE.90.030902.

[63]O. D'Huys, J. Lohmann, N. D. Haynes, and D. J. Gauthier, "Super-transient scaling in time-delay autonomous boolean network motifs," Chaos **26**, 094810 (2016), http://dx.doi.org/10.1063/1.4954274.

Chapter 6

The fragmentation of production amplifies systemic risk in supply chains

This paper is a final draft intended to be submitted to the journal *Proceedings of the National Academy of Sciences*. The main text is followed by the supplementary information.

Authors: Célian Colon, Åke Brännström, Elena Rovenskaya and Ulf Dieckmann. AB, ER and UD are affiliated to the Internation Insitute for Applied System Analysis, Autria. AB is also affiliated to Umeå University, Sweden, and ER to Moscow State University, Russia.

Abstract: Unexpected localized disruptions can cascade along supply chains and induce disproportionately high losses. Mitigating such risks can be challenging as nowadays, through outsourcing, supply chains are becoming more complex and specialized. We formulate a stylized model in which firms in a supply chain mitigate the risk of supply disruption using inventories. The mitigating strategy of one firm influences the profit of the other; we analyze such interactions using evolutionary game theory. We find that the mitigating effort that each firm should commit largely varies depending on the position of a firm in the supply chain. Vertical fragmentation, whereby the design and production stages of a good or service are split across multiple firms, reduces their incentives to maintain inventories and gives rise to systemic risk. Finally, we show how decision-makers can mitigate systemic risk using a network indicator based on the ecological concept of "trophic level" to allocate inventory.

The fragmentation of production amplifies systemic risk in supply chains

Introduction

Supply chain disruptions raise significant concerns for businesses (1–6) and their adverse financial effects have been empirically established (7–9). Trigger events include natural disasters, industrial accidents, bankruptcies, and social movements. Localized disruptions may cascade from one firm to another and cause significant economic losses in distant locations (10). For example, such ripple mechanisms gave Tohoku's earthquake and Thailand's 2011 floods a global reach (11–13). Even minor accidents may generate sizeable impacts to supply chains (e.g., 12), especially when they affect the production of very specific inputs (9).

Firms often lack visibility over the supply chain in which they are a part (15–17). In this context, incurring losses due to a cascading disruption appears to be a systemic risk, a concept more commonly associated with financial systems (18). Systemic risk emerges in networked systems, in which the state of a node depends on the activity of the others. Production systems are becoming a global network as a result of large-scale transformations developed over the past decades, namely offshoring, outsourcing and vertical specialization (19–21). In many sectors, production has been split into multiple sequential stages operated by geographically diverse firms. Many manufactured goods are now assembled from a large number of outsourced components. These trends have resulted in longer and more interconnected supply chains, whose shapes can be tracked with sectorial input–output tables (e.g., 22) or supplier–buyer data (e.g., 23). The consequence of a greater structural complexity of production networks for the systemic risk has started to be investigated empirically (13) and theoretically (24, 25).

Another effect of outsourcing and vertical specialization is the increased fragmentation of supply chains, whereby production stages get highly segmented and each segment is run by a legally distinct firm (19). Fragmentation creates additional challenges to the mitigation of systemic risk. Even though at their level firms are taking risk-mitigating measures, such as inventories, supplier diversification, or operational flexibility, their exposure to systemic risk also depends on the measures implemented by others. For instance, in a lean management perspective, manufacturers reduce inventory by working with few and highly reliable suppliers. Conversely, if a supplier decides to engage in more risk-prone operations, its clients may, in response, build larger inventories or find alternative suppliers. In a supply chain, even if firms first aim to design a risk-mitigating strategy that improves their own profitability, in practice this strategy depends on the one implemented by the others. If now a supply chain becomes more fragmented, then its exposure to systemic risk depends on an even larger number of other firms. We aim to evaluate how this proliferation of distinct yet interdependent risk-mitigating strategies affects the overall level of systemic risk in a supply chain.

The strategies adopted by economic agents that interact and aim to maximize their profit can be adequately studied with game theory. This analytical framework has been used in operations research and management sciences to elicit optimal strategies for firms to mitigate supply disruptions (26) and to identify ways to foster cooperation along supply chains (27, 28). The assumption of strong rationality, according to which agents instantaneously process the full decision-trees of all players over an infinite time horizon, has however limited the application of game theory to small or very idealized supply chains, in which the link between systemic risk and fragmentation cannot be addressed. To overcome this limitation, we develop a model of supply chain based on the evolutionary dynamics, which belong to the class of evolutionary games on networks (29, 30). Firms follow simple behavioral rules to explore and adjust risk-mitigating strategies in order to increase their profits. We are able to elicit the outcome of the strategic interactions in complex supply chains and study the effect of fragmentation.

In our model, final producers attempt to fulfill a fixed demand from households. They produce goods using inputs from suppliers, who themselves purchase inputs from other firms, and so on up to primary producers, thus forming a supply chain. Production of each single firm is subject to randomly occurring failures. Firms use an inventory to mitigate the risk of supply disruptions. Given the level of systemic risk they experience, they adjust the rate at which inventory is replenished in order to increase their expected profit. If the supply chain is fully fragmented, each firm aims to increase its own profit; if it is fully integrated, all firms are concerned with the total profit of the supply chain. Intermediate fragmentation scenarios are also studied.

We found that supply chain fragmentation inherently fosters systemic risk. When the different stages of a supply chain get operated by an increasing number of firms, the overall level of inventory is reduced, resulting in a higher systemic risk. Moreover, the risk-mitigating efforts of firms are heterogeneous and highly depend on their position in the supply chain. To address this issue, we investigate network indicators that could offer guidance for the allocation of inventories, and find that an indicator equivalent to the ecological "trophic level" prescribes the mitigation strategy rather effectively. This approach requires a precise mapping of the whole supply chains and could help business managers, insurers or policy makers mitigate fragmentation-induced systemic risk.

Model

Supply chain as input–output network. We model a supply chain as a directed acyclic network of n firms with a predefined adjacency matrix M, such that $m_{ij} = 1$ if firm i is supplying goods to firm j and $m_{ij} = 0$ otherwise. No firm supplies to itself and hence $m_{ii} = 0$. Firms that have no incoming links in the network produce using raw materials and are called "primary producers"; at the other end of the chain, firms that do not have outgoing links to other firms sell their production to households and are called "final producers". Since the supply chain is acyclic, all other firms are intermediary producers. The economic activity is driven by a fixed final demand from households, represented by vector D, where $d_i = 1/n_f$ if firm i is one of the n_f final producers and $d_i = 0$ otherwise. To meet this demand, final producers order inputs from their suppliers, which themselves order inputs from their suppliers, and so on up to primary producers. Firms equally divide the total amount of input they need between their suppliers. Each firm has a linear production function, i.e., it transforms quantity x_i of input into quantity y_i of output with productivity $z > 1$—the same for all firms—such that $y_i = z\, x_i$, where x_i and y_i are expressed in the same monetary terms. Inputs are assumed to be fully substitutable and storable with durability v, which means that, at the end of each time step, while all inputs that a firm did not use are added to its inventory, a portion $1 - v$ of this inventory gets obsolete and is thrown away. In the absence of external perturbations, firms order the exact quantity of inputs required to meet the demand they face. We form an input–output matrix A, whose coefficients are $a_{ij} = m_{ij}/(z\, s_i)$, where s_i is the number of suppliers of firm i. It describes how much input from firm j is needed by firm i to produce one unit of output. Using linear algebra, we obtain that the vector of production targets Y is equal to $(I - A)^{-1}D$, where I is the identity matrix. In the absence of a supply disruption, each firm produces its production target y_i. In these conditions, the profit of each firm, π_{0i}, defined as sales minus inputs costs, is equal to $y_i(1 - 1/(z\, s_i))$; all other costs involved in production such as labor and capital costs are considered to be fixed and are omitted from the model.

Dynamic responses to external perturbations. To model supply disruptions, we assume that at each time step, every firm can lose its entire production with probability $p \in [0,1]$ which is the same for all firms. Such perturbed firms are unable to supply goods to their clients, who may as a result lack the necessary inputs to meet their demand. Rationing may occur and the disruption may cascade further along the supply chain, leading to profit losses by firms located downstream from the initial failure. To mitigate this risk, firms build inventories of inputs by ordering at each time step some extra units from their suppliers. Specifically, if firm i faces demand y_i, it constantly orders a quantity $y_i(1 + r_i)/(z\, s_i)$ of inputs from each of its supplier, in which $r_i > 0$ is the overordering rate specific to each firm and constant over time. Overordering leads to greater input costs, such that when no perturbation occurs, profit is reduced; but in the event of a supply disruption, it compensates for potential losses. The input–output coefficients become $a_{ij} = m_{ij}(1 + r_i)/(z\, s_i)$; they are used to compute the production target y_i of each firm. Because, over time, production disruptions occur randomly, the actual production of firms varies over time, and so do their profits. To evaluate the impact of firms' overordering on their profits, we conduct numerical simulations and calculate the average profits of each firm $\bar{\pi}_i$ over a long time horizon T. For simple supply chains, we derive reduced-form dynamical equations; see *SI Text, S1*. In addition, for specific classes of layered supply chains, we have developed an algorithm that enables us to calculate the exact expected value of firms' profits; see *SI Text, S5*.

The aggregate losses of the entire supply chain measure the decrease in all firms' profit, using as a baseline the case without perturbations and without overordering:

$$L = \sum_i (\pi_{0i} - \bar{\pi}_i). \qquad [1]$$

Aggregate losses can be split into direct losses L_D, incurred by perturbed firms, and indirect losses L_I, resulting from the propagation of disruption throughout the supply chain. In a simulation, direct losses can be evaluated by summing the profit loss of firms only when they are externally perturbed. Indirect losses are then the difference between aggregate and direct losses.

To evaluate the "mitigation success" S produced by a vector of overordering rates $R = \{r_1, r_2, \dots, r_n\}$, we measure a relative change in the indirect losses compared to a counterfactual case in which firms ignore disruptions risks and do not overorder, i.e., $R_0 = \{0, 0, \dots, 0\}$:

$$S(R; M, z, v, p) = \frac{L_\mathrm{I}(R) - L_\mathrm{I}(R_0)}{L_\mathrm{I}(R_0)}. \qquad [2]$$

Adjustment of overordering and supply chain fragmentation. Firms can adjust their overordering rate to achieve a certain objective. In this analysis we assume firms to be risk-neutral. We consider a scenario of "full fragmentation", in which firms overorder at a rate that maximizes their own expected profits. Since the overordering rate chosen by one firm may affect the profits of other firms, firms interact strategically, which means that each firm responds optimally to the decisions of others. The vector of overordering rates at which no firm can unilaterally increase its profit corresponds to a Nash equilibrium; we denote it by R^*. To study this situation, we apply an evolutionary process based on a stochastic gradient ascent algorithm, whereby each firm iteratively tries and tests various rates and adopts the ones that increase its profit. The details are presented in *SI Text*, *S6*. We demonstrate the existence and uniqueness of the Nash equilibrium analytically for simple supply chains in *SI Text, S4*; numerical evidence is provided for the general case; see *SI Text*, *S7*. We then evaluate the mitigation success S^* that is achieved when all firms adopt the Nash equilibrium overordering rates.

Next, we contrast the "full fragmentation" scenario with scenarios of a partial fragmentation. Specifically, we consider firms allocated into groups, such that, within a group, each firm adjusts its overordering rate to maximize the group's profit. A group can only be composed of adjacent firms: each one has to be the supplier or the client of one other firm in the group. A supply chain with g groups has a fragmentation level $f = (g - 1)/(n - 1)$. We generate a large number of group configurations, and study how fragmentation f affects mitigation success S^*.

Numerical and analytical study. General results are derived from numerical investigation of large ensembles of random supply chains generated with the classic algorithm for Erdős–Rényi graphs restricted to the upper triangle of the adjacency matrix (31). As a baseline, we have chosen supply chains with $n = 30$ firms and an average of $c = 2$ suppliers per firm; we also perform a robustness checks for $10 \leq n \leq 100$ and $1 \leq c \leq 4$. We explore the full parameter space: $z \geq 1$, $0 \leq v \leq 100\%$, and $0 \leq p \leq 100\%$, as well as the cases with distributed values of the firm-level parameters, in which a different z, v, and p is given to each firm. To illustrate the results, we selected representative examples by using the following benchmark values: $z = 2$, $v = 50\%$ and $p = 10\%$. To advance the understanding of the role of each parameter in the overordering decisions, we perform analytical studies of simpler supply chains: a single producer supplied by multiple firms and a class of multi-layered networks. These analytical results, given in *SI Text*, *S1* to *S5*, are qualitatively similar to the results in the general case and helped facilitate its interpretation.

Results

Optimal levels of inventory are widely unbalanced along supply chains. Through the evolutionary process, firms gradually adapt their overordering rates to increase their profits. This objective can be met by diminishing their loss induced by the supply disruptions. Since the exposure to this risk largely differs from one firm to another, these decentralized profit-increasing decisions lead to very heterogeneous overordering rates. Figure 1(a) shows for the benchmark example the evolution of the overordering rates, initially at 0%, in a fully fragmented supply chain represented in Fig. 1(b). For some firms, overordering has a strong impact on their profits. They rapidly increase their rate to cope with the 10% failure rate. In this example, the evolutionary trajectory largely fluctuates around a stationary value. This volatility is due to the time-averaging procedure done by the firms to assess the profitability of different overordering rates. Since perturbations are stochastic, the time-averaged profit associated to a particular overordering rate may vary from one evolutionary time step to the other. The impact of the stochasticity on the evolutionary process is discussed in further details in *SI Text, S6*. For other firms, in contrast, the marginal effect of overordering on their profits is smaller, so that they exhibit slower and less volatile trajectories.

Figure 1(b) shows how the resulting overordering rates are distributed in the supply chain. In this instance, more than a half of the firms do not overorder at all, mainly those located upstream that have five or fewer total suppliers—“total” meaning that suppliers of all tiers are counted. This particular observation lies in accordance with the distributions of overordering rates obtained from an ensemble of 2,000 fragmented supply chains with similar number of firms and average connectivity but different topologies; see Fig. 1(c). Given that the inflow of raw materials is not subject to perturbations, primary producers never overorder. As we move downstream, firms become increasingly subject to supply disruptions, because each supplier, direct and indirect, is a potential source of disruption. Risks gradually pile up, until thresholds are crossed and overordering becomes beneficial. Using simpler supply chains, we demonstrate analytically the existence of such thresholds, and show how they arise from the limited number of independent suppliers and from the non-durability of goods; see *SI Text, Figs. S2* and *S4*. The threshold value of five total suppliers observed in Fig. 1(c) diminishes with greater failure rates, more productive firms or more durable goods.

As seen in Fig. 1(c), after the threshold, there is still a positive relationship between overordering rates and number of total suppliers, which shows that, on average, having an additional supplier exposes a firm to a larger risk. However, the horizontal dispersion of the results implies that this behavior does not apply to all situations. A supplier that maintains large inventories abates the risk of supply disruption for its clients, who may then overorder less. In Fig. 1(b), for instance, the two green final producers with 17 total suppliers overorder less than their blue suppliers with 12 total suppliers. This type of interactions also explains that the directions of some trajectories of Fig. 1(a) significantly change along the evolutionary time. In specific supply chains, this mechanism may lead to surprising patterns, as shown in *SI Text, Fig. S6*. Additional results on potential correlations between the position of the firms and their optimal overordering rates are presented in *SI Text, S10*.

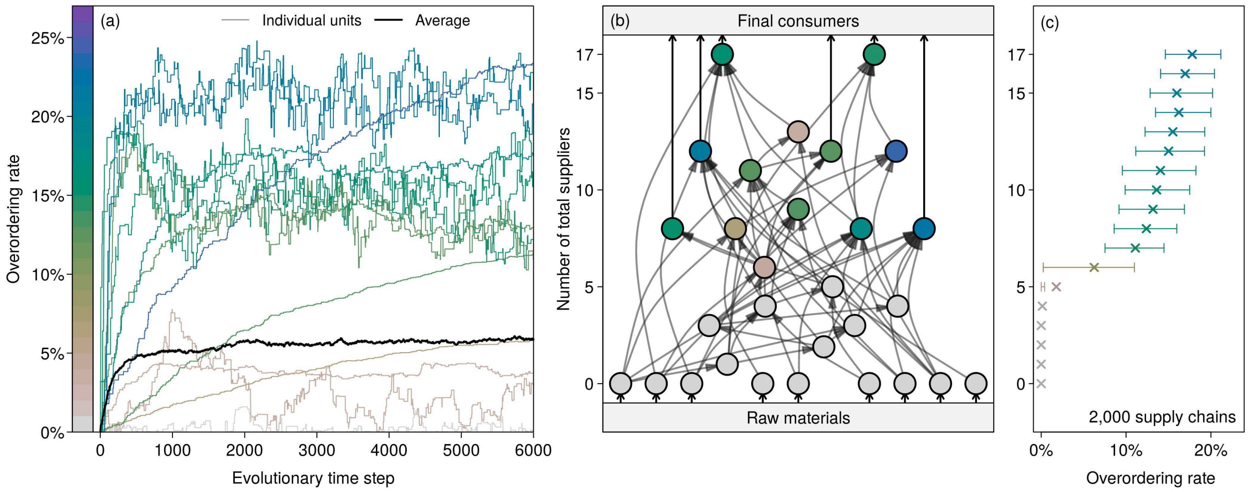

Fig. 1. Heterogeneous overordering patterns emerge from strategic interactions. Panel (a) presents the evolution of the overordering rates of the 29 firms of the supply chain displayed in panel (b). Firms start without overordering, then adjust their rate to increase their own profit. The thick black curve indicates the average overordering rate. Each other curve corresponds to a firm; it is colored according to the final overordering rate adopted by the firm. In panel (b), firms are nodes, colored in correspondence to the curves of panel (a). The 61 grey arrows represent supplier–buyer interactions, while the black arrows indicate the flows that go in and out the chain: inflows of raw materials and outflows of final goods. The vertical position of the firms is proportional to their number of total suppliers. Panel (c) uses the same vertical axis to compare this specific pattern with statistics from an ensemble of 2,000 supply chains with the same n and c. The $\times$ symbols indicate the mean, and the bars the interquartile interval.

Inventories alleviate disruption cascades. Without inventories, most economic losses provoked by external perturbations are indirect. Any supply disruption propagates downstream, leading to large disruption cascades. Systemic risk is larger in longer and more interconnected supply chains. For instance, in the fairly complex supply chain of Fig. 1(b), a random external perturbation that disrupts one firm generates profit losses for 5.4 other firms on average, and indirect losses are more than twice as high as direct ones; see Fig. 2(a). Note that, because we assumed that inputs are perfectly substitutable, these indirect losses are certainly smaller than in situations with only partial or without substitutability. Once firms have picked the overordering rates that maximize their profits, they maintain inventories, which act as buffers against disruption cascades; in Fig. 2(a), for instance, the average size of disruption cascades is more than halved, down to 2.1 firms. In particular, the chance that a final producer experiences an input shortage following the disruption of a primary producer is reduced from 1 to 0.55 for the supply chain on Fig. 1(b), leading to a 39% drop of indirect losses; see Fig. 2(b). We generally observe an increase in direct loss associated with overordering. Because they buy more inputs, the overordering firms are running a more costly production process. When externally perturbed, they lose their production but still have to pay for the extra inputs they ordered, and thus experience greater direct loss. This negative impact remains moderate compared with the mitigation of indirect losses. Even in a fully fragmented supply chain, the decentralized profit-driven decisions allow to generate inventories that decrease systemic risk.

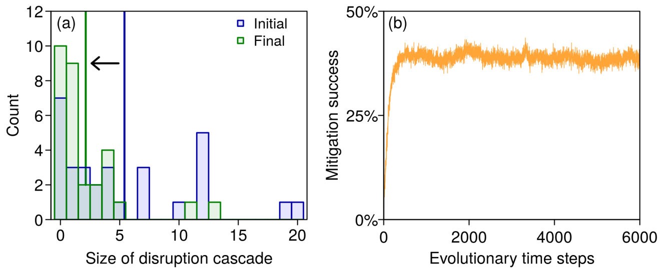

Fig. 2. Overordering diminishes disruption cascades and mitigates risks. Both panels refer to the supply chain of Figs. 1(a–b). Panel (a) shows how the distribution of the size of disruption cascades changes between the initial state in blue, in which no firms overorder, and the end of the evolutionary process in green. The thick vertical lines indicate the mean, which moves from 5.4 to 2.1 firms. The cascade size is the number of firms affected by supply shortage following one external perturbation; the distribution is obtained by perturbing each firm one by one. Panel (b) displays how mitigation success changes during the evolutionary process of Fig. 1(a).

Supply chain fragmentation disincentivizes overordering. When firms are grouped together and aim at increasing the group profit instead of their own, they overorder more. This behavior induces larger inventories, and lead to a stronger risk mitigation. This result is valid over the whole parameter space and is robust to changes of the supply chain structure. It is shown in Fig. 3 for six classes of networks. Mitigation success is minimal for the case of the full fragmentation, and maximal for the case of the full integration. For supply chains with 30 firms and two suppliers per firm, for instance, full integration helps increase the mitigation success by two thirds compared to full fragmentation. This stronger mitigation comes from the internalization of positive externalities. When a firm overorders, it generates positive outcomes both upstream and downstream: upstream firms receive a larger demand; downstream firms are less subject to disruption cascades. For them, these benefits do not cost anything: they are externalities. If now the firm is grouped together with some of its suppliers or customers, a share of these indirect benefits feedbacks into its decision-making process, making overordering more attractive. Integration therefore enables the internalization of the positive externalities associated with overordering, resulting in larger inventories and less risks of supply disruptions. The steepest slopes for low levels of fragmentation show that, in otherwise fully integrated supply chains, a slight degree of fragmentation has a relatively high impact. The vertical ordering of the curves also suggests that mitigation is larger in more interconnected supply chains. Although such systems are prone to longer disruption cascades, firms are better able manage them because they have access to a larger number of fully substitutable suppliers. The positive impact of supplier diversification is shown in the analytical results of *SI Text, Figs. S2* and *S4*.

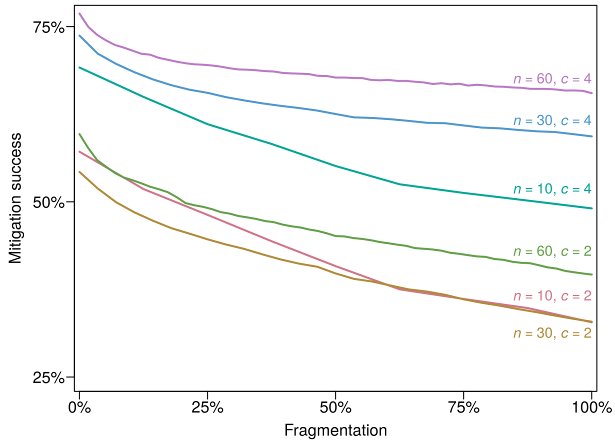

Fig. 3. Supply chain integration favors risk mitigation. The figure presents how mitigation success changes with fragmentation for six classes of supply chains, defined by the number of firms n and the average number of supplier per firm c. Fragmentation is defined as follows: $(g-1)/(n-1)$, where g represents the number of groups of integrated firms. Each curve is the average over 20 supply chains, and for each of them, $10 \times n$ group configurations are assessed. The dispersion of the data is shown in *SI Text, Fig. S6*.

Durable inventories enable robust risk mitigation. While systemic risk is robustly reduced by supply chain integration, the exact level of optimal mitigation depends on the three parameters: productivity z, failure rate p and durability v. The behavior of the mitigation success in this parameter space exhibit some regularities; there are shown in Fig. 4 for fully integrated supply chains. First, when failure rate p is high compared to productivity z, supply chains can become unproductive. This phenomenon occurs when $p \geq 1 - 1/z$, whatever durability v and the supply chain; see the grey regions of Fig. 4's three panels. There, firms use on average more than one unit of input to produce one unit of output, i.e. they are unproductive. Next, inside the productive region, the mitigation success peaks for intermediate failure rates; see vertical intersects in Fig. 4. When firms get more productive—moving rightward within each panel—or when goods become more durable—moving rightward across the panels—this peak gradually flattens and becomes a plateau; see in particular Fig. 4(c) for $z \geq 2$. With durable goods, the cost of replenishing the inventory is equal to the cost of the used inputs, which, within the productive region, is smaller than the additional sales it generates in case of disruption. Keeping an inventory is therefore always profitable, leading to a high mitigation success for any failure rate. With less durable goods, the cost of maintaining an inventory is no longer proportionate to sales. For high failure rates, very large overordering rates are needed. Building such large inventories may become unprofitable, so that the mitigation success drops; see the upper limit of the productive regions in Figs. 4(a–b). On the other hand, for low failure rates, firms may prefer to undergo occasional disruptions than to permanently maintain inventories, hence we observe a weaker mitigation successes at the bottom of Figs. 4(a–b). The mechanisms that underpin this behavior are analytically assessed in simple supply chains; see *SI Text, Figs. S2* and *S3*.

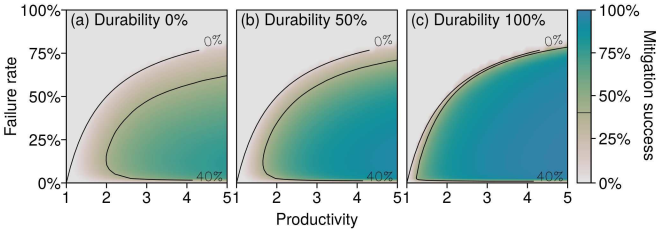

Fig. 4. Durable goods lead to robust mitigation. The three panels present the mitigation success of integrated supply chains in the parameter plane (z, p) and for three levels of durability: (a) 0%, (b) 50%, and (c) 100%. The 0% contour corresponds to the boundary between the productive and the unproductive regions. Results are averages over 10 supply chains with 30 firms and an average of two suppliers per firms.

Mapping supply chains helps identify benchmarks for mitigation. So far, we have elicited the optimal overordering rates through a decentralized process that takes into account strategic interactions between firms. We now examine whether a simple mapping of the supply chain can help decision-makers allocate, in a top-down manner, some reasonable overordering rates. To that end, we define ten different indicators that capture information on the position of each firm in the supply chain; see *SI Text, Table S2* for a full list and definition. For each indicator, for instance the number of suppliers, each firm i is associated with a value s_i. To compare across indicators, we center and normalize the values of s_i for each indicator; the resulting s_i' values average to 0 and their standard deviation is 1. We then determine the overordering rate of each firm i as $r_i = a + bs_i'$, in which a is a prescribed average overordering rate and b is an elasticity factor that modulates the information captured by the indicator. For each indicator, we pick the values of a and b that lead to the highest mitigation success. Figure 5(a) illustrates the results for the three most and the three least successful indicators, and Fig. 5(b) compares the maximum mitigation successes obtained over a large ensemble of supply chains. These quantitative results depend on the choice of parameters but illustrate a qualitative behavior that is general in the model.

The three least-performing indicators fail to significantly outperform a uniform allocation, whereby all firms receive the same overordering rate. These are the number of clients, and two centrality measures from network theory: closeness and betweenness centrality (33). Instead, three other indicators significantly improve the mitigation outcome: the number of direct suppliers, the number of total suppliers, and the supply-chain level. The latter is formally equivalent to the trophic level used in ecology (34): it is the average number of links connecting a firm to primary producers, taking into account all possible pathways. It has so far not been used to describe the position of firms in supply chains. In our model, it captures the most appropriate information to allocate the mitigation efforts. For the specific yet representative case displayed in Fig. 5(a), the average overordering rate at which the mitigation success peaks is similar across the indicators. This similarity illustrates that the stronger mitigation success of the top three indicators is not merely due to larger risk-mitigating efforts but to more appropriately allocated ones. In addition, the top three indicators significantly reduce systemic risk compared to decentralized decisions in fragmented supply chains—the right side of the sloping bar of Fig. 5(b). Nevertheless, even supply-chain level does reach the level of mitigation achieved when supply chains are fully integrated—the left side of the same bar. For the parameter value chosen, the average maximum mitigation success reached by supply-chain level is 48%, achieved with an average overordering rate of 18%, whereas full integration reaches 56% mitigation success with an average rate of 14%. This comparison demonstrates that a decentralized optimization process, whereby strategic interactions are taken into account, mitigates risk not only more effectively—delivering a greater mitigation success—but also more efficiently—keeping smaller inventories. In addition, the peaks of Fig. 5(a) are relatively narrow, suggesting that wrong decisions on the overall overordering efforts, or inaccurate information on the position of the firm, can rapidly deteriorate mitigation success. Combining indicators do not improve significantly the mitigation success. A more detailed statistical analysis on the information provided by these indicators are presented in *SI Text, S10*.

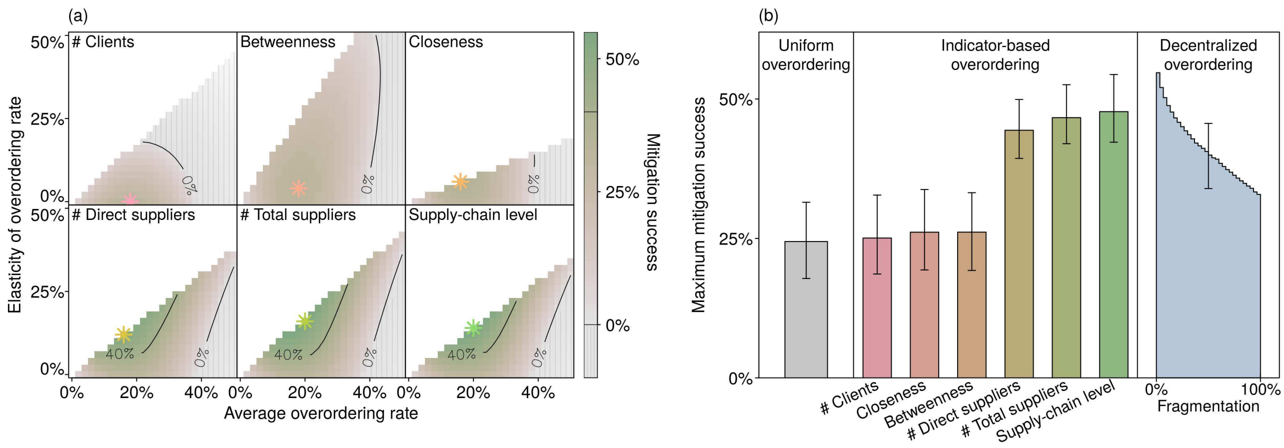

Fig. 5. Network indicators help allocate inventories. Panel (a) shows, for a specific supply chain with 30 firms and 60 supplier–buyer relationships, the mitigation success of six indicators. In each subpanel, the n values of the indicator are centered, normalized, then mapped into 26^2 vectors of overordering rates using an affine transformation: the average rate corresponds to the x-axis, the elasticity to the y-axis. With high elasticity, some rates may fall below 0%, implying that some firms should underorder. Such combinations are removed from the study, hence the upper white triangle. The eight-branch star symbols pinpoint the maximum mitigation successes. Panel (b) displays the maximum mitigation successes of the six indicators averaged over 200 supply chains. The vertical arrows indicate the interquartile intervals. These performances are contrasted with the uniform allocation of overordering rates, whereby all firms receives the same rate, and with the decentralized evolutionary process.

Discussion

Systemic risk occurs due to cascading failures that propagate far through economical systems, resulting in potentially large financial loss. Here, we have for the first time demonstrated that, under very general conditions, supply chain fragmentation increases systemic risk. The more fragmented a supply chain is, the more likely small disruptions propagate and get amplified. This additional risk arises from the strategic interactions between individual firms. In fragmented supply chains, the system-level benefits of inventory become externalities, in the economic sense, and individual firms have less incentive to maintain them. This theoretical finding is also consistent with the empirical observations that inventories have been decreasing during the outsourcing boom. Although these practices have allowed firms to be more competitive, we argue that, if not managed, they can lead to a larger systemic risk as side effect. Systemic risk could thus be seen as a common good problem: as a whole, the supply chain benefits from the provision of inventories, but firms are not sufficiently incentivized to do so.

The benefits of having more integrated decision-making processes along a supply chain have been described a long ago in the supply chain management literature (33). Coordination among firms could re-incentivize risk-mitigating measures in fragmented supply chains. In practice, it could take various forms (36, 37). For instance, bilateral supply chain contracts such as revenue sharing contracts could facilitate information sharing and directly extend the scope of risk management (39). Sales rebate, buy-back, and quantity flexibility contracts could also lessen the financial risk of maintaining a safety stock (see 39 for a review of supply chain contracts). Third-party “orchestrators” could also help firms coordinate larger and specialized subcomponents of the chain (41, 42).

Our work shows that, through a precise supply chain mapping, several simple indicators can be used to define the inventory levels that firms should keep to minimize systemic risks. In practice, which agents could use such benchmark levels? Central the banks are legitimate decision-makers to deal with systemic risk in financial systems, but no equivalent agents exist for supply chains. We suggest that three types of agents could be interested in such a top-down approach to systemic risk mitigation. First, within large corporations, supply chain managers could use this information to facilitate coordination between subsidiaries or production sites. Next, to secure the provision of critical goods, such as food or health-related products, policy-makers could be interested in setting minimum inventory requirements within the relevant supply chains. Last, insurers are increasingly asked to cover the economic losses generated by supply chain disruptions. The use of such indicators could thus help them tailor their insurance policy according to the position of firms in their supply chains.

Our results also point to a trade-off between environmental performance and economic resilience. Supply chains are able to deliver a steadier flow of outputs in the face of external perturbations through the maintenance of inventories. This resilient behavior comes with a higher input consumption, especially when goods are perishable, leading to a loss of material efficiency. For instance, in our model, with the benchmark parameter values, the sales of an integrated supply chain can be 22% greater compared to a fragmented one, but it will consume 40% more raw materials. These figures suggests a possible trade-off between a green (43) and resilient supply chain (44). This trade-off could be particularly marked for perishable goods such as food. For instance, to ensure high on-shelf availability of food products (45), retailers might build larger stocks, inducing extra wastage (46, 47). In a turbulent environment, securing a disruption-free supply of such goods can thus be a conflicting objective with the reduction of environmental degradation.

Acknowledgements. This study was enabled by the financial and organizational support of the International Institute for Applied System Analysis, through the Young Scientific Summer Program.

References

1. Goldin I (2010) Globalisation and risks for business - Implications of an increasingly interconnected world (Lloyd's, London).

2. Allianz Global Corporate & Specialty (2012) Managing disruptions: Supply chain risk: an insurer's perspective (Allianz, Munich).

3. World Economic Forum (2012) New Models for Addressing Supply Chain and Transport Risk (WEF, Geneva).

4. Gledhill R, Hamza-Goodacre D, Ping Low L (2013) Business-not-as-usual: Tackling the impact of climate change on supply chain risk (PWC).

5. Glendon L, Bird L (2013) Supply Chain Resilience 2013: An international survey to consider the origin, causes and consequences of supply chain disruption (Business Continuity Institute, Zurich).

6. Punter A (2013) Supply Chain Failures: A study of the nature, causes and complexity of supply chain disruptions (Airmic, London).

7. Hendricks KB, Singhal VR (2003) The effect of supply chain glitches on shareholder wealth. *J Oper Manag* 21(5):501–522.

8. Hendricks KB, Singhal VR (2005) An empirical analysis of the effect of supply chain disruptions on long-run stock price performance and equity risk of the firm. Prod Oper Manag 14(1):35–52.

9. Barrot J-N, Sauvagnat J (2016) Input specificity and the propagation of idiosyncratic shocks in production networks. Q J Econ:qjw018.

15. Wang YI, Li J, Anupindi R (2015) Risky Suppliers or Risky Supply Chains? An Empirical Analysis of Sub-tier Supply Network Structure on Firm Risk in the High-Tech Sector (University of

Michigan, Ann Arbor MI).

10. Nanto DK, Cooper WH, Donnelly JM (2011) Japan's 2011 Earthquake and Tsunami: Economic Effects and Implications for the United States (Congressional Research Service, Washington DC).

11. Chongvilaivan A (2012) Thailand's 2011 Flooding: Its Impact on Direct Exports and Global Supply Chains (ARTNeT Working Paper Series No. 133, Bangkok).

12. Todo Y, Nakajima K, Matous P (2013) How Do Supply Chain Networks Affect the Resilience of Firms to Natural Disasters? Evidence from the Great East Japan Earthquake (RIETI Discussion Paper Series 13-E-028, Tokyo).

14. Norrman A, Jansson U (2004) Ericsson's proactive supply chain risk management approach after a serious sub-supplier accident. *Int J Phys Distrib Logist Manag* 34(5):434–456.

15. Blackhurst J, Craighead CW, Elkins D, Handfield RB (2005) An empirically derived agenda of critical research issues for managing supply-chain disruptions. *Int J Prod Res* 43(19):4067–4081.

16. Katunzi TM (2011) Obstacles to process integration along the supply chain: Manufacturing firms perspective. Int J Bus Manag 6(5):105–113.

17. KPMG (2013) Global Manufacturing Outlook: Competitive advantage (KPMG International Cooperative, Switzerland).

21. National Research Council of the National Academies (2007) New directions for understanding systemic risk: a report on a Conference Cosponsored by the Federal Reserve Bank of New York and the National Academy of Sciences (Federal Reserve Bank of New York, National Research Council, Washington DC)

19. Hummels D, Ishii J, Yi K-M (2001) The nature and growth of vertical specialization in world trade. *J Int Econ* 54(1):75–96.

20. Jones R, Kierzkowski H, Lurong C (2005) What does evidence tell us about fragmentation and outsourcing? *Int Rev Econ Finance* 14(3):305–316.

21. Baldwin R, Lopez-Gonzalez J (2015) Supply-chain Trade: A Portrait of Global Patterns and Several Testable Hypotheses. *World Econ* 38(11):1682–1721.

22. Xu M, Allenby BR, Crittenden JC (2011) Interconnectedness and Resilience of the U.S. Economy. *Adv Complex Syst* 14(05):649–672.

23. Fujiwara Y, Aoyama H (2010) Large-scale structure of a nation-wide production network. *Eur Phys J B* 77(4):565–580.

24. Coluzzi B, Ghil M, Hallegatte S, Weisbuch G (2011) Boolean delay equations on networks in economics and the geosciences. *Int J Bifurc Chaos* 21(12):3511–3548.

25. Henriet F, Hallegatte S, Tabourier L (2012) Firm-network characteristics and economic robustness to natural disasters. *J Econ Dyn Control* 36(1):150–167.

26. Snyder LV, et al. (2016) OR/MS models for supply chain disruptions: A review. *IIE Trans* 48(2):89–109.

27. McCarter MW, Northcraft GB (2007) Happy together?: Insights and implications of viewing managed supply chains as a social dilemma. *J Oper Manag* 25(2):498–511.

28. Nagarajan M, Sošić G (2008) Game-theoretic analysis of cooperation among supply chain agents: Review and extensions. *Eur J Oper Res* 187(3):719–745.

29. Lieberman E, Hauert C, Nowak MA (2005) Evolutionary dynamics on graphs. *Nature* 433(7023):312–316.

30. Szabó G, Fáth G (2007) Evolutionary games on graphs. *Phys Rep* 446(4–6):97–216.

31. Erdös P, Rényi A (1959) On random graphs, I. *Publ Math Debr* 6:290–297.

24. Karrer B, Newman MEJ (2009) Random graph models for directed acyclic networks. Phys Rev E 80(4):046110.

25. Newman M (2010) Networks: An Introduction (Oxford University Press, Oxford).

34. Levine S (1980) Several measures of trophic structure applicable to complex food webs. *J Theor Biol* 83(2):195–207.

27. Lambert DM, Cooper MC, Pagh JD (1998) Supply chain management: Implementation issues and research opportunities. Int J Logist Manag 9(2):1–20.

28. Simatupang TM, Wright AC, Sridharan R (2002) The knowledge of coordination for supply chain integration. Bus Process Manag J 8(3):289–308.

37. Hennet J-C, Arda Y (2008) Supply chain coordination: A game-theory approach. *Eng Appl Artif Intell* 21(3):399–405.

38. Cachon G (2003) Supply chain coordination with contract. *Supply Chain Management: Design, Coordination and Operation*, Handbooks in Operations Research and Management Science. (de Kok A and Graves S), pp 227–339. Elsevier.

31. Cachon G, Lariviere M (2005) Supply chain coordination with revenue-sharing contracts: Strengths and limitations. Manag Sci 51(1):30–44.

32. Höhn MI (2010) Literature review on supply chain contracts. Relational Supply Contracts, Lecture Notes in Economics and Mathematical Systems. (Springer, Berlin), pp 19–34.

33. Bitran GR, Gurumurthi S, Sam SL (2007) The need for third-party coordination in supply chain governance. MIT Sloan Manag Rev 48(3):30.

34. Zacharia ZG, Sanders NR, Nix NW (2011) The emerging role of the third-party logistics provider (3PL) as an orchestrator. J Bus Logist 32(1):40–54.

43. Srivastava SK (2007) Green supply-chain management: A state-of-the-art literature review. *Int J Manag Rev* 9(1):53–80.

36. Christopher M, Peck H (2004) Building the resilient supply chain. Int J Logist Manag 15(2):1–14.

45. Daniel Corsten, Thomas Gruen (2003) Desperately seeking shelf availability: an examination of the extent, the causes, and the efforts to address retail out-of-stocks. *Int J Retail Distrib Manag* 31(12):605–617.

46. Osner R (1982) Food wastage. *Nutr Food Sci* 82(4):13–16.

39. Trautrims A, Grant DB, Fernie J, Harrison T (2009) Optimizing on-shelf availability for customer service and profit. J Bus Logist 30(2):231–247.

SI Text

The SI Text is composed of three parts.

1. Sections S1 to S5 present analytical results for simple supply chains. They allow us to identify the mechanisms that drive the results shown in the Main Text. Section S1 to S4 focus on a single producer connected to multiple primary producers. The dynamical equations for inventory and profit are established in Section S1. Section S2 shows how the overordering rate that maximizes profits changes with parameters. Section S3 describes the mechanism that determines this behavior for fully durable goods. Section S4 presents the analytical treatment for fully perishable goods. Section S5 exposes a method to algorithmically compute the exact expected values of profits and overordering for a large class of complex supply chain.
2. Sections S6 and S7 provide information on the evolutionary process. Section S6 describes in details the evolutionary process used in the simulations. Section S7 provides evidence on the existence of evolutionary equilibria.
3. Sections S8 to S10 present additional numerical results. Section S8 shows a topologically periodic distribution of the overordering rates obtained with a layered supply chain. Section S9 presents the distribution of the mitigation success as a function of fragmentation. Section S10 presents the statistical correlations between the profit-maximizing overordering rates and a selection of ten network indicators.

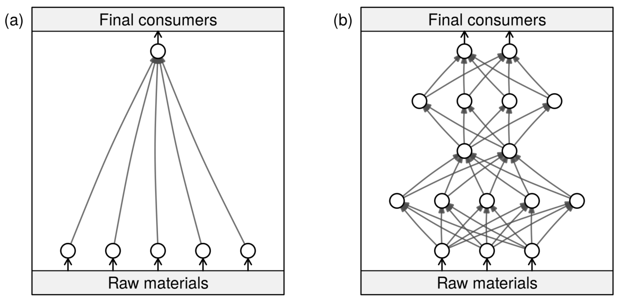

Figure S1. Analytical results are derived for simpler supply chains. Panel (a) displays a two-layer supply chain with one final producer supplied by five primary producers. Panel (b) shows a fully connected five-layer supply chain. The network topology is summarized by the vector $(3,5,2,4,2)$, which gives the number of firms that corresponds to each one of the five layers: 3 primary producers, 5 layer-two firms, …, and 2 final producers. This supply chain is fully connected, because each on of the layer-l firms is supplied by all of the layer-$(l-1)$ firms, for $l = 2, \dots, 5$.

S1: A single producer supplied by multiple firms: dynamical equations. This situation is illustrated in Fig. S1(a) for $s = 5$ suppliers. The s suppliers are primary producers. Since the inflow of raw materials is not subject to external perturbations, they do not overorder. We focus on the inventory of the final producer, denoted by x_t. It changes through time as follows:

$$x_{t+1} = x_t + \mathcal{I}_t - \mathcal{O}_t - (1-v)(r_t + \mathcal{I}_t - \mathcal{O}_t), \qquad [S2]$$

where $\mathcal{I}_t$ is the quantity received, $\mathcal{O}_t$ the quantity used for production. The last term represents the impact of non durability: a share $1-v$ of the remaining inventory is lost at each time step. This expression can be rewritten as follows:

$$x_{t+1} = v(r_t + \mathcal{I}_t - \mathcal{O}_t). \qquad [S3]$$

We denote by K_t the random variable representing the number of externally perturbed suppliers at time t. This variable — which can take up to $s+1$ values: $0, 1, \dots, s$ — follows a binomial distribution:

$$\Pr(K = k) = \binom{s}{k} p^k (1-p)^{s-k}. \qquad [S4]$$

When K_t suppliers are perturbed, the quantities $\mathcal{I}_t$ and $\mathcal{O}_t$ are:

$$\mathcal{I}_t = \frac{s - K_t}{s}\frac{1+r}{z}, \qquad [S5]$$

$$\mathcal{O}_t = \min\left(\frac{1}{z}, r_t + \mathcal{I}_t\right). \qquad [S6]$$

To eliminate the min function, we determine the maximum number of suppliers that can simultaneously fail without impacting final production. It is the largest K_t such that $x_t + \mathcal{I}_t \geq 1/z$. Using Eq. [S4] in the inequality, this number is the largest integer lower than or equal to:

$$\bar{s}_t = \frac{s\,r + z\,x_t}{1+r}. \qquad [S7]$$

We can thus rewrite Eq. [S2] by distinguishing whether is threshold is crossed:

$$x_{t+1} = \begin{cases} v\left(x_t + \frac{r}{z} - \frac{K_t}{s}\frac{1+r}{z}\right), \text{if } K_t \leq \frac{sr + zx_t}{1+r}, \\ 0, \text{otherwise.} \end{cases} \qquad [S8]$$

The profit — sales minus input costs — can be derived from the inventory:

$$\pi_t = \begin{cases} P_t - \frac{s-K_t}{s}\frac{1+r}{z}, \text{if } K_t \leq \frac{sr + zx_t}{1+r}, \\ P_t z x_t + \frac{s-K_t}{s}(1+r)\left(1 - p - \frac{1}{z}\right), \text{otherwise,} \end{cases} \qquad [S9]$$

where P_t is a random variable equals to 0 with probability p and 1 otherwise. If either inventory or overordering gets larger, the threshold value $\bar{s}_t$ also grows. The firm is less vulnerable to supply disruption and meet the full demand more often; see the first Eq. of [S8]. If both inventory and overordering are low enough, a combination of perturbation may induce a shortage. The entire inventory is used for production and a share of the demand remains unmet; see the second equations of [S5] and [S6].

S2: A single producer supplied by multiple firms: a summary of the influence of parameters on the optimal overordering rate. We present how the overordering rate that maximizes the expected profit of the final producer, denoted by r^*, changes with durability v, failure rate p, productivity z, and number of suppliers s. We focus on the productive region, defined by $p < 1 - 1/z$. Results are shown in Fig. S2, and are commented for three scenario of durability.

- When $v = 100\%$, there is a smooth continuous relationship between r^* and p, namely: $r^* = p/(1-p)$. This equation is not affected by z or s. The mechanism underpinning this result is explained in Section S3.
- When $v = 0\%$, the relationships between r^* and p and between r^* and z are discontinuous. The optimal rate r^* can take up to s values, equal to $i/(s-i)$ with $i = 0, 1, \ldots, s-1$. It jumps from one of this value to another as p or z crosses specific threshold values; these values are explicitly derived in Section S4. With more numerous suppliers, a larger set of values is accessible to r^*, so that the firm can more finely manage a particular failure rate. For instance, considering the three 0%-durability curves in Fig. S1, we observe that it is never profitable to overorder with one or two suppliers, whereas for five suppliers the optimal rate r^* jumps from 0 to 25% when p crosses 25%.
- The behavior of r^* for intermediate durability interpolates between the features described for $v = 100\%$ and $v = 0\%$. In Fig. S2, as v decreases, a threshold behavior appears for low and high failure rates. Overordering is profitable only for intermediate failure rates. This p-interval gets reduced as v decreases. The set of accessible r^*-values gets also smaller, leading to a more discontinuous behavior. Having mores suppliers smoothen these nonlinearities; see the 90%-durability curves across all three panels of Fig. S2.

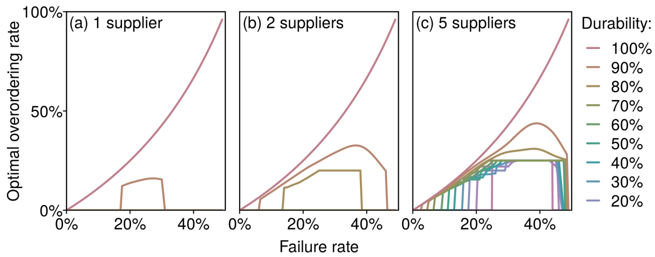

Figures S2. Profit-maximizing overordering rates depends nonlinearly on parameters. These curves concern a final producer supplied by (a) one, (b) two and (c) five suppliers, as illustrated in Fig. S1(a). The panels contain 11 curves, corresponding to different durability. Productivity is 2, and only the productive region of the parameter space is shown, i.e. with failure rates between 0 to 50%.

S3: Origin of the large overordering rates when goods are fully durable. When the final producer is supplied by a single primary producer, the dynamics of its inventory, denoted by x_t, can be interpreted as a one-dimensional asymmetric random walk in the positive real line. At each time step, inventory increases by r/z with probability $1-p$, or decreases by $\min(x_t, 1/z)$. The origin of the positive real line, 0, is a so-called sticky wall: because of the min function, any trajectory below $1/z$ that undergoes a negative step simply lands on the wall. This behavior is to be distinguished from that of reflecting walls, on which trajectories bounce back, and of absorbing walls, in which trajectories get caught. In this class of random walk, trajectories are expected to diverge if the expected growth rate $\mathbb{E}(x_{t+1})/x_t$ is higher than one, i.e. when the positive step has a larger expected size than the negative step. Otherwise, trajectories are expected to sometimes touch the wall. In our model, this condition is $(1-p)\,r/z \geq p/z$. The overordering rate that maximize profit, r^*, is the one that turns this inequality into an equality:

$$r^* = \frac{p}{1-p}. \tag{S10}$$

This solution can be explained by the following decision-making heuristics. When r is higher than $p/(1-p)$, inventory eventually diverges. Consequently, most extra inputs purchased are not used, implying that the amount of sales could be achieved with less overordering. Conversely, when r is lower than $p/(1-p)$, inventory is sometimes below $1/z$, which leaves the firm vulnerable to supply disruption, and some sales are missed. With fully durable goods, however, it is always profitable not too miss sales. When one unit of output is sold, cost only consists of the associated quantity of input consumed — there is not need to purchase extra inputs to replace an obsolete inventory. As a consequence, if sales are missed, it is profitable to increase overordering. This heuristics also applied when the firm has more than one supplier.

S4: Nonlinear behavior of the optimal overordering rate when goods are not durable. We first aim to write an explicit equation of the expected profit of a final producer supplied by s primary producers, as in Fig. S1(a), for $v = 0\%$. To that end, we determine for one time step all the possible value of profit and their associated probability. Since inputs are not storable, the firm can only tap into the inputs received during the same time step. Costs are directly proportional to the number of failed suppliers, denoted by $k = 0, \dots, s$. Sales depend nonlinearly on k: they are proportional to k but cannot exceed the final demand, which equals one. Combining Bernoulli distributions, we obtain the expression of the expected profit $\mathbb{E}(\pi)$:

$$\mathbb{E}(\pi) = \sum_{k=0}^{s} \binom{s}{k} p^k (1-p)^{s-k} \left[(1-\mathrm{p}) \min\left(\frac{s-k}{s}(1+r), 1\right) - \frac{s-k}{s}\frac{1+r}{z}\right]. \tag{S11}$$

We note that the overordering rates of the primary producers do not affect $\mathbb{E}(\pi)$. The min function corresponds to the fact that sales cannot exceed the demand. To eliminate this function in [S8], we identify the largest k-value for which the min expression yields one. It is immediate that this value, denoted by $\hat{s}(r)$, is:

$$\hat{s}(r) = U\left(\frac{sr}{1+r}\right), \tag{S12}$$

where operator U transform a real number into the highest integer less than or equal to this number. Integer $\hat{s}(r)$ represents the maximum number of suppliers that, for a given level of overordering, can be shocked without loss of sales. Using $\hat{s}(r)$, expression [S8] can be rewritten as:

$$\mathbb{E}(\pi) = (1-p)\left[\sum_{k=0}^{\hat{s}(r)} \binom{s}{k} p^k (1-p)^{s-k} \left[1 - \left(1 - \frac{k}{s}\right)(1+r)\right] \right.$$
$$\left. + (1+r)\left(1 - p - \frac{1}{z}\right)\right]. \qquad \text{[S13]}$$

In the full fragmentation scenario, the objective of the final producer is to select the overordering rate r^* that maximize its expected profit $\mathbb{E}(\pi)$. We define on $\mathbb{R}^+$ the function $\mathcal{G}: r \longmapsto \mathbb{E}\big(\pi(r)\big)$; it represents the fitness landscape. For any $z > 1$, any $p \in [0,1]$ and any $s \in \mathbb{N}^*$, function $\mathcal{G}$ is continuous and piecewise linear. As r increases from 0% onward, $\hat{s}(r)$ jumps from one integer value to the next, from 0 all the way to $s-1$. Each time $\hat{s}(r)$ increases, a new term in the sum of [S9] is added, leading to a new linear piece for $\mathcal{G}$. The number of linear pieces of $\mathcal{G}$ is equal to the number of values that $\hat{s}(r)$ can take, which is s. Using Eq. [S11], we find the $(s-1)$ values of r separating the s pieces:

$$r^i = \frac{i}{s-i}\,, \qquad \text{[S14]}$$

with $i = 1, \dots, s-1$. We add to this ensemble the term $r^0 = 0$, which corresponds to the left boundary of the first linear piece. The last linear piece of $\mathcal{G}$ lies on the interval $[r^{s-1}, +\infty[$. There, given [S12], $\mathcal{G}$ is decreasing in r with coefficient of variation $-(1-p)^2/\mathrm{z}$. It follows that, since $\mathcal{G}$ is continuous, it reaches a maximum on the interval $[r^0, r^{s-1}]$. Suppose that a maximum is located between two boundaries, say r^j and r^{j+1}. Then, because $\mathcal{G}$ is linear on the segment $\left[r^j, r^{j+1}\right]$, it would necessarily be maximum on the whole segment. Consequently, it suffices to look for maxima of $\mathcal{G}$ among the boundaries $r^0, \dots, r^{s-1}$. Using [S12], we can write the expression of $\mathcal{G}(r^i)$:

$$\mathcal{G}(r^i) = (1-p)\left[\left(1 - p - \frac{1}{z}\right)\frac{s}{s-i} + \sum_{k=0}^{i} \binom{s}{k} p^k (1-p)^{s-k} \frac{k-i}{s-i}\right]. \qquad \text{[S15]}$$

We now demonstrate that the set $\{\mathcal{G}\big(r^i\big)\}$ has a unique maximum. When $s = 1$, the set has only one value; $\mathcal{G}$ is therefore maximum for $r^0 = 0$. When $s > 1$, we study the sign of the difference $\mathcal{G}(r^{i+1}) - \mathcal{G}(r^i)$ using Eq. [S14] for $i = 0, \dots, s-2$:

$$\mathcal{G}\big(r^{i+1}\big) - \mathcal{G}\big(r^i\big) = \frac{s\,(1-p)}{(s-i-1)(s-i)}\left(\theta_i(p) - \frac{1}{z}\right), \qquad \text{[S16]}$$

where $\theta_i(p)$ is the term:

$$\theta_i(p) = 1 - p - \sum_{k=0}^{i} \binom{s}{k} p^k (1-p)^{s-k} \left(1 - \frac{k}{s}\right). \quad \text{[S17]}$$

From Eq. [S15], we observe that, unless $p = 1$, for which $\mathcal{G}$ is always null, the sign of $\mathcal{G}(r^{i+1}) - \mathcal{G}(r^i)$ is determined by the relative value of $\theta_i(p)$ and $1/z$. From Eq. [S16], the $\theta_i(p)$s are decreasing when i increases from 0 to $s-2$. We are left with three possibilities.

1. When $\theta_0(p) < 1/z$, we have $\mathcal{G}(r^{i+1}) < \mathcal{G}(r^i)$ for $i = 0, \dots, s-2$. It implies that $\mathcal{G}$ is maximum at $r^0 = 0$.
2. When $\theta_{s-2}(p) > 1/z$, we have $\mathcal{G}(r^{i+1}) > \mathcal{G}(r^i)$ for $i = 0, \dots, s-2$. It implies that $\mathcal{G}$ is maximum at $r^{s-1} = s-1$.
3. Otherwise, we can find an integer i^* between 0 and $s-2$ such that $\theta_i(p) > 1/z$ for $i < i^*$ and $\theta_i(p) \leq 1/z$ for $i \geq i^*$. It implies that $\mathcal{G}$ is maximum at $r^{i^*} = i^*/(s-i^*)$.

For particular values of p and z, defined by the following equations:

$$z = 1/\theta_i(p), \quad \text{[S18]}$$

with $i = 0, \dots, s-2$, we have $\mathcal{G}(r^{i+1}) = \mathcal{G}(r^i)$. It implies that $\mathcal{G}$ is maximum both at r^i and r^{i+1}, and therefore on the whole segment $[r^i, r^{i+1}]$. In these particular cases, we suppose that firms select the smallest overordering rate that maximizes $\mathcal{G}$, i.e., r^i. In conclusion we have established that, for a combination of z and p values, the profit-maximizing overordering rate is unique. As z and p vary, it can take only a limited set of values: $i/(s-i)$ with $i = 0, \dots, s-1$. Equation [S17] defines the regions of the (z, p) parameter plane corresponding to the different profit-maximizing overordering rates. They are shown in Fig S3. A small modification of z or p either has no impact on overordering decisions, or lead to a discontinuous adjustment. With more suppliers, the number of potentially optimal overordering rates increases; see the growing number of regions in Fig. 3 from panel (a) to (c). Consequently, discontinuities fade out as the number of suppliers grows; see Fig. S4(a). In other words, the wider supplier base, the finer firms can adapt to a particular level of risk. The loss due to supplier failures thus decreases as $1/\sqrt{s}$; see Fig. S4(b).

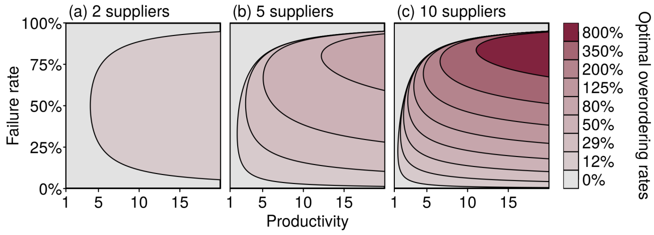

Figures S3. The optimal overordering of fully perishable inputs discontinuously changes with productivity and failure rate. The three panels show, in the parameter plane (z, p), the overordering rates that maximize the profit of a firm supplied by (a) $s = 2$, (b) $s = 5$ or (c) $s = 10$ primary producers. The regions are separated by the curves defined in Eq. [S17].

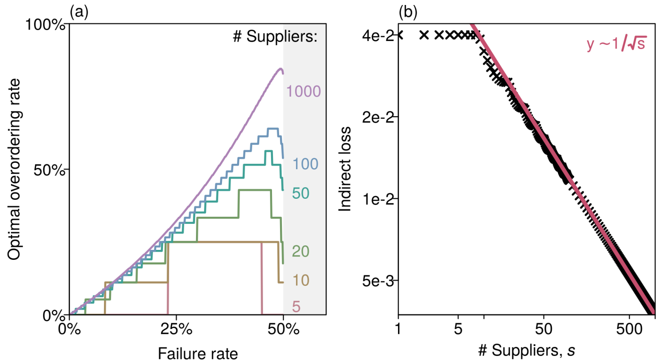

Figure S4. A larger supplier base enables finer adaptation to risks. Both panels concern a single firm supplied by multiple primary producers. Panel (a) shows how the relationship between profit-maximizing overordering rate and failure rate changes with the number of suppliers. In particular, the 5- and 10-supplier curves are the vertical intersects of Fig. S3(b) and (c) for $z = 2$. Note that over 50% failure rate, in the grey region, firms are unproductive. Panel (b) presents how the expected indirect loss decreases with the number of suppliers for a failure rate of 10%. The red curve is a fit, showing that indirect loss decreases as $1/\sqrt{s}$.

In the full integration scenario, all firms belong to the same group. They aim to maximize the expected profit of the group, denoted by $\mathbb{E}(\pi_G)$. We infer from the symmetry of the supply chain that all primary producers choose the same overordering rate r_P and have the same expected profit $\mathbb{E}(\pi_P)$:

$$\mathbb{E}(\pi_P) = \frac{1 + r_F}{s\,z}\left(1 - p - \frac{1 + r_P}{z}\right), \qquad \text{[S19]}$$

where r_F the overordering rate of the final producer. The group profit $\mathbb{E}(\pi_G)$ is thus equal to $\mathbb{E}(\pi_F) + s\mathbb{E}(\pi_P)$, where $\mathbb{E}(\pi_F)$ is the expected profit of the final producer defined in Eq. [S10]. Since r_P only influences $\mathbb{E}(\pi_P)$ and not $\mathbb{E}(\pi_F)$, primary producers choose the overordering rate that maximizes their own profit. From Eq. [S18], this overordering rate is 0%, whatever the choice of the final producer. As for the latter, we define on $\mathbb{R}^+$ the function $\mathcal{H}: r_F \mapsto \mathbb{E}(\pi_G(r_F))$, which is, as $\mathcal{G}$, piecewise linear and has the same boundaries r^i between linear pieces, given in Eq. [S13]. The last linear piece on $[r^{s-1}, +\infty]$ is decreasing in r_F with coefficient of variation $-1/z^2$, which ensures that, as $\mathcal{G}$, $\mathcal{H}$ has a unique maximum among the values r^i, with $i = 0, \ldots, s-1$.

S5: Algorithmic computation of the expected profits in fully connected and layered networks. In large acyclic networks, we cannot write an explicit expression of expected profits for each firm. For the general case, we approach these values through the numerical simulations of the stochastic process. For a specific class of structure, however, we can write a deterministic algorithm that allows us to access the exact values of the expected profit. An example of such network is shown in Fig. 1(b). It is said to be "layered", because, firms are organized in layers: at layer 1 lie the primary producers, at layer 2 the direct customers of primary producer, and layer 3 the direct customers of layer-2 firms, and so on all the way to final producers. It is said to be "fully connected", because each firm at one layer is supplied by all the firms of the layer underneath, except primary producers which are externally supplied. The topology is described by the number of firms n^l occupying each layer $l = 1, \dots, L$, where L denotes the number of layers. In this class of supply chain, all firms occupying the same layer share the exact same suppliers and customers. They all face the exact same demand and the same supply risk. This symmetry allows us to make the following analytical simplification: all firms at one layer have the exact same behavior. In particular, they choose the same overordering rate r^l. The production targets of each firm can either be computed using the input–output relationships, as proposed in the Main Text for general acyclic networks, or using the following relationships:

$$\begin{cases} \overline{y^l} = \dfrac{1}{s^l} \quad \text{for} \quad l = L, \\ \overline{y^{l-1}} = \dfrac{s^l \overline{y^l}(1 + r^l)}{s^{l-1} z} \quad \text{for} \quad l = 1, \dots, L-1. \end{cases} \qquad \text{[S20]}$$

In addition, all firms at one layer simultaneously receive the exact same amount of inputs. We denote by Q^l the random variable representing the quantity of inputs received by a layer-l firm. The random variable Q^l is discrete; we denote by q_j^l each of its j_l realizations, with $j = 1, \dots, j_l$. The core of the algorithm consists in computing, layer by layer, the probability distribution of Q^l. After computing all production targets $\overline{y^l}$ using Eq. [S19], we initialize the process with the primary producers, $l = 1$. The probability distribution of Q^1 is $\overline{y^1}/z(1 + r^1)$ with probability one. Next, suppose that we know the probability distribution of Q^l, i.e., the value of its realization q_j^l and its associated probability $\Pr(Q^l = q_j^l)$. To find the probability distribution of Q^{l+1}, we distinguish between $n^l + 1$ cases, each case corresponding to the number of direct layer-l firms perturbed: case (1) no firm is perturbed; case (2) one firm is perturbed; case (3) two firms; and so on up to case $(n^l + 1)$ in which all of the n^l firms are perturbed. For each case, we do the following computation.

1. We evaluate the probability of the case using combinatory formulas. For instance, the probability of case $(i + 1)$, in which i layer-l firms is perturbed, is $\binom{n^l}{i} p^i (1-p)^{l-i}$.

2. We determine the probability distribution of the total quantity produced by layer-l firms, using the known probability distribution of Q^l and production targets $\overline{y^l}$. For the case $i+1$, the total quantity produced by layer-l firms is $(n^l - i)\min\left(zQ^l, \overline{y^l}\right)$.
3. We deduce the probability distribution of inputs received by layer-$(l+1)$ firms. For the case $i+1$, each layer-$(l+1)$ firms receives $(n^l - i)\ /n^{l+1} \min\left(zQ^l, \overline{y^l}\right)$ inputs.

Each case thus provides a part of the probability distribution of Q^{l+1}. Case $(i+1)$ provides the following potential realizations of Q^{l+1}:

$$\frac{(n^l - i)}{n^{l+1}}\min\left(zq_j^l, \overline{y^l}\right),\ \text{for } j = 1, \dots, j_l, \qquad \text{[S21]}$$

along with their corresponding probabilities:

$$\binom{n^l}{i} p^i (1-p)^{n^l - i}\Pr\left(Q^l = q_j^l\right),\quad \text{for } j = 1, \dots, j_l. \qquad \text{[S22]}$$

We recombine all of the $n^l + 1$ cases to elicit the complete probability distribution of Q^{l+1}. By applying the recursive process from primary producers all the way to final producers, we can determine the probability distributions of Q^l for all $l = 1, \dots, L$. Next, we deduce directly from these distribution the probability distribution of the sales, denoted by Y^l. Sales are null with probability p or otherwise equal to $\min\left(zQ^l, \overline{y^l}\right)$. Last, knowing the probability distribution of the inputs and sales of each firms, we can compute the expected profits $\mathbb{E}(\pi^l) = \mathbb{E}(Y^l - Q^l)$.

S6: Detailed description of the evolutionary process. The optimization problem of each firm is to find the overordering rate that maximizes the profit of the group it belongs to. We define an evolutionary process to elicit the solutions. We call strategy the choice of a particular overordering rate. The set of strategies for which no firm has any interest in choosing another strategy is called the set of evolutionarily stable strategies (ESSs); it corresponds to a Nash equilibrium. We call fitness landscape of firm i at evolutionary step τ the mapping of its overordering rate r_i^τ into the expected profit of the group $\mathbb{E}(\pi_g^\tau)$; it is determined by the topology M, by the firm-level parameters z, v and p, and by the overordering rates of the other firms $r_{j\neq i}^\tau$. The evolutionary process proceeds through gradient ascent. One firm at a time performs an explore-and-adjust procedure: it explores its fitness landscape by testing different strategies, then makes a small adjustment to move up the landscape. We denote by $\mathcal{U}_\tau$ the ensemble of firms that have not reached their ESS at the evolutionary step τ. The initial ensemble $\mathcal{U}_0$ gathers all firms except primary producers. Since the latters receive riskless supply of raw materials, they always find it more profitable not to overorder. An initial overordering rate of typically 0% is attributed to each firm. At evolutionary step τ, firms in $\mathcal{U}_\tau$ perform the explore-and-adjust procedure, one after the other, in a random order. Exploration consists in three trials, whereby to three strategies are tested: $\max(0, r_i^\tau - \Delta), r_i^\tau$ and $r_i^\tau + \Delta$. To test a strategy, we run the model over T time steps and compute the corresponding time-averaged group profit $\langle \pi_g^\tau \rangle_T$. For the three tests, we apply the same sequence of perturbations, randomly generated by n simultaneous Bernoulli processes—one per firm—of length T and probability p. The three pairs $\{r_i^\tau, \langle \pi_g^\tau \rangle_T\}$ are used to estimate the local geometry of the fitness landscape. An estimate of the gradient, denoted by γ_i^τ, is given by the derivative in r_i^τ of a parabola fitted in a least square sense to the three points. The overordering rate of firm i is then updated as follows: $r_i^\tau = r_i^\tau + B_\delta(h\,\gamma_i^\tau)$, where h is a scaling constant and B_δ a bounding function that returns δ if its argument exceeds δ, -δ if its argument falls below $-\delta$, or the argument itself otherwise. These bounds limit the size of the updating step. Once all firms in $\mathcal{U}_\tau$ have gone through this procedure, all updated strategies are carried forward: $r_i^{\tau+1} = r_i^\tau$. Some firms may have reached their ESS and will therefore be removed from the new ensemble of updating firm $\mathcal{U}_{\tau+1}$. The whole process is repeated until $\mathcal{U}_\tau$ becomes empty. A firm is considered to have reached its ESS if its strategy has become stationary. Stationarity is tested as follows. Within an evolutionary-time window of length W, which spans the interval $[\tau - W + 1, \tau]$, we randomly select two smaller windows that are longer than $W/2$. An evolutionary time series is considered stationary when the linear trend on each one of the two windows falls below a threshold w. In this case, the ESS is estimated by the average value over the last W steps. Table S1 summaries the relevant parameters and their values.

Table S1. Summary of the parameters used in the evolutionary process

Parameter	Definition	Value
T	Duration of the trials, in economic time step	100
Δ	Exploration step	5.10^{-2}
δ	Maximum updating step size	2.10^{-2}
W	Evolutionary time window for testing stationarity	30
w	Stationary threshold	10^{-4}

The stochastic nature of the external perturbations poses several challenges to the design of the evolutionary process. The three trials only provide estimates of the fitness landscape. When each trial is made under different sequences of perturbations, we observe that the estimated fitness landscape sometimes lead to ambiguous results. Specifically, as soon as the local geometry of the expected fitness landscape becomes flatter, the estimated landscape gets rugged, even with longer duration of the trials, such as $T = 10{,}000$. Instead, when the three trials use a common sequence of perturbations, they produce comparable results and enable unambiguous adjustments. This solution however generates evolutionary fluctuations. Since a new sequence of perturbations is used at each evolutionary time step, the estimation of the same fitness landscape may slightly vary. These varying estimates produce noises in the evolutionary time series of the strategies, as observed in Fig. 1(a) of the Main Text. Consequently, to determine whether a firm has reached its ESS, we use a stationarity condition. Note that, using the same sequence of perturbation over a whole simulation would lead to overordering decisions that are adapted to this precise sequence, but not to the overall failure rate, leading to large variability across simulations. In Tab. S1, we selected the parameter values that lead, within reasonable computation time, to reproducible results: the standard deviations over the evolutionary stable overordering rates is below 1%. For fully connected and layered networks, illustrated in Fig. 1(b), we can use the algorithm of Sec. S5 to obtain the exact expected profits. At each evolutionary time step, we have access to the exact fitness landscape. For this class of supply chain, we can therefore determine the exact ESS.

S7: Evidences for the existence and uniqueness of Nash equilibria. As studied in Secs. S2 to S4, a firm supplied by multiple primary producers has a unique solution to its optimization problem, both in the fully fragmented and in the fully integrated scenarios. For specific combinations of z, v and p — e.g., Eq. [S17] — a continuous range of strategies could solve the optimization problem. To ensure uniqueness, we have assumed that firms have a waste-minimizing behavior: when a range of overordering rates yield similar outcome, they choose the smallest one. The uniqueness of the solution applies to any two-layer supply chains. Strategic interactions occur in supply chain of three or more layers. The strategy chosen by a layer-2 firm influences the fitness landscape of layer-3 firms. In fact, extensive numerical simulations show that all fitness landscapes have a unique maximum, as those of studied in Sec. S4. Examples are shown in Fig. S5 for $v = 0\%$, both for the fully fragmented scenario in panels (b) and (e) and for the fully integrated one in panels (c) and (f). In fully connected and layered network, as in Figs. S5(a–c), the number of linear pieces increases as we move down the supply chains. In random acyclic network, as in Figs. S5(d–f), the fitness landscape become even smoother. This property of the fitness landscapes suggests that a unique Nash equilibrium exist generically in a supply chain. Numerical experiments using very diverse set of initial conditions show that the evolutionary process leads to similar ESSs, within 1% standard deviation. The remaining variability is attributed to the fluctuations discussed in Sec. S6.

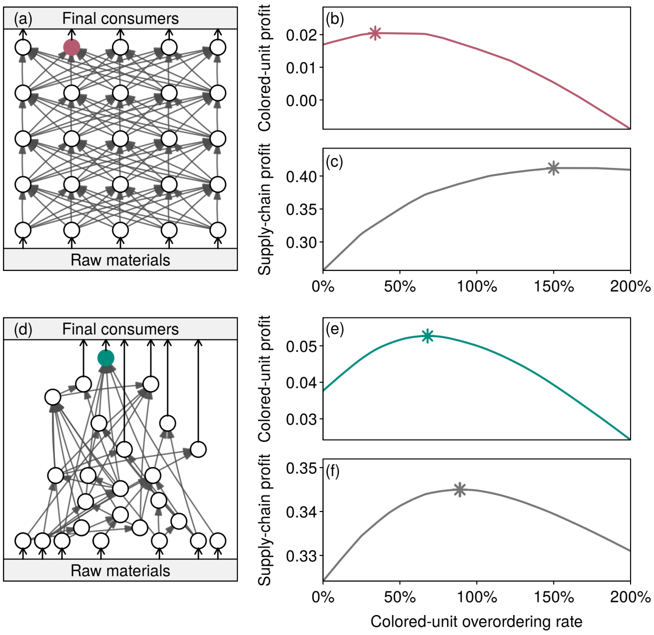

Figure S5. Fitness landscapes always have a unique maximum. Panels (b–c) (resp. panels (e–f)) show the fitness landscape at ESS of the colored firm of the supply chain displayed in panel (a) (resp. panel (d)). Panels (a) and (e) concern full fragmentation: the fitness landscape is the relationship between the colored-firm profit and its overordering rate. Panels (b) and (f) concern full integration: it shows the relationship between the profit of the whole supply chain and the colored-unit overordering rate. In all panels, $p = 30\%, z = 2$. Durability is 0% in panels (b–c) and 50% in panels (e–f).

S8: Periodic patterns of inventory emerging from threshold behavior. As mentioned in the Main Text, two main mechanisms shape the overordering decisions. First, as each supplier, both direct and indirect, is a potential source of hazard, leading to stronger overordering for firms located downstream. Next, the inventory maintained by a supplier may sufficiently damp disruption cascade, so that can its clients may overorder less. In random acyclic network, the first mechanism dominates, as shown in Fig. 1(c) of the Main Text, but the second generates a large variability. For layered structures, however, firms belonging to the same layer share a very similar position, and tend to act alike. Consequently, the second mechanism gets more detrimental in shaping the outcome. Figure S6 presents the periodic pattern that emerges from these interactions in a fully connected and layered network. According Sec. S4, with two suppliers and non-durable goods, the overordering rates that maximize the profit of firm is either 0% or 100%. Clients of primary producers face too low risks, so that overordering is not profitable. As we move down, risks pile up. At layer 9 a threshold is crossed and a 100%-overordering becomes profitable. Because of this decision, the level of risks is reduced so much that layer-10 firms have no incentive to overorder. As we move the next layers, risks pile up again until a new threshold is met, and overordering becomes profitable, at layer 15. This sequence repeats and leads to a periodic pattern of length 5.

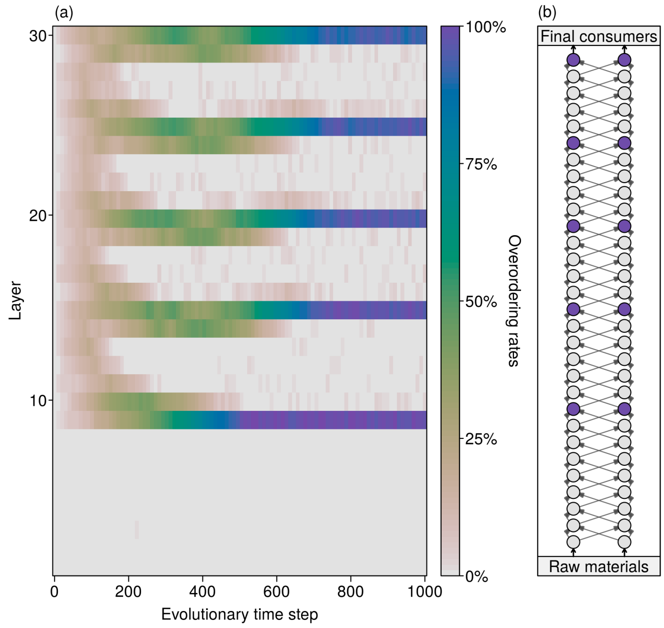

Fig. S6. A periodic overordering pattern emerges from strategic interactions. Panel (a) presents the evolutionary dynamics corresponding of the full fragmentation scenario that settles in the fully connected 30-layer supply chain with 2 firms per layer displayed on panel (b). The average overordering rate of each of the 30 layers is indicated by a color code: grey corresponding to no overordering and purple to a 100%-overordering rate. Panel (b) displays the resulting pattern: only firms located at layers 9, 15, 20, 25 and 30 overorder.

S9: Robustness check of the negative impact of fragmentation on mitigation. Figure 3 of the Main Text shows how the average mitigation success changes with fragmentation for six classes of acyclic random network. Each point of these curves is, for a given level of fragmentation, an average over 20 supply chains, and for each supply chain with n firms, over $10\times n$ group configurations. Using the same colors, each panel of Fig. S7 presents the dispersion of underlying data. The top subpanels show the inter-network dispersion: how mitigation success, averaged over the group configurations, varies across the 20 networks. The bottom subpanels present the inter-group dispersion: how mitigation success, scaled by the average over all networks, varies across the $10\times n$ group configurations. Such variability is sizeable, indicating that, for specific group configurations, a slightly more fragmented supply chain may have a larger mitigation success. But the overall finding remains robust: in average fragmentation hampers risk mitigation. The variability between networks is much larger, indicating that the overall mitigation success is strongly influenced by the structure of the supply chain. This finding point towards further investigations aiming at identifying the structural features that influence risk mitigation.

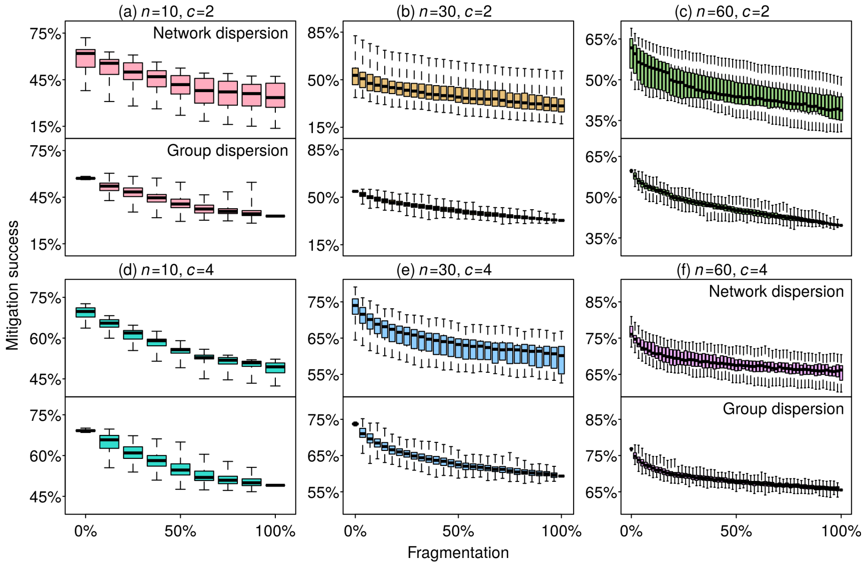

Figure S7. Dispersion of the data underpinning the six curves of Fig. 3 of the Main Text. Each panel corresponds to one of the curves. For each fragmentation level, two distributions of mitigation success are shown. The top one represents the network dispersion: it is made of 20 data points, which are the average mitigation success over the $10\times n$ group configuration generated for each network. The bottom one represents the group dispersion, made of $20\times 10\times n$ data points. To shown only the group-configuration-induced variability, we remove the network dispersion effect by rescaling each data points by the average mitigation success. Specifically, each data point is the mitigation success obtained with one network and one group configuration, minus the average mitigation success over all configurations for the specific network, plus the average over all configurations and all networks. The bottom and top of the boxes indicates the first and third quartiles, the heavy horizontal lines inside the boxes pinpoint the medians, and the whiskers extends to the extrema.

S10: Predicting the optimal overordering rates with network indicator. Could the optimal overordering rate of a particular firm be predicted by its position in the supply chain, without an explicit analysis of the strategic interactions? We use linear and multilinear regression analyses to test the ten network indicators presented in Table S2. Each of them captures a particular aspect of the position of the firm in the supply chain. Three indicators focus on the supply side: the number of direct suppliers, of total suppliers, and the supply-chain level. Three others are their counterparts for the demand side: the number of direct clients, of total clients, and the inverted supply-chain level. The number of similar firms captures the density of firms sharing the same clients. The three last indicators are centrality measures: closeness and betweenness centrality, page ranks.

Table S2. Summary of the ten network indicators.

Name	Explanation
# Direct suppliers	Number of direct suppliers.
# Total suppliers	Number of all direct and indirect suppliers, up to primary producers.
Supply-chain level	Average length—i.e. number of links—of all pathways connecting the firm to primary producers. It is equivalent to the ecological trophic level (26).
# Direct clients	Number of direct clients.
# Total clients	Number of all direct and indirect clients, up to primary producers.
Inverted supply-chain level	Average length of all pathways connecting the firm to final producers. It is the supply-chain level of the network in which all links have been reverted.
# Similar firms	Number of other suppliers of the firm's clients
Closeness centrality	Inverse of the sum of the length of the shortest path connecting the firm to all others (25).
Betweenness centrality	Importance in connecting any two regions of the network (25).
Page ranks	Importance in supplying clients that are themselves important suppliers (25).

We performed linear and multilinear regressions of the indicators on the ESSs, both full fragmentation and full integration. We exhaustively tested combinations of indicators, using stepwise algorithms for model selection. For each scenario, the dataset contains 60,000 points, corresponding to 2,000 directed acyclic random networks with $n = 30$, $c = 3$, $z = 2$, $v = 50\%$ and $p = 10\%$. We first performed linear regressions using one indicator at a time. Results are presented in Table S3. The highest coefficient of determination is reached by the number of total suppliers in the fragmentation scenario, and by the supply-chain level in the integration one. Overall, the indicators focusing on the supply side, including page rank, outperform those focusing on the demand side. This difference is slightly reduced in the integration scenario, in which the impact of overordering on clients is taken into account by firms. We note, in particular, that closeness and betweenness centrality do not capture relevant information for the allocation of overordering rates. These results confirm the findings exposed in Fig. 5 of the Main Text. The overordering rates leading to the higher mitigation success are those of the full integration scenario. Therefore, supply-chain level is the most accurate tool that decision-makers can use to find an allocation of overordering rates that reduces systemic risks. With full fragmentation, after removing the variability captured by the number of total suppliers, a large dispersion of the overordering rate remains, as seen in Fig. 1(c) of the Main Text. No other indicator, however, is able to capture the remaining variability. Even a multilinear model containing all indicators increases the coefficient of determination by only 0.03. With full integration, a similar multilinear model increases more significantly the coefficient of determination, from 0.48 with supply-chain level only to 0.62. Using stepwise model selection, we found that the inverted supply-chain level is the second best indicator. This result confirms that, in integrated supply chains, the position of a firm in relation to its clients could also be taken into account to improve the allocation of overordering rates. The large remaining variability however suggests that strategic interactions fail to be captured by linear models. Decentralized decisions always outperform centralized ones based on linear models.

Table S3. Results of the linear regressions made for each indicator of Table S2 on the evolutionary stable overordering rates of individual firms for the fully fragmented and fully integrated scenarios. Each regression contains only one indicator at a time. For each scenario, the indicator with the highest coefficient of determination is highlighted. All p-values are below 10^{-10}. Each dataset contains 60,000 points, corresponding to 2,000 networks with parameters $n = 30$, $c = 3$, $z = 2$, $v = 50\%$ and $p = 10\%$.

Indicator	Full fragmentation		Full integration	
	Estimated coefficient (standard error)	Coefficient of determination	Estimated coefficient (standard error)	Coefficient of determination
# Direct suppliers	0.033 (0.00018)	0.59	0.052 (0.00060)	0.20
# Total suppliers	**0.016 (0.000049)**	**0.69**	0.023 (0.00017)	0.40
Supply-chain level	0.042 (0.00027)	0.49	**0.11 (0.00066)**	**0.48**
# Direct clients	-0.019 (0.00024)	0.20	-0.060 (0.00058)	0.26
# Total clients	-0.0064 (0.000079)	0.21	-0.018 (0.00019)	0.24
Inverted supply-chain level	-0.030 (0.00033)	0.26	-0.096 (0.00073)	0.36
# Similar firms	-0.0054 (0.000095)	0.12	-0.019 (0.00022)	0.19
Closeness centrality	9.97 (0.21)	0.084	-3.41 (0.54)	0.0013
Betweenness centrality	0.0014 (0.000069)	0.017	-0.0022 (0.00017)	0.0055
Page ranks	2.34 (0.014)	0.55	4.42 (0.042)	0.27

Chapter 7

Research outlook

Conceptual framework and methods. The conceptual framework of Fig. 3.2 has helped us formulate two theoretical models for economic resilience. In both models, the building blocks are economic agents who follow simple dynamical rules. The flexibility of ABMs has enabled the study of both short dynamics and long term adaptive behavior. From the engineering resilience standpoint, we can apply simple statistical methods and measure the amplitude and timing of disruption cascades. But for ecological resilience, we may need a wider toolbox, including, for instance, feedback control and advanced spectral analysis. The study of adaptive resilience, which implies longer time scale, may be performed using evolutionary approaches and the theory of adaptive dynamics.

In the first paper, ABM analysis was productively steered by the results of the ODE model. Without this guidance, we perceived that formulating an ABM may quickly resemble a 'kitchen sink' approach: many ingredients are put together, but we loose sight of their impacts on the outcomes. Many ABM users have expressed this risk. Like Gallegati and Kirman (2012), we argue that purely simulation-based analyses should be avoided. Instead, we may advance the exploration of an ABM step by step, through a hierarchy of models of intermediate complexity that are analytically solvable.

We applied this approach in the two subsequent papers. In the large and complex ER and SF–FA networks, we zoomed in on smaller structures to uncover the dynamics of 'fast desaturation' and 'fine detuning'. In the last paper, we reformulated our dynamical system on simpler and symmetrical supply chains in order to solve the evolutionary trajectories either explicitly or algorithmically. These intermediate steps have allowed us to build more robust conclusions. We have however noticed that tractability may be quickly lost with complex and more realistic typologies. That is why, even with detailed data on real production systems, generic motifs (e.g., loops, tree) and classes (e.g., Erdős–Rényi graphs) are still useful for exploring the dynamics of the aggregate system.

Novel hypotheses on economic resilience. The BDE model has offered a rich view on the potential structural fragility of production systems. While the adverse effect of superconnected hubs is now fairly recognized in economics (e.g., Acemoglu et al., 2012), the negative impact of stock unbalances found in our model has only been recently investigated (Hallegatte, 2014). Inventory data being disclosed by publicly-traded firms in the U.S., we believe that the empirical study of our finding could be undertaken. For instance, Barrot and Sauvagnat (2016) have correlated these data with the U.S. structure of production and disasters data, and assessed the damping effect of inventory on disruption propagation.

Following the preliminary results of Coluzzi et al. (2011), our second paper has uncovered the striking role of production delays and their heterogeneity. We have found that short and unbalanced production delays between interdependent processes may hamper their recovery to shocks. The formal sobriety of BDEs has allowed us to identify the dynamical and topological patterns from which this nonlinear behavior originates. It would be interesting to identify how frequent are these 'short interacting loops' in the U.S. and Japanese production systems, using for instance the data explored by Fujiwara and Aoyama (2010) or Mizuno et al. (2014). In addition, consistent dataset on production delay has not yet been published. We argue such data may be highly relevant to better grasp the dynamics of production systems and their resilience.

The behavior of the BDE model also suggests potential conflicts between firm-level and system-level resilience. For instance, from a managerial standpoint, it may seem adequate to shorten production delays and to ask suppliers to deliver more rapidly, not only for efficiency purposes but to also enable quicker response to disruptions. But if such reductions take place between interdependent industries, it may actually take longer to recover. This concern for speed has also been expressed in financial systems, in which, according to professionals, efficiency-driven reduction of time lags have increased fragility (National Research Council of the National Academies, 2007).

In the last model, the evolutionary adaptation of agents, albeit limited to ordering, has allowed us to evaluate the level of resilience that emerges from optimal risk-mitigating strategies. We have found that systemic risks, in the form of disruption cascades, increase with the fragmentation of the supply chains. Although the set of observations presented in Sec. 2.1.2 seems to support this view, a specific empirical investigation may still be undertaken to test statistically this theoretical finding.

In reality, fragmentation results from business strategies and is implemented by firms to cope with competition. Through outsourcing, a share of the risks that could before be internally managed is externalized to the production system. The economy may as a result become more turbulent. As suggested in Sec. 2.2.2, firms may compensate for the higher fragility of their supply chains by being more agile. Turbulence is an opportunity to compete through resilience. This interpretation could fit within the idea of a self-organized criticality (Bak and Chen, 1991): competitive pressure drives the system towards higher systemic risk, leading to disruption avalanches. The most resilient firms adapt through new strategies, and systemic risk builds up again.

We then could, as proposed by May et al. (2008) for the banking systems, use such ABM models to test potential firm-level regulations or incentives that could pull the system back to a 'subcritical' state. Such investigations would be of high interest for insurers and reinsurers, who are increasingly asked to cover for systemic risks.

Indicators, heuristics, and 'Black Swans'. To deal with such risks, there is a tendency to overemphasize the role of quantitative indicators. Designing metrics is for instance the top priority of the expert panel on systemic risks of the World Economic Forum (2012). This dissertation has highlighted significant limitations for the measurement of resilience. For both models of disruption propagation, we have designed quantitative indicators linked to specific classes of 'well behaved' shocks. In reality, disasters and accidents are much wilder, and vary in their duration, intensity, spatial extent, and may exhibit spatial and temporal correlations.

In the BDE model, our metrics were linked to short perturbation affecting single agents one by one. Although interesting findings on resilience could be built on such indicators, it became ineffective to apprehend the response of the system to stochastic shocks. A series of small perturbations, occurring in a certain order and at specific place, could destabilize the whole network. With only 1,000 firms, robustly assessing the resilience of the network to these rare sequences of events is very challenging.

In the third paper, production units were independently hit by failures that follow a simple stochastic, Poisson process. Agents could learn from these perturbations through time-averaging procedure and update their strategy accordingly. Real shocks seem however to behave more erratically, and are better represented by fat-tailed distributions. Our measurement of resilience would become meaningless. Using 'Black Swan' events (Taleb, 2007) as external perturbations, the evolutionary process would have probably not converged, and the notion of 'optimal strategy' would have to be redefined.

This more realistic setting leads to reassess our assumption on the decision-making process of agents and their expectations. With such wild uncertainties, it may be, as in Dosi et al. (2015), that agents with very simple heuristic-based decisions outperform those using advanced analytics to infer trends.

We argue that designing an indicator of resilience that is freed from any assumption on the shocks is impossible. Resilience is not purely determined by internal structures and processes, but by how these factors interact with the environment. The extended conceptual framework of Fig. 7.1 makes these interactions more explicit.

An extended conceptual framework for the Anthropocene. We have emphasized in the general introduction that the forcing exerted by human societies on environmental processes is likely to generate higher variability. This dissertation has contributed to uncover economic processes that may amplify such instabilities. However, by limiting our scope to purely economic processes, we have found limits in our evaluation of resilience.

Since environmental shocks may increasingly be linked with economic activities, as suggested by the Anthropocene paradigm, we propose to extend our conceptual framework to explicitly account for this feedback; see Fig. 7.1. In other words, we make the same step as Holling did with other resilience scientists in the 1990s, but the other way around. While they realized that, in an anthropogenized planet, socioeconomic dynamics had to be included in the study of ecological resilience, we here propose, for the exact same reason, to account for environmental processes in the study of economic resilience.

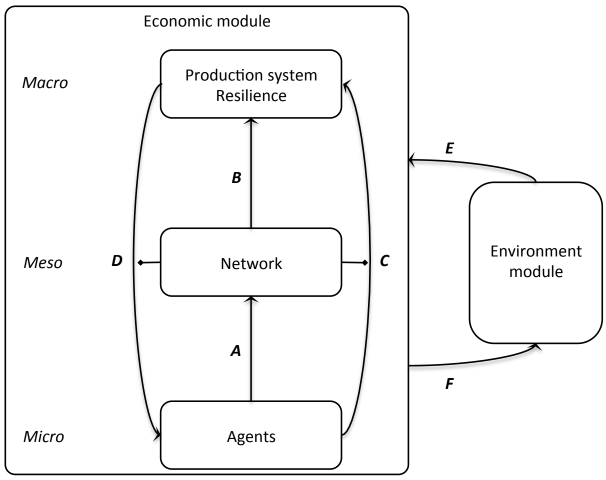

Figure 7.1: Conceptual framework for the modeling of economic resilience in the Anthropocene. The economy exerts a forcing on environmental processes (E–arrow), which in turn affect the economy (F–arrow). The F–arrow could represent, for instance, climate-and-weather–related extreme events. The description of the economic module can be found in Fig. 3.2.

This extended conceptual framework opens novel exciting perspectives. For instance, in our model of supply chain fragmentation, we may link perturbation frequency with the waste generated by the economy. We expect that this feedback loop will penalize the building of high safety stocks. Firms may accept a certain degree of fluctuations in order to avoid getting into an even more turbulent environment. However, as for the climate and other common goods, pollution is caused by individuals but damages are felt globally. This coordination issue however differs from most studies of such 'tragedy of the commons' (Hardin, 1968), in that agents share the same supply chain and are therefore interdependent.

Evolutionary path of production systems. Already within the original conceptual framework, our models can be extended in many directions: studying more realistic decision-making processes, better representing the production process, its constraints and its flexibility, introducing multiple sectors, calibrating input–output relationships from data, etc. One particularly interesting direction is to investigate the evolutionary path of the structure of production through the B–D–A–loop, and especially how the shocks, i.e. the F-arrow or the E–F–arrow, are memorized into the network.

A somewhat similar approach was adopted by Weisbuch and Battiston (2007) on the emergence of spatial pattern in an initially symmetric production network. In models studying the emergence of production network, as in Gualdi and Mandel (2015), we could study how different classes of perturbation regimes — well-behaved and wilder ones — may affect the resulting topology.

We have started to explore this question in the BDE model. By allowing agents to replace disrupted suppliers by others, highly interconnected structures quickly disappear, and the resilience of the system greatly increases. This result is in line with Holling's hypothesis (1973): systems subject to environmental fluctuations evolutionarily encode more resilient structures, while unperturbed ones become fragile. We have also observed that the amount and quality of information processed by agents when they change suppliers significantly boost the resilience of the system.

We thus believe that our thesis has opened a wide research outlook. New theoretical hypotheses may be empirically tested, and new data collected. The extended conceptual framework may usefully guide new theoretical projects, whether based on the models presented in our papers, or on new ones.

References

Acemoglu, D., Carvalho, V. M., Ozdaglar, A., Tahbaz-Salehi, A., 2012. The Network Origins of Aggregate Fluctuations. Econometrica 80 (5), 1977–2016.

Bak, P., Chen, K., 1991. Self-Organized Criticality. Scientific American 264 (1), 46–53.

Barrot, J.-N., Sauvagnat, J., 2016. Input Specificity and the Propagation of Idiosyncratic Shocks in Production Networks. The Quarterly Journal of Economics, qjw018.

Coluzzi, B., Ghil, M., Hallegatte, S., Weisbuch, G., 2011. Boolean delay equations on networks in economics and the geosciences. International Journal of Bifurcation and Chaos 21 (12), 3511–3548.

Dosi, G., Napoletano, M., Roventini, G. D. M. N. A., Stiglitz, J. E., Treibich, T., 2015. Expectation Formation, Fiscal Policies and Macroeconomic Performance when Agents are Heterogeneous and the World is Changing.

Fujiwara, Y., Aoyama, H., 2010. Large-scale structure of a nation-wide production network. The European Physical Journal B 77 (4), 565–580.

Gallegati, M., Kirman, A., 2012. Reconstructing economics: Agent based models and complexity. Complexity Economics 1 (1), 5–31.

Gualdi, S., Mandel, A., 2015. On the emergence of scale-free production networks. arXiv 1509 (01483).

Hallegatte, S., 2014. Modeling the Role of Inventories and Heterogeneity in the Assessment of the Economic Costs of Natural Disasters. Risk Analysis 34 (1), 152–167.

Hardin, G., 1968. The tragedy of the commons. Science 162 (3859), 1243–1248.

May, R. M., Levin, S. A., Sugihara, G., 2008. Complex systems: Ecology for bankers. Nature 451 (7181), 893–895.

Mizuno, T., Souma, W., Watanabe, T., 2014. The Structure and Evolution of Buyer-Supplier Networks. PLoS ONE 9 (7), e100712.

National Research Council of the National Academies, 2007. New directions for understanding systemic risk: a report on a Conference Cosponsored by the Federal Reserve Bank of New York and the National Academy of Sciences. Tech. rep., Federal Reserve Bank of New York, National Research Council, Washington, DC.

Taleb, N. N., 2007. The Black Swan: The Impact of the Highly Improbable. Random House, New York City, NY.

Weisbuch, G., Battiston, S., 2007. From production networks to geographical economics. Journal of Economic Behavior & Organization 64 (3–4), 448–469.

World Economic Forum, 2012. New Models for Addressing Supply Chain and Transport Risk. Tech. rep., World Economic Forum.

Conclusion

We cannot understand the resilience of economies without a deep look at their structure. Businesses now operate through a variety of networked infrastructures and are engaged in complex supply chains. Such increased interconnectivity generates economic volatility, which may be also amplified by a more turbulent climate. By modeling the economy as a dynamic network, we have identified factors that could attenuate these phenomena: less concentrated sectors, shorter and more integrated supply chains, less inventory unbalances, more even production delays. These findings now wait to be empirically investigated.

What perspective do they bring for managing our 'Spaceship Earth'? First, they indicate that the conventional formula "if you can't measure it, you can't manage it" does not quite apply for resilience. It is hard to quantitatively capture this property, even in theoretical models. Instead, we should investigate the wide set of economic processes that underpin it, and assess, in light of some general principles that we are starting to uncover, whether they contribute or not to resilience. We may start with the following questions: Are there any weak points in the supply of basic services? How interdependent are the critical players and how fast do they interact? To which extent supply chains are visible to consumers and businesses?

We should however not forget why there is a need for resilience. Indeed resilience has become a solution to climate change due to the collective inability to sustainably manage socioeconomic development. Steering our societies towards resilience should not be an end in itself but a mean to tackle the roots of the initial problem.

In fact, most economic volatility is not yet caused by climate change, nor by another environmental transformation, but arose from internal economic processes. Through technological innovation and heightened competition, firms have engaged in outsourcing and inventory reduction, making supply chains more sensitive to shocks. They have simultaneously become more agile, more able to cope in a changing environment. Nowadays, many of them embrace resilience as the process of 'perpetual reconstruction', which, in the end, may increase economic fluctuations.

Resilience is not intrinsically virtuous, and we suggest that, when presented as a practical solution, it should always be questioned. However, regardless of its socioeconomic implications, the concept is extremely valuable for complex system scientists. This mainly qualitative notion opens very rich perspectives to reassess the dynamics of our anthropogenized planet. It also opens new interpretations on how complex systems co-evolve with their environment and may persist through time.

Our thesis has been an exciting intellectual journey. We have explored a broad spectrum of disciplines, discussed innovative methods, and manipulated intriguing mathematical objects. The conceptual framework we have formulated was helpful to make a start on our exploration of resilience. We believe that it can guide the development of many more projects, and hope that this dissertation will contribute to advancement of knowledge on complex systems.

Résumé long en français

Introduction

Les défis climatiques et environnementaux s'accompagnent d'incertitudes et d'instabilités grandissantes. Le changement climatique ne conduit pas seulement à une hausse progressive des températures moyennes, il se traduit également par une modification de la variabilité interne des processus climatiques et de leurs interactions. En conséquence, les évènements climatiques extrêmes se transforment, et pourraient devenir plus fréquents, plus intenses, et affecter de nouvelles régions du globe.

Pour devenir soutenable, il ne suffit donc pas de réduire notre empreinte écologique, il faut aussi s'adapter à ces turbulences. Comment s'adapter à un environnement changeant et incertain ? Pour beaucoup, la solution réside dans la résilience, cette capacité à rebondir après des chocs, à se réadapter rapidement face à de nouvelles conditions. Comment ce concept, surtout développé en écologie, se traduit-il en terme économique ? Comment bâtir une économie résiliente face aux chocs environnementaux ? Nous nous concentrons dans cette thèse sur l'un des mécanismes amplifiant l'impact des catastrophes naturelles sur l'économie : la propagation des ruptures d'approvisionnement dans les systèmes de production.

Etant donné l'originalité du sujet abordé et sa dimension interdisciplinaire, nous consacrons les trois premiers chapitres à introduire la problématique, à en exposer les enjeux, et à expliciter nos choix méthodologiques. Nous développons d'abord une discussion approfondie du concept de résilience et exposons certaines de ses implications socio-politiques. Nous relions ensuite notre problématique aux enjeux économiques actuels, en particulier à l'interconnexion grandissante des processus de production et à l'émergence du risque systémique. Enfin, à partir d'une revue multidisciplinaire des modèles existants, nous justifions nos choix méthodologiques et proposons un cadre conceptuel nouveau pour modéliser de la résilience économique.

La deuxième partie rassemble les trois articles préparés au cours du travail de thèse. Ils en constituent le substrat scientifique. La première étude valide, à partir d'un système dynamique proie–prédateur classique en écologie, l'approche multi-agent proposée dans notre cadre méthodologique. Nous analysons ensuite l'impact de l'hétérogénéité des délais d'approvisionnement sur la résilience des chaînes de production, à partir d'un modèle original basé sur des équations booléennes à retard. Le troisième article mobilise la théorie des jeux évolutionnaires pour montrer comment la fragmentation des chaînes de production exacerbe le risque systémique et diminue la résilience.

Pourquoi et comment modéliser la résilience économique ? Contexte, enjeux et méthodes

La résilience invite à saisir la complexité dynamique des systèmes

En 1973, Holling introduit le concept de résilience en écologie pour souligner le caractère fondamentalement dynamique des écosystèmes. Son argument se base sur l'observation de certaines communautés d'espèces dont les populations persistent dans le temps tout en étant très fluctuantes, et d'autres qui, d'apparence très stable, s'effondrent brusquement. Etudier la stabilité d'un écosystème n'est donc pas suffisant pour comprendre sa capacité à perdurer dans le temps. Il propose de s'intéresser à leur résilience, c'est-à-dire à leur capacité à rester ou à retourner dans un même état qualitatif malgré des perturbations extérieures. Du point de vue mathématique, il s'agit de passer de l'analyse des points d'équilibre et de leurs stabilités locales à une étude des comportements dynamiques globaux, caractérisés par la géométrie des bassins d'attractions et la survenance de bifurcations.

Des dynamiques socio-économiques ont été intégrées à l'étude écologique de la résilience, notamment dans un contexte d'exploitation de ressources renouvelables. Ce faisant, plusieurs auteurs ont proposé d'intégrer le concept de résilience dans le corpus théorique des systèmes complexes adaptatifs, lequel s'intéresse aux phénomènes d'auto-organisation, de rétroactions multi-échelles, d'adaptation et d'apprentissage. Au-delà de la capacité d'un système à retrouver son état normal après un choc, la résilience devient dans cette perspective la faculté d'un système à s'adapter à des chocs, à apprendre pour évoluer vers un nouvel état.

Ces différentes définitions montrent que, suivant les échelles de temps et les processus considérés, l'analyse de la résilience peut s'effectuer selon différentes profondeurs de champ. Trois niveaux sont généralement admis : (i) la résilience ingéniériale — le temps de retour à l'équilibre, (ii) la résilience écologique — la capacité à rester dans le même état qualitatif, et (iii) la résilience adaptive — la capacité à se réorganiser face à de nouvelles contraintes.

Le concept de résilience porte également des enjeux socio-politiques, qu'il convient d'identifier tant la pratique scientifique ne peut s'en extraire. Dans le champ scientifique, de très nombreuses communautés se sont saisies de ce concept, dans les sciences politiques ou la géographie par exemple. Il est souvent utilisé pour réinterroger des hypothèses de travail, ou même pour proposer un changement de paradigme ; l'article de Holling en est l'exemple archétypal. Si le concept est jugé inutile par certains car trop flou, pour d'autres il constitue un « objet-frontière », dont la malléabilité stimule les échanges interdisciplinaires. Le concept de résilience est par ailleurs très largement répandu dans la « zone grise » entre sciences, politiques publiques, et institutions internationales. Du fait de son écho novateur et fédérateur, le terme y est parfois utilisé dans des jeux de pouvoir et des logiques institutionnelles dépassant sa portée scientifique.

L'interconnexion des chaînes de production, une menace pour la résilience ?

Etudier la résilience économique, c'est étudier les facteurs qui déterminent la façon dont une économie répond à des chocs. Le concept de résilience semble adéquat, car, à l'instar des écosystèmes, le système économique est hautement dynamique, et les grandeurs macroéconomiques sont sujettes à de larges variations. Dans cette thèse, nous nous concentrons sur l'un des mécanismes amplificateurs des chocs exogènes dans l'économie, à savoir les liens d'interdépendances au sein des chaînes de production. Ce phénomène, encore mal compris, constitue un enjeu économique majeur.

Depuis plusieurs décennies, les processus de production de biens et de services sont marqués par la désintégration verticale des industries manufacturières et un développement exceptionnel de la sous-traitance à l'échelle mondiale. En conséquence, les chaînes de production sont plus longues, plus complexes et plus fragmentées. Un dysfonctionnement à un point de ces chaînes peut engendrer des ruptures d'approvisionnement, qui, par effet ricochet, risquent de se propager d'une entreprise à l'autre. De tels phénomènes ont été mis en évidence empiriquement, et de nombreux rapports émanant d'assureurs et d'organisations professionnelles témoignent de la difficulté des entreprises à faire face à ce type de risque.

Dans un système productif devenu réseau mondialisé hautement interconnecté, ces phénomènes sont perçus comme un risque systémique. Ce risque tend à être exacerbé par les forces concurrentielles, car elles limitent certaines pratiques renforçant la résilience du système, comme les stocks-tampons ou la diversification des sources d'approvisionnement. Pour être individuellement résilientes, certaines entreprises développent des capacités organisationnelles d'anticipation, de réactivité et d'agilité afin de s'adapter aux turbulences économiques.

S'intéresser à la résilience des systèmes de production conduit donc à articuler deux niveaux d'analyse. D'une part, le réseau des interdépendances entre processus de production est la matrice à travers laquelle se propagent et s'amplifient les chocs. D'autre part, les entreprises, qui sont les nœuds de ce réseau, anticipent, réagissent et s'adaptent à ces perturbations. Leurs décisions, soumises aux forces concurrentielles, modifient la forme du réseau et sa résilience.

Pour une modélisation multi-échelle de la résilience des réseaux de production

De nombreux modèles exploitent les tableaux de comptabilité intersectorielle entrée–sortie pour analyser les interdépendances productives. Ils permettent d'obtenir des estimations quantitatives des répercussions d'un choc exogène sur l'ensemble des secteurs d'une économie. Ces estimations dépendent d'hypothèses technologiques et économiques : ajustement des prix, flexibilité des processus de production, recours à des stocks, réactivité des entreprises, etc.

Le défi principal de ces modèles est leur granularité, car l'agrégation sectorielle ne rend compte que de manière très partielle du processus de propagation de choc. Ce dernier s'opère précisément du fait de l'éclatement structurel de la production entre des agents différents. Il est donc nécessaire de modéliser le réseau de production à l'échelle des firmes. Un tel projet se heurte cependant à l'absence de jeux de données déjà structurés. Des travaux sont en cours pour résorber ce problème. Par exemple, des données fournisseurs–clients ont déjà permis de reconstituer la majorité du réseau de production du Japon. Ce résultat sera utilisé pour calibrer l'un de nos modèles.

Modéliser la propagation des chocs sur des réseaux aussi complexes est un autre défi scientifique, et rejoint la question plus générale des processus dynamiques et adaptatifs au sein des réseaux. D'importants résultats ont été obtenus par la modélisation des cascades de défauts sur les dettes, ce qui a permis de mieux caractériser le risque systémique dans les réseaux interbancaires. La modélisation des réseaux de production et des ruptures d'approvisionnement en est encore à ses débuts. Quelques modèles ont commencé à étudier le lien entre topologie et risque systémique, un autre a mis à jour la tendance de ces réseaux à concentrer la production sur quelques nœuds. Ces contributions établissent la base de travail sur laquelle s'appuient nos modèles.

Ces processus dynamiques et adaptatifs déterminent la réponse de ces réseaux à des chocs exogènes. C'est à partir de ces réponses que nous évaluons la résilience du système. La résilience est donc une propriété macroéconomique qui émerge du comportement des entreprises et de leurs interactions. Nous adoptons une modélisation dite multi-agent. A la différence des modèles macroéconomiques classiques qui utilisent des agents représentatifs, cette approche granulaire est adaptée à l'étude de propriétés émergentes. Notre revue de littérature montre plus généralement les limites de l'analyse économique classique pour l'étude de ce phénomène. La majorité des modèles économiques se concentrent sur les états d'équilibre, alors que la résilience relève justement des comportements hors équilibre. Pour étudier de telles trajectoires dynamiques, nous n'adoptons pas les hypothèses de rationalité parfaite et d'anticipations rationnelles, et modélisons les agents économiques par des règles comportementales adaptatives.

Le cadre de modélisation que nous proposons articule trois niveaux d'agrégation : les entreprises (micro), la structure du réseau (méso), et le système productif (macro).

Ces trois niveaux interagissent : par exemple, en fonction des risques macroéconomiques, les entreprises ajustent leur stratégie microéconomique, ce qui peut modifier la forme du réseau. En formulant des modèles de différents niveaux de complexité, nous pouvons méthodiquement étudier plusieurs niveaux de détails, et ce faisant, faire varier la profondeur de champ de notre analyse de la résilience.

La résilience ingénieriale caractérise l'ampleur des phénomènes de propagation qui suivent un choc exogène. Nous la mesurons à partir des trajectoires dynamiques de variables macroéconomiques. La résilience écologique décrit la vulnérabilité du système à des changements de régime. Nous l'évaluons par la géométrie des bassins d'attraction et à la survenance de bifurcations. Enfin la résilience adaptative, qui présuppose la modélisation de processus évolutionnaire d'apprentissage, se mesure par l'amélioration, sur une échelle de temps plus longue, de la résilience ingénieriale et écologique.

Trois contributions scientifiques pour modéliser la résilience

Analyser les bifurcations d'un modèle multi-agent

Nous avons identifié la pertinence des modèles multi-agents pour modéliser les réseaux de production. Or, l'analyse de cette classe de modèles est encore peu standardisée. Il n'existe en particulier aucune méthode établie pour détecter les bifurcations, étape fondamentale pour étudier la résilience. Nous nous attaquons à ce problème à partir d'un système classique d'équations différentielles. Il s'agit du modèle Rosenzweig–MacArthur avec effet Allee sur la proie, qui décrit la dynamique d'interaction entre une proie et son prédateur. Nous formulons un modèle multi-agent qui en reprend les caractéristiques principales. La définition du modèle respecte strictement le paradigme de la modélisation multi-agent, à savoir qu'aucune propriété dynamique globale n'est encodée a priori dans les règles comportementales des agents. Nous concevons ensuite des méthodes statistiques afin de détecter les bifurcations.

La séquence de bifurcations du modèle multi-agent est qualitativement équivalente à celle du modèle original. La bifurcation de Hopf est détectée grâce à des méthodes avancées d'analyse des séries temporelles ; les points-selles sont localisés grâce à des algorithmes de rétroactions issus du contrôle automatique. Ce résultat valide l'utilisation des modèles multi-agents pour l'étude de la résilience. En outre, nous montrons que les signaux annonciateurs des changements de régime, comme le ralentissement des rétroactions ou l'asymétrie des séries temporelles, sont très dépendants de la nature des bifurcations sous-tendant les transitions.

Enfin, notre travail démontre l'intérêt de s'appuyer sur une hiérarchie de modèles de différents niveaux de complexité. Le comportement d'un modèle éclaire celui de l'autre, et leur comparaison facilite l'identification du lien entre comportement dynamique et hypothèses de modélisation. Ce premier travail valide notre modélisation de la résilience dans un champ où ce concept est déjà connu. Dans les deux autres articles, nous la mettons en œuvre pour étudier la résilience économique.

Désynchronisation et perte de résilience dans des réseaux de production hétérogènes

Une caractéristique incontournable des réseaux de production est la présence de délais d'approvisionnement. Ces délais sont extrêmement hétérogènes : de la seconde pour l'électricité à plusieurs mois pour certains composants technologiques spécifiques. Jusqu'à présent, les modèles de propagation considèrent implicitement que ces délais sont égaux. Plus généralement, l'impact de l'hétérogénéité des délais d'interactions entre nœuds sur la dynamique des réseaux n'a encore jamais été étudié.

Nous analysons la résilience de réseaux de production dans lesquels les délais d'approvisionnement sont hétérogènes. Notre modèle est constitué d'équations booléennes à retard. Ce formalisme a été introduit récemment pour l'étude des interactions entre phénomènes climatiques dont la fréquence d'apparition est hétérogène. Dans notre modèle, l'activité des firmes dépend de la production de leurs fournisseurs, et, en cas de rupture d'approvisionnement, de l'existence de stocks-tampons. L'ensemble des firmes forme un réseau complexe. Nous évaluons la réponse dynamique de ce système à des chocs, définis comme l'arrêt soudain de la production d'une firme pendant une certaine durée. Nous comparons différentes topologies de réseaux, depuis des réseaux de réseaux très idéalisés à des structures calibrées sur des résultats empiriques.

De manière générale, l'hétérogénéité des délais d'approvisionnement réduit la résilience de ces systèmes. Grâce à une étude détaillée du processus de propagation, nous identifions les méso-structures topologiques qui déterminent ce résultat macro. La présence au sein de ces réseaux de plusieurs chaînes circulaires en interactions les rend vulnérables à des phénomènes de désynchronisation. Lorsque les délais sont homogènes, les firmes se rétablissent mutuellement et conjointement; dans le cas contraire, l'asynchronie des processus empêche ce retour à la production et amplifie les ruptures d'approvisionnement. Ce risque est d'autant plus marqué dans des réseaux observés empiriquement, dans lesquels quelques firmes sont extrêmement interconnectées. Dans une moindre mesure, l'hétérogénéité des stocks peut également conduire à une perte de résilience.

Nous construisons et testons un indicateur évaluant la contribution de chaque firme au risque systémique. Il s'agit de la durée minimale d'arrêt de la production engendrant une paralysie générale. L'agrégation de ces durées fournit une mesure de la résilience qui est très pertinente dans le cas de chocs ponctuels et isolés, mais devient inopérante en cas d'attaques coordonnées. Une série de chocs affectant certaines firmes dans un certain ordre peut, même dans un réseau a priori résilient, engendrer un dysfonctionnement généralisé. Ce résultat montre combien tout indicateur de résilience dépend largement des chocs auxquels est soumis le système. Par ailleurs, nous mettons en lumière des oscillations de relaxation métastable. Ces comportements remarquables sont encore mal compris dans ces réseaux booléens. Dans certaines régions de l'espace des paramètres, un choc initial peut engendrer des vagues de dysfonctionnements périodiques, qui s'installent dans une partie du réseau puis se déplacent vers d'autres, avant de s'éteindre ou de s'étendre à l'ensemble du système.

La fragmentation de la production amplifie les risques systémiques

Les systèmes de production ont subi de profondes transformations au cours des dernières décennies. La désintégration verticale des industries manufacturière, la complexité grandissante de certains produits et la généralisation de la sous-traitance a conduit à la fragmentation des chaînes de production. En d'autres termes, un nombre grandissant d'entreprises distinctes participent à la conception, la production et le transport d'un même produit. Quel est l'impact de cette fragmentation des supply chains sur le risque systémique de rupture d'approvisionnement ? Si des cas isolés suggèrent une corrélation entre fragmentations des supply chains et difficulté de gérer le risque systémique, aucun modèle théorique n'a encore été proposé pour étudier ce lien.

Dans une supply chain, la défaillance d'une firme peut générer des ruptures d'approvisionnement en chaîne. Chaque firme met en œuvre, à son niveau, des mesures pour gérer ce risque. Les mesures prises par une firme sont susceptibles de modifier l'exposition aux risques des autres membres de la supply chain. Si un fournisseur décide d'augmenter son stock-tampon, ses clients seront moins sensibles à des dysfonctionnements intervenant chez les fournisseurs de ce fournisseur. Ils sont donc susceptibles d'en profiter et de décider de réduire leur propre stock. Cet exemple montre que les stratégies face aux risques sont interdépendantes. Plus la chaîne est fragmentée, plus ces interdépendances se multiplient. Quel est l'effet de cet accroissement sur le risque systémique ?

Pour répondre à cette question, nous formulons un modèle basé sur la théorie des jeux évolutionnaires en réseau. Une supply chain est modélisée par un graphe acyclique. Chaque nœud est une firme, dont la production peut être temporairement interrompue. Chaque firme a besoin des produits de ses fournisseurs pour fonctionner. Afin d'amortir les ruptures d'approvisionnement, les entreprises maintiennent un stock-tampon. Le niveau de ce stock est évolutionnairement ajusté pour accroître le profit du groupe auquel appartient la firme. Dans une supply chain intégrée, toutes les firmes appartiennent au même groupe ; chaque firme correspond à un seul groupe dans une supply chain fragmentée.

Notre modèle montre que plus une supply chain est fragmentée, moins les firmes ont intérêt à maintenir un stock, engendrant une propagation accrue des ruptures d'approvisionnement et donc une perte de résilience. Ce comportement est dû au fait que, plus une supply chain se fragmente, plus les effets positifs des stocks-tampons deviennent des externalités, au sens économique du terme. En effet, lorsqu'une firme accroît son stock, ses clients sont mieux protégés contre les risques et ses fournisseurs bénéficient de ventes additionnelles. Si ces entreprises appartiennent au même groupe, tous ces bénéfices sont intégrés dans la décision de maintenir ou non un stock. Si le groupe est fragmenté, chaque firme ne prend compte que son propre bénéfice, si bien qu'elle réduit le niveau de son stock-tampon.

En l'absence de mécanisme de coordination, la fragmentation des supply chains génère donc un transfert du risque des entreprises individuelles vers le système. Comment contrebalancer ce phénomène ? Nous montrons que le risque systémique peut être en partie réduit en prescrivant aux firmes des niveaux de stock-tampon en fonction de leur position dans la supply chain. L'indicateur permettant d'allouer le plus efficacement les stocks provient de l'écologie : il s'agit du niveau trophique, qui décrit la position d'une espèce dans une chaîne alimentaire. Un tel indicateur pourrait par exemple servir aux assureurs dans la conception de produits couvrant les risques d'approvisionnement.

Perspectives de recherche : vers un couplage des dynamiques économiques et environnementales

Modéliser la résilience économique face aux chocs environnementaux invite à s'interroger sur les liens entre décisions microéconomiques, structure des réseaux et dynamique macroéconomique. En construisant des modèles multi-agents, analysés grâce à la théorie des systèmes dynamiques, des graphes et des jeux évolutionnaires, nous avons mis en lumière certains facteurs susceptibles d'affecter la résilience des chaînes de production : des formes particulières d'interdépendance entre entreprises, l'hétérogénéité des délais d'approvisionnement et des stocks, la fragmentation des supply chains. Ces résultats théoriques sont appelés à être testés par des analyses empiriques. De nombreuses extensions de ces deux modèles sont en outre envisageables. Par exemple, endogénéiser la structure des réseaux permettrait d'examiner l'évolution de la résilience en fonction de la manière dont les firmes adaptent leurs choix de fournisseurs aux chocs. Plus généralement, les principes de modélisation énoncés dans la première partie offrent un cadre fertile pour générer de nouvelles études théoriques et structurer la comparaison de leurs résultats.

Enfin, notre thèse a montré que la résilience ne saurait être une propriété intrinsèque d'un système, mais ne se définit, au contraire, qu'en relation avec le régime de perturbations auquel il est soumis. Pour concevoir des stratégies de résilience face aux chocs environnementaux, il faut non seulement étudier la topologie du système économique et ses rétroactions internes, mais aussi caractériser finement les interactions entre ce système et les processus environnementaux. L'élaboration de modèles dynamiques couplant économie et environnement constitue donc une perspective de recherche prometteuse pour approfondir notre compréhension de la résilience économique.

ÉCOLE DOCTORALE
Sciences de l'environnement d'île-de-France (SEIF)

Titre : Modéliser la résilience économique

Mots clefs : systèmes complexes, systèmes dynamiques, réseaux, modèles multi-agents, supply chains, risques systémiques

Résumé : De grandes transformations écologiques et climatiques sont aujourd'hui à l'œuvre. Elles sont sources d'instabilité environnementale, à l'image d'évènements climatiques extrêmes devenus plus fréquents, plus intenses, et touchant de nouvelles régions du globe. A défaut de pouvoir empêcher ces changements, comment les sociétés humaines pourraient-elles s'y adapter ? Pour beaucoup de chercheurs et de décideurs, c'est par la résilience qu'elles y parviendront. Ce concept semble renfermer des solutions nouvelles, adaptées à un monde turbulent et incertain. Par définition, les systèmes résilients sont capables de rebondir face à des chocs inattendus, d'apprendre rapidement et de s'adapter à des conditions inédites. Malgré l'intérêt suscité par cette notion, les processus qui permettent à une société d'être résiliente restent encore mal connus. Cette thèse développe un cadre conceptuel nouveau permettant, via la modélisation mathématique, d'explorer les liens théoriques entre mécanismes économiques et résilience. Ce cadre repose sur une analyse critique de la résilience en écologie — domaine d'origine du concept — et en économie — notre champ d'application. Nous l'appliquons aux systèmes de production économique, modélisés comme des réseaux de firmes et analysés à travers la théorie des systèmes dynamiques. Cette thèse évalue l'aptitude de tels modèles, dits multi-agents, à générer des profils de bifurcations, étape incontournable de l'analyse mathématique de la résilience. Nous étudions pour cela une dynamique proie–prédateur très générale en écologie et en économie. Ensuite, cette thèse s'attaque à un facteur majeur qui entrave la résilience : les fortes interdépendances entre activités économiques, par lesquelles les retards et interruptions de production se propagent d'une entreprise à l'autre. En utilisant des réseaux de production réalistes, nous montrons comment les délais d'approvisionnement, lorsque intégrés dans des topologies particulières, démultiplient ces phénomènes de propagation. Ensuite, grâce à un modèle évolutionnaire, nous mettons en lumière l'existence d'un risque systémique : les cascades d'incidents ont lieu alors même que tous les agents possèdent des inventaires adaptés au niveau de risque. Ce phénomène s'amplifie lorsque les chaînes d'approvisionnement se spécialisent et se fragmentent. Ces résultats théoriques ont une valeur générale, et pourront servir à orienter de futures recherches empiriques. Cette thèse fait en outre avancer les connaissances sur des méthodes et objets mathématiques très récents, comme les équations booléennes à retard formant un réseau complexe, et les dynamiques évolutionnaires sur les graphes. Les modèles et le cadre conceptuel proposés ouvrent de nouvelles perspectives de recherche sur la résilience, en particulier sur l'impact des rétroactions environnementales sur l'évolution structurelle des réseaux de production.

Title : Modeling Economic Resilience

Keywords : complex systems, dynamical systems, agent-based modeling, networks, supply chains, systemic risks

Abstract : A wide range of climatic and ecological changes are unfolding around us. These changes notably manifest themselves through an increased environmental variability, such as shifts in the frequency, intensity, and spatial distribution of weather-related extreme events. If human societies cannot mitigate these transformations, to which conditions should they adapt? To many researchers and stakeholders, the answer is resilience. This concept seems to subsume a variety of solutions for dealing with a turbulent and uncertain world. Resilient systems bounce back after unexpected events, learn novel conditions and adapt to them. Theoretical models, however, to explore the links between socioeconomic mechanisms and resilience are still in their infancy. To advance such models, the present dissertation proposes a novel conceptual framework. This framework relies on an interdisciplinary and critical review of ecological and economic studies, and it is based on the theory of dynamical systems and on the paradigm of complex adaptive systems. We identify agent-based models as crucial for socioeconomic modeling. To assess their applicability to the study of resilience, we test at first whether such models can reproduce the bifurcation patterns of predator–prey interactions, which are a very important factor in both ecological and economic systems. The dissertation then tackles one of the main challenges for the design of resilient economic system: the large interconnectedness of production processes, whereby disruption may propagate and amplify. We next investigate the role of delays in production and supply on realistic economic networks, and show that the interplay between time delays and topology may greatly affect a network's resilience. Finally, we investigate a model that encompasses adaptive responses of agents to shocks, and describes how disruptions propagate even though all firms do their best to mitigate risks. In particular, systemic amplification gets more pronounced when supply chains are fragmented. These theoretical findings are fairly general in character and may thus help the design of novel empirical studies. Through the application of several recent ideas and methods, this dissertation advances knowledge on innovative mathematical objects, such as Boolean delay equations on complex networks and evolutionary dynamics on graphs. Finally, the conceptual models herein open wide perspectives for further theoretical research on economic resilience, especially the study of environmental feedbacks and their impacts on the structural evolution of production networks.

Université Paris-Saclay
Espace Technologique / Immeuble Discovery
Route de l'Orme aux Merisiers RD 128 / 91190 Saint-Aubin, France